Defining the mechanism and functional consequences of PAI-2-mediated uPA/uPAR endocytosis

David R. Croucher
University of Wollongong

Defining the mechanism and functional consequences of PAI-2- mediated uPA/uPAR endocytosis

A thesis submitted in partial fulfillment of the requirements for the award of the degree

Doctor of Philosophy

from

University of Wollongong

by

David R Croucher

Bachelor of Biotechnology (Honours 1st Class)

School of Biological Sciences
University of Wollongong

2006

I, David R Croucher, declare that this thesis, submitted in partial fulfillment of the requirements for the award of Doctor of Philosophy, in the School of Biological Sciences, University of Wollongong, is wholly my own work unless otherwise referenced or acknowledged. The document has not been submitted for qualifications at any other academic institution.

David R Croucher
12th October 2006

List of Publications

Croucher D, Saunders DN, Ranson M. The Urokinase/PAI-2 Complex: A New High Affinity Ligand for the Lipoprotein Receptor-Related Protein. Journal of Biological Chemistry 281: 10206-10213 (2006)

Al Ejeh F, **Croucher D**, Ranson M. Kinetic analysis of plasminogen activator inhibitor type-2:urokinase complex formation and subsequent internalisation by carcinoma cell lines. Experimental Cell Research 297(1):259-271 (2004)

Stutchbury TK, Al-ejeh F, Stillfried G, **Croucher D**, Allen B, Irving D, Andrews J, Links M, Ranson M. Preclinical evaluation of PAI-2-DTTA-^{213}Bi (alpha-PAI-2) in an orthotopic murine xenogenic model of human breast carcinoma. *Manuscript in press - Molecular Cancer Therapeutics*

Samson A, Niego B, Daniel P, Weiss TW, **Croucher D**, Lawrence DA, Medcalf RL. Tissue-type Plasminogen Activator Requires a Co-Receptor to Enhance NMDA receptor function. *Submitted to Journal of Biological Chemistry*

Croucher D, Saunders DN, Stillfried GE, Ranson M. Structural Basis of Differential Signaling by PAI-1 and PAI-2 in Breast Cancer: Implications for Metastatic Potential *Submitted to Cancer Research.*

List of Conference Presentations

Conference Oral Presentations

Croucher D, Saunders D, Ranson M**.**
PAI-2 is internalised by receptor mediated endocytosis.
IX International Workshop on Molecular and Cellular Biology of Plasminogen Activation, Isle of Capri, Italy (2003).

Croucher D, Saunders D, Ranson M.
Characterising the receptor mediated endocytosis of PAI-2.
International Society for Fibrinolysis and Proteolysis, Melbourne, Victoria (2004).

Croucher D, Saunders D, Leung H, Ranson M.
Structural basis of the differential signaling by initiated by PAI-1 and PAI-2: Implications for metastatic potential.
18th International Congress on Fibrinolysis and Proteolysis, San Diego, US (2006).

Samson AL, Niego B, Daniel PB, Weiss TB, **Croucher D,** Lawrence DA, Medcalf RL.
Tissue-type plasminogen activator can promote NMDA-induced neuronal stimulation via LDL receptor and plasmin-dependent mechanisms.
18th International Congress on Fibrinolysis and Proteolysis, San Diego, US (2006).

Conference Poster Presentations

Croucher D, Al-Ejeh F, Ranson M. The binding kinetics and cellular internalisation of PAI-2 by prostate cancer cells: Validating its use for targeted cancer therapy.
15th Lorne Cancer Conference, Lorne, Victoria (2003)

Al Ejeh F, **Croucher D,** Ranson M. Binding and internalisation characteristics of plasminogen activator inhibitor type 2 (PAI-2) on human breast and prostate cancer cell lines. IX International Workshop on Molecular and Cellular Biology of Plasminogen Activation, Isle of Capri, Italy (2003)

Croucher D, Saunders D, Ranson M. The PAI-2/urokinase complex: A new ligand for the low density lipoprotein receptor-related protein X International Workshop on Molecular and Cellular Biology of Plasminogen Activation, Washington DC (2005)

Croucher D, Saunders D, Ranson M. Annexin II, a novel cell surface receptor and avenue of endocytosis for PAI-2. Serpins Conference, Cairns, Australia (2005)

Lobov S, **Croucher D**, and Ranson M. Assessment of known/potential binding sites in the PAI-2 CD-loop for interaction with annexin II and endocytosis receptors. XVIIIth International Congress on Fibrinolysis and Proteolysis, San Diego, USA, (2006)

List of Tables

List of Figures

List of Abbreviations

Absorbance	A
Amino Terminal Fragment	ATF
Basement Membrane	BM
Bovine Serum Albumin	BSA
Deoxyribonucleic Acid	DNA
Disabled-1	Dab-1
Epidermal Growth Factor	EGF
Epidermal Growth Factor Receptor	EGFR
Ethylenediaminetetraacetic Acid	EDTA
Extracellular Matrix	ECM
Extracellular Signal-Regulated Kinase	ERK
Fluorescein Isothiocyanate	FITC
Foetal Calf Serum	FCS
Glycophosphoinositol	GPI
Gram	g
Gravity	*g*
High Molecular Weight	HMW
Horse Radish Peroxidase	HRP
Hour	h
4-(2-hydroxyethyl)-1-piperazineethanesulfonic Acid	HEPES
Immunoglobulin G	IgG
Association Rate	k_a
Dissociation Rate	k_d
Dissociation Constant	K_D

Kilodalton	kDa
Lipopolysaccharide	LPS
Litre	L
Low Density Lipoprotein Receptor	LDLR
Low Density Lipoprotein Receptor-Related Protein	LRP
Low Molecular Weight	LMW
Matrix Metalloprotease	MMP
Metre	m
Micro	μ
Milli	m
Minute	min
Molar	M
Nano	n
N-hydroxysuccinimide	NHS
Para-formaldehyde	PFA
Phenylmethylsulphonylfluoride	PMSF
Phosphate Buffered Saline	PBS
Plasminogen Activator Inhibitor	PAI
Poly-Acrylamide Gel Electrophoresis	PAGE
Propidium Iodide	PI
Reactive Centre Loop	RCL
Receptor Associated Protein	RAP
Retinoblastoma	Rb
Revolutions per Minute	rpm
Sodium Dodecyl Sulphate	SDS

Second	sec
Serine Protease Inhibitor	Serpin
Standard Error of the Mean	SEM
Surface Plasmon Resonance	SPR
Tissue Plasminogen Activator	tPA
Transforming Growth Factor-α	TGF-α
Tris Buffered Saline	TBS
Tumour Necrosis Factor-α	TNF-α
Urokinase Plasminogen Activator	uPA
Urokinase Plasminogen Activator Receptor	uPAR
Very Low density Lipoprotein Receptor	VLDLr
Volts	V

Acknowledgements

After three and a half years or so there are a lot of people to whom I owe a debt of gratitude, but thanks must go firstly to my supervisor Marie Ranson. Marie always had time to listen, help out, offer suggestions or read the many piles of paper I placed on her desk. Marie allowed me the freedom and the funding to follow the many tangents I came up with along the way, but never allowed me to stray too far from the big picture. Working in Marie's lab gave me many experiences and opportunities I may have otherwise not had. An appreciation of good food, wine, coffee, and also learning to order something other than chicken, seem just as important as all the finer aspects of research.

My co-supervisor Darren Saunders was an invaluable sounding board for most of the experiments and theories that arose during my research. Thanks must go to him for the sheer amount of time and effort he put in to assisting me in every aspect of this thesis. Darren also provided me with a link to the facilites at the Garvan Institute without which much of this work would have been simply impossible.

My co-supervisor Tamantha Stutchbury was a continual source of wisdom for all research, personal and confectionary related matters. An indispendisble part of any PhD.

Thankyou to all the members of the Ranson lab over the last three and a half years. They were always there to help, to have a laugh with or simply to put up with my reluctance to face the fact that it was my turn to do the washing up. Many thanks go to Gillian Hicks, Fares Al-Ejeh, Kara Perrow, Martina Sanderson-Smith, Fiona McKay, Sergei Lobov, Adam Lowe, Helen Leung, Jodi Lee, Blake Cochran and Laurel Morrisey.

Many thanks to those who looked after me whilst I was overseas. Particularly Niels Behrendt from the Finsen Laboratory in Copenhagen who went to great efforts to make me feel welcome in his lab and also to show me the sites of Denmark. Also to Chris Madsen, Nicolai Sidenius, Orla Cunningham and Macarena Lahores of IFOM in Milan who happily spent a lot of time helping me in their lab and showing me the restaurants and bars of Milan. Not that the latter took much convincing!

Thanks must also go to Rob Medcalf, Dudley Strickland, Dan Lawrence, Dieter Blaas, Phil Hogg, Teresa Compton and Peter Lenting, all of whom generously provided me with proteins and reagants without which I could not have completed this research.

Finally to my parents, Tom and Jenny, who supported, fed and encouraged me, in and out of home, without question and without reserve. To you I owe the biggest debt of gratitude of all. Thank you.

Abstract

Plasminogen is converted to its active form plasmin by two major serine proteases; the urokinase plasminogen activator (uPA) and tissue plasminogen activator (tPA). De-regulated plasmin formation is associated with tumour growth and progression. Whilst tPA is primarily involved in blot clot dissolution, uPA, along with its cell surface receptor uPAR, are commonly over-expressed at the leading edge of a tumour and by the tumour-associated stroma, contributing to plasmin formation, cell proliferation and migration. Soluble and receptor bound uPA is efficiently inhibited by two members of the serine protease inhibitor (serpin) superfamily; the plasminogen activator inhibitors type 1 (PAI-1) and 2 (PAI-2) (Serpin E1 and B2 respectively).

The purpose of this thesis was; **(1)** to examine the fate of cell surface bound PAI-2, a largely un-explored aspect of the plasminogen activation system, with particular focus on the possibility of the internalisation of uPA bound PAI-2; **(2)** to characterise the interaction between PAI-2, uPA:PAI-2 and any putative receptors involved in the internalisation of these proteins; and **(3)** to determine the functional consequences of the process of PAI-2 internalisation, in terms of regulation of uPA/uPAR levels and cell signaling responses.

Confocal microscopy and a novel flow cytometry based internalisation assay were used to both visualise and measure the interaction of PAI-2 with human carcinoma cancer cell lines. This data provided definitive proof that uPA bound PAI-2 was internalised into the endosomes and lysosomes of these cells, mediated through an interaction with endocytosis receptors of the low density lipoprotein receptor (LDLR) family. This finding may lead to the development of a more effective PAI-2 cancer therapeutic utilising the intracellular delivery of cytotoxins to cancer cells.

Surface plasmon resonance and further applications of the flow cytometry based internalisation assay were used to investigate the interactions of uPA:PAI-2 with two receptors of the LDLR family. This lead to the characterisation of the interaction between uPA:PAI-2 and the low density lipoprotein receptor-related protein (LRP) and the very low density lipoprotein receptor (VLDLr). The biochemical analysis of these interactions, in comparison to that of uPA:PAI-1, led to the discovery of a novel difference in the kinetics and affinities of the interactions between uPA:PAI-1, uPA:PAI-2 and these receptors. Differing positive electrostatic potentials and conservation of a putative LDLR binding motif within helix D of these two serpins, specifically surrounding a conserved arginine residue, were implicated in the higher affinity of uPA:PAI-1 for these receptors.

The consequences of this variation in receptor binding were revealed using MCF-7 breast cancer cells. As previously demonstrated, the binding of the high affinity helix D site in uPA:PAI-1 to VLDLr on MCF-7 cells resulted in the propagation of intracellular signaling events and cell proliferation. As uPA:PAI-2 does not contain this high affinity site, these cell signaling events were not induced upon uPA:PAI-2 binding to VLDLr, however the complex was still efficiently endocytosed.

The data presented in this thesis therefore proposes a novel mechanism behind the disparity in patient prognosis associated with tumour expression of PAI-1 and PAI-2. The negative prognostic impact of PAI-1 may be mediated through the mitogenic effects of its high affinity LDLR binding site, whereas the positive prognostic impact of PAI-2 stems from its ability to efficiently inhibit and clear cell surface uPA without inducing the mitogenic effects associated with PAI-1.

Table of Contents

Chapter 1

1. Review of the Literature

1.1 INTRODUCTION

Tumour cells have acquired mutations allowing them to bypass their regulatory systems and proliferate unabated (Bertram, 2000). Malignant cells can also gain the ability to detach from the cells surrounding them and the network of structural proteins that hold them in place, the extracellular matrix (ECM) and the basement membrane (BM). The dysregulated activation of proteolytic systems by these cells leads to the degradation of the ECM and BM and allows them to escape into the bloodstream or lymphatic system in the final stages of cancer progression (Blasi, 1999; Dano et al., 2005). It is this ability of cancerous cells to escape a primary tumour and initiate disease in healthy tissue, a process called metastasis, which is the cause of 90% of cancer deaths (Hanahan and Weinberg, 2000).

Current approaches to cancer therapy aim to localise drug delivery to the cancerous tissue, reducing side effects and unwanted toxicity (Allen, 2002; Leszczyniecka et al., 2001; Rihova, 1998). This can be achieved through the use of agents that specifically target cancer cells, conjugated to a cytotoxin (Allen, 2002; Rihova, 1998). One such system that was recently proposed as a rich source of targets for cancer therapy is the plasminogen activation system (Dano et al., 2005; Duffy and Duggan, 2004; Schmitt et al., 2000). This system plays a role in many physiological processes, including wound healing, tissue remodeling and thrombolysis, through a tightly regulated system of protease activation and inhibition (Andreasen et al., 1997; Behrendt, 2004; Blasi, 1999; Dano et al., 1999). However, dysregulation of the plasminogen activation system due to acquired mutations can contribute to many patho-physiological processes, including catalysing the degradation of the ECM associated with metastasis (Andreasen et al., 2000; Blasi, 1999; Dano et al., 2005; Mignatti and Rifkin, 1993). This strong association of plasminogen activation with metastasis makes

it a viable target for the development of drugs to target metastatic cancer (Dano et al., 2005; Duffy and Duggan, 2004; Schmitt et al., 2000).

This literature review will provide an outline of the plasminogen activation system and how this system contributes to the pathology of cancer. Detail will be provided on the individual components of the system and their interactions at the cell surface, particularly focusing on the plasminogen activator inhibitors (PAI-1 and PAI-2). The mechanisms of PAI endocytosis, the signaling events associated with this process and their relevance to cancer progression will be discussed in detail. The use of PAI-2 in cancer therapy will also be addressed, with a focus on understanding the biology of PAI-2 in order to increase its efficiency as a cancer targeting agent.

1.2 THE PLASMINOGEN ACTIVATION SYSTEM

1.2.1 Proteolytic Functions

Many tumours over-express the urokinase plasminogen activator receptor (uPAR) (Dano et al., 1999; Schmitt et al., 2000). This receptor has many different roles, one of which is binding its ligand, the urokinase plasminogen activator (uPA) (Plesner et al., 1997). The protease uPA is produced in an inactive form (pro-uPA) (Dano et al., 1985) by both tumour cells and the surrounding tumour-associated stroma (Andreasen et al., 1997; Dano et al., 1999). Activation of pro-uPA can be catalysed by various proteases that are found in the extracellular fluid (e.g. cathepsins) (Goretzki et al., 1992; Kobayashi et al., 1991) or bound to the cell membrane (e.g. matriptase) (Lee et al., 2000). Once activated by proteolytic cleavage, uPA can then activate plasminogen to its active form, plasmin. Plasmin is a broad spectrum protease that can cleave collagens, fibrin and various proteins involved in cell adhesion, the ECM and the BM as well as

activate zymogens such as pro-uPA and pro-matrix metalloproteases (MMP) (Dano et al., 1985). By degrading these structures and also by activating other proteases that catalyse further degradation, plasmin allows cancer cells to escape from a primary tumour during metastasis (Andreasen et al., 1997). Circulating plasmin is inhibited by α_2-antiplasmin (Mullertz et al., 1984), whereas cell-surface plasminogen activation by uPA is inhibited by PAI-1 and PAI-2 (Andreasen et al., 1994) (Summarised in Figure 1.1). The major components of the system; plasminogen, uPA, uPAR and the PAI's will be discussed in detail below. For details on other components shown (e.g. MMPs, cathepsins, matriptase) the reader is referred to the following papers (Chakraborti et al., 2003; Goretzki et al., 1992; Kobayashi et al., 1991; Lee et al., 2000).

1.2.2 Plasminogen/Plasmin

Plasmin, the active form of plasminogen, is a trypsin-like serine protease with broad substrate specificity (Ponting et al., 1992). Plasmin is capable of degrading components of the ECM, both directly and indirectly by the activation of pro-MMPs, a family of potent degradative enzymes (Dano et al., 1985). Plasmin is also capable of activating latent growth factors (e.g. transforming growth factor-α, TGF-α) (Rakic et al., 2003), providing tumours with stimuli for both mitogenic and motogenic responses.

Plasminogen is secreted as a single chain glycoprotein of 791 amino acids and is present in plasma at a concentration of ~2 μM in a form called glu-plasminogen, in which the N-terminal residue is glutamate (Dano et al., 1985). A single proteolytic cleavage by uPA, at Arg^{560}-Val^{561}, activates glu-plasminogen to two chain plasmin in which the two chains are connected via two disulphide bonds (Andreasen et al., 1997). The C-terminal (light) chain (25 kDa) of plasmin consists of the serine protease domain.

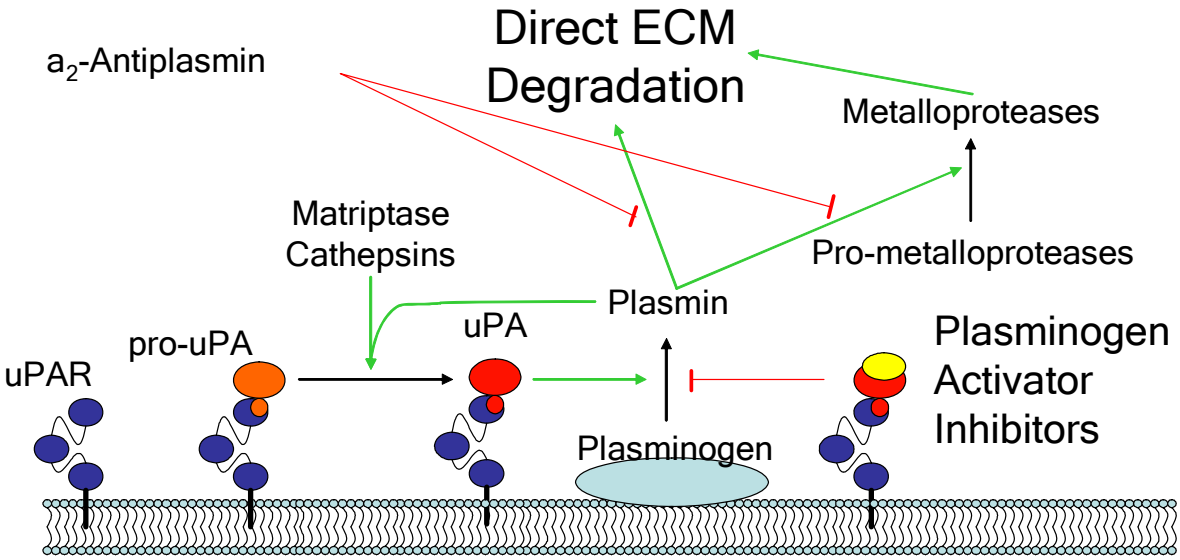

Figure 1.1: Schematic diagram of the pericellular proteolytic activity of the plasminogen activation system. uPAR (blue) is shown at the surface of a cancer cell. Pro-uPA (orange) binds to uPAR and is activated to uPA (red) by various proteases. uPA is then able to catalyse the conversion of receptor bound plasminogen to the active plasmin. Plasmin is then able to reciprocally activate pro-uPA, forming a positive feedback with the potential to generate large amounts of plasmin. Plasmin can then degrade the extracellular matrix (ECM) directly or indirectly by activating pro-matrix metalloproteases. α_2-antiplasmin is able to directly inhibit ECM degradation by inhibiting plasmin. The plasminogen activator inhibitors are able to inhibit plasmin formation by inhibiting uPA activity. Black arrows indicate a conversion from inactive to active state, green arrows indicate catalysis and red arrows indicate inhibition.

The N-terminal (heavy) chain (65 kDa) consists of the N-terminal peptide and five 'kringle' domains (Ponting et al., 1992), which are triple-disulphide-bonded polypeptides with unique secondary and tertiary structure. The first, fourth and fifth kringle domains in plasminogen contain lysine binding sites which mediate binding to various proteins that contain exposed lysine groups; including fibrin, a large group of heterogenous cellular receptors such as α-enolase (Andronicos et al., 2000; Felez, 1998) and the annexin II heterotetramer (Kwon et al., 2005). Once activated, plasmin is also able to generate additional binding sites via the cleavage of cell surface proteins, revealing C-terminal lysine residues to which its kringle domains are able to bind (Kwon et al., 2005; Syrovets and Simmet, 2004). Plasminogen can also bind to a bacterial cell surface receptor known as the plasminogen-binding group A streptococcal M protein via a high affinity interaction with kringle 2 (Wistedt et al., 1998). This binding is mediated by arginine and histidine residues in the amino terminal binding domain of plasminogen-binding group A streptococcal M protein that together resemble a pseudo lysine-like ligand (Sanderson-Smith et al., 2006). The lysine binding sites also help maintain the right-handed spiral conformation of glu-plasminogen, which is resistant to activation, by an interaction with internal lysine residues in the N-terminal peptide. The removal of the N-terminal peptide converts glu-plasminogen to a readily activated, open U-shaped form that is termed lys-plasminogen (Marshall et al., 1994).

The receptor binding of plasminogen results in a more open conformation which allows more efficient activation (Andronicos et al., 2000; Markus, 1996; Namiranian et al., 1995; Ponting et al., 1992). Plasmin is usually found complexed with its circulatory inhibitor, α_2-antiplasmin (Mullertz et al., 1984), however receptor-bound plasmin is protected from inhibition by α_2-antiplasmin, as receptor binding is competitive for α_2-antiplasmin inhibition. α_2-Antiplasmin interacts with plasmin through binding sites in

the first and potentially the fourth and fifth kringle domain, and also through inhibition of the protease domain of plasmin via its serpin mechanism (Felez, 1998; Ponting et al., 1992) (see section1.2.4.1).

For more detail on the structure, activity and cell surface binding of plasminogen, the reader is referred to the following review papers (Castellino and Ploplis, 2005; Kwon et al., 2005; Markus, 1996; Ranson and Andronicos, 2003).

1.2.3 Urokinase Plasminogen Activator (uPA)

The two major mammalian serine proteases that can catalyse the activation of plasminogen to plasmin are uPA and the tissue plasminogen activator (tPA). tPA is predominantly involved in fibrinolysis and thrombolysis, as it has a high affinity for fibrin (Castellino and Ploplis, 2005; Lijnen, 2001; Melchor and Strickland, 2005; Mosesson, 2005; Sheehan and Tsirka, 2005), and also in neurobiology where it plays a role in synaptic plasticity (Melchor and Strickland, 2005; Sheehan and Tsirka, 2005). uPA appears to have a very different biological role, being involved in tissue remodeling, wound healing and cell migration (Aguirre Ghiso et al., 1999; Andreasen et al., 2000; Blasi, 1999; Dano et al., 2005; Dano et al., 1999; Han et al., 2005; Kjoller, 2002; Rakic et al., 2003; Rosenberg, 2001). As the role of uPA in cancer biology is more pertinent to this thesis, the function of tPA will not be discussed further.

In vivo, uPA is synthesised as a partially active zymogen pro-uPA (Dano et al., 1985) by kidney tubule cells, phagocytic cells, pneumocytes, keratinocytes, fibroblasts and trophoblasts (Schmitt et al., 2000). *In vitro*, uPA is expressed by various malignant cell lines (Dano et al., 1985). The expression of pro-uPA is regulated by various growth factors (e.g. epidermal growth factor, EGF), oncogenes (e.g. *HER2/neu*) and tumour promoters (e.g. phorbol esters), although the effect of each of these seems to be

dependent on cell type (Aguirre Ghiso et al., 1999). uPA is present in the blood at a concentration of ~20 pM, however this is mostly in an inactive or PAI-1 complexed form (Andreasen et al., 1994). uPA is also present in the urine, at a concentration of ~800 ng/mg of urinary protein (du Toit et al., 1997).

Pro-uPA is a single chain glycosylated polypeptide consisting of 411 amino acids and with a molecular mass of 55 kDa (Dano et al., 1985). Pro-uPA is activated to uPA by cleavage at Lys^{158}, resulting in a two chain structure joined by a single disulphide bond (Figure 1.2). This cleavage is known to be catalysed *in vivo* by plasmin (Dano et al., 1985) and *in vitro* by matriptase (Lee et al., 2000), kallikrein, cathepsin-B and cathepsin-L (Kobayashi et al., 1991; Schmitt et al., 2000). It is unknown whether the latter enzymes activate pro-uPA *in vivo*.

The A chain of uPA contains a single kringle domain and an N-terminal growth factor domain with homology to the receptor binding regions in EGF and TGF-α (Andreasen et al., 1997). The A chain is involved in binding to uPAR via the amino terminal fragment (ATF) situated in the growth factor domain. The enzymatic activity of pro-uPA is increased 2-3 fold upon receptor binding (Higazi et al., 1995) even though the serine protease catalytic triad (His^{204}, Asp^{255} and Ser^{356}) is situated in the B chain. Although the catalytic site is situated on the B chain, there is evidence to suggest a possible plasminogen interacting site on the A chain of uPA (Gly^{149}-Lys^{158}) (Andronicos and Ranson, 2001; Ellis et al., 1999).

uPA can also be converted to a smaller form, *in vitro* and *in vivo*, by removal of the growth factor domain via cleavage at an alternate site (Lys^{135}-Lys^{136}). This form of uPA, termed low-molecular-weight uPA (LMW uPA), consists only of the protease domain and therefore retains its activity but not its ability to bind uPAR (Andreasen et al., 1997; Dano et al., 1985). The structure of uPA is depicted in Figure 1.2.

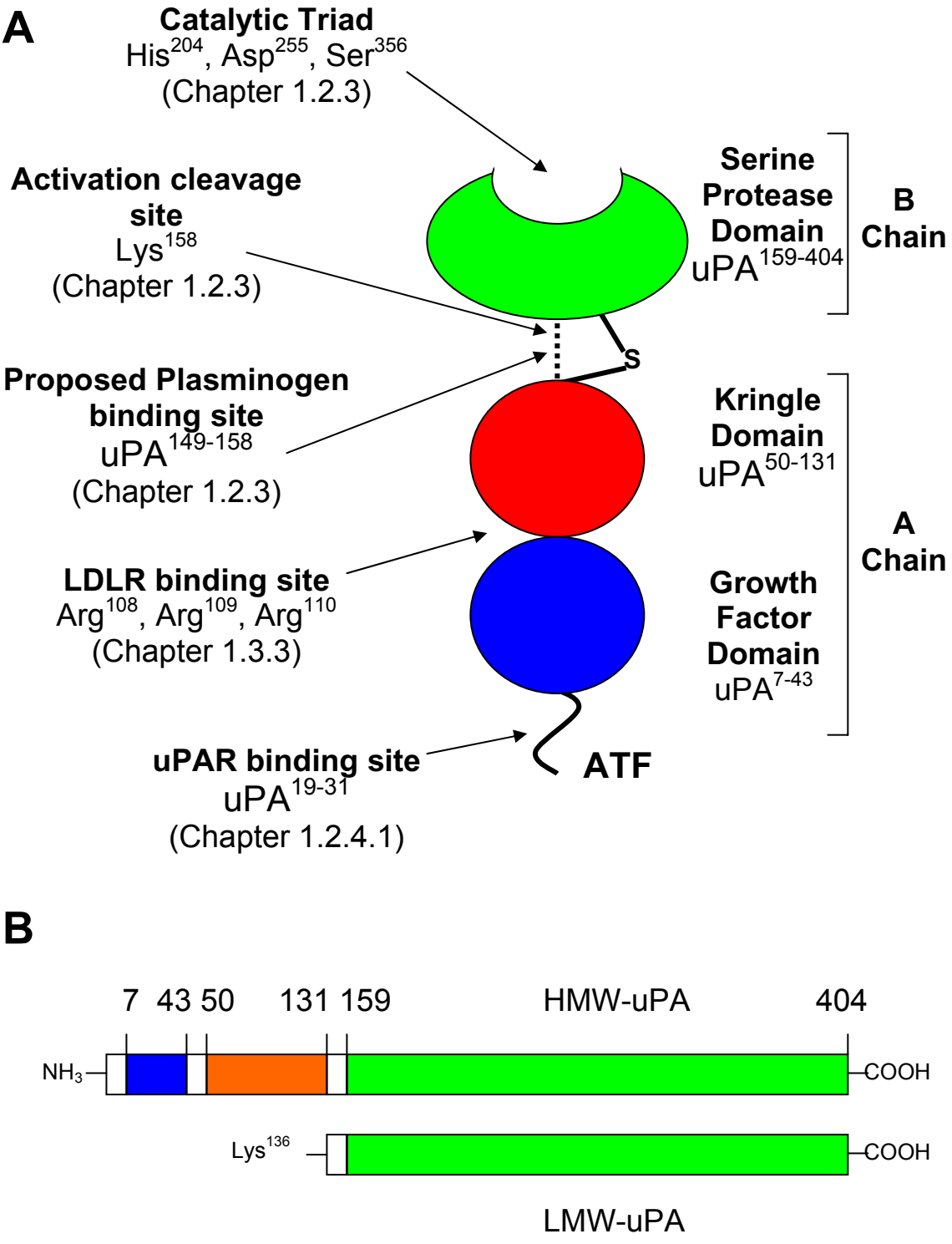

Figure 1.2: Schematic diagram of the structural and functional domains of uPA. (A) A simplified structure of uPA is shown. The B-chain protease domain is shown in green, the A-chain consisting of the kringle domain in red and the growth factor domain in blue is also shown. The amino-terminal fragment is labeled (ATF). The point of cleavage for activation (dotted line) and the disulphide bond joining the A- and B-chain are shown. The approximate positions of binding for uPA interacting proteins are indicated (black arrows). **(B)** a box version of uPA structure is shown in the same coloring. The components of both high and low molecular weight uPA are shown.

The tissue expression of uPA has been a controversial area of research, with many conflicting findings (Dano et al., 1999; Duffy, 1993; Schmitt et al., 2000). *In vitro*, many malignant tumour cell lines are capable of synthesising uPA (Dano et al., 1985) and uPA is known to localise at the invasive front of a tumour (Andreasen et al., 2000; Sidenius and Blasi, 2003; Zhou et al., 2000). However, uncertainty arose from the question of whether uPA was expressed by tumour cells, or by the stroma surrounding the tumour *in vivo*. As uPA is a secreted protein, it may be found bound to cells that are not actually responsible for expressing it. Nielsen et al. (2001) demonstrated that the mRNA of uPA is highly expressed in the myo-fibroblasts surrounding ductal breast cancers, while the protein itself was most always localised to the myo-fibroblasts and macrophages. The protein was also found in tumour associated epithelial cells (~50% of cases) and in a sub-population of cancer cells (~12% of cases). However, other studies using immuno-histochemistry and *in situ* hybridization have shown that uPA is expressed by both tumour associated fibroblasts and cancer cells (Andreasen et al., 1997; Dano et al., 1999; Robert et al., 1999; Umeda et al., 1997). The variation between the tissue of origin of tumours and the hormonal regulation of uPA expression, underly variation in cells expressing uPA and those it binds to after secretion. There is, however, no doubt that uPA over-expression is correlated to the metastasis of cancer cells (Aguirre Ghiso et al., 1999; Andreasen et al., 2000; Bouchet et al., 1999; Dano et al., 2005; Duffy, 2004; Duffy and Duggan, 2004; Foekens et al., 2000; Han et al., 2005; Mignatti and Rifkin, 1993; Schmitt et al., 2000; Sidenius and Blasi, 2003; Spyratos et al., 2002).

1.2.4 Urokinase Plasminogen Activator Receptor (uPAR)

uPAR is synthesised as a single chain, heterogenously glycosylated polypeptide consisting of 283 amino acids and with a molecular mass of 50-60 kDa. The uPAR molecule contains three globular domains which mediate the binding of multiple ligands (discussed below). uPAR is not a trans-membrane receptor, but is anchored to the cell membrane via a GPI moiety (Ploug et al., 1991). The GPI-anchor is added post-translationally, simultaneous with the removal of a C-terminal signal sequence, by cleavage at Gly^{283}.

uPAR is synthesised by neutrophils, B-lymphocytes, granulocytes, monocytes, migrating keratinocytes and by many metastatic cancer cell lines *in vitro* (Blasi, 1993). Elevated levels of a soluble form of uPAR (suPAR) have also been detected in the plasma and urine of patients with cancer or inflammatory conditions. suPAR is released from the cell membrane through cleavage of the GPI-anchor by the GPI specific phospholipase-D (Wilhelm et al., 1999). It is suggested that plasma levels of suPAR are indicative of total uPAR levels in the patient, which may be important in evaluation of conditions that involve an increase in activity of the plasminogen activation system (Gao et al., 2001; Ronne et al., 1995; Sier et al., 1999).

The proteolytic cleavage of domain 1 of uPAR was revealed by the presence of two forms of uPAR (a 35 kDa and 27 kDa form) after complete de-glycosylation of isolated membrane proteins from U937 cells. uPAR was cleaved in the linker region between domain 1 and 2 at Arg^{83}-Ala^{84} or Arg^{89}-Ser^{90} (Hoyer-Hansen et al., 1997). Enzymes with trypsin- or chymotrypsin-like specificity, including uPA, are able to cleave this domain from uPAR (Behrendt, 2004). While the physiological role of this cleavage is unknown, it may present another point of regulation of plasmin formation since the 27 kDa form of uPAR is unable to bind uPA (Hoyer-Hansen et al., 1992).

The three domains of uPAR are 90 residue repeats presenting upwards of 60% homology with each other. The domains of uPAR show a high homology to those of the Ly6 genes, a family of single domain glycoproteins, and also to snake venom neurotoxins (Plesner et al., 1997; Ploug and Ellis, 1994). The homology of uPAR to Ly6 allowed the initial characterisation of the structure and consequently, the function of the uPAR molecule. More recently the crystal structure of uPAR (Llinas et al., 2005) and the uPAR/ATF complex (Huai et al., 2006) were solved, allowing a more detailed characterisation of this and other interactions. The structure of uPAR is described in Figure 1.3.

1.2.4.1 The uPA/uPAR Interaction

The binding of pro-uPA to uPAR at the cell surface potentiates its activation via proximity to membrane bound activators such as matriptase (Andreasen et al., 2000; Romer et al., 2004). Furthermore, uPAR binding confines the uPA mediated activation of plasminogen to the cell surface, an important event in cell migration and tissue remodeling because it allows localised degradation of the ECM (Burgle et al., 1997; Plesner et al., 1997).

uPAR was initially identified as a cell surface receptor for uPA on monocytes (Stoppelli et al., 1985; Vassalli et al., 1985) and has long been known to bind uPA with high affinity, with reported K_D values ranging from 0.1 – 1 nM (Behrendt, 2004). The uPA molecule binds to domain 1 of uPAR via the ATF in the N-terminal growth factor domain of uPA (Gardsvoll et al., 1999) (Figure 1.2). uPA^{19-31} was shown to form the minimal epitope for receptor binding, forming a flexible ring like structure via a seven residue Ω loop from Asn^{22} to Ile^{28} (Burgle et al., 1997).

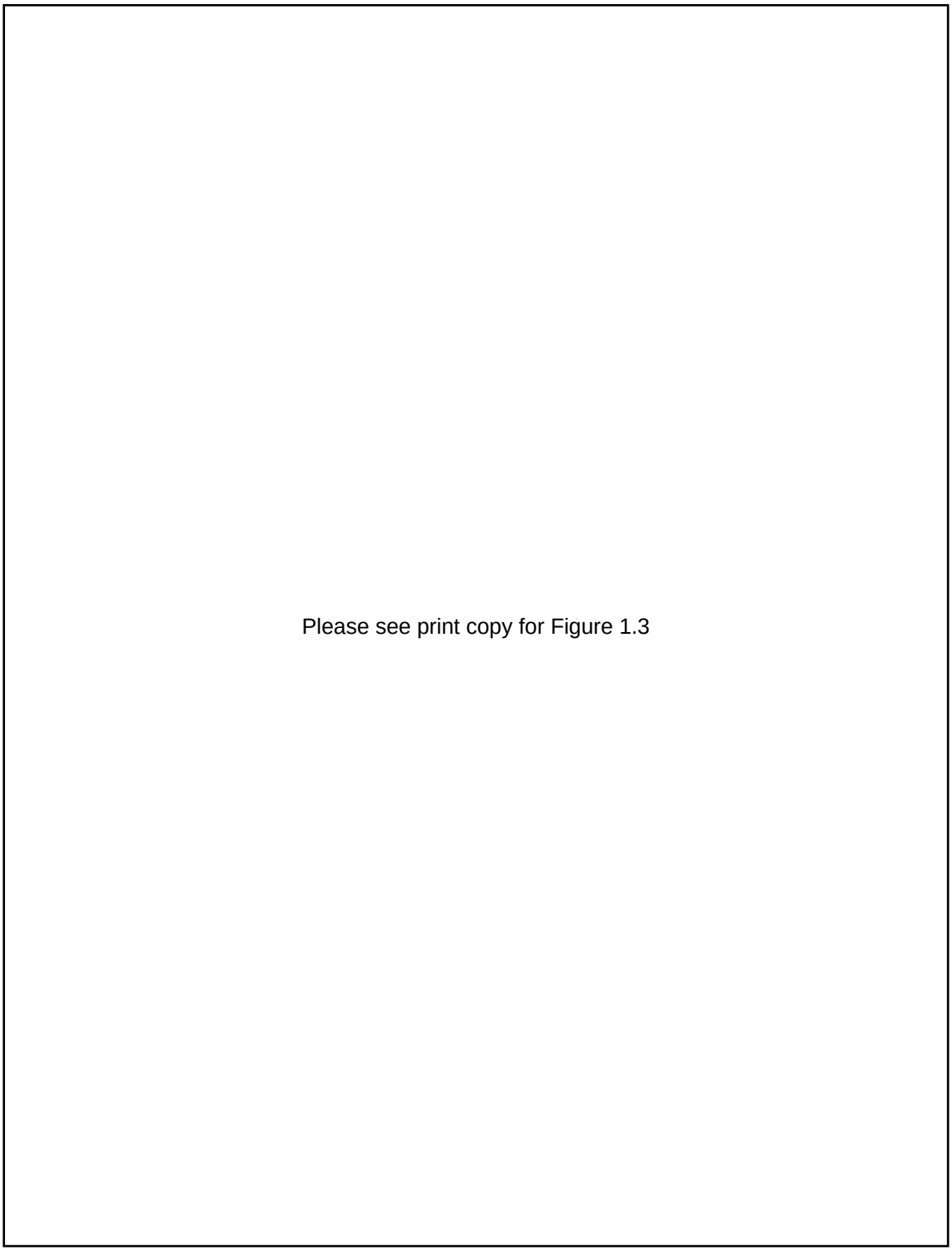

Figure 1.3: The structural and functional domains of cell surface uPAR. (A) The crystal structure of uPAR, attached to the cell membrane through a GPI anchor is shown. The amino terminal fragment of uPA (Red) is shown binding to the concave cavity of uPAR. The residues of uPA involved in this interaction are labeled and the corresponding residues of uPAR are colored yellow (section 1.2.4.1). Figure from (Llinas et al., 2005). **(B)** A simplified structure of uPAR showing the three domains and approximate positions of integrin and vitronectin binding sites is shown.

The uPA molecule is capable of binding uPAR in its activated (two chain) or single chain (pro-uPA) forms, and also whilst complexed with inhibitors (Blasi, 1993). The three domains of uPAR combine to form a concave cavity into which the ATF of uPA inserts (Huai et al., 2006) (Figure 1.3). This recent study also confirmed the presence of the binding determinants within uPA^{19-31}. Ser^{21}, Asn^{22}, Lys^{23} and Tyr^{24} all form contacts with domain 2 of uPAR and Ser^{26} interacts with domain 1. Tyr^{24} also forms 5 hydrogen bonds with residues in domains 1, 2 and 3 of uPAR. Phe^{25}, Ile^{28} and Trp^{30} all interact with the β-strands of domain 1 of uPAR in a hydrophobic manner, contributing greatly to the high affinity of the uPA/uPAR interaction. A further hydrogen bond and Van der Waals forces from domain 1 of uPAR contacting with the ATF contribute a third binding site at the edge of the cavity (Huai et al., 2006). Thus, whilst the high affinity binding of uPA is the result of contacts with all three domains of uPAR, the interaction is dependent upon the presence of domain 1, as its cleavage renders uPAR unable to bind uPA (Hoyer-Hansen et al., 1992).

1.2.4.2 Alternative Roles for uPAR

Apart from its role in proteolysis, a number of non-proteolytic functions have been ascribed to uPAR, including roles in cell-cell and cell-ECM adhesion, migration and proliferation (Kjoller, 2002; Ragno, 2006). An interaction between uPAR and the ECM protein vitronectin (Wei et al., 1994), mediated through sites in domain II of uPAR (Li et al., 2003) and clusters of hydrophobic residues in the somatomedin B domain of vitronectin (Kamikubo et al., 2004), has been described (Figure 1.3). The affinity of the interaction between uPAR and vitronectin is greatly increased upon the ligation of pro-uPA to uPAR (Plesner et al., 1997).

Even though uPAR does not contain a trans-membrane region, it still contributes

to signal transduction across the cell membrane by its association with integrins and protein kinases (Bohuslav et al., 1995; Simon et al., 1996; Xue et al., 1997). Integrin binding sites have been described in both domains II (Degryse et al., 2005) and III of uPAR (Chaurasia et al., 2006) (Figure 1.3). The binding of uPAR to multiple integrin partners has been described (Chapman and Wei, 2001; Kugler et al., 2003). Through association with integrins, the binding of uPAR to vitronectin induces activation of the signaling molecule Rac1, leading to a rearrangement of the actin cytoskeleton and an increase in cell motility (Kjoller, 2002; Kjoller and Hall, 2001). The uPA-induced association of uPAR with integrins generally results in increased cell motility and increased protease (i.e. uPA, MMP-9) secretion (Ahmed et al., 2003; Ghosh et al., 2000; Tarui et al., 2006). Cell migration is enhanced through modulation of integrin attachment to components of the extracellular matrix and also motogenic cytoskeletal rearrangements mediated through associated protein-kinases (Chapman and Wei, 2001; Kugler et al., 2003). Interestingly, a uPAR independent interaction between the kringle domain of uPA and the $\alpha_5\beta_3$ integrin has been recently described (Tarui et al., 2006). Whilst this interaction promoted plasminogen activation and cell migration, it was of a much lower affinity than the uPA/uPAR interaction, suggesting that it may only be of consequence in the absence of uPAR.

A complex interplay exists between uPAR, vitronectin, PAI-1 and various integrins in which binding interactions are modulated by the binding of ligands and various signaling events are mediated. These events are thoroughly detailed in the following review papers (Blasi and Carmeliet, 2002; Chapman and Wei, 2001; Kugler et al., 2003; Loskutoff et al., 1999; Ragno, 2006; Reuning et al., 2003; Rosenberg, 2001). Further detail on the signaling events mediated through the binding of uPA to uPAR is provided in section 1.3.4.

1.2.5 Plasminogen Activator Inhibitors (PAI's)

Circulating plasmin is inhibited by a direct interaction with α_2-antiplasmin (see section 1.2.2). However, as receptor bound plasmin is protected from inhibition by α_2-antiplasmin (Mullertz et al., 1984), a key regulatory mechanism of peri-cellular plasminogen activation is through direct inhibition of uPA (and also tPA) by PAIs, members of the super-family of serine protease inhibitors (serpins). Four types of PAIs (PAI-1, 2, 3 and 4) are known to inhibit uPA and tPA. The role of PAI-1 in the plasminogen activation system has been well characterised (Andreasen et al., 2000; Blasi, 1999; Dano et al., 2005; Stefansson et al., 2003) (discussed in section 1.2.6), whereas the role of PAI-2 is less well understood (discussed in section 1.2.7). The actions of both PAI-3 (Protease nexin-1) and PAI-4 (Protein C inhibitor) are not restricted to the plasminogen activation system and these inhibitors react much more slowly with uPA and tPA than PAI-1 and PAI-2 (Andreasen et al., 1997).

Regulation of cell surface uPA/uPAR proteolytic activity is an important step in the tight control of pericellular plasminogen activation. Additionally, uPA, uPAR and PAI-1 play significant non-proteolytic roles in the regulation of cell adhesion and migration (see sections 1.3.4, 1.2.4.2 and 1.2.6 respectively). Consequently, PAI-1 and PAI-2 may play an important role in regulating many normal physiological processes, including wound healing, cell migration, and thrombolysis, while they also take part in the patho-physiological processes of metastasis and inflammation (Agirbasli, 2005; Blasi, 1999; Kruithof et al., 1995).

1.2.5.1 Serpin Structure and the Serpin Inhibition Mechanism

The serpins are a large superfamily consisting of both inhibitory and non-inhibitory proteins. While serpins generally inhibit trypsin-like serine proteases,

examples of cysteine protease inhibiting serpins have been described (Silverman et al., 2001). Additionally, non-inhibitory functions such as hormone transport (SerpinA6), corticosteroid-binding (SerpinA7), blood pressure regulation (SerpinA8) and chromatin condensation (MENT) (Silverman et al., 2001) have also been described.

Serpins have a highly conserved secondary structure that consists of 3 β-sheets (A,B and C) and at least 7, but typically 9, α-helices (Silverman et al., 2001). They were recently categorised into sub-groups (clades) based on their sequence homology (Silverman et al., 2001). Approximately 500 serpins have so far been identified, ranging from eukaryotic to prokaryotic and viral species. Phylogenetic analyses has placed these serpins into 16 separate clades (Silverman et al., 2001).

Serpins react with their target proteases as 'suicide' substrates, forming a covalent serpin-protease complex, mediated by a conformational change in the serpin from a 'stressed' state to a more thermodynamically favourable 'relaxed' state. Crystal structures of serpin-protease complexes have demonstrated that the mechanism of this transformation is the result of cleavage of the reactive centre loop (RCL) by the protease, and the insertion of the RCL into β-Sheet A, a large central structure of the serpin consisting of six anti-parallel β-strands (Harrop et al., 1999; Huntington and Carrell, 2001) (Figure 1.4). The protease initially interacts with amino acids surrounding the RCL cleavage site (P1-P1`) in a non-covalent Michaelis-like manner. However, upon cleavage of the P1-P1` site, a covalent-ester bond is formed between the serine of the protease active site and the carbonyl of the P1 residue (Carrell and Huntington, 2003). Cleavage of the RCL also results in its insertion into β-Sheet A and the translocation of the covalently bound protease to the base of the serpin, where it is 'crushed' against the body of the serpin (Carrell and Huntington, 2003).

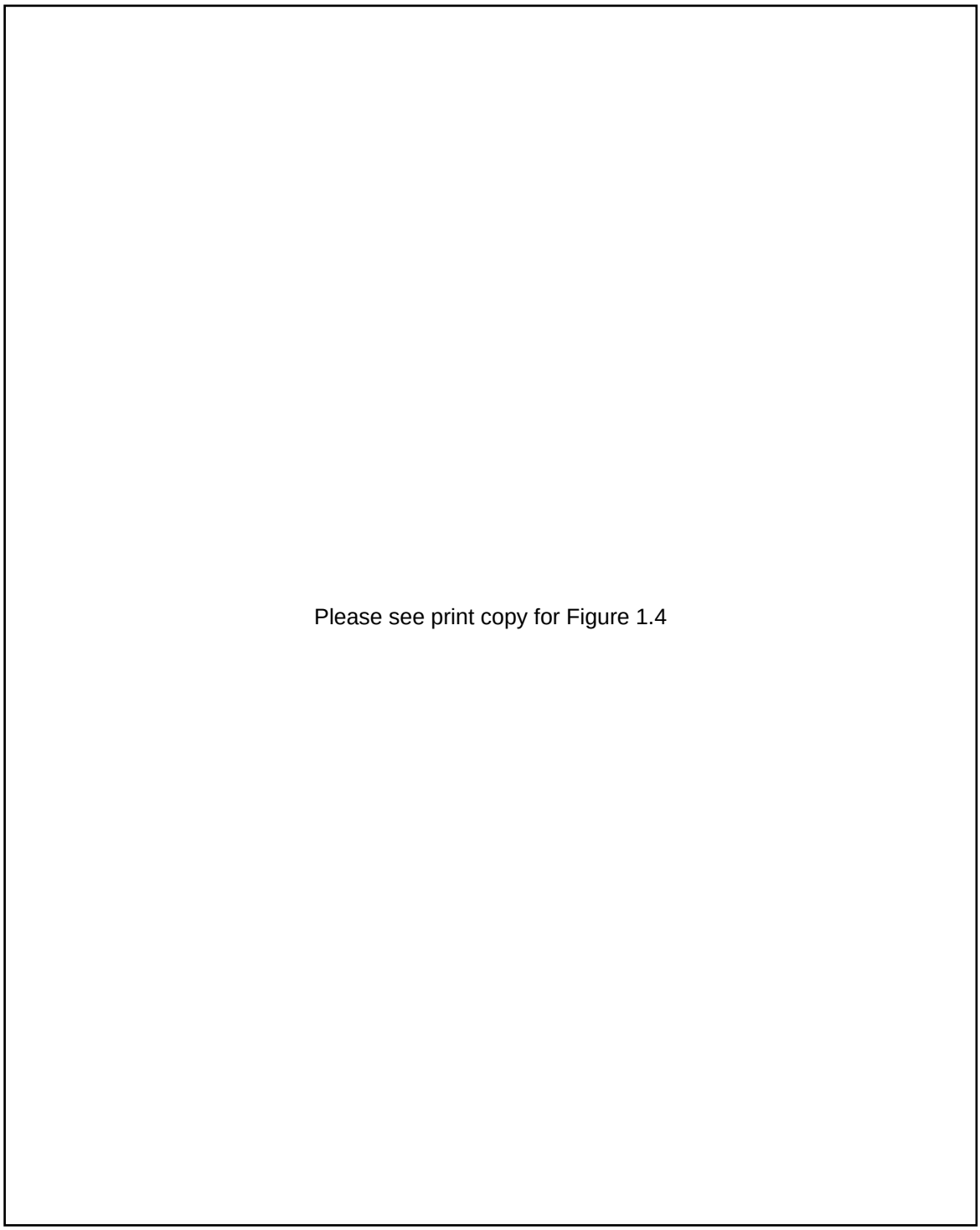

Figure 1.4: The generalised mechanism of serpin inhibition. (A) The inhibition of trypsin (cyan and magenta) by α1-antitrypsin (red and grey) is shown with trypsin in position to cleave the reactive centre loop (yellow) of α1-antitrypsin. The side chain of the P1 residue shown **(B)** The complex of α1-antitrypsin and trypsin following the insertion of the reactive centre loop into the β-sheets (red) of α1-antitrypsin and the translocation of trypsin to the base of α1-antitrypsin. The disorded structures in the complexed trypsin are shown as interrupted lines. Figure taken from Huntington et al. (2000).

The conformational change resulting from this inhibition is apparently irreversible and the consequential distortion of the active site of the protease locks the serpin and the protease together, thereby inhibiting its activity (Wright and Scarsdale, 1995) and also generating neo-epitopes that may act as cryptic binding sites for receptors specific for serpin:protease complexes (Horn et al., 1998; Perlmutter et al., 1990; Stefansson et al., 1998). The insertion of a synthetic peptide mimicking the RCL can also result in the transition of a serpin from the stressed to the relaxed conformation, without cleavage of the *in situ* RCL. This process has previously been used to investigate changes in serpin conformation associated with this transition, without the need of a protease (Bjork et al., 1993; Jankova et al., 2001; Saunders et al., 1998; Saunders et al., 2001).

Despite their ability to inhibit uPA, PAI-1 and PAI-2 separate into distinct sub-groups (SerpinE1 and SerpinB2, respectively) (Silverman et al., 2001), highlighting key differences in the amino acid sequence of these serpins which have important implications for their individual functions.

1.2.6 Plasminogen Activator Inhibitor type 1 (PAI-1)

PAI-1 (SerpinE1) is thought to participate in many diverse plasmin-dependent physiological processes including thrombolysis, ovulation, embryogenesis, intima proliferation and wound repair (Agirbasli, 2005). *In vivo*, PAI-1 is secreted as a 379 amino acid, 52kDa single chain glycoprotein (Pannekoek et al., 1986). It is present in normal human plasma at 6-80 ng/ml and is produced by both endothelial cells and activated platelets (Agirbasli, 2005). Its role in inhibiting thrombolysis through the rapid inhibition of tPA is especially well documented (Huber, 2001).

In keeping with its serpin structure, PAI-1 consists of three β-sheets and nine

α-helices (Figure 1.5). However, unlike many other serpins, the active form of PAI-1 is highly unstable and reverts to an inactive, latent form with a half life of 2 h at 37°C. In this latent form, the RCL of PAI-1 is inserted into β-sheet A, rendering the molecule inactive and uncleavable (Agirbasli, 2005). Various mutations of PAI-1, including the introduction of cysteine residues (Chorostowska-Wynimko et al., 2003) and a reduction in length of the RCL (Na and Im, 2005) have been shown to increase the half life of active PAI-1. A study involving a randomly mutated recombinant PAI-1 expression library produced a PAI-1 clone (K154T, Q319L, M354I, N150H) with a functional stability that was increased ~72 fold over wildtype PAI-1, whilst retaining inhibitory and vitronectin binding capabilities (Berkenpas et al., 1995). This version of PAI-1, termed 14-1b, is commonly used in biochemical studies to prevent complications arising from the formation of latent PAI-1. These and other findings related to the latency transition of PAI-1 are discussed in detail in the following review paper (Chorostowska-Wynimko et al., 2004).

PAI-1 is able to inhibit uPA both in solution and bound to uPAR (Cubellis et al., 1989), resulting in a reduction in the ECM degradation associated with uPA activity (Cajot et al., 1990; Shirasuna et al., 1993). However, it has been suggested that PAI-1 may play a larger role in the regulation of cell adhesion and migration, rather than in just cell surface proteolysis, through its interaction with the ECM protein vitronectin and modulation of integrin/uPAR/uPA interactions with the ECM (Stefansson and Lawrence, 2003). PAI-1 binds to the somatomedin B domain of vitronectin via a region extending through helix E, β-strand1A and helix F of PAI-1 (Figure 1.5) (Lawrence et al., 1994; Schroeck et al., 2002; Zhou et al., 2003) and therefore competes with uPAR and integrins for vitronectin binding. This complex interaction of PAI-1, uPA, uPAR, integrins and vitronectin serves to regulate cell migration and adhesion (Czekay and

Loskutoff, 2004; Deng et al., 1996; Stefansson and Lawrence, 1996). The binding of PAI-1 to vitronectin also stabilises the conformation of PAI-1, preventing it from reverting to the inactive, latent form that is un-able to bind uPA (Lindahl et al., 1989). The binding of uPA by PAI-1 reverses this competitive situation by dramatically reducing the affinity of PAI-1 for vitronectin (Lawrence et al., 1997). Furthermore, inhibition of uPA/tPA by PAI-1 induces high affinity interactions with the low density lipoprotein receptor (LDLR) family of endocytosis receptors (discussed in section 1.3). This further modulates the interaction of uPAR with integrins, and possibly other cell signaling mediators, further regulating cell adhesion, migration and proliferation (Czekay et al., 2003; Czekay and Loskutoff, 2004; Kjoller, 2002; Loskutoff et al., 1999; Webb et al., 2001).

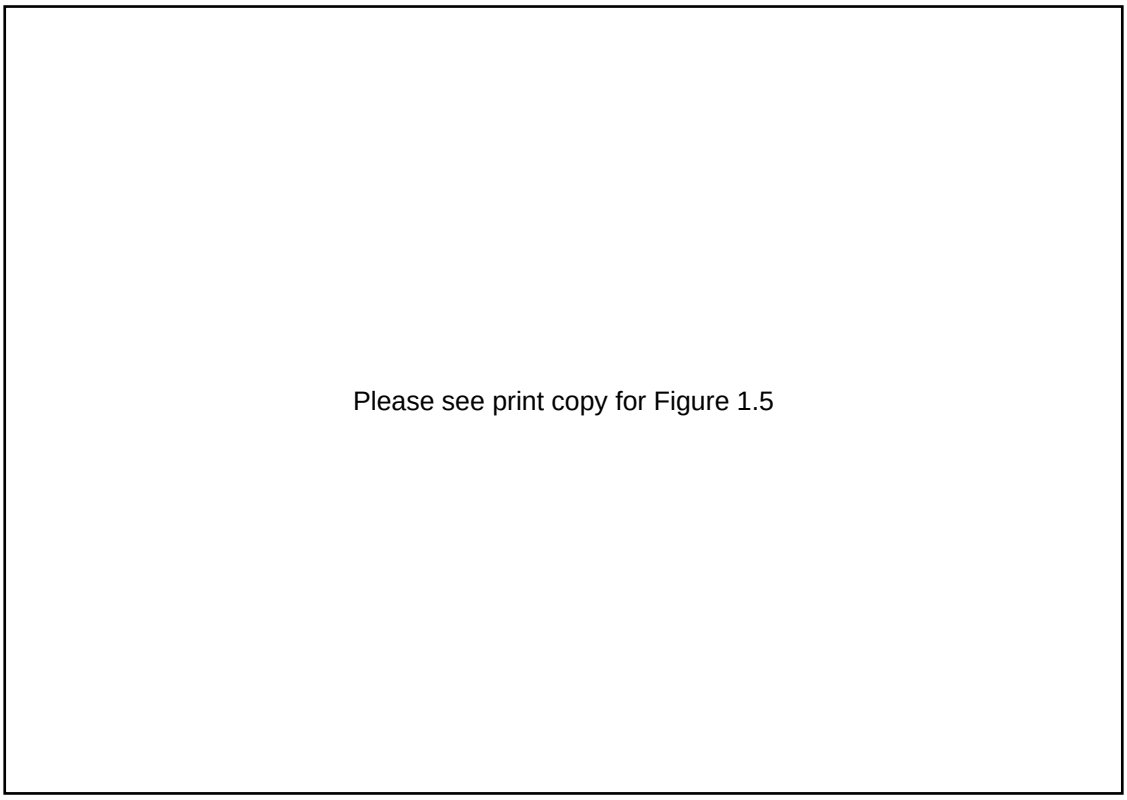

Figure 1.5: The structure of PAI-1. A ribbon diagram of the latent conformation of PAI-1 (PDB accession 1dvn) is shown. The α-helices are shown as cyan, the β-sheet A is shown as blue and inserted RCL is shown as red. β-sheets B and C are shown in purple. The vitronectin binding domain (helix E, β-strand1A and helix F) and the position of the cryptic LDLR binding site (Helix D) are indicated. Protein structure analysis and figure preparation was performed using the PyMol software package (DeLano Scientific).

1.2.7 Plasminogen Activator Inhibitor type 2 (PAI-2)

PAI-2 (SerpinB2) was first isolated from the human placenta (Kawano et al., 1968) and found to have a similar structure to the chicken protein ovalbumin (Ye et al., 1989), indeed PAI-2 and ovalbumin are both categorised into serpin clade B (Silverman et al., 2001). A unique feature of PAI-2 is that it is present in both the cytosol (47 kDa) and in an extracellular, glycosylated form (60 kDa) (Belin et al., 1989; Genton et al., 1987; Kruithof et al., 1995; Wohlwend et al., 1987). A weak, uncleaved signal peptide is responsible for this uneven distribution (Belin et al., 1989), with only 20-30% of PAI-2 glycosylated in the endoplasmic reticulum and secreted (Kruithof et al., 1995). Mutation of this signal peptide to increase its hydrophobicity increased the percentage of secreted PAI-2 (von Heijne et al., 1991). It has also been proposed that the polymerisation of PAI-2 may contribute to this inefficient secretion (Mikus and Ny, 1996). Although as this polymerisation has been shown to be redox sensitive (Lobov et al., 2004; Wilczynska et al., 2003), the reducing conditions present in the intracellular environment make this hypothesis unlikely.

A large increase in blood and placental concentration of PAI-2 is found during late pregnancy (Ye et al., 1989), largely due to PAI-2 secretion by the trophoblast cells of the placenta. This suggests that PAI-2 plays a role in the regulation of the maternal or fetal fibrinolytic system (Kruithof et al., 1987), although the amount of PAI-2 expressed by these cells was shown to be in excess of the amount required to completely inhibit uPA (Zini et al., 1992). The exact role of this increase in PAI-2 expression has not been elucidated, however decreased plasma levels of PAI-2 correlate with intrauterine growth retardation, indicating that this role is vital to correct fetal development (Astedt et al., 1998). Importantly, these data demonstrate that high levels of PAI-2 in the bloodstream do not exert a toxic effect on the body, a promising aspect for anti-cancer therapy using

PAI-2 as a targeting agent (see section 1.4).

PAI-2 is also expressed by activated human monoctyes and macrophages, differentiated keratinocytes, placental trophoblasts and certain cancerous cell lines (Belin et al., 1989; Kruithof et al., 1995; Umeda et al., 1997). Whilst PAI-2 is not detectable in plasma, it is present in human gingival crevicular fluid, saliva and also in seminal plasma (Kruithof et al., 1995). The target protease of PAI-2 in human gingival crevicular fluid and saliva is thought to be tPA. However, the target protease in seminal plasma remains unknown (Kruithof et al., 1995). PAI-2 expression can be significantly increased by induction with the tumour promoter phorbol-12-myristate-13-acetate, tumour necrosis factor-α (TNF-α) and bacterial lipopolysaccharide (LPS) (Tierney and Medcalf, 2001).

The crystal structure of PAI-2 has been solved in both the stressed (Harrop et al., 1999) and relaxed (Jankova et al., 2001) conformation (Figure 1.5). The movement of specific residues during this transition has also been mapped (Saunders et al., 2001). Like most serpins, PAI-2 consists of three β-sheets and nine α-helices. However a unique feature of PAI-2 is an extended 33 amino acid loop between the C and D helices, termed the CD loop. The mobile nature of the CD loop meant that crystalisation of PAI-2 (Figure 1.5A and B) required its deletion, however a predicted conformation for the CD loop has been published (Lobov et al., 2004) and is shown in Figure 1.5C. The CD loop is thought to be involved in many non-inhibitory interactions with proteins other than uPA. These interactions are detailed in the following sections.

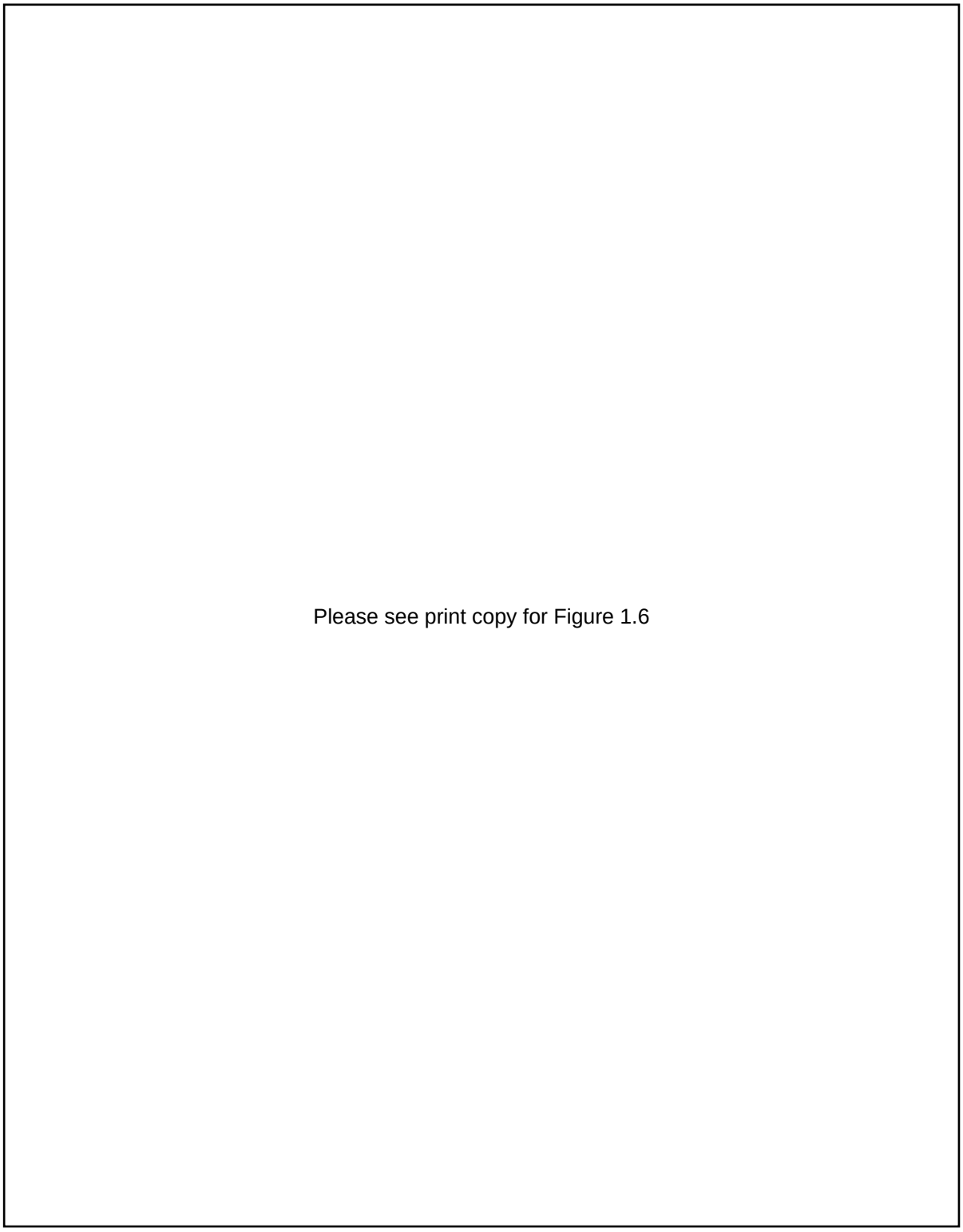

Figure 1.6: The structure of PAI-2. Ribbon diagrams of the CD loop deletion mutant of PAI-2 in the **(A)** stressed (PDB accession 1by7, Harrop et al., 1999) and **(B)** relaxed (peptide inserted) (PDB accession 1jrr, Jankova et al., 2001) state. The α-helices are shown as cyan, β-sheet A is shown as blue, β-sheets B and C are shown as purple. α-helices A, D, E, F, G, and I are labeled in A, α-helices B, C and H are behind the molecule in this view. The disordered reactive centre loop is not shown in A, however the inserted reactive centre loop is shown as red in B. **(C)** a ribbon diagram of PAI-2 showing the proposed positions of the mobile CD-loop (dark blue) and RCL (orange), the β-sheet A is shown as red and cysteine residues are shown as green balls (Lobov et al., 2004). Protein structure analysis and figure preparation was performed using the PyMol software package (DeLano Scientific).

1.2.7.1 Extracellular PAI-2

Whilst *in vitro* studies have demonstrated that both 47 and 60 kDa PAI-2 inhibit uPA with identical kinetics (Mikus et al., 1993) and that PAI-2 can inhibit cell surface uPA (Al-Ejeh et al., 2004; Ellis et al., 1990), whether PAI-2 inhibits cell surface uPA *in vivo* has been a point of contention. Several immuno-histochemical studies have detected the presence of relaxed PAI-2 *in vitro* (Williams et al., 1999) and *in vivo* (Lindberg et al., 2001; Risse et al., 2000; Tsatas et al., 1997; Williams et al., 1999). Whilst this indicates that PAI-2 has interacted with a protease, no definitive data for the topological localisation of the PAI-2 was presented and therefore the interacting protease may not have been uPA. However, transfection of melanoma cells used for tumour xenografts with PAI-2 cDNA resulted in the complete inhibition of cell surface uPA activity, demonstrating that, at least in this system, extracellular PAI-2 is able to inhibit cell surface uPA (Laug et al., 1993). Further evidence for the *in vivo* inhibition of uPA by PAI-2 is presented in section 1.2.8.

Expression of PAI-2 by peripheral blood monocytes *in vitro* has been shown to increase in the presence of bacterial LPS (Schwartz and Bradshaw, 1992) and various inflammatory mediators, including TNF-α (Kruithof et al., 1995; Medcalf et al., 1988) and interleukin-1/2 (Zoellner et al., 1993). Whilst this may also relate to the potential role of PAI-2 in apoptosis, a suggested function for PAI-2 during the inflammatory response is to prevent proteolytic degradation of new ECM laid down in the process of wound healing (Liew et al., 2000). Extracellular PAI-2 also exerts an anti-proliferative effect on THP-1 monocytic cells, whilst decreasing their cell-cell adhesion and preventing phorbol ester induced differentiation (Yu et al., 2002). Using PAI-2 with a mutation in the P1-P1` residues, rendering the serpin uncleavable and therefore inactive, these effects were demonstrated to be specific to the inhibitory activity of PAI-2,

suggesting that PAI-2 inhibition of uPA at the cell surface modulates signaling events involved in the proliferation and differentiation of monocytes. This effect may also be facilitated through the inhibition of uPA-mediated plasmin generation, as the formation of plasmin activated receptors (i.e. annexin II heterotetramer) has been shown to induce signaling events that increase the proliferation of monocytes (Syrovets and Simmet, 2004)

The anti-proliferative effect of PAI-2 is not restricted to monocytic cells and has been shown in multiple cell types (Hibino et al., 1999). This effect is especially prevalent in keratinocytes, the cells of the epidermis that produce the tough outer layer, keratin. Keratinocytes have been shown to synthesize the components of the plasminogen activation system, however PAI-2 concentrations are found to be 50 times higher than that of the other components (Jensen et al., 1995). In keratinocytes, PAI-2 is found cross-linked to the cell membrane during terminal differentiation, via the enzyme transglutaminase and is incorporated into the cornified envelope (Kruithof et al., 1995). Whilst the effects of PAI-2 upon keratinocyte proliferation and differentiation may be mediated via intracellular interactions (see section 1.2.7.3), additional evidence has shown that the uPA induced proliferation of keratinocytes was inhibited by the addition of exogenous PAI-2 (Hibino et al., 1999). Whilst the role of PAI-2 in this system is still not well defined, these studies suggest that PAI-2 may indeed have several functions and interact with different protein partners depending upon its topological localisation.

1.2.7.2 PAI-2 and Annexins

PAI-2 has also been shown to interact with various members of the annexin family (Annexins I, II, IV, and V) and in some cases this interaction is via the CD-loop (Jensen et al., 1996). Whilst the authors suggest that this interaction may be of an intracellular nature, annexin II is known to be expressed at the cell surface of many different cells lines as a heterotetramer with its ligand p11 (Kwon et al., 2005), a translocation thought to be induced by the tyrosine phosphorylation of annexin II (Deora et al., 2004). Additionally, a 26 kDa cell surface receptor for the annexin II heterotetramer was recently identified (Lu et al., 2006). This raises the possibility that extracelluar PAI-2 may bind to annexin II on the surface of various cell lines, although this hypothesis has not been tested.

1.2.7.3 Intracellular PAI-2

As discussed above, whilst extracellular PAI-2 is likely involved in the regulation of uPA activity at the cell surface, at least *in vitro* (Kruithof et al., 1995), the intracellular form of PAI-2 is known to interact with various intracellular proteins; including retinoblastoma protein (Rb) (Darnell et al., 2003), interferon regulatory factor–3 (Zhang et al., 2003), proteosome subunit beta type 1 (Fan et al., 2004a), pre-mRNA processing factor 8 (Fan et al., 2004b) and fusion kinase ZNF198/FGFR1 (Kasyapa et al., 2006). However, the functional outcomes of these interactions are somewhat conflicting.

A role for intracellular PAI-2 in the regulation of apoptosis was first proposed when a cleaved, yet still active, isoform of PAI-2 was detected in apoptotic human NB4 cells and in the homogenates of apoptotic leukemic cells (Jensen et al., 1994). This suggested the possible presence of an unidentified protease acting on PAI-2 during

apoptosis, as cleavage by uPA would render PAI-2 inactive (Kruithof et al., 1995).

The inhibition of TNF-α induced apoptosis by intracellular PAI-2 was first proposed by Kumar and Baglioni (1991). Human HT-1080 fibrosarcoma cells transfected with PAI-2 were shown to have a higher resistance to TNF-α than non-transfected cells (Kumar and Baglioni, 1991). This was later reproduced in HeLa cells, in which PAI-2 conferred a similar protection against TNF-α (Dickinson et al., 1995) in a CD-loop dependent manner (Dickinson et al., 1998). However, varying expression levels of transfected PAI-2 mutants makes interpretation of this data somewhat problematic.

Interactions between the CD-loop of PAI-2 and interferon regulatory factor–3 (Zhang et al., 2003) and proteosome subunit beta type 1 (Fan et al., 2004a) were also identified. It was hypothesised by the authors that these interactions may play a role in the regulation of apoptosis by PAI-2, however no functional data was shown to support this hypothesis. An interaction was also proposed with pre-mRNA processing factor 8 (Fan et al., 2004b), however it was concluded that this interaction was not involved with the regulation of apoptosis.

Recently, an interaction between the CD-loop of PAI-2 and Rb was discovered (Darnell et al., 2003). Rb is a known tumour suppressor involved in the regulation of the cell cycle, apoptosis and differentiation (Harbour and Dean, 2000). PAI-2 inhibited the papilloma virus mediated degradation of Rb and as such it may serve to maintain Rb levels and therefore regulate its ability to act as a tumour suppressor. However, no definitive link between this interaction and a role in regulation of apoptosis has been shown. Furthermore, the relevance of this interaction in a viral free environment has not been addressed. Additional evidence of a role for PAI-2 in resistance to apoptosis has been demonstrated through a direct interaction with the fusion kinase ZNF198/FGFR1

(Kasyapa et al., 2006). Transfection of HEK-293 cells with ZNF198/FGFR1 induced PAI-2 expression and also conferred resistance to TNFα-induced apoptosis.

Despite the studies summarised above, the reproducibility of some of these experiments has been questioned. A recent study (Fish and Kruithof, 2006) used HeLa, HT-1080 and Isreco-1 cells to examine the effect observed by Kumar and Baglioni (1991) and Dickinson et al. (1995). They found that while TNF-α stimulation increased PAI-2 expression in HT-1080 and Isreco-1 cells, over-expression of PAI-2 in all cells lines conferred no protection against TNF-α induced apoptosis (Fish and Kruithof, 2006).

Due to these conflicting results, the exact mechanism of PAI-2's potential protective role in apoptosis remains unclear. It is also important to note that these observations are restricted to intracellular PAI-2 and no role in apoptosis regulation has been proposed for extracellular PAI-2. In support of this, the addition of exogenous PAI-2 to HeLa cells did not confer resistance to TNF-α induced apoptosis (Saunders and Ranson, *unpublished data*).

1.2.8 PAI-2 and Cancer

Elevated expression of both uPA and PAI-1 by tumours is a potent prognostic marker of poor survival for patients with solid tumours, particularly when taken in combination (Duffy, 2004; Harbeck et al., 2002; Schmitt et al., 2000; Weigelt et al., 2005). While PAI-1 has been shown to inhibit receptor bound uPA *in vitro*, the role of PAI-1 in metastasis may not be related to its ability to inhibit uPA mediated proteolysis. Rather its effect may be mediated through the induction of cell detachment by PAI-1, facilitated by the interaction between PAI-1 and vitronectin (Stefansson and Lawrence, 2003) and the internalisation of uPAR associated integrins (Czekay et al., 2003;

Stefansson and Lawrence, 2003), by mitogenic signaling events initiated following PAI-1 binding to cell surface uPA (discussed in section 1.3.4) or by the inhibition of anoikis induced apoptosis (Kwaan et al., 2000). However, it appears that PAI-2 tumour expression is prognostic marker for positive patient outcome in the presence of high uPA expression, especially in breast cancer (Duffy, 2004; Foekens et al., 1995; Foekens et al., 2000). The mechanism underlying this positive outcome remains unknown, although it is interesting to note that in the absence of uPA expression, PAI-2 expression loses its prognostic significance (Duffy and Duggan, 2004). This suggests that the inhibition of uPA, and not an intracellular target, is responsible for this positive relationship.

In vivo experiments have demonstrated a reduction in tumour metastasis associated with PAI-2 expression. PAI-2 has been shown in rodent models to modulate xenograft growth, either by intravenous injection of PAI-2, or by transfection of the cells used for the xenograft with a PAI-2 expression vector. In all cases a tumour was formed that was surrounded by a dense collagenous capsule and the incidence of metastases was reduced or completely absent in the presence of PAI-2 (Laug et al., 1993; Mueller et al., 1995; Praus et al., 1999). Additionally, the down-regulation of uPA, uPAR, tPA, PAI-1 and the up-regulation of PAI-2 expression associated with adenovirus EIA infection of tumour cells supports a tumour suppressor function for PAI-2 (Fernandez-Soria et al., 2006). As viral infection with E1A is associated with decreased tumour growth and decreased metastatic potential, it is possible that PAI-2 may facilitate this tumour suppression. However, there was no direct link provided between the up-regulation of PAI-2 and the observed tumour suppression or data shown for the topological localisation of this PAI-2. Although, the up-regulation and enhanced secretion of PAI-2 induced by phorbol ester (12-O-tetra-decanoylphorbol-13-acetate)

treatment of TSU-Pr1 prostate cancer cells was shown to decrease the malignancy of these cells (Shimizu et al., 2003). While this action was shown to be mediated by extracellular PAI-2, the inhibition of uPA expression or activity by other means (i.e. chemical inhibitors, RNA interference) was not undertaken to confirm uPA inhibition as the means of tumour suppression.

Some studies indicate that PAI-2 expression may be correlated with a negative outcome in some cancer types (Nordengren et al., 2002; Osmak et al., 2001). These studies are restricted to cancers of ovarian or endometrial origin and involve small population numbers. Studies with large cohorts (~100-2500 patients) consistently demonstrate a positive outcome associated with PAI-2 expression, particularly for breast cancer patients (Bouchet et al., 1999; Duffy, 2004; Duffy and Duggan, 2004; Duggan et al., 1997; Foekens et al., 1995; Foekens et al., 2000; Spyratos et al., 2002; Umeda et al., 1997) or a negative outcome associated with decreased PAI-2 expression (Ishikawa et al., 1996; Yoshino et al., 1998). It has been suggested that the induction of PAI-2 secretion by colony stimulating factor-1 increased the invasive phenotype of ovarian cancer (Chambers et al., 1997). However, in this study the effect of colony stimulating factor-1 on PAI-2 secretion was only shown *in vitro*, and an inverse relationship between PAI-2 and colony stimulating factor-1 expression was observed *in vivo*.

Studies into the prognostic value of PAI-2 are also complicated by the differential localisation of PAI-2 expression. As studies have predicted both pro- and anti-apoptotic roles for intracellular PAI-2 (section 1.2.7.3), and tumour promoting and suppressing roles for extracellular PAI-2, there are clearly other factors involved in the effect of PAI-2 expression upon cancer cells. These factors may include differing receptor expression or even the topological localisation of PAI-2 expression.

It is becoming increasingly apparent that the expression of components of the plasminogen activation system by the stroma supporting tumours plays a significant role in cancer progression. Both tumour size and the number of metastates were greatly reduced when human tumour xenografts were grown in $uPA^{-/-}$ mice, as compared to wildtype mice, demonstrating the importance of uPA expression by tumour associated stroma for tumour growth and metastasis (Frandsen et al., 2001). The expression of PAI-1 by tumour associated stroma has been shown to increase invasiveness and angiogenesis of tumour xenografts while tumour expression of PAI-1 imparted no such effects (Bajou et al., 2004). Indeed one study examining patients with esophageal squamous cell carcinoma indicated that uPA expression by both cancer cells and fibroblasts, and PAI-2 expression by cancer cells, decreased survival. However, when PAI-2 expression was detected in the fibroblasts, increased survival was observed (Shiomi et al., 2000). This effect was most pronounced when low levels of uPA expression were observed in the cancer cells. Another study examining lung cancer progression in humans demonstrated that uPA and PAI-1 expression was detected in the tumour and fibroblasts, however its expression in the fibroblasts was more frequently associated with high-grade tumours than low or intermediate tumours (Robert et al., 1999). The expression of PAI-2 was restricted to fibroblasts and associated with the absence of metastasis.

To date, no studies into the prognostic value of PAI-2 have differentiated between intracellular or extracellular expression of PAI-2 in relation to positive prognosis, however this would be difficult to assess using currently available technology. As discussed above, possible tumour suppressor roles have been suggested for intracellular PAI-2 (Darnell et al., 2003). However, the only direct *in vivo* data that has not solely relied on the correlation of PAI-2 expression levels with the effect of a

known tumour suppressor/promoter and has also provided a mechanism for the effect of PAI-2, has implicated the inhibition of cell surface uPA in this tumour suppression (Laug et al., 1993; Mueller et al., 1995; Praus et al., 1999).

1.3 INTERNALISATION OF PLASMINOGEN ACTIVATION SYSTEM COMPONENTS AND FUNCTIONAL CONSEQUENCES

The serpin inhibition of a protease is known to produce a covalent complex that is recognised by members of the LDLR endocytosis receptor family, often with a greatly increased affinity than that of the individual serpin and protease (Andreasen et al., 1994; Kasza et al., 1997; Strickland and Ranganathan, 2003). The receptor mediated endocytosis of PAI-1 has been thoroughly characterised (discussed in detail below, section 1.3.3), and the receptor mediated endocytosis of other uPA inhibitors, protease nexin-1 (PN-1) (Kasza et al., 1997; Knauer et al., 1997; Knauer et al., 1996) and protease-C inhibitor (Andreasen et al., 1997) have been described. In contrast, the fate of cell surface bound of PAI-2 is not clear as there have been few studies directed at this aspect of PAI-2 and of these there are contradictory findings. Given that the inhibition of uPA by PAI-2 has been associated with tumour suppression (section 1.2.8) but that the expression of uPA/PAI-1 is strongly associated with tumour progression (section 1.2.8 and Chapter 4), there may be key differences in the cellular interactions of the uPA:PAI-1 and uPA:PAI-2 complexes. Investigation of the interactions between receptors of the LDLR family and uPA:PAI-1 compared to uPA:PAI-2 may help describe the current disparity between the consequences of uPA inhibition by PAI-1 and PAI-2 for tumour progression.

1.3.1 The LDLR Family of Endocytosis Receptors

The LDLR family consists of several receptors that are defined by common repeated complement-like, EGF and β-propeller regions (Nykjaer and Willnow, 2002; Strickland et al., 2002). These receptors bind a multitude of ligands and they are responsible not only for cargo transport but also mediate cell signaling responses to a variety of stimuli (Strickland and Ranganathan, 2003). The three receptors from this family shown to mediate endocytosis of uPA:serpin complexes are the low density lipoprotein receptor-related protein (LRP), a 600 kDa receptor comprising of an 85 kDa transmembrane domain and a 515 kDa extracellular domain, the very low density lipoprotein receptor (VLDLr) and LRP-2 (also known as Megalin and gp330) (Strickland et al., 2002). Both VLDLr and megalin are single chain receptors of 120 and 600 kDa in size, respectively (Figure 1.7) (Strickland et al., 2002).

An intracellular chaperone of LRP and other receptors of the LDLR family, called the receptor associated protein (RAP) is often used as an inhibitor of receptor binding in ligand binding or internalisation assays (Herz and Strickland, 2001; Nykjaer and Willnow, 2002; Strickland et al., 2002; Strickland and Ranganathan, 2003). Through an interaction with three clusters of ligand binding repeat regions in LRP (Clusters 2, 3 and 4) (Figure 1.6) (Strickland et al., 2002), RAP is thought to induce an allosteric change in the structure of LRP that prevents further ligand binding (Horn, 1997). Whilst the physiological function of this allosteric inhibition is likely to involve the prevention of ligand binding during trafficking to the cell surface, the inhibitory function of RAP is commonly exploited in biochemical assays.

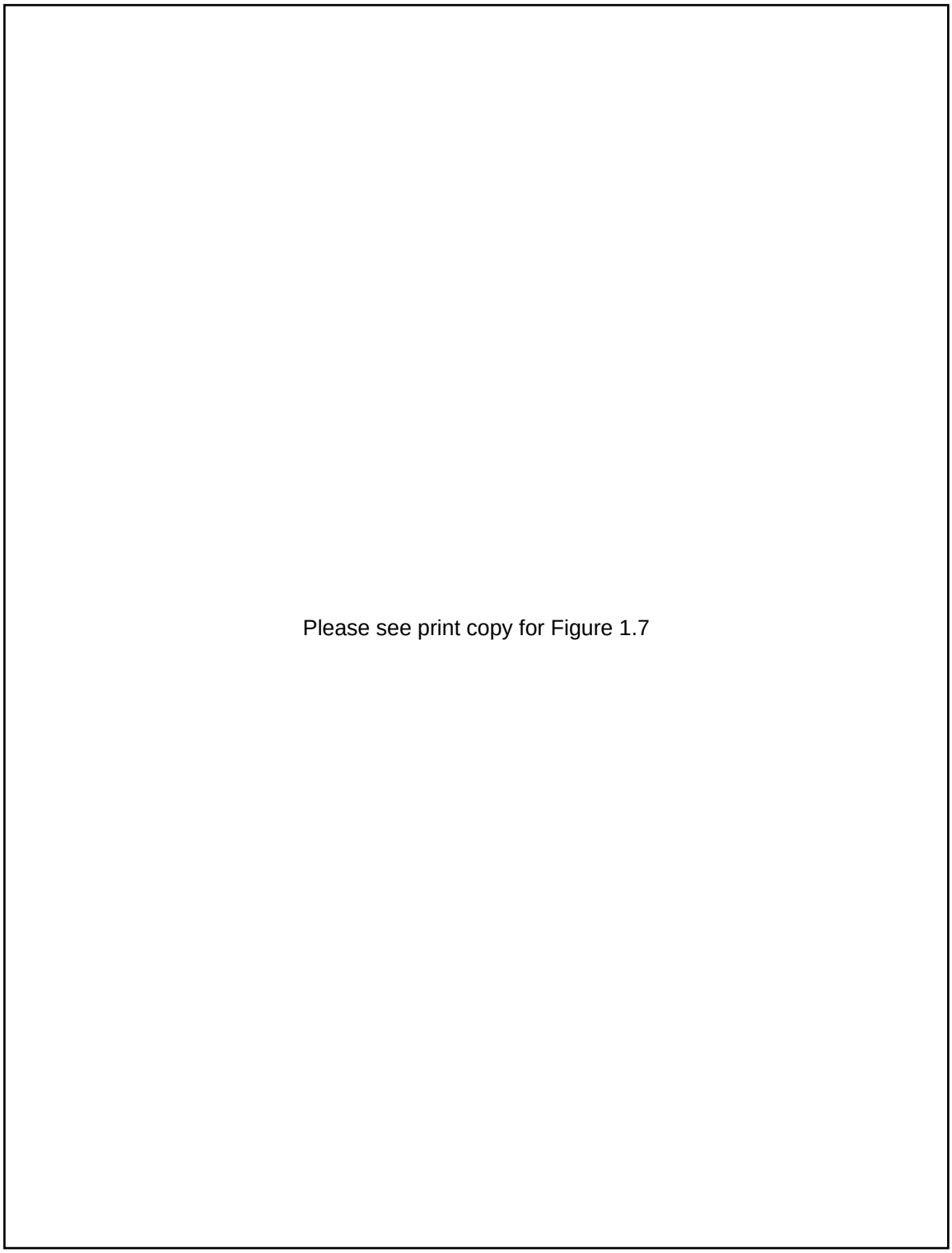

Figure 1.7: Structures of the three endocytosis receptors responsible for the internalisation of uPA:PAI-1 complexes. The very low density lipoprotein receptor (VLDLr), low density lipoprotein receptor-related protein (LRP) and Megalin (also known as LRP-2 or gp330). The four ligand binding regions, or clusters, of LRP are shown. Figure adapted from Strickland et al. 2002.

Cell surface LDLRs localise within clathrin coated pits via an NPxY motif in their cytoplasmic domain that is thought to bind to clathrin heavy chains and also a variety of signal transducing molecules (Hussain et al., 1999; Nykjaer and Willnow, 2002; Strickland and Ranganathan, 2003). Clathrin coated pits continuously internalise by budding from the cell membrane to form intracellular vesicles, resulting in the constitutive endocytosis of the receptors within them (Hussain et al., 1999). The association of uPAR within clathrin coated pits does not occur until the binding of uPA:PAI-1 induces an interaction with an LDLR family member. The LDLR/uPAR/uPA:PAI-1 complex then localises into the clathrin coated pit and is endocytosed (Czekay et al., 2001). The work by Czekay *et al.* (2001) suggested that a direct interaction between uPAR and LRP was necessary for the internalisation of uPA:PAI-1. They also suggested that uPAR may bind directly to LRP, independent of uPA:PAI-1 binding, through domain 3 of uPAR. However, previous research found no evidence supporting this interaction (Nykjaer et al., 1994).

As is the case for most LDLR family ligands, the internalised LDLR/uPAR/uPA:PAI-1 complex is directed into the early endosomes (Czekay et al. 2001). Here the uPA:PAI-1 complex is dissociated and targeted to the lysosome for degradation (Jensen et al. 1990, Hussain et al. 1999), while uPAR and LRP are recycled back to the cell surface (Hussain et al., 1999; Misra and Pizzo, 2001; Nykjaer et al., 1997).

The protein expression of LRP varies between human tumour cell lines and appears to be characteristic of tumour cell type and stage (Jensen et al., 1989; Li et al., 1997; Van Leuven et al., 1979). A wide range of LRP levels (300 - 6300 sites per cell, Li et al., 1998) and a positive correlation between high LRP expression and invasiveness has been reported in breast carcinoma (Chazaud et al., 2002; Li et al.,

1998). In contrast to LRP, the high expression of VLDLr shows a negative correlation with invasiveness in breast cancer cell lines (MCF-7 and MDA-MB-231), whereas gp330 is not expressed at significant levels in these carcinoma cell lines (Chazaud et al., 2002). In prostate carcinoma, LRP may be expressed on the surface of both benign and malignant prostate epithelial cells (Kancha et al., 1994). However, LRP may be inversely related to invasiveness since invasive subclones of the PC-3 cell line were observed to express reduced levels of LRP mRNA relative to non-invasive subclones (Asplin et al., 2000; Kancha et al., 1994). Whilst levels of these LDLR family molecules may impact upon the invasiveness of cells, they are unlikely to be directly involved in the process of invasion. Rather, they are more likely to elicit indirect effects by regulating the levels and activity of other proteins (i.e. uPA, uPAR, MMPs) involved in this process.

1.3.2 Caveolae Mediated Endocytosis

An alternate mechanism of uPAR internalisation that does not involve LDLR receptors or clathrin coated pits, but distinct membrane sub-domains called caveolae, has been observed in some cell lines (Vilhardt et al., 1999). Caveolae are rounded plasma membrane invaginations, typically around 50-80 nm in diameter. The intracellular leaflet of caveolae are coated with a protein called caveolin-1 (caveolin-3 in muscle cells), which serves to stabilise caveolae structure and may actually regulate the internalisation rate of caveolae (Pelkmans and Helenius, 2002). Caveolae can be experimentally characterised by their resistance to non-ionic detergent solubilisation at 4°C, due to the highly ordered structure of lipids in the plasma membrane of caveolae (Pelkmans and Helenius, 2002).

GPI-anchored proteins have been reported to localise within caveolae (Pelkmans

and Helenius, 2002) and also within lipid rafts (Mayor and Riezman, 2004). Localisation within caveolae remains somewhat controversial, as studies exist which claim that this localisation exists only after artefactual cross-linking that occurs during the isolation process (Mayor and Riezman, 2004). There are however, studies showing the localisation of uPAR and uPA within caveolae (Stahl and Mueller, 1995; Vilhardt et al., 1999), a direct interaction between uPAR and caveolin (Stahl and Mueller, 1995), and a regulation of uPAR and pro-uPA expression by caveolin-1 expression (Cavallo-Medved et al., 2005). uPA/uPAR present in caveolae has been shown to increase plasmin generation (Stahl and Mueller, 1995) by inducing close juxtaposition of plasminogen activation system components and associated proteases (Cavallo-Medved et al., 2005), and also associate with Janus Kinase 1 (Jak1) inducing Signal Transducers and Activators of Transcription 1 (Stat1) phosphorylation (Koshelnick et al., 1997). Caveolae are internalised in a clathrin-independent, RAP in-sensitive fashion (Vilhardt et al. 1999) into intracellular vesicles called caveosomes (Figure 1.7) that are not detectable with markers of the endosomes, lysosomes, golgi or endoplasmic reticulum. From here, the contents of the 'caveosome' may be directed to the endoplasmic reticulum, the golgi body, the early endosomes or other as yet unknown locations (Pelkmans and Helenius, 2002).

A dimeric form of uPAR that preferentially associates with lipid rafts has also been observed (Cunningham et al., 2003). The localisation of this form of uPAR into lipid rafts was shown to increase the incidence of uPA mediated uPAR cleavage and preferentially associate with vitronectin. Lipid rafts are small, highly ordered, cholesterol and glycosphingolipid rich microdomains that are distinct from caveolae (Parton and Richards, 2003). They are internalised in a clathrin and caveolin independent manner (Pelkmans and Helenius, 2002) into RAB5-negative early

endosomes that are not marked by either caveolin or clathrin (Mayor and Riezman, 2004) (Figure 1.7). Therefore lipid rafts present another avenue through which uPAR and consequently uPA and PAI-1/PAI-2 may interact with co-receptors and also be internalised.

The classic model of LRP mediated endocytosis involves LRP binding to a multitude of different ligands and associating with clathrin coated pits to facilitate the endocytosis of these ligands (Strickland et al. 2002). However, recent research has revealed that LRP transiently enters lipid rafts (Wu et al., 2004) and caveolae (Boucher et al., 2002; Loukinova et al., 2002) and may remove uPAR from the lipid rafts or caveolae to facilitate its endocytosis through clathrin coated pits. Phosphorylation of the cytoplasmic tail of LRP by the non-receptor tyrosine kinase Src is also facilitated through its association with caveolae, but the function of this phosphorylation event is unknown (Boucher et al., 2002; Loukinova et al., 2002).

Hence there are several pathways through which uPAR, and any associated ligands or co-receptors, may be internalised. However, nothing is known about the relationship of uPA:PAI-2 complex formation, any resulting co-receptor interactions or pathways of internalisation.

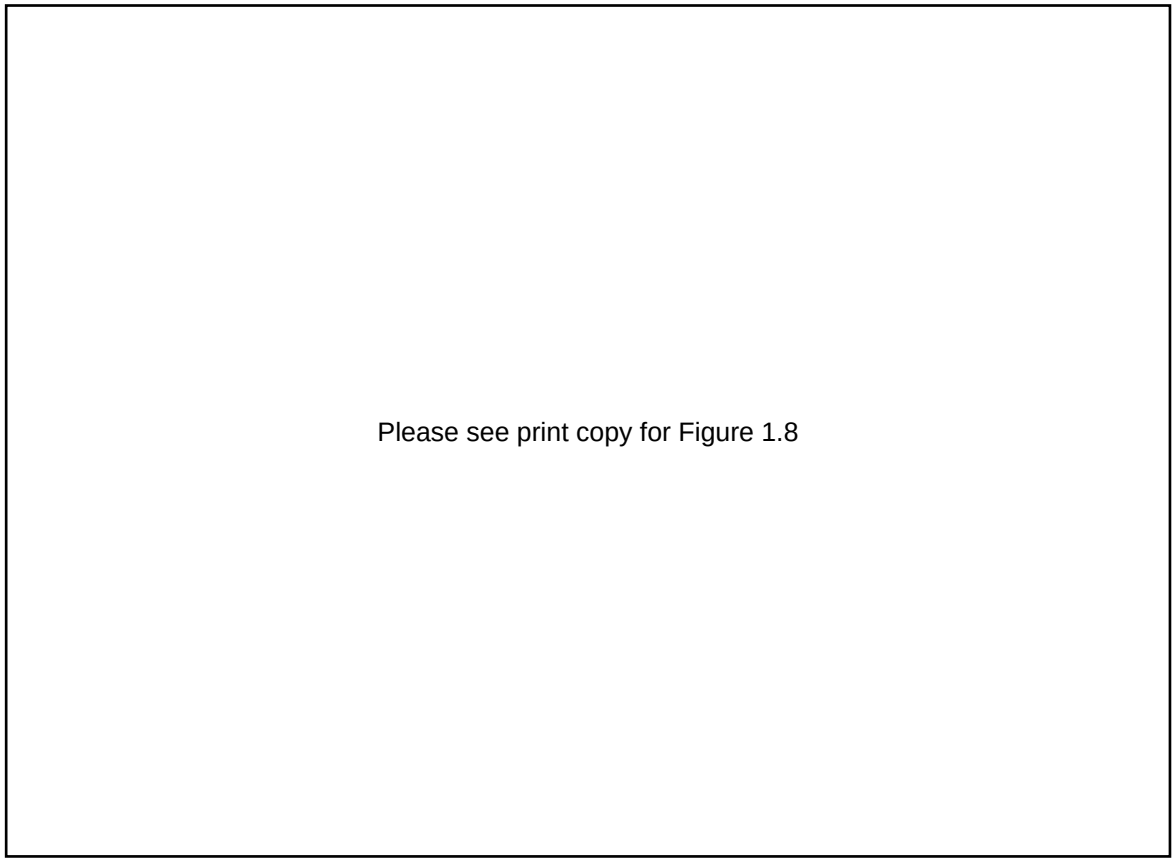

Figure 1.8: A schematic diagram showing the main pathways of endocytosis. Endocytosis routes through clathrin coated pits into a series of intracellular endosomes, through caveolae into the caveosome, endoplasmic reticulum, golgi body, nucleus or the early endosome, or through lipid rafts into an unknown but distinct vesicle are depicted. Figure adapted from Pelkmans and Helenius (2002).

1.3.3 Receptor Mediated Endocytosis of uPA:PAI-1

PAI-1 is known to be internalised by an interaction with at least three members of the LDLR family of endocytosis receptors, LRP (Herz et al., 1992; Kounnas et al., 1993), VLDLr (Argraves et al., 1995; Rettenberger et al., 1999; Webb et al., 1999) and LRP-2 (Stefansson et al., 1995) (Figure 1.6). Although free PAI-1 can bind weakly to these receptors, once PAI-1 is complexed with uPA via its classical inhibitory mechanism, either at the cell surface or in solution, the complex is able to bind to these receptors with high affinity. This increase in affinity for LDLR receptors results in greatly enhanced internalisation and degradation of uPA:PAI-1, as compared to that of uPA alone (Cubellis et al., 1990; Zhang et al., 1998). The affinities of the interactions of uPA, uPA:PAI-1 and other components of the plasminogen activation system are listed in Table 1.1. It should be noted that many of these affinities were determined using different methodologies and as such it may be difficult to directly compare values between different assays. Nonetheless, many of the obtained values reach close agreement despite being determined using different techniques.

Whilst uPA:PAI-1 is known to bind to complement repeat regions in clusters 2 and 4 of LRP and in LRP-2 and VLDLr (Strickland et al., 2002), the location of the uPA:PAI-1 epitope that facilitates binding to these endocytosis receptors has been somewhat controversial. Nykjaer et al. (1994) proposed that regions in PAI-1, and both the uPA A chain and serine protease domain were responsible for the interaction between uPA:PAI-1 and LRP. Indeed, more recent studies have confirmed that regions in both the serpin and protease moieties of the complex are able to interact with LRP (Andersen et al., 2001).

Table 1.1: Reported affinities of plasminogen activation system components for receptors of the low density lipoprotein receptor family

Please see print copy for Table 1.1

While either component alone (i.e. free uPA and PAI-1) is capable of binding to LDLR's with low affinity, the affinity of the complex is substantially higher (Nykjaer et al., 1994) (Table 1.1). Stefansson et al. (1998) demonstrated that this increase in affinity is largely due to a cryptic LDLR binding site centred around Arg^{76} within the helix D of PAI-1, which is exposed by conformational changes associated with uPA inhibition. This binding site was independent of the identity of the complexed protease, as the cryptic site in PAI-1 was revealed even when complexed with the non-uPAR binding protease tPA (Horn et al., 1998).

Pro-uPA is also able to bind to LRP (Kounnas et al., 1993) and LRP-2 (Stefansson et al., 1995), through binding sites in the ATF and serine protease domain (Nykjaer et al., 1994). It is thought that once pro-uPA is bound to uPAR and/or activated to twin-chain uPA, the binding site is blocked and is only revealed once complexed with PAI-1 (Nykjaer et al., 1994). However, other studies have reported an interaction between twin-chain uPA and LRP, LRP2 and VLDLr (Heegaard et al., 1995; Kounnas et al., 1993; Nykjaer et al., 1994; Stefansson et al., 1995). The interaction between pro-uPA and LRP is reported to be higher than that of twin-chain uPA (Kounnas et al., 1993; Nykjaer et al., 1994) (Table 1.1), although this observation is reversed for LRP-2 (Stefansson et al., 1995) and has not been investigated in the case of VLDLr (Table 1.1).

The interaction of ligands with LRP and other LDLR family receptors is thought to be mediated by positive electrostatic potential on the surface of the ligand, and complementary negative potential on the ligand binding region of the receptor (Hussain et al., 1999) (More detail provided in Chapter 4). Studies involving the selective mutagenesis of PAI-1 to remove basic amino acids have implicated arginine (Arg^{76} and Arg^{118}) and lysine (Lys^{80} and Lys^{122}) residues within and around the helix D of PAI-1 in

the high affinity binding of uPA:PAI-1 to LRP and VLDLr (Rodenburg et al., 1998; Stefansson et al., 1998). The binding site of thrombin:PN-1 complexes to LRP, within the complexed inhibitor, was identified using a peptide library prepared from the sequence of PN-1 to inhibit the endocytosis of thrombin:PN-1 by LRP (Knauer et al., 1997). This study revealed a binding site in a loop structure between Pro^{47}-Ile^{58} of PN-1. Whilst this region does not contain either arginine or lysine residues, it does contain two basic histidine residues which may contribute to LRP binding (Knauer et al., 1997).

1.3.4 Cell Signaling Through uPAR and the LDLR Family

As discussed in section 1.2.4.2, the association of uPAR with its various ligands and integrins induces the potentiation of intracellular signaling (Kjoller, 2002). As uPAR is a GPI-anchored protein, and as such has no transmembrane region, signaling by uPAR is mediated by integrins and co-receptors (e.g. EGF receptor, EGFR) that interact with uPAR (Liu et al., 2002; Resnati et al., 2002). The binding of uPA to uPAR results in the activation of various signaling molecules, including $p56/p59^{hck}$ (Konakova et al., 1998), Jak/Stat (Dumler et al., 1999; Koshelnick et al., 1997), focal adhesion kinase (Nguyen et al., 2000; Tang et al., 1998; Yebra et al., 1999), protein kinase Cε (Busso et al., 1994), casein kinase 2 (Dumler et al., 1999) and extracellular signal-regulated kinases 1/2 (ERK) (Aguirre Ghiso et al., 1999; Kanse et al., 1997; Nguyen et al., 1998). On MCF-7 cells, the ligation of uPA to uPAR stimulates transient ERK phosphorylation and vitronectin dependent cell migration (Nguyen et al., 1999; Webb et al., 2001). The binding of uPAR to vitronectin also stimulates cell migration by activating Rac1 (Kjoller and Hall, 2001; Kraynov et al., 2000), resulting in the regulation of various effector proteins involved in initiating and stabilising the new actin polymers of advancing lamellipodia (Ridley, 2001).

As discussed in section 1.3.3, the inhibition of uPA by PAI-1 results in the formation a covalent complex that has an increased affinity for certain members of the LDLR family, resulting in an enhanced rate of uPA:PAI-1 endocytosis (Andreasen et al., 1994). These interactions with members of the LDLR family can indirectly effect signaling activity by regulating levels of uPA/uPAR on the cell surface (Webb et al., 2000) and also directly transmit signals through cytoplasmic domains of the LDLRs (Herz and Strickland, 2001).

The inhibition of uPA by PAI-1 sustains the phosphorylation of ERK in MCF-7 cells, through an as yet un-identified mechanism, which stimulates enhanced cell proliferation (Webb et al. 2001). These events are facilitated by an interaction with VLDLr and mediated through the high affinity binding site within the PAI-1 molecule (Webb et al. 2001), unveiled after inhibition of uPA (Stefansson et al. 1998). This sustained ERK phosphorylation is also uPAR dependent as tPA:PAI-1 is not able to elicit the same response (Webb et al. 2001). PAI-1 is also capable of stimulating cell migration independently of uPA, tPA and vitronectin. Degryse et al. (2004) showed that a direct interaction between PAI-1 and LRP activates the Jak/Stat pathway, resulting in the polarisation of actin filaments and a shift of activated Stat1 into the nucleus. For a thorough review of the signaling events initiated through the binding of ligands to uPAR and members of the LDLR family, see Kjoller et al. (2002) and Herz and Strickland (2001), respectively. A brief summary of the interactions between uPAR, uPA, PAI-1, LDLR family members, vitronectin and integrins is presented in Figure 1.8. Some relevant aspects of these interactions will also be discussed in detail in Chapter 4.

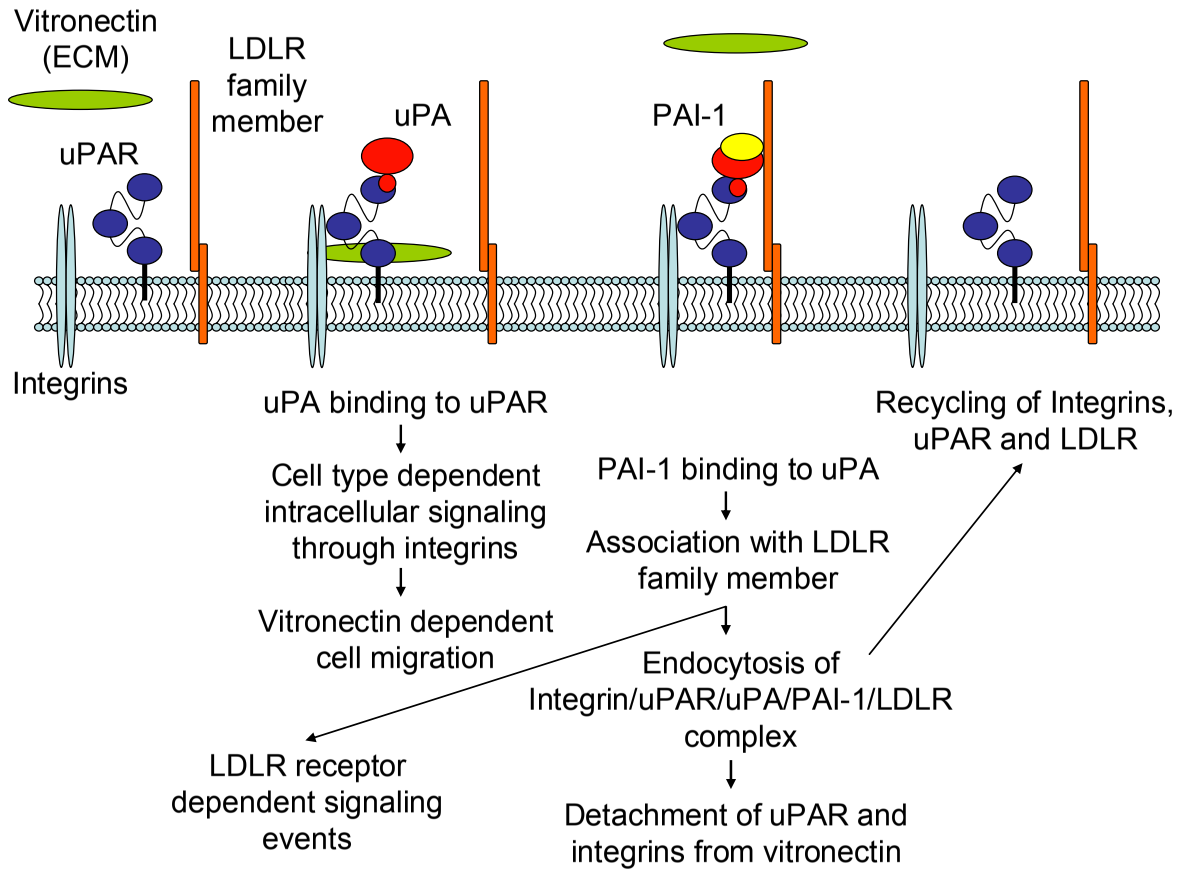

Figure 1.8: A brief schematic diagram of the interactions between uPAR, integrins, vitronectin, uPA, PAI-1, members of the LDLR family and the functional consequences of these interactions. The binding of uPA (red) to uPAR at the surface of a cancer cell and the consequences of the resulting integrin (light blue) and vitronectin (green) interactions with uPAR are detailed. The inhibition of uPA by PAI-1 (yellow), the subsequent signaling and endocytic events following interaction of the uPAR/uPA:PAI-1/integrin complex with an LDLR family member (orange) are shown.

The interactions between uPA:PAI-1 and members of the LDLR family (namely LRP1, VLDLr and LRP2) have been thoroughly characterised and as such the signaling events following these interactions at the cell surface are reasonably well understood. Conversely, the interactions between uPA:PAI-2 and LRP (Croucher et al., 2006) (Chapter 3), as well as uPA:PAI-2 and VLDLr (Chapter 4) have only been recently described. Thus whether any signaling events are initiated by PAI-2, or upon the inhibition of cell surface uPA by PAI-2, remains unknown. Given the role of PAI-1 signaling in cancer metastasis, investigating the role of extracellular PAI-2 in signaling, if any, through uPAR or LDLR receptors is vital for a thorough understanding of the role of PAI-2 in cancer biology and normal physiology.

1.4 RATIONALE AND AIMS OF THE THESIS

As addressed in section 1.2, the over-expression of uPA/uPAR by tumours, the role of these proteins in tumour progression and therefore their attractiveness as potential targets for cancer therapy, is well established. Although little is known about the biology of extracellular PAI-2, its ability to bind rapidly and specifically to cell surface uPA (Al-Ejeh et al., 2004) presents it as an attractive candidate as an agent for the delivery of a cancer therapy to tumours that over-express uPA/uPAR.

The conjugation of a cytotoxin (i.e. radioactive molecule or biological toxin) to PAI-2 molecules allows specific delivery to metastatic cells by targetting the over-expression of uPA commonly associated with metastatic cells (Allen et al., 2001; Allen et al., 2003; Li et al., 2002; Ranson et al., 2002). Preliminary work on the pharmacokinetics of an ^{125}I:PAI-2 conjugate in *nu/nu* mice with uPA over-expressing human colon cancer xenografts showed that ^{125}I:PAI-2 quickly localised and accumulated in the xenograft. Localisation to the kidney and liver was observed, but

was cleared rapidly from these organs. The radioactivity present was excreted in a degraded form in the urine of the mice (Hang et al., 1998). Furthermore, PAI-2 conjugated to the alpha-emitting radioisotope ^{213}Bi has been used successfully to treat breast, prostate and melanoma xenografts in mouse models (Allen et al., 2001; Allen et al., 2003; Li et al., 2002; Ranson et al., 2002). This treatment was shown to inhibit tumour growth by inducing apoptosis in uPA expressing cells, presumably through massive radiological insult to target cells (Li et al., 2002).

The use of PAI-2 in a therapeutic setting presents many advantages over PAI-1. Firstly, PAI-2 is significantly less active towards tPA than PAI-1 and does not bind to vitronectin (Mikus et al., 1993), reducing the complication of effects on normal fibrinolysis and hemostasis. PAI-2 is not prone to converting to a latent, inactive form, or to oxidative inactivation, in contrast to PAI-1, providing superior stability *in vivo* (Baker et al., 1990). Also, prolonged exposure to high levels of PAI-2 *in vivo* are not likely to present a health risk as increased levels of PAI-2 are commonly found in late pregnancy (Ye et al., 1989).

Taken together, the proven ability of PAI-2 to target cancer cells *in vitro* and *in vivo*, its ability to inhibit the growth and spread of tumours and its advantage as a human therapeutic, make it an attractive protein for use as a cancer cell targeting molecule. If PAI-2, like PAI-1, is internalised by cancer cells once it is uPA bound, this presents another avenue to greatly increase the cytotoxicity of any PAI-2 based therapies by the delivery of cytotoxin intracellularly (Rihova, 1998). This makes understanding the binding and possible internalisation of PAI-2 by cancer cells vital to the development of specific and effective cancer therapy against metastatic cancer. Furthermore, given the wide involvement of the LDLR gene family in processes of uPA:serpin complex endocytosis (Nykjaer and Willnow, 2002; Strickland et al., 2002)

(section 1.3.3), it is reasonable to hypothesise that this gene family may be responsible for endocytosis of uPA:PAI-2 complexes, although this has not been previously investigated.

Considering the lack of clear data pertaining to the internalisation of PAI-2, and its relevance to the use of PAI-2 as a cancer targeting agent for the delivery of an intracellular cytotoxin, the overall aim of this thesis is to characterise the fate of cell surface bound PAI-2. Specifically, the pathways and kinetics of internalisation of PAI-2 upon inhibition of cell surface uPA will be examined (Chapter 2), followed by a detailed characterisation of interactions with putative receptors responsible for this internalisation (Chapters 3 and 4). The functional consequences of interactions with these receptors will also be addressed (Chapter 4), along with implications for understanding prognostic outcomes of tumour expression of PAI-1 and PAI-2 (Chapter 4).

Chapter 2

2. Characterisation of the Pathways of PAI-2 Internalisation

2.1 INTRODUCTION

As previously discussed in Chapter 1.4, the use of PAI-2 as an agent to target cancer cells that over-express the serine protease uPA is well established. However, the ^{213}Bi radioisotope used as the cytotoxin is expensive and has a short half life of 46 min, meaning that delivery to patients of an active PAI-2:^{213}Bi conjugate could present logistical issues. Therefore, the use of an alternative, non-radioactive cytotoxin would be an attractive possibility, however such a cytotoxin would most likely need to enter the cell to be effective. While it is known that PAI-1 is internalised into cancer cells upon inhibition of uPA, no definitive research has been conducted into the internalisation of PAI-2. Thus an investigation into the internalisation of PAI-2 would provide data necessary for the intracellular delivery of a cytotoxin and also address an area of cell biology that has been largely ignored.

There is very little literature describing the interaction of PAI-2 and uPA at the cell surface. The PAI-2 inhibition of uPA on the surface of U937 cells, as assessed indirectly by measuring plasmin activity, was determined to have a 2nd order rate constant of 5.3×10^5 $M^{-1}s^{-1}$ (Ellis et al., 1990). This was ~10 fold slower than the rate for PAI-1 inhibition of uPA (4.5×10^6 $M^{-1}s^{-1}$). Using a more direct method, it was demonstrated that PAI-2 inhibits uPA with a K_I of 60-80 pM on carcinoma cells (Al-Ejeh et al., 2004). Using an indirect method of detecting ^{125}I labeled uPA degradation on the human choriocarcinoma cell line JAR, Jensen et al. (1990) showed that the addition of PAI-2 increased the lysosomal degradation of cell surface bound uPA from 15% to 40%, whilst PAI-1 increased degradation to 50%. Estreicher et al. (1990) observed a 70 kDa fragment of uPA:PAI-2 that was cleared from the surface of THP-1 cells, however showed no direct evidence of endocytosis of this fragment. While these results suggest that PAI-2 is internalised after inhibiting cell surface uPA, a study by

Ragno et al. (1995) suggested that uPA:PAI-2 complexes were cleaved at the cell surface into two separate 70 and 22 kDa fragments, and not internalised. The 22 kDa fragment containing the ATF of uPA stayed bound to uPAR, whilst the remaining portion of uPA and PAI-2 was released into the media. The conclusions of this paper came to dominate the field of uPA:serpin internalisation and were published in three review papers (Andreasen et al., 2000; Andreasen et al., 1997; Schmitt et al., 2000).

Consequently, this chapter aims to thoroughly address the possibility of PAI-2 internalisation following uPA inhibition. Using information obtained from previous studies into the internalisation of PAI-1 (summarised in Chapter 1.3.3) and by developing novel flow cytometry and confocal microscopy techniques to both visualise and quantitate the internalisation of PAI-2, the results in this chapter demonstrate that PAI-2 is indeed internalised following inhibition of cell surface uPA. This process appears to be via receptor mediated endocytosis, as internalised PAI-2 was taken up into the endosomes and then lysosomes of human carcinoma cell lines by a predominantly RAP-sensitive mechanism.

2.2 MATERIALS AND METHODS

2.2.1 Proteins, Antibodies and Reagents

Recombinant human PAI-2 (47 kDa form) was provided by PAI-2 Pty Ltd (Sydney, Australia). Active human HMW/LMW uPA mixture was from Chemicon (CA, USA). Purified human RAP and rabbit anti-LRP polyclonal antibody were a kind gift from Prof Dudley Strickland (American Red Cross, MD, USA). 2H5 anti-relaxed PAI-2 monoclonal antibody produced as previously described (Saunders et al., 1998). Anti-PAI-2 (#3750), anti-uPA (#394) and anti-uPAR (#3936) monoclonal antibodies

were from American Diagnostica Inc (USA). Anti-VLDLr (H-95) and anti-LRP2 (H-245) polyclonal antibodies were from Santa Cruz (CA, USA). p36 anti-serum was from Dr Teresa Compton (University of Wisconsin Medical School, Madison, USA). Purified bovine annexin II heterotetramer was from Biodesign International (Maine, USA). Transferrin:$Alexa_{488}$ was a kind gift from Dr Ellen Van Dam (Garvan Institute, Sydney, Australia). The $Alexa_{488}$ labeling kit and $Alexa_{488}$ polyclonal antibody were from Molecular Probes (OR, USA). PD-10 columns were obtained from Pharmacia Biotech (Uppsala, Sweden). Mono-C ion exchange spin columns were from Sartorius (Goettingen, Germany). 30 kDa cut-off protein concentration spin columns were from Millipore (MA, USA). BIAcore CM5 chips and Amine linking kit were from BIAcore (Melbourne, Australia). Bovine serum albumin (BSA), Streptavidin-FITC, propidium iodide (PI), Hank's balanced salts powder, ethyldiaminetriacetic acid (EDTA), Goat anti-mouse IgG-FITC and Goat anti-rabbit IgG-FITC, chlorpromazine and nystatin were from Sigma-Aldrich (MO, USA). Reagents for SDS-PAGE and broad-range unstained molecular weight marker were from Bio-Rad Laboratories, (NSW, Australia). RPMI-1640 powder and foetal calf serum were from Trace Bioscientific (NSW, Australia).

2.2.2 Detection of Cell Surface Antigens by Dual Colour Flow Cytometry

PC-3 prostate epithelial carcinoma cells, grown to sub-confluency over a 48 hour period, were detached using PBS/EDTA (5 mM) (Appendix 1), washed with ice cold binding buffer (Appendix 1) and centrifuged at 300 x *g*, at 4˚C. The cells were incubated with primary anti-mouse antibodies (5 μg/mL) or primary rabbit or goat polyclonal antibodies (5 μg/mL) in binding buffer for 45 min, on ice. After three washes

with ice-cold binding buffer, the cells were incubated with either goat anti-mouse IgG-FITC or goat anti-rabbit IgG-FITC as required (1:50 dilution) for 45 min, on ice. After three washes, the cells were resuspended in PBS containing propidium iodide (PI) (1 μg/mL) and cell surface expression of various antigens analysed by dual colour flow cytometry. This is based on the exclusion of PI by live cells, as previously described (Ranson et al., 1998) and detailed in Appendix 2. The exclusion of non-viable cells from fluorescence calculations ensures that the measurement is based only on cell surface levels of antigens, as cells with permeabilised membranes would allow antibodies access to intracellular antigens.

2.2.3 Fluorescence Microscopy

2.2.3.1 Localisation of PAI-2 in Endosome and Lysosomes

PC-3 cells were detached with PBS/EDTA (5 mM) for 5 min at 37ºC, centrifuged at 300 x g and resuspended in ice-cold binding buffer at $1x10^6$ cells/mL. The cells were then incubated with PAI-2:Cy5 (5 μg/mL) and Transferrin:$Alexa_{488}$ (50 μg/mL) in binding buffer for 20 min, on ice. The cells were centrifuged at 4ºC and washed twice in ice cold binding buffer. Following resuspension in pre-warmed binding buffer containing Lysotracker Yellow DND-68 (75 nM), the cells were incubated at 37ºC for 15, 30 or 45 min, and washed twice in ice cold binding buffer. For viewing by confocal microscopy, 20 μl of cell suspension was placed onto a microscope slide and covered by a coverslip. Transferrin:$Alexa_{488}$ and Lysotracker Yellow DND-68 were both excited with the 488 Argon laser and the emissions collected at 500-530 nm and 550-600 nm respectively. The PAI-2:Cy5 signal was obtained separately to prevent interference from the Lysotracker signal, it was excited at 633 nm by the Helium-Neon

laser and the emission collected from 650-800 nm. A Leica TCS SP system (Leica, Heidlberg, Germany) was used and the obtained images were overlayed using Confocal Assistant v4.02 (Written by Todd Clark Brelje).

2.2.1.1 Internalisation of PAI-2 by HEK-293 Cells

This work was conducted at IFOM in Milan, Italy with the assistance of Mr Chris Madsen and Dr Nicolei Sidenius. PAI-2 was biotinylated as per manufacturers instructions (Pierce). uPA:PAI-2 complexes were formed by incubating 300 μg of biotinylated PAI-2 with 100 μg of uPA for 1 h at 37°C. The crude complexes were diluted 5-fold into sodium phosphate buffer (50 mM) pH 6 (Appendix 1) and applied to a pre-equilibrated mono-C spin column in 400 μL aliquots. After three washes with sodium phosphate buffer (50 mM) pH 6 the complexes were eluted by applying 400 μL of sodium phosphate buffer (50 mM) pH 6 containing 500 mM NaCl (see Chapter 3.3.4 for more detail). 10 μg of biotinylated PAI-2 or uPA:PAI-2 complexes were pre-incubated with streptavidin-FITC (4 μL in 200 μL) for 30 min on ice.

HEK-293 cells, either wild-type or cells stably transfected with uPAR cDNA (Madsen and Sidenius, *unpublished data*), were grown on glass coverslips for 24 h, washed twice with ice-cold PBS and incubated with streptavidin-FITC labeled biotinylated PAI-2 (10 nM) or uPA:PAI-2 complexes (10 nM) for 1 h at 37°C, in PBS/BSA (0.1%)/$CaCl_2$ (1mM). Following this, the cells were washed twice with ice-cold PBS and fixed with 3.75% para-formaldehyde (PFA) for 15 min on ice. The cell monolayers were washed twice with ice-cold PBS and permeabilised by incubation with 0.1% triton-X in PBS for 5 min on ice. After washing with ice-cold PBS, the cells were incubated with DAPI (1:500) in PBS for 15 min on ice. Following a further two washes

with ice-cold PBS, the coverslips were mounted onto slides and viewed by epi-fluorescence. DAPI nuclear stain was excited at 360 nm and the emission collected from 460-520 nm. FITC was excited at 488 nm and the emission collected from 520-610 nM.

2.2.2 Internalisation assays

2.2.2.1 Internalisation Rate Assay

The labeling of PAI-2 with $Alexa_{488}$ (Molecular Probes) was undertaken according to manufacturer's instructions. PC-3 cells, grown to sub-confluency over a 48 hour period, were detached using PBS/EDTA (5 mM), washed with ice cold binding buffer and centrifuged at 300 x *g*, at 4˚C. The cells were resuspended at $1x10^6$ cells/mL in phenol red free binding buffer and incubated with PAI-2:$Alexa_{488}$, for 20 min, on ice. The cells were then washed twice, a 600 µl sample taken and the rest resuspended in binding buffer adjusted to 37˚C. Further 600 µl samples were taken at various time points for 40 min. Each sample was diluted into 5 mL of ice cold binding buffer and centrifuged at 300 x *g*, at 4˚C. The cells were then resuspended at 2 x 10^6 and incubated with or without 4 µg/mL of anti-$Alexa_{488}$ polyclonal antibody for 30 min, on ice.

After this incubation period, the cells were centrifuged at 300 x *g* at 4˚C, the supernatant was decanted and the cells resuspended in ice-cold PBS containing PI (1 µg/mL) and analysed by dual colour flow cytometry as previously described (Ranson et al., 1998). Cells not treated with PAI-2:$Alexa_{488}$ were used as a measure of auto-fluorescence, the mean value of two samples was calculated and subtracted from all values (Figure 2.1A). Cells treated with PAI-2:$Alexa_{488}$ but without the anti-$Alexa_{488}$ antibody represented the total amount of cell associated PAI-2 (Cell surface and internalised, Figure 2.1B), whilst the cells treated with both PAI-2:$Alexa_{488}$ and the

quenching antibody represented the internalised PAI-2 (Figure 2.1C) (Further described in Appendix 3). A mean value for the total PAI-2 was taken, and the values for internalised PAI-2 were calculated as a percentage of this, with the standard error of the mean being derived from these three values. For control experiments testing the efficiency and cytotoxicity of chlorpromasine and nystatin, transferrin:Alexa$_{488}$ was used in the same manner as PAI-2:Alexa$_{488}$.

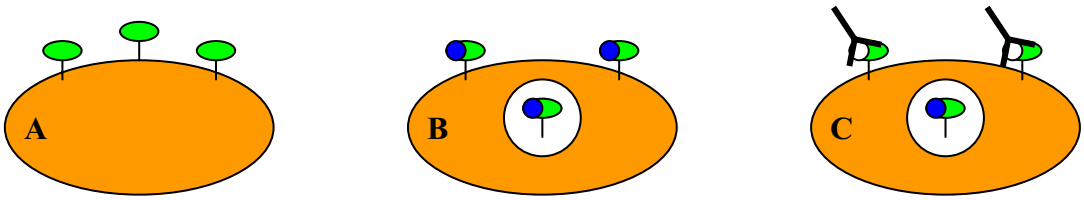

Figure 2.1: The method of fluorescence quenching used to measure the internalisation of PAI-2. (A) shows a cell incubated with neither PAI-2:Alexa$_{488}$ (Blue) or the quenching antibody (black), this cell provides a measure of autofluorescence. **(B)** shows a cell with both internalized PAI-2:Alexa$_{488}$ and at the cell surface, this provides a measure of the total amount of cell associated PAI-2. **(C)** shows a cell with both internalized PAI-2:Alexa$_{488}$ and at the cell surface, as in B, however the fluorescence associated with the cell surface PAI-2 has been quenched using the polyclonal antibody towards Alexa$_{488}$. This gives a measure of the internalized PAI-2.

2.2.2.2 Attached Cell Internalisation Assay

To obtain a more physiological response to the endocytosis inhibitors used, the internalisation assay was altered slightly for the use of attached cells. Briefly, PC-3 cells grown in a six-well plate to sub-confluency over a 48 h period were washed once with 1 mL binding buffer and then incubated for 1 h at 37˚C in binding buffer to pre-cycle cell surface receptors (Hahn-Dantona et al., 2001). The cells were pre-incubated for 15 min with either RAP (100 nM), anti-uPA monoclonal antibody (5 µg/mL), annexin II anti-serum (1:20 dilution) chlorpromazine (40 µM), nystatin (20 µM) or combinations of these as indicated. PAI-2:Alexa$_{488}$ was then added to a concentration of 10 nM and the cells incubated at 37˚C for the time period indicated. Following this, the cell monolayers were washed twice with ice-cold binding buffer, detached with PBS/EDTA

(5 mM) for 3 min at room temperature and resuspended at 2 x 10^6/mL in ice cold binding buffer. The cells were then incubated in the presence of 4 μg/mL of anti-$Alexa_{488}$ polyclonal antibody for 30 min on ice.

After this incubation period the cells were centrifuged at 300 x *g* at 4˚C, resuspended in ice-cold PBS containing the vital fluorescent stain PI (1 μg/mL) and analysed by dual colour flow cytometry as previously described (Ranson et al., 1998). Cells not incubated with PAI-2:$Alexa_{488}$, but subjected to the same treatments, were used as a measure of autofluorescence. The mean value of two autofluorescence samples was calculated and subtracted from all relevant values.

2.2.2.3 Determination of Cell Viability Following Chlorpromazine and Nystatin Treatment

PC-3 cells, grown to sub-confluency over a 48 hour period, were detached using PBS/EDTA (5 mM), washed with ice cold binding buffer and centrifuged at 300 x *g*, at 4˚C. The cells were re-suspended at 1x10^6 cells/mL incubated in the presence of chlorpromazine (30 μM) for the time periods indicated, or with nystatin for 10 min at the concentrations indicated. Following this, the cells were centrifuged at 300 x *g*, at 4˚C, and washed twice with ice-cold binding buffer. Cells were re-suspended in PBS containing PI (1 μg/mL) and analysed by flow cytometry for PI fluorescence. Viable cells were counted based on their ability to exclude PI.

2.2.3 BIAcore Analysis of the Annexin II/PAI-2 Interaction

PAI-2 was immobilised to a CM5 BIAcore chip according to manufacturer's instructions. Briefly, the chip was activated using a 1:1 mixture of 0.2M *N*-ethyl-*N'*-(3-dimethylaminopropyl)carbodi-imide and 0.05M *N*-hydroxysuccimide. PAI-2 was

coated to the chip at 20 μg/mL in 10 mM sodium acetate (pH 3) to ~10,000 response units. The un-occupied binding sites were blocked using 1M ethanolamine, pH 8.5 (An example of immobilisation is shown in Appendix 4). Ligands were diluted into running buffer (Appendix 1) before applying to the BIAcore chip at 20 μL/min. Regeneration of the chip was achieved using 10 mM EDTA. All buffers were filtered and degassed before use. For kinetic analysis, a blank cell was used as the reference cell and data was analysed using BIAevaluation software (Version 4). A one-binding site model with a drifting baseline provided the best fit according to χ^2 values and analysis of residual plots (An example of BIAcore analysis is provided in Appendix 5).

2.3 RESULTS

2.3.1 Characterisation of the PC-3 Cell Line

The binding of PAI-2 to the cell surface is known to be dependent on the presence of uPAR bound uPA (Al-Ejeh et al., 2004). To establish the PC-3 cell line as an adequate model for the internalisation of cell surface bound PAI-2, the presence of endogenous uPA and uPAR checked by flow cytometry. High cell surface levels of both uPA and uPAR were found on the PC-3 cells (Figure 2.2). Additionally, no PAI-1 or PAI-2 was detected in the conditioned media of PC-3 cells (*Data not shown*). As receptor mediated endocytosis of uPA:PAI-1 is known to be mediated by three members of the LDLR family, namely LRP, LRP-2 and VLDLr, the levels of these receptors was also measured (Figure 2.2). LRP was present at high levels on the PC-3 cells, VLDLr was present at low levels and LRP-2 was absent. Annexin II, a protein also thought to interact with PAI-2 (Jensen et al., 1996), was also present on the surface of PC-3 cells.

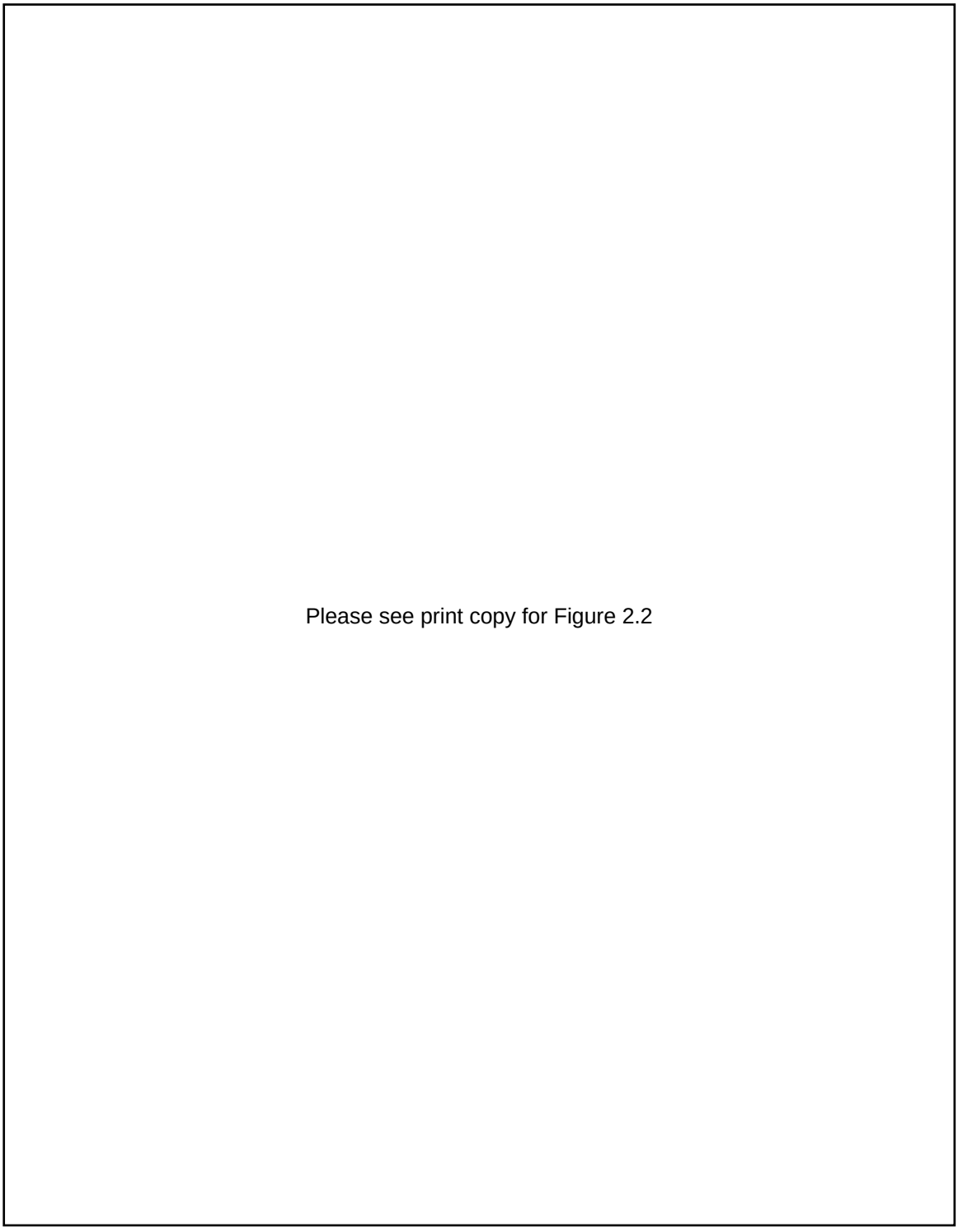

Figure 2.2: Cell surface expression profile of the PC-3 cell line. PC-3 cells were probed with monoclonal antibodies towards uPA and uPAR (5 µg/mL), and polyclonal antibodies towards LRP, VLDLr, megalin and Annexin II (5 µg/mL) (all shown in black). Relevant secondary IgG-FITC antibodies were used to detect primary antibodies (1:50 dilution). Non-specific binding was determined by the use of a species specific irrelevant isotype (shown as grey outline). Cell surface fluorescence was measured using dual colour flow cytometry as previously described (Ranson et al., 1998). Values shown are geometric means of specific primary antibody fluorescence minus non-specific irrelevant isotype antibody fluorescence (Values are mean ± SEM, n=3).

2.3.2 Relaxed PAI-2 at the Cell Surface

The specificity of PAI-2 binding to uPA at the surface of PC-3 and MDA-MB-231 cells has been previously established using 125I:PAI-2 binding assays (Al-Ejeh et al., 2004). However, to confirm that this binding is the result of the serpin inhibition mechanism and therefore that a uPA:PAI-2 complex is formed, the conversion of PAI-2 from a stressed to a relaxed state upon binding uPA on the surface of PC-3 cells, under conditions that prevent endocytosis, was monitored using an antibody directed specifically towards the relaxed form of PAI-2, 2H5 (Saunders et al., 1998). The total amount of PAI-2 was detected by using a generic PAI-2 monoclonal antibody (ADI #3750). No endogenous PAI-2 was detected by either antibody (Figure 2.3) Without exogenous uPA pre-incubation, exogenous PAI-2 binding was detected by the 2H5 antibody (Figure 2.3). The increased level of 2H5 binding compared to #3750 may be reflective of the relative affinities of these antibodies for their specific epitopes. However, when the cells were pre-incubated with uPA, significantly larger amounts of PAI-2 were detected by both the 2H5 and #3750 antibodies. This finding also demonstrates that a substantial portion of cell surface uPAR is un-occupied on this cell line as previously found in the ^{125}I:PAI-2 binding assays (Al-Ejeh et al., 2004).

2.3.3 Intracellular Localisation of Internalised PAI-2

To provide a preliminary indication of PAI-2 internalisation and to observe the intracellular localisation of any internalised PAI-2, the fate of PAI-2:Cy5 was tracked by confocal microscopy using transferrin as a marker of endosomes (van Dam et al., 2002) and Lysotracker DND-68 (Molecular Probes) as a marker of lysosomes.

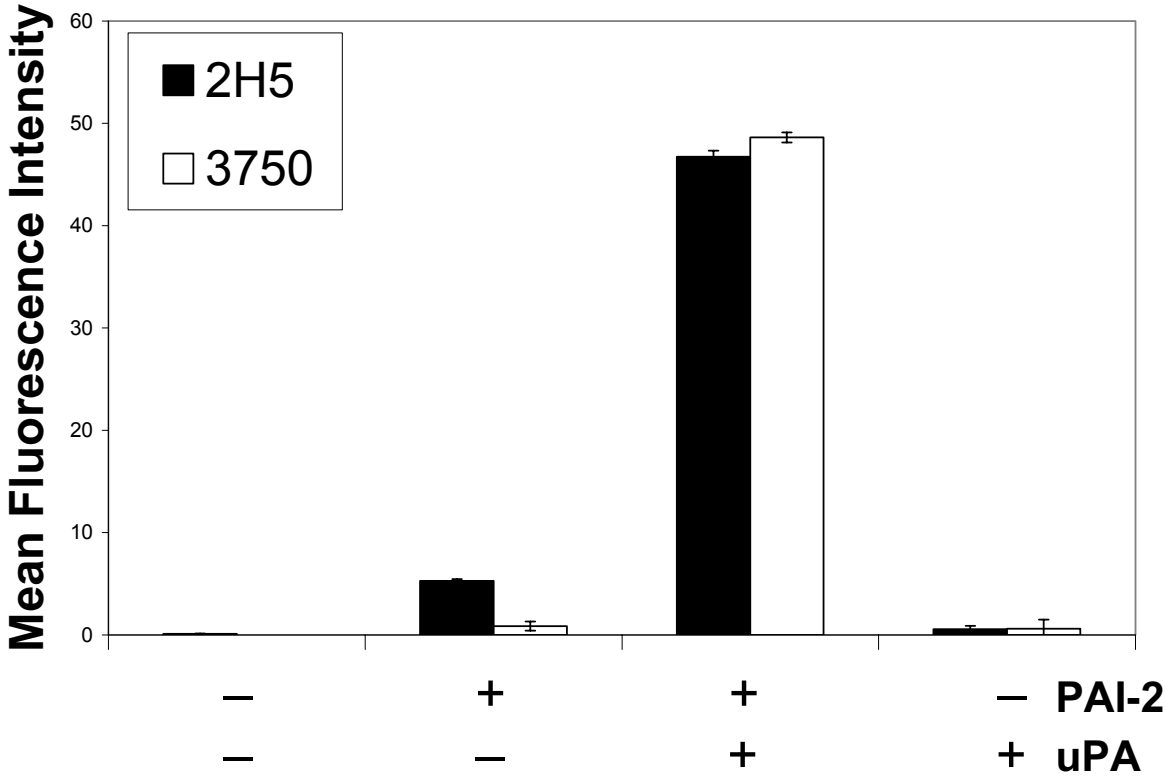

Figure 2.3: PAI-2 forms complexes with uPA at the surface of PC-3 cells. PC-3 cells were detached with PBS/EDTA and incubated in the presence or absence of uPA (10 nM) for 30 min, on ice, in binding buffer. The cells were washed three times with ice cold binding buffer and incubated with PAI-2 (10 nM) for 30 min, on ice. Following further washes, cell surface PAI-2 was detected using a monoclonal antibody directed specifically towards relaxed PAI-2 (2H5) and a generic monoclonal antibody towards PAI-2 (#3750) (Both at 5 µg/mL). These were detected using anti-mouse IgG-FITC (1:50 dilution) and measured using dual colour flow cytometry. Values shown are geometric means of specific primary antibody fluorescence minus non-specific irrelevant isotype antibody fluorescence (Values are mean ± SEM, n=3).

Intracellular tracking of PAI-2 revealed that it progressed firstly from the cell surface into transferrin-labeled endosomes and then into lysosomes. After 30 min at 37ºC, PAI-2 could be localised in endosomes, however none was present in the lysosomes (Figure 2.4). After a further 15 min incubation, the majority of PAI-2 was present in lysotracker-labeled lysosomes with a small amount still present in the endosomes (Figure 2.4).

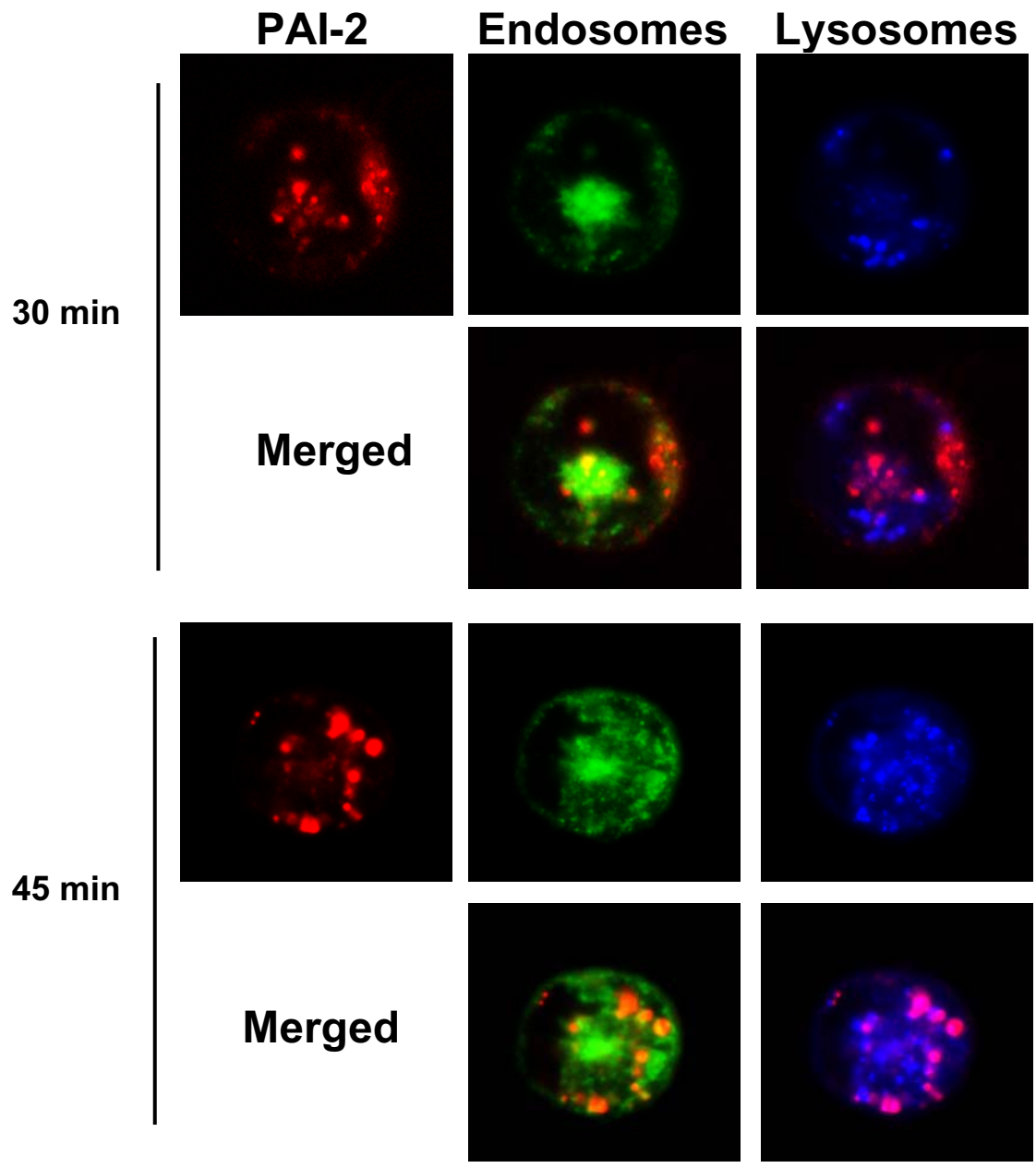

Figure 2.4: The intracellular localisation of internalised PAI-2. Cells from the PC-3 cell line were incubated with 5 µg/mL PAI-2:Cy5 and 25 µg/mL transferrin:$Alexa_{488}$ for 20 min, on ice. The cells were centrifuged, washed with ice cold binding buffer and resuspended in binding buffer adjusted to 37ºC, containing lysotracker (75 nM). After 30 min, the cells were diluted into 5 mL of ice cold binding buffer, centrifuged and analysed by confocal microscopy. The transferrin:$Alexa_{488}$ and lysotracker were excited by the Argon 488 nm laser and the emission collected at 520-540 nm and 560-600 nm, respectively. The PAI-2:Cy5 was excited by the helium/neon 633 nm laser and the emission collected at 750-900 nm. PAI-2 (red) and transferrin (green) co-localisation appears as yellow. PAI-2 and lysotracker (blue) co-localisation appears as pink.

2.3.4 Optimisation of Internalisation Assay

To both visualise and quantify the internalisation of PAI-2 by PC-3 cells, an internalisation assay was developed using $Alexa_{488}$ labeled PAI-2 and a polyclonal antibody that quenches the fluorescence of $Alexa_{488}$. The conditions for PAI-2 binding to PC-3 cells and the efficient quenching of cell surface PAI-2:$Alexa_{488}$ by the polyclonal $Alexa_{488}$ antibody were optimised in order to ensure the accuracy of the internalisation assay. The time required for PAI-2:$Alexa_{488}$ to saturate cell surface uPA on PC-3 cells was determined using a time course of PAI-2 binding (Figure 2.5A). These measurements were not intended to provide an accurate kinetic analysis of the quenching antibody, merely to provide parameters with which to conduct the internalisation assay.

At a concentration of 10 nM, sufficient to saturate PAI-2 binding to PC-3 cells (Al Ejeh et al., 2004), PAI-2 binding reached saturation levels after 2.5 min at 4°C, as measured by dual colour flow cytometry. The concentration of polyclonal quenching antibody needed to completely quench cell surface PAI-2:Alexa bound to PC-3 cells at 4°C was found to be 2 μg/mL (Figure 2.5B). Complete quenching was observed by 10 min of incubation (Figure 2.5C). To ensure complete quenching in the internalisation assay, the concentration of antibody used was 4 μg/mL and the incubation time was 30 min.

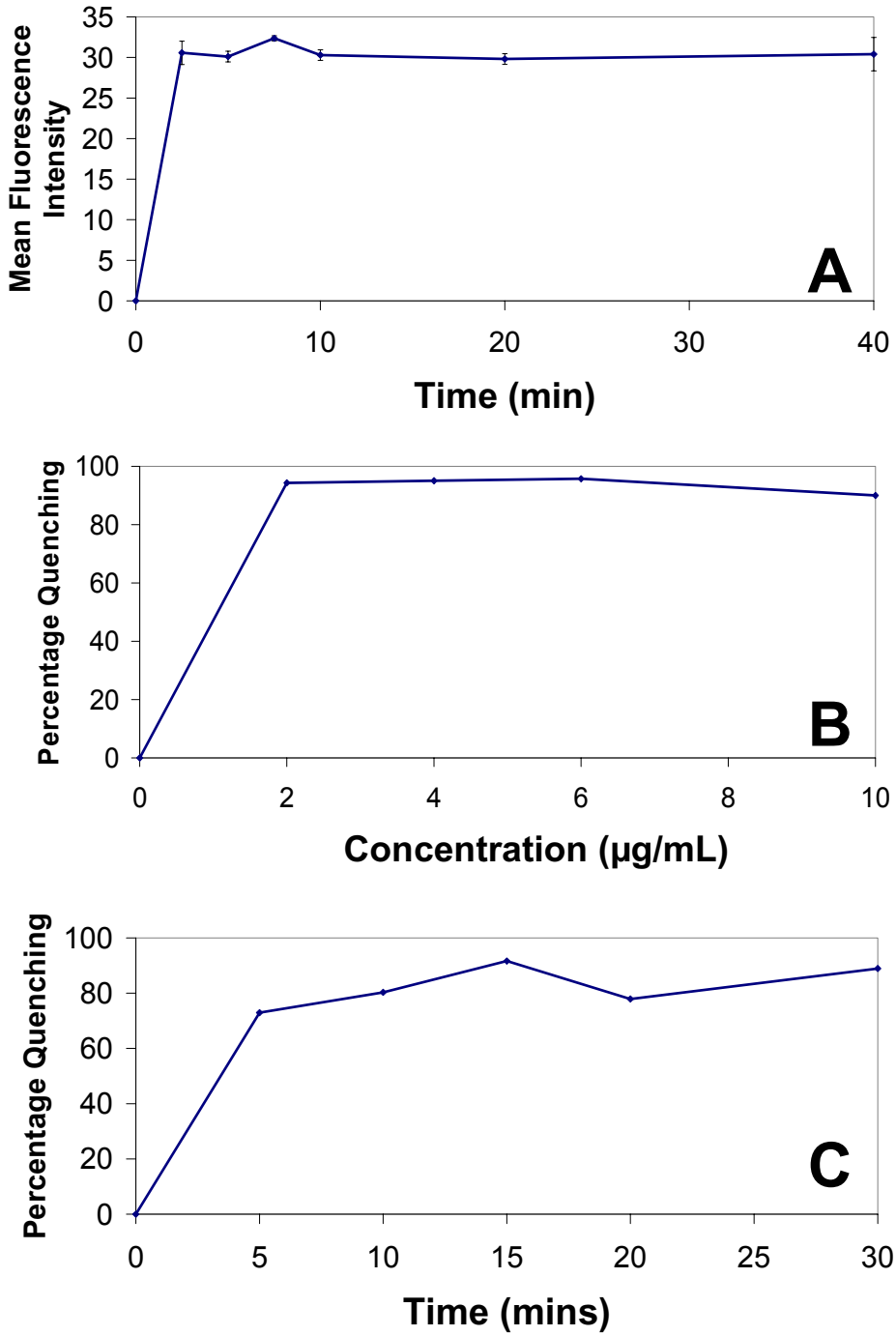

Figure 2.5: Optimisation of the PAI-2:Alexa$_{488}$ fluorescence quenching internalisation assay. (A) shows the binding of PAI-2:Alexa$_{488}$ to PC-3 cells. PC-3 cells were incubated with PAI-2:Alexa$_{488}$ (10 nM) in ice cold binding buffer for the time periods indicated, washed three times with ice cold binding buffer and viable cells analysed for Alexa$_{488}$ fluorescence by dual colour flow cytometry. **(B)** shows the quenching of cell surface PAI-2:Alexa$_{488}$ fluorescence by the addition of the quenching antibody. PC-3 cells were incubated with PAI-2:Alexa$_{488}$ (10 nM) for 20 min, on ice. Following three washes with ice cold binding buffer the cells were re-suspended in binding buffer containing the quenching antibody at the concentrations indicated for 1 h on ice. The quenching of cell surface PAI-2:Alexa$_{488}$ was measured as in A. **(C)** shows a time course of quenching of PAI-2:Alexa$_{488}$ by the quenching antibody. PC-3 cells were incubated with PAI-2:Alexa$_{488}$ (10 nM) for 20 min, on ice. Following three washes with ice cold binding buffer the cells were re-suspended in binding buffer containing the quenching antibody (4 µg/mL) for the time periods indicated. Following this the cell surface PAI-2:Alexa$_{488}$ fluorescence was analysed as in A.

2.3.5 Visualisation and Quantification of PAI-2 Internalisation

The internalisation of PAI-2:Alexa$_{488}$ was visualised using the fluorescence quenching internalisation assay and confocal microscopy. At 4ºC, PAI-2 was seen to bind to the cell surface of PC-3 cells (Figure 2.6, time point 0 min). The fluorescence associated with this cell surface bound PAI-2 was completely quenched by the addition of the quenching antibody. Once the cells were placed at 37ºC, PAI-2 began to concentrate into intracellular, vesicular compartments (time points 5-20 min). With further incubation at 37ºC, PAI-2 completely disappeared from the cell surface and subsequently increased intracellularly (time points 30-40 min). By combining flow cytometry and the fluorescence quenching internalisation assay, the process of PAI-2 internalisation was quantified by determining the amount of cell surface and internalised PAI-2 at each time point (Figure 2.7). It was seen that approximately 80% of cell surface bound PAI-2 was internalised by PC-3 cells, after a 40 min incubation at 37ºC, with a calculated $t_{1/2}$ of 8 min.

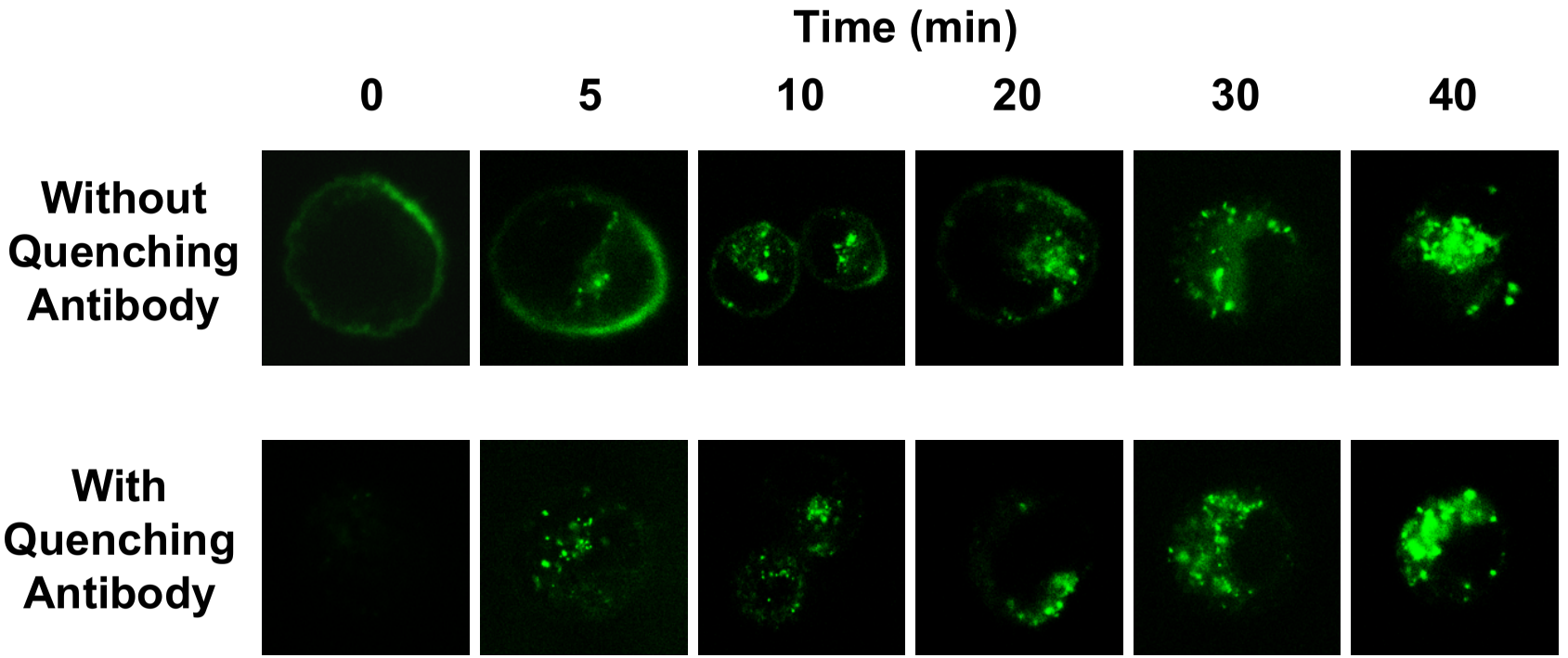

Figure 2.7: Confocal fluorescence microscopy analysis of the internalisation of PAI-2 by PC-3 cells. PC-3 cells were incubated with PAI-2:Alexa488 (10 nM) for 20 min, on ice. Following three washes with ice cold binding buffer the cells were re-suspended in binding buffer pre-warmed to 37°C. At each time point, an aliquot of cells was taken and diluted ~20 times into ice cold binding buffer. The cells were then incubated in the presence or absence of the quenching antibody (4 µg/mL) for 30 min on ice. The cells were mounted and viewed by confocal microscopy to detect PAI-2:Alexa488.

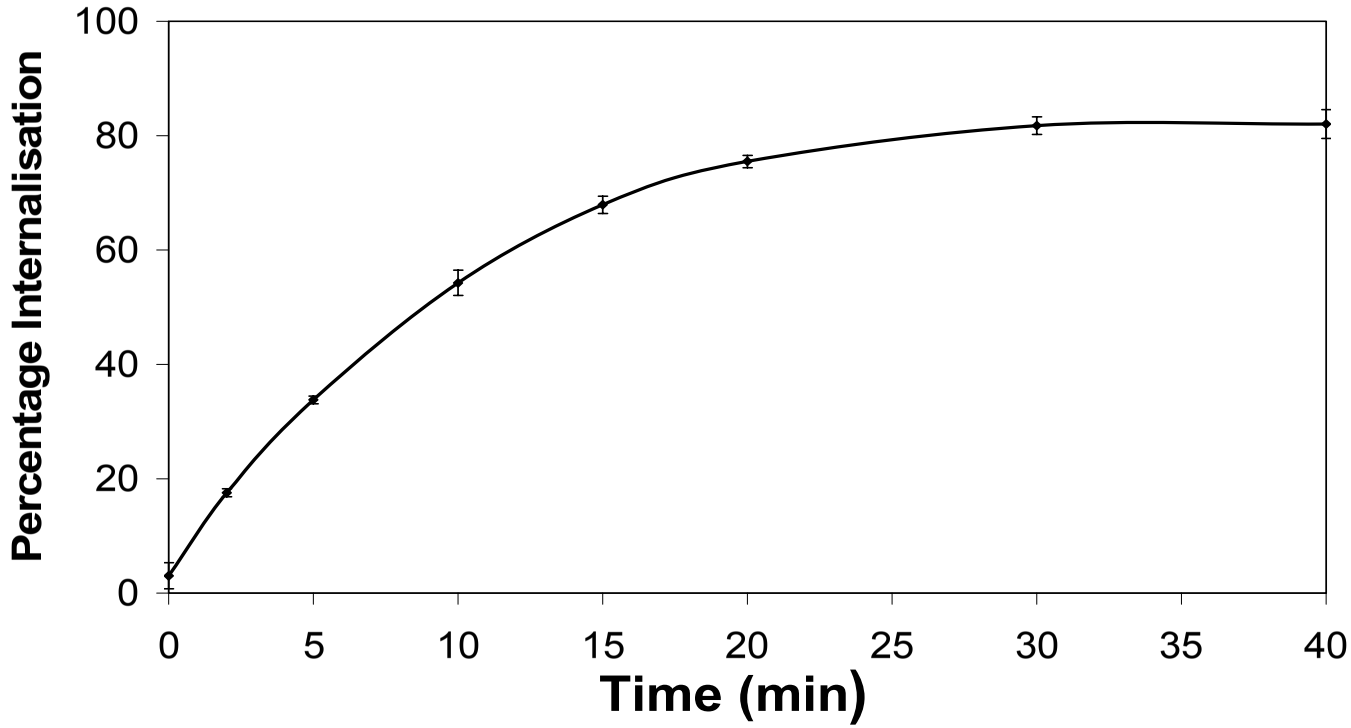

Figure 2.8: Quantification of PAI-2:Alexa488 internalisation by PC-3 cells. PC-3 cells were incubated with PAI-2:Alexa488 (10 nM) for 20 min, on ice. Following three washes with ice cold binding buffer the cells were re-suspended in binding buffer pre-warmed to 37°C. At each time point, an aliquot of cells was taken and diluted 20 times into ice cold binding buffer. The cells were then incubated in the presence or absence of the quenching antibody (4 µg/mL) for 30 min on ice. The PAI-2:Alexa488 fluorescence of viable cells was measured using dual colour flow cytometry. Values in the absence of the quenching antibody represented total PAI-2:Alexa488, whilst values in the presence of the quenching antibody represented internalised PAI-2:Alexa488. Percentage internalisation was calculated by taking the values for internalised PAI-2:Alexa488 was a percentage of the average of the values for total PAI-2:Alexa488, at each time point. (Values are ± SEM, n=3). Data was fit to a one-phase exponential association (*r2*= 0.99) which was used to calculate t1/2 values. Data were fitted using GraphPad v4 (Prism).

2.3.6 Inhibition of PAI-2 Internalisation

Inhibitors of various pathways of endocytosis were used to determine the route of PAI-2 entry into the cell. Chlorpromazine, an inhibitor of clathrin coated pit formation (Anderson et al., 1996) was used to inhibit clathrin coated pit-dependent internalisation and RAP was used to specifically inhibit the LDLR family of endocytosis receptors (Moestrup et al., 1993a). Nystatin, a cholesterol sequestering agent that disrupts caveolae and lipid rafts (Anderson et al., 1996) was used to investigate clathrin-independent pathways. Initially, the potential cytotoxicity of nystatin and chlorpromazine was established to prevent the introduction of artefacts into the internalisation assay due to any effects on cell viability. This was determined by the ability of the cells to exclude PI after incubation with either chlorpromazine or nystatin (Figure 2.8). Chlorpromazine concentrations up to 40 μM and nystatin concentrations up to 20 μM did not substantially reduce cell viability (<70%) compared to that in the absence of these compounds (Figure 2.8). Higher concentrations reduced cell viability to below 50% or resulted in total cell death, suggesting that concentrations of 40 and 20 μM are safe working concentrations for chlorpromazine and nystatin, respectively.

To determine if chlorpromazine was able to inhibit clathrin coated pit mediated endocytosis at a concentration of 40 μM, the internalisation of transferrin:$Alexa_{488}$ was analysed, as transferrin is known to be internalised through clathrin coated pits (van Dam et al., 2002). Almost complete inhibition of receptor mediated endocytosis of transferrin by 40 μM chlorpromazine was achieved after a 10 min incubation at 37°C (Figure 2.9A). The disruption of the cell membrane caused by treatment with nystatin is known to have effects upon receptor mediated endocytosis, if used at high concentrations (Dr Ellen van Dam, Garvan Institute, *personal communication*).

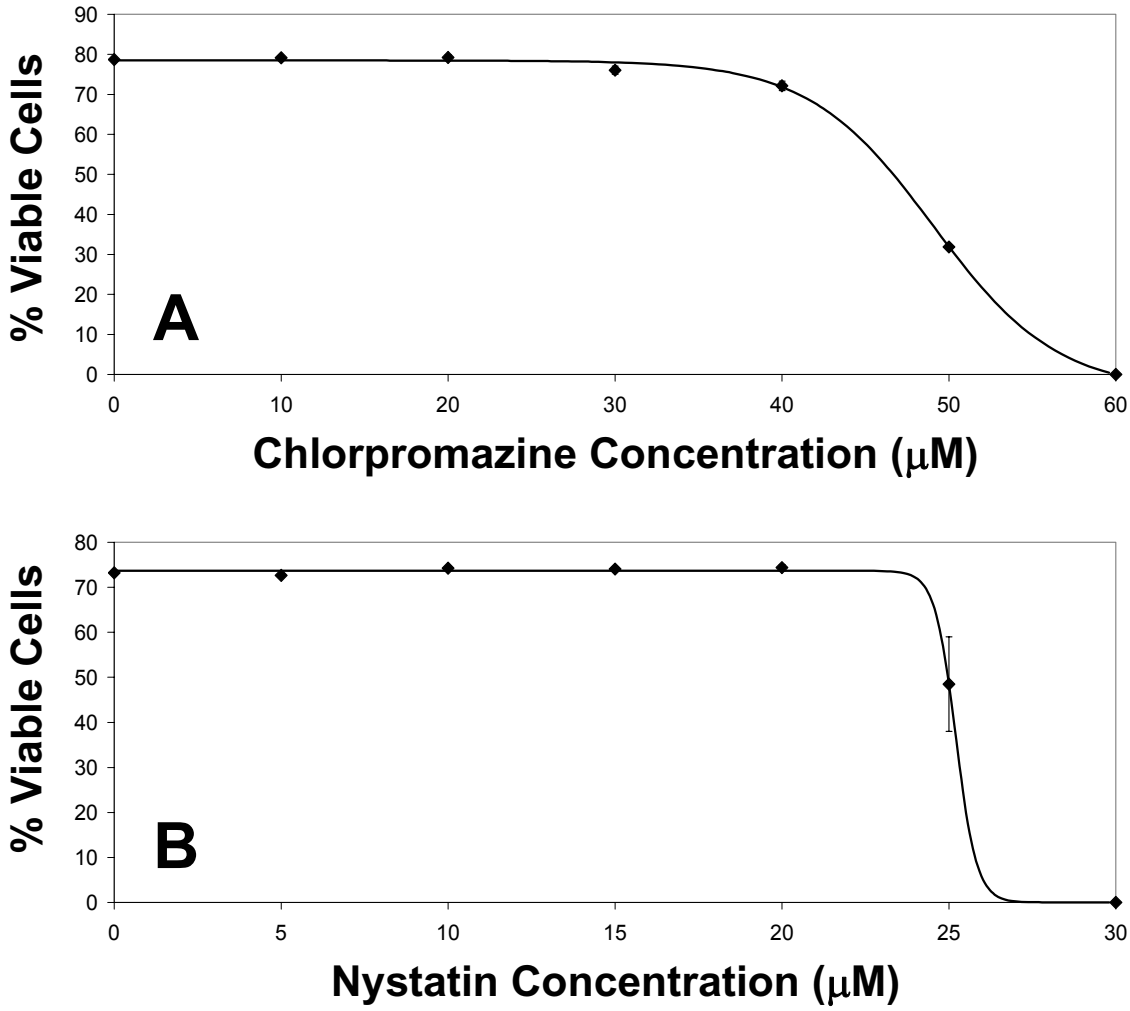

Figure 2.8: Cytotoxicity of the endocytosis inhibitors chlorpromazine and nystatin towards PC-3 cells. PC-3 cells were incubated with **(A)** chlorpromazine or **(B)** nystatin in binding buffer at the concentrations indicated for 30 min at 37°C. Following three washes with ice cold binding buffer, the cells were analysed for viability by PI exclusion and flow cytometry. (Values are ± SEM, n=3). Data were fitted using GraphPad v4 (Prism).

To check that the level of nystatin used was not interfering with receptor mediated endocytosis and to confirm that any inhibition observed was only of clathrin-independent pathways, the ability of nystatin to affect the internalisation of transferrin was examined. Pre-incubation with nystatin at concentrations up to 20 μM for 10 min at 37°C had no effect upon the internalisation of transferrin by PC-3 cells (Figure 2.9B).

Chlorpromazine, nystatin, RAP and an anti-catalytic anti-uPA monoclonal antibody, known to inhibit the binding of PAI-2 to PC-3 cells (Al-Ejeh et al., 2004), were utilised within the internalisation assay to analyse the pathways of PAI-2 internalisation by PC-3 cells (Figure 2.10). Both RAP and the anti-uPA antibody inhibited ~70% of PAI-2 internalisation, whilst chlorpromazine inhibited ~30% and nystatin ~20%. The addition of both nystatin and RAP resulted in the complete inhibition of PAI-2 internalisation.

The dependence of uPA, uPAR and members of the LDLR family upon PAI-2 internalisation was also demonstrated using uPAR negative HEK-293 cells (Madsen and Sidenius, *unpublished data*) (Figure 2.11). Wild-type HEK-293 cells incubated with a pre-formed biotinylated uPA:PAI-2/streptavidin-FITC complex showed no internalisation of uPA:PAI-2 (Figure 2.11A), as did HEK-293 cells stably transfected with uPAR cDNA and incubated with biotinylated PAI-2/streptavidin-FITC complex (Figure 2.11B). However, when uPAR transfected cells were incubated with biotinylated uPA:PAI-2/streptavidin-FITC complex, significant amounts of uPA:PAI-2 was internalised, resulting in peri-nuclear accumulation of uPA:PAI-2 (Figure 2.11C). This internalisation was completely inhibited by the addition of RAP (Figure 2.11D) as the uPA:PAI-2 no longer accumulated in a peri-nuclear position but was seen as a diffuse staining at the surface of the HEK-293 cells.

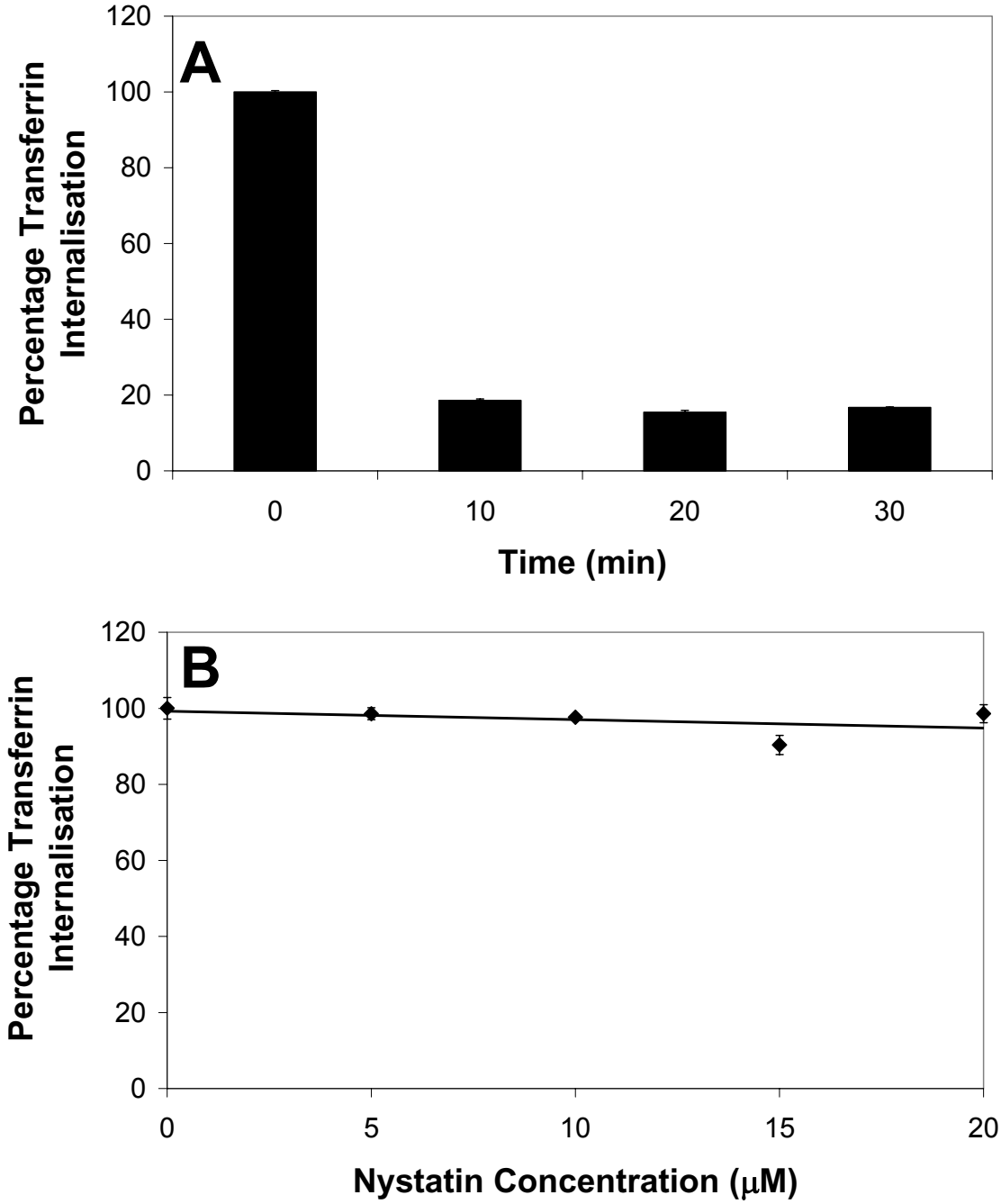

Figure 2.9: The effects of chlorpromazine and nystatin on transferrin internalisation. PC-3 cells were incubated with **(A)** chlorpromazine (40 μM) for the time periods indicated, or **(B)** nystatin (at the concentrations indicated) for 10 min, in binding buffer, at 37°C. Following three washes with ice-cold binding buffer, the cells were incubated with transferrin:Alexa$_{488}$ (10 nM) for 20 min, on ice. Following another three washes with ice cold binding buffer the cells were re-suspended in binding buffer pre-warmed to 37°C for 45 min. The cells were then incubated in the presence or absence of the quenching antibody (4 μg/mL) for 30 min on ice. The amount of internalised PAI-2:Alexa$_{488}$ fluorescence of viable cells was measured using dual colour flow cytometry (Values are ± SEM, n=3). Data were fitted using GraphPad v4 (Prism).

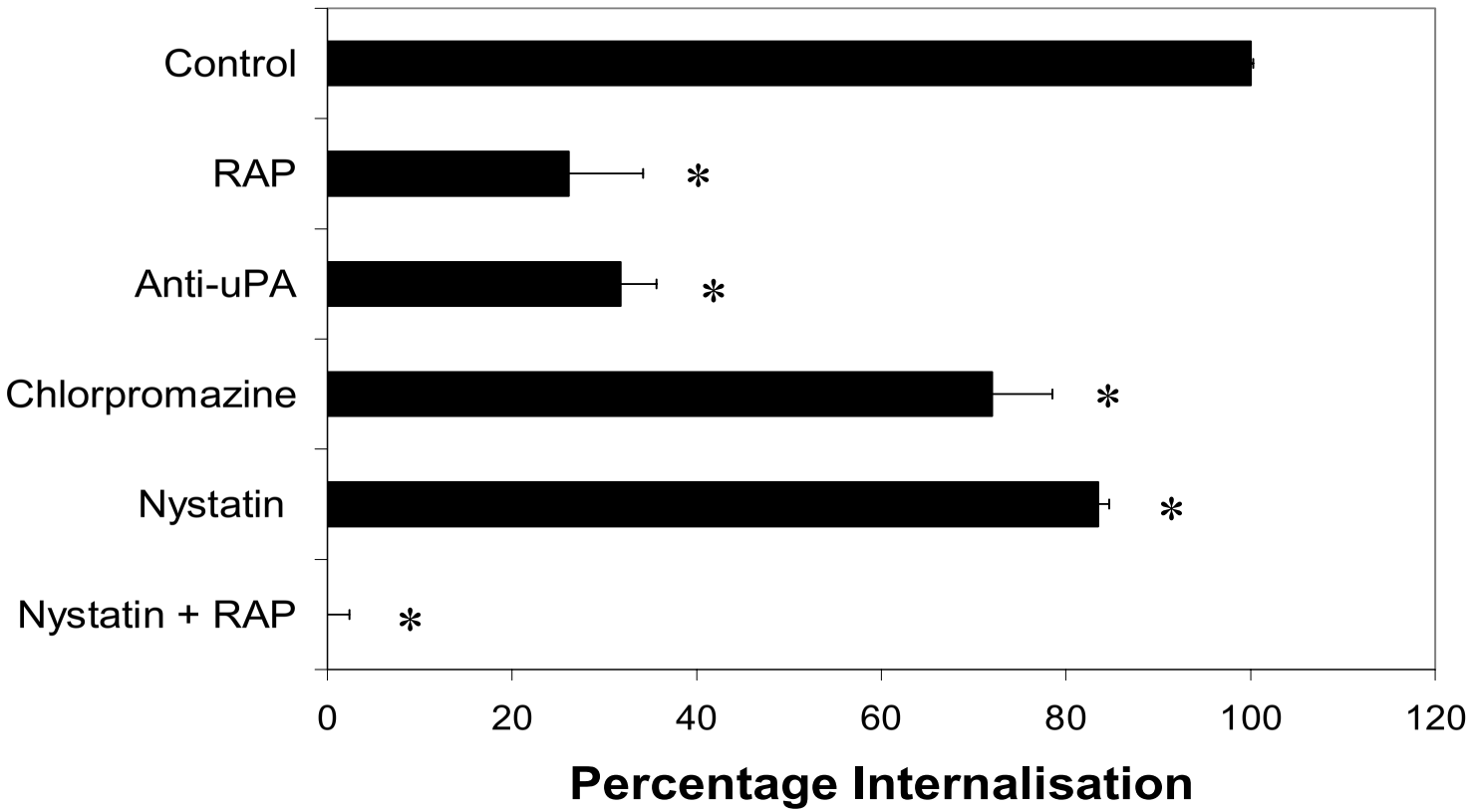

Figure 2.10: PAI-2 endocytosis can be prevented by inhibitors of clathrin dependent and independent processes. PC-3 cells were treated with either RAP (200 nM), anti-uPA monoclonal antibody (20 µg/mL), chlorpromazine (40 µM) or nystatin (20 µM) for 10 min at 37ºC, or a combination of these as indicated, prior to analysis of PAI-2:Alexa488 internalisation by the fluorescence quenching internalisation assay. Each value for internalised PAI-2 was taken as a percentage of the relevant control (values are ± SEM, n=3). Values obtained for all treatments are significantly different to the control (*$p<0.05$).

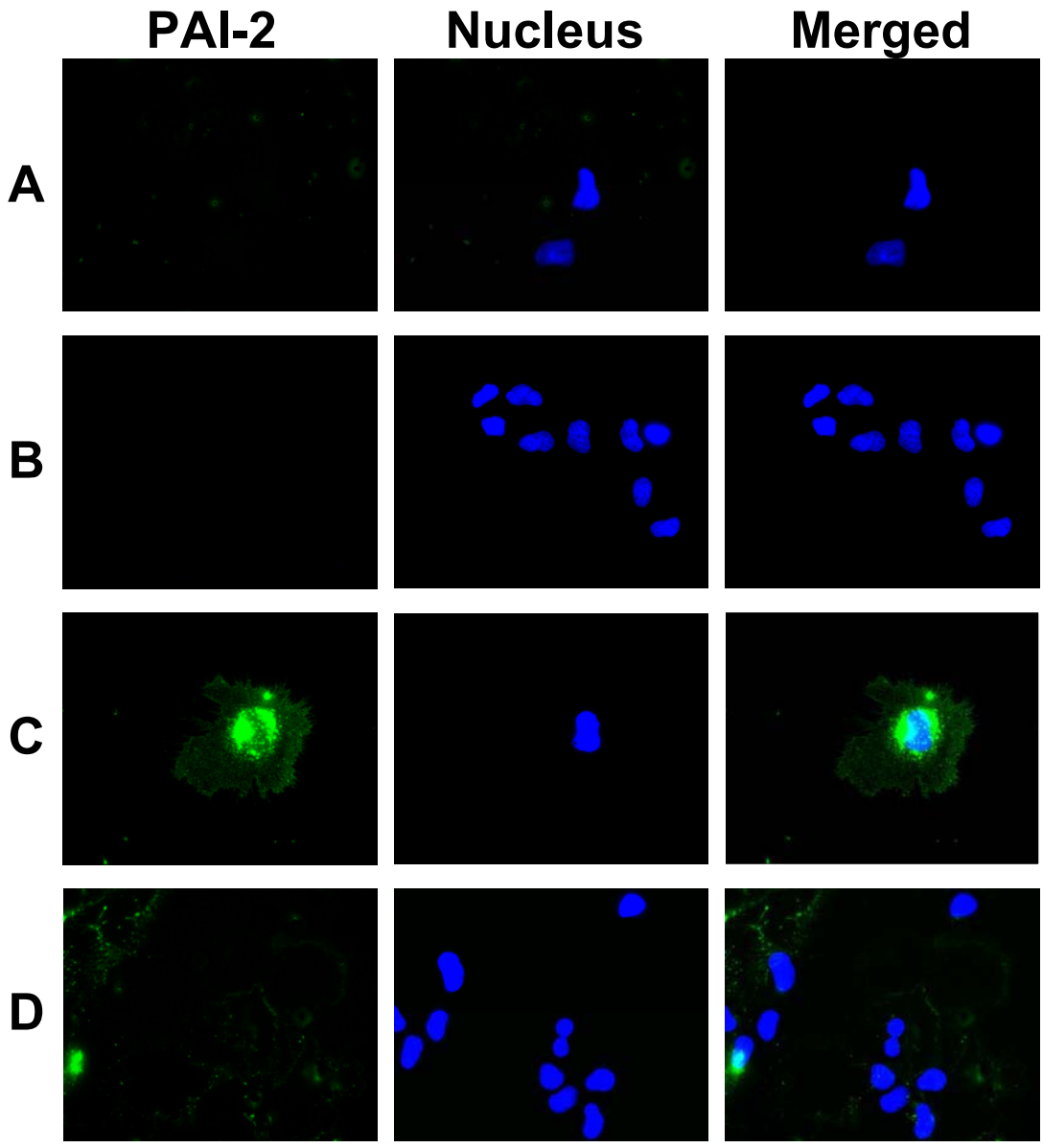

Figure 2.11: PAI-2 is internalised in a uPA, uPAR and LDLR specific manner by HEK 293 cells. HEK 293 cells, either wild-type **(A)** or transfected with uPAR **(B,C and D)** were grown on glass coverslips and incubated with either biotinylated PAI-2/Streptavidin-FITC (green) **(B)** or biotinylated PAI-2/Streptavidin-FITC in complex with uPA **(A,C and D)**, in the presence **(D)** or absence **(A,B and C)** of RAP (200 nM) for 1 h at 37°C. The cell monolayers were then washed three times with ice cold binding buffer, fixed with 3.75% PFA for 15 min on ice, permeabilised with 0.1% triton-X for 5 min on ice and incubated with DAPI (blue) (1:1000 dilution) for 15 min on ice. Following another two washes with ice cold binding buffer, the coverslips were mounted and viewed using epifluorescence.

2.3.7 Annexin II Dependent PAI-2 Internalisation

The incomplete inhibition of PAI-2 internalisation in the presence of RAP or the anti-uPA antibody (section 2.3.6) suggests that an alternative binding site for PAI-2 exists on the surface of PC-3 cells. As an interaction between annexin II and PAI-2 has been previously proposed (Jensen et al., 1996) and annexin II was present on the surface of these cells (section 2.3.1), it was therefore hypothesised that this interaction may be responsible for the RAP-insensitive, uPA-independent internalisation. Pre-incubation of PC-3 cells with an polyclonal antibody against annexin II, previously used to examine the binding of viral particles to cell surface annexin II (Pietropaolo and Compton, 1999), inhibited ~30% of PAI-2 internalisation (Figure 2.12), equivalent to the amount of RAP-insensitive, uPA-independent internalisation observed in these cells (section 2.3.6).

Annexin II is often present at the cell surface as a heterotetramer, consisting of two sub-units of annexin II and two of p11 (Gerke and Moss, 2002). To confirm that PAI-2 is able to interact with the heterotetrameric form of annexin II, SPR analysis of this interaction was undertaken. Annexin II heterotetramer bound to immobilised PAI-2 with a K_D of ~172 nM (χ^2 of 6.2).

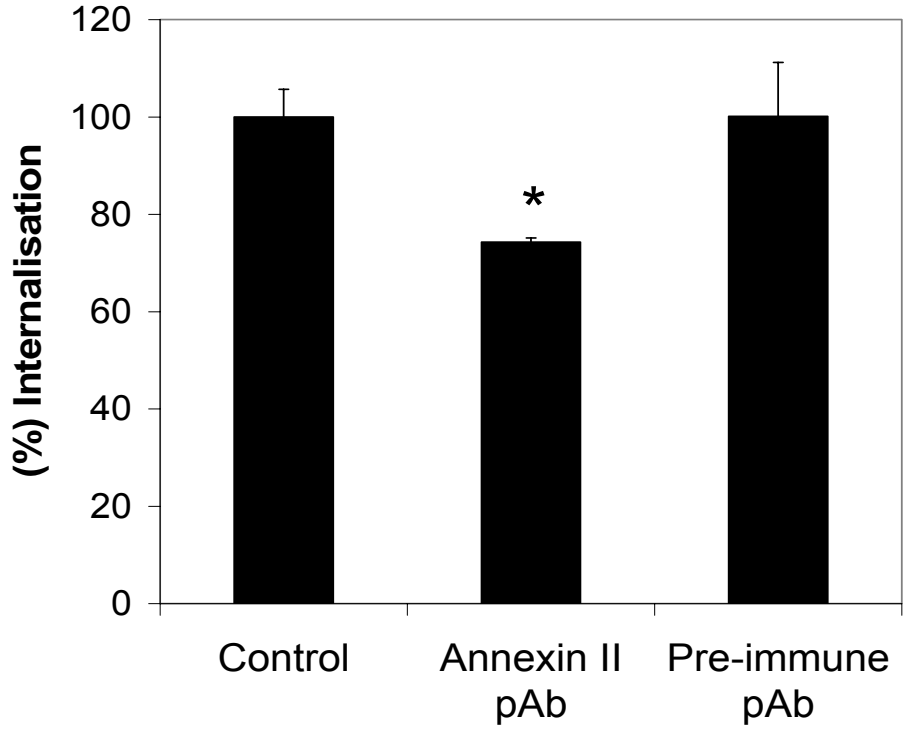

Figure 2.12: PAI-2 is internalised in a partially annexin II dependent manner on PC-3 cells. PC-3 cells were treated with either protein-G purified antibodies from annexin II anti-serum or pre-immune anti-serum (1:20 dilution) for 15 min at 37ºC, prior to analysis of PAI-2:$Alexa_{488}$ internalisation by the fluorescence quenching internalisation assay. Each value for internalised PAI-2 was taken as a percentage of the PAI-2 internalisation in the absence of inhibitors (control) (values are ± SEM, n=3). Values marked with an asterisk are significantly different from the control (*p<0.05).

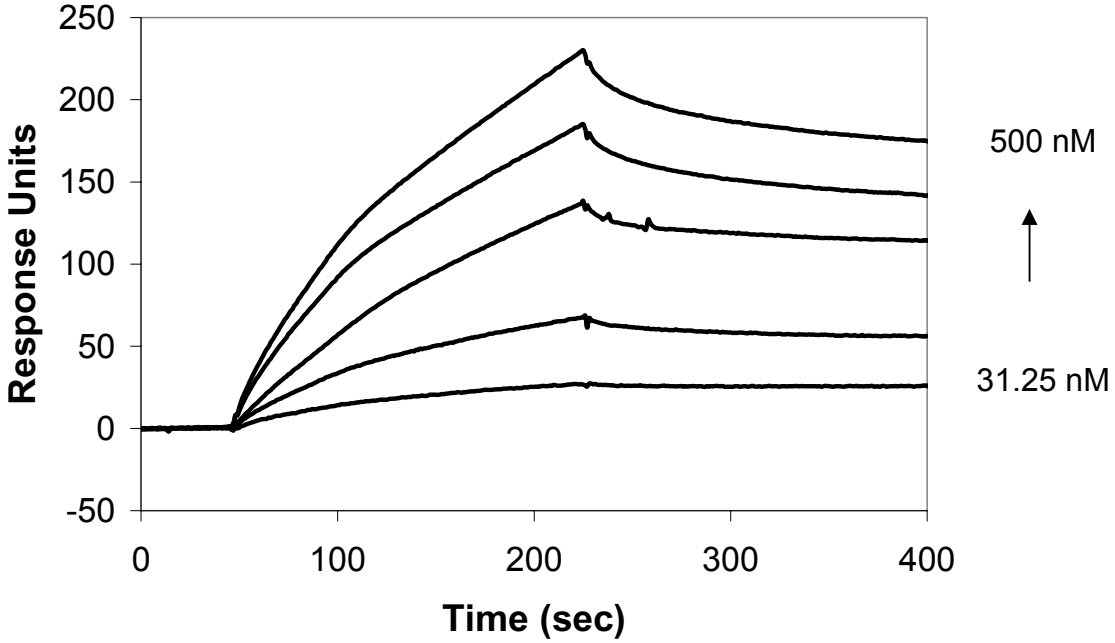

Figure 2.13: The interaction of bovine annexin II heterotetramer and PAI-2, measured by surface plasmon resonance. A sensorgram showing dose dependent binding of bovine annexin II heterotetramer (31.25 – 500 nM) to immobilised PAI-2 is shown.

2.4 DISCUSSION

Previous research into PAI-2 internalisation by Ragno *et al*. (1993 and 1995) was self-contradicting. A paper published by this group in 1993 claimed that cell surface uPA bound PAI-2 was cleaved into two fragments, a 22 kDa fragment consisting of the ATF of uPA and a 70 kDa fragment consisting of the PAI-2 molecule and the remaining uPA. It was claimed that the 22 kDa fragment remained bound to the cell surface, whilst the 70 kDa fragment was internalised by an un-determined mechanism, suggested to be endocytosis mediated by LRP. The cleavage of the uPA:PAI-2 complex was declared to be caused by 'stretching' of uPA:PAI-2 between uPAR and another receptor. In 1995, the same group recanted and claimed that the 70 kDa fragment was not internalised, instead this fragment was released into the medium.

However, the formation of these fragments from the uPA:PAI-2 complex is a process that is not reliant on uPAR nor another receptor. These fragments can be reproduced by the incubation of the uPA:PAI-2 complex with excess uPA (Al-Ejeh et al., 2004), they are the product of proteolysis caused by the action of the free serine protease upon itself, once complexed with PAI-2. Therefore, the production of these fragments was most likely facilitated through the experimental procedure of Ragno et al. (1993 and 1995). THP-1 cells were acid stripped and then incubated with radio-iodinated uPA:PAI-2 pre-formed complex that contained a large amount of un-complexed uPA. This excess uPA would have not only caused the cleavage of the uPA:PAI-2 complex into the observed fragments, regardless of uPAR binding, but would also have caused a competitive binding situation between labeled uPA and uPA:PAI-2. The conclusion that the 70 kDa fragment was released into the medium was because it was not able to bind to cell surface uPAR because it lacked the ATF, which stayed bound to the cell surface. Consequently, the combination of reduced uPA:PAI-2

binding and the production of fragments which were artefacts of experimental procedure most likely lead to the contradictory conclusions published. The latter conclusion of Ragno et al. that PAI-2 was cleaved at the cell surface and released was thus accepted in the literature, despite the evidence to the contrary (Estreicher et al., 1990; Jensen et al., 1990).

In contrast to this, the data presented in this chapter provides definitive proof that PAI-2 is indeed internalised following the inhibition of cell surface uPA. By utilising the PC-3 cell line, which expresses high levels of uPAR and also active uPA, the uPA dependent binding of PAI-2 to the surface of these cells has been thoroughly demonstrated (Al-Ejeh et al., 2004). This was further demonstrated here by the use of the 2H5 antibody which preferentially recognises the relaxed form of PAI-2. PC-3 cells incubated sequentially with uPA and PAI-2 presented high levels of binding by both the 2H5 antibody and also a generic PAI-2 monoclonal antibody.

The internalisation of PAI-2 was first observed in PC-3 cells using confocal microscopy. By using transferrin:$Alexa_{488}$ a marker of early endosomes (van Dam et al., 2002) and lysotracker, a marker of lysosomes, PAI-2 was observed to be internalised firstly into endosomes and then lysosomes. However, in order to obtain detailed data about the pathway through which PAI-2 is internalised, a quantitative internalisation assay was developed utilising PAI-2 labeled with $Alexa_{488}$ and a polyclonal antibody capable of quenching the fluorescence of $Alexa_{488}$.

The necessary conditions for the internalisation assay were obtained by determining the length of time needed to saturate PAI-2:$Alexa_{488}$ binding to the surface of PC-3 cells (2.5 min), the concentration of antibody (2 μg/mL) and incubation period (10 min) needed to fully quench the bound PAI-2:$Alexa_{488}$. After obtaining this data, an

internalisation assay was developed based on a generous amount of time or concentration for each parameter (see method in section 2.3.4).

Firstly, the internalisation of PAI-2 was observed in a qualitative manner using confocal microscopy. After a 20 min incubation on ice, PAI-2 could be seen bound to the surface of the PC-3 cells. This PAI-2 was completely quenched by addition of the polyclonal antibody. Upon increasing the temperature to 37°C, the PAI-2 increased intracellularly and decreased at the cell surface. By using flow cytometry to measure the quenchable/unquenchable fluorescence, the amount of internalised PAI-2 and consequently the rate of internalised PAI-2 was measured. The rate of PAI-2 internalisation was similar to that observed for PAI-1 by determining the amount of non-acid extractable ^{125}I:uPA:PAI-1 internalised by U937 cells (Cubellis et al., 1990). This paper extended the time frame of the experiment out to three hours in order to observe the degradation of the uPA:PAI-1 complex, which occurred rapidly after ~40 min, a time frame which is supported by the delivery of PAI-2 to the lysosomes after 45 min, as observed using confocal microscopy.

To gain a more detailed analysis of PAI-2 internalisation, inhibitors of endocytosis pathways were employed to determine the contribution of each of these pathways to PAI-2 internalisation. Chlorpromazine, which breaks down clathrin coated pits, and nystatin, a cholesterol sequestering agent that disrupts caveolae and lipid rafts were used (Anderson et al., 1996), however both of these chemicals can have significant cytotoxic effects if used at high concentrations. To determine a safe concentration for these inhibitors, cytotoxicity assays were undertaken based on the ability of viable cells to exclude PI. It is interesting to note that the sub-toxic concentrations determined by these assays are very similar to those used in other studies (Deckert et al., 1996; Pho et al., 2000; Stuart et al., 2002; Vendeville et al., 2004).

By using RAP, an inhibitor of the LDLR family, and an anti-uPA antibody capable of blocking PAI-2 inhibition of uPA (Al-Ejeh et al., 2004), it was clearly demonstrated that the majority of PAI-2 internalisation occurred through the sequential binding of uPA and an LDLR endocytosis receptor, as indicated by the equal amounts of inhibition seen by the use of either RAP or the anti-uPA antibody. However, as pre-incubation with either RAP or the anti-uPA antibody was unable to completely inhibit PAI-2 internalisation, the presence of an alternative (ie uPA- and LDLR-independent) PAI-2 binding site is possible. The inefficient inhibition by chlorpromazine also suggests the presence of an alternative mechanism of PAI-2 endocytosis. The amount of inhibition by chlorpromazine should be reflected in that of RAP, as chlorpromazine was an efficient inhibitor of transferrin internalisation, and the transferrin receptor is known to be internalised through clathrin coated pits (van Dam et al., 2002) as are the LDLR family (Hussain et al., 1999).

The inhibition of PAI-2 internalisation by nystatin also suggested the involvement of lipid rafts and/or caveolae in PAI-2 endocytosis. It should be noted that nystatin did not effect the internalisation of transferrin under these conditions, indicating that the inhibition observed by the use of nystatin was specific to caveolae and/or lipid rafts and not due to non-specific disruption of clathrin coated pits. LRP has been recently detected within caveolae and lipid rafts (Boucher et al., 2002; Wu et al., 2004), suggesting that nystatin treatment may also interfere with LDLR dependent endocytosis of PAI-2, however the cumulative effects of nystatin and RAP in this assay do not support this as their effects on PAI-2 endocytosis seem to be additive and not cooperative. Furthermore, the presence of LDLR family members within caveolae may also explain the persistence of uPA:PAI-2 internalisation in the presence of chlorpromazine, whilst transferrin internalisation (which is not mediated by receptors of

the LDLR family) was almost completely inhibited. uPAR dependent endocytosis of uPA:PAI-2 by caveolae is also not unfeasible, as uPAR is known to localise into these regions (Stahl and Mueller, 1995). However, given that in the presence of both nystatin and RAP, PAI-2 internalisation was completely abolished, an additional unknown uPA- and LDLR-independent mechanism of PAI-2 internalisation mediated via caveolae or lipid rafts must also be operating in these cells.

The inhibition of the RAP-insensitive PAI-2 internalisation by both annexin II polyclonal antibodies and nystatin, and the interaction of annexin II and PAI-2 by SPR, provide evidence to suggest that annexin II, present at the surface of these cells as a heterotetramer, and localised in lipid rafts or caveolae, is responsible for this proportion of PAI-2 binding and internalisation. Supporting this data, various cell types are known to express annexin II at their cell surface, including; carcinoma cells (Andronicos and Ranson, 2001), endothelial cells (Hajjar et al., 1994), epithelial cells (Ma et al., 1994), fibroblasts (Pietropaolo and Compton, 1999), macrophages (Falcone et al., 2001) and monocytes (Brownstein et al., 2004). Furthermore, its localisation into detergent-insoluble membrane domains (i.e. caveolae and/or lipid rafts) has also been established (Garver et al., 1999; Myers and Stanley, 1999; Stahl and Mueller, 1995). Annexin II, present at the plasma membrane facilitates cell adhesion through direct interaction with cell adhesion molecules (Kirshner et al., 2003) and in the formation of tight junctions (Lee et al., 2004). It has also been implicated in the activation of plasminogen on endothelial cells, through its role as a co-receptor for plasminogen and tPA, either on its own or as a heterotetramer consisting of to annexin II (p36) and two p11 subunits (Hajjar et al., 1994; Kwon et al., 2005; MacLeod et al., 2003; Waisman, 2005). This suggests that physiologically the interaction of PAI-2 with annexin II may exert effects on both cell adhesion and pericellular protease activity. Furthermore, annexin II may

present an alternative and possibily deleterious target for ^{213}Bi:PAI-2. However the biochemical details and functional consequences of this interaction are currently under further investigation and are beyond the scope of this thesis.

A further example of the receptor mediated endocytosis of PAI-2 is the uPAR and LDLR specific internalisation of uPA:PAI-2 by HEK-293 cells. Wild-type cells that do not express detectable uPAR or annexin II heterotetramer (MacLeod et al., 2003) did not internalise either uPA:PAI-2 or PAI-2, however upon transfection with uPAR significant amounts of uPA:PAI-2 was seen inside the cells. That this internalisation was almost completely inhibited by the addition of RAP is a strong indication of the involvement of LDLR receptors in this process.

This data therefore presents a mechanism through which PAI-2 inhibits and clears cell surface uPA by forming a covalent complex which is then recognised by members of the LDLR family of endocytosis receptors, leading to internalisation and degradation of uPA:PAI-2 in the lysosomes. The particular members of the LDLR family that are involved in this process and the details of the interaction between uPA:PAI-2 and these members are the focus of the two subsequent chapters of this thesis.

This data also provides valuable information for the use of PAI-2 as a cancer therapeutic, as the internalisation of PAI-2 into the lysosomes presents an opportunity for an alternative form of PAI-2 cancer therapy that does not involve the use of expensive and short half-life radioisotopes, but instead depends on a cytotoxin attached to PAI-2 through an acid labile linker. Upon exposure to the decreased pH of the late endosomes and lysosomes, this linker would be cleaved and the cytotoxin released from PAI-2, allowing it to exert its toxic effect on the cell.

Chapter 3

3. The Role of LRP in the Receptor Mediated Endocytosis of uPA:PAI-2

3.1 INTRODUCTION

Inhibition of uPA proteolytic activity at the cell surface is an important step in the regulation of pericellular plasminogen activation (Chapter 1.2). This process is facilitated by members of the serpin superfamily, most notably by PAI-1 and PAI-2 (SerpinE1, SerpinB2, respectively) (Chapter 1.2.5). Whilst both are efficient uPA inhibitors, PAI-1 and PAI-2 are structurally and functionally quite distinct serpins, as recognised by their grouping into different serpin sub-family groups (Silverman et al., 2001). For example, PAI-1 also has alternative non-uPA inhibitory activities that affect cell adhesion, intracellular signalling and cell migration that have not been demonstrated for PAI-2 (Chapter 1.2.6).

It was recently reported that the efficient and rapid inhibition of uPAR bound uPA by PAI-2 at the surface of MDA-MB-231 and PC-3 carcinoma cells led to the rapid internalisation of the uPAR/uPA:PAI-2 complex and delivery into endosomes and lysosomes (Al-Ejeh et al., 2004) (See also Chapter 2). The internalisation of PAI-2 was shown to be uPA dependent and partially inhibited by RAP, indicating the involvement of LDLR family members in the receptor mediated endocytosis of uPA:PAI-2. However, the mechanism/s of PAI-2 endocytosis are unknown.

The receptor mediated endocytosis of uPA:PAI-1 complexes is known to be mediated by a high affinity interaction with at least three different members of the LDLR family of endocytosis receptors; LRP (Herz et al., 1992; Kounnas et al., 1993), VLDLr (Argraves et al., 1995; Rettenberger et al., 1999; Webb et al., 1999) and LRP-2 (megalin or gp330) (Stefansson et al., 1995). Following endocytosis, the uPA:PAI-1 complex is degraded in the lysosomes (Cubellis et al., 1990; Jensen et al., 1990) and uPAR is recycled back to the cell surface (Nykjaer et al., 1997). All three interactions are inhibitable by RAP (Andreasen et al., 1994; Heegaard et al., 1995) and are calcium

dependent, as the conformation of the receptor is dependent upon the binding of calcium ions (Moestrup et al., 1993a). In terms of the endocytosis of serpin:uPA complexes, LRP is the most thoroughly characterised LDLR family member (Andreasen et al., 1994; Gonias et al., 2004; Nykjaer and Willnow, 2002; Strickland et al., 2002). LRP binds and internalises numerous, structurally diverse ligands and has been implicated in a range of biological processes including receptor endocytosis, cell signaling, antigen presentation, phagocytosis, and regulation of vascular permeability (Gonias et al., 2004).

Comprehensive analysis of the interaction between uPA:PAI-1, PAI-1 and LRP has previously been undertaken (Andersen et al., 2001; Nykjaer et al., 1994; Rodenburg et al., 1998; Stefansson et al., 1998). This has not been the case for PAI-2, possibly as a result of a previous study using denatured bovine LRP that found no interaction between uPA:PAI-2 and LRP (Heegaard et al., 1995). Herein, this chapter shows for the first time that PAI-2 is internalised by a process of receptor mediated endocytosis. Furthermore, by using techniques that maintain the native, calcium-dependant conformation of human LRP, that this involves a high affinity interaction between uPA:PAI-2 and native LRP. These results also suggest that the high affinity binding sites for LRP lie solely within the uPA moiety of the uPA:PAI-2 complex, as there was no evidence of a corresponding site within either relaxed or stressed PAI-2 molecule. This indicates a clear distinction with PAI-1, where a high affinity site within the PAI-1 moiety of uPA:PAI-1 complex contributes significantly to LRP binding (Stefansson et al., 1998). Furthermore, the uPA:PAI-2 complex is still able to bind LRP in the presence of uPAR, indicating the validity of this interaction at the cell surface. This has important physiological implications for pericellular proteolytic control, through the inhibition of plasmin formation (Chapter 1.2.2) and also the clearance/recycling of

uPA/uPAR (Chapter 1.3), and also for cell signaling mechanisms that involve interactions between uPA, uPAR and the LDLR family (Chapter 1.3.4 and Chapter 4). This data also provides further characterisation of the pathways through which PAI-2 is internalised by cancer cells.

3.2 MATERIALS AND METHODS

3.2.1 Proteins, Antibodies and Reagents

Many proteins, antibodies and reagents used in this chapter are previously described (Chapter 2.2.1). Additionally, the PAI-2 CD loop mutant (residues 66-98 deleted) (Harrop et al., 1999) was provided by PAI-2 Pty Ltd (Sydney, Australia). Purified human placental LRP was a kind gift from Prof Phillip Hogg (University of New South Wales, Sydney, Australia). Human HMW uPA was from American Diagnostica (CT, USA). Anti-LRP heavy chain (#3402) was from American Diagnostica. Recombinant human uPAR was from Calbiochem (CA, USA). Anti-DNP rabbit polyclonal isotype control was from DakoCytomation (Glostrup, Denmark). Biotin NHS and enhanced chemiluminescence kit were from Pierce (IL, USA). Rabbit anti-mouse IgG-HRP, Neutravidin-HRP and nitrocellulose were from Bio-Rad Laboratories, (NSW, Australia).

3.2.2 Fluorescence Quenching Internalisation Assay

Internalisation assays were undertaken as described in Chapter 2.2.4.2

3.2.3 Co-localisation Studies using Confocal Microscopy

Confocal fluorescence microscopy was performed essentially as previously described (Andronicos and Ranson, 2001), with the exception of the PAI-2 binding and internalisation step. Briefly, PC-3 cells were grown on glass coverslips, washed with ice-cold binding buffer and pre-incubated for 1 h in binding buffer at 37˚C to pre-cycle cell surface receptors. Following this, the cell monolayers were pre-incubated in the presence or absence of RAP (100 nM) for 15 min at 37˚C and then with 10 nM PAI-2:$Alexa_{488}$ for 1 h at 18˚C. After a further washing with ice-cold PBS, the cells were fixed with 3.75% PFA for 20 min on ice. The cells were permeabilised using 0.1% Triton-X100 in PBS for 5 min at room temperature, washed with ice-cold PBS and non-specific sites blocked by incubation with PBS/BSA (0.1%) for 30 min on ice. LRP was detected by incubation with 10 µg/mL of anti-LRP polyclonal antibody in PBS/BSA (0.1%) for 45 min on ice. After two washes with ice cold PBS, the cells were incubated with goat anti-rabbit IgG-Cy5 (1:50 dilution) in PBS/BSA (0.1%), for 45 min on ice. After two washes with ice-cold PBS, the cells were analysed by confocal microscopy using a Leica TCS SP system (Leica, Heidlberg, Germany).

3.2.4 Binding of uPA:PAI-2 to Immobilised LRP

Ligand blotting was undertaken for the initial characterisation of uPA:PAI-2 binding to LRP as this procedure is often used to investigate the interaction between LRP and potential ligands (Andersen et al., 2001; Misra et al., 2002; Wang et al., 2004). Purified LRP (1 µg) was dotted onto nitrocellulose and dried for 30 min at 37˚C. The membrane was then blocked by incubation in Tris-buffered saline (Appendix 1) containing Tween 20 (0.05%) (TBST) and 3% gelatin for 1 h at room temperature. After three 10 min washes with TBST/$CaCl_2$ (1 mM), the membranes were incubated with

various biotinylated ligands or monoclonal antibodies for 1 h at room temperature in TBST/1% gelatin/$CaCl_2$. It has been previously demonstrated that incubation of an equimolar ratio of uPA to PAI-2 results in almost complete inactivation of uPA by conversion to uPA:PAI-2 complex (Saunders et al., 1998). However, complexes between uPA and biotinylated PAI-2 were formed by incubating a 10 molar excess of PAI-2 with uPA at 37˚C for 90 min to facilitate maximal formation of uPA:PAI-2 complexes, while minimising formation of cleavage products from excess uPA (Al-Ejeh et al., 2004). In some cases, the membranes were pre-incubated with RAP (100 nM) or EDTA (5 mM) in TBST/1% gelatin/$CaCl_2$ for 30 min, at room temperature then washed prior to adding ligands or antibodies. In the case of EDTA inhibition, EDTA (5 mM) was also present during the incubation with uPA:PAI-2 to prevent the restoration of calcium binding by LRP. After another three 10 min washes with TBST, the membranes were incubated with neutravidin-HRP (1:10,000 dilution) or rabbit anti-mouse IgG-HRP (1:50 dilution) for 1 h at room temperature in TBST/1% gelatin/$CaCl_2$. Following a further three 10 min washes with TBST/$CaCl_2$, the membranes were finally washed with TBS/$CaCl_2$ for 10 min and then developed by enhanced chemiluminescence.

3.2.5 Surface Plasmon Resonance Analysis

3.2.5.1 Protein Preparation/Purification

To further analyse the interaction between the uPA:PAI-2 complex and LRP, surface plasmon resonance (SPR) assays were performed using a BIAcore 2000 (BIAcore AB, Uppsala, Sweden). Purified complexes were necessary for SPR analysis, as excess proteins would significantly interfere with measurements. In order to prepare HMW and LMW uPA:PAI-2 complexes, a 10 fold molar excess of PAI-2 was incubated

with a mixture of HMW and LMW uPA for 30 min at 37˚C. The crude mixture of uPA:PAI-2 complexes was buffer exchanged into 50 mM phosphate buffer (pH 6) using 30 kDa cut-off spin columns. The crude mixture was applied to a mono-C ion-exchange spin column which was centrifuged at 300 x *g* for 4 min. Following three 400 µL washes with 50 mM phosphate buffer, the bound proteins were eluted using a NaCl step gradient (0 – 0.5 M) by applying 400 µL aliquots of increasing NaCl concentration to the column, between each centrifugation/elution step (Saunders et al., 1998). Non-reducing SDS-PAGE confirmed the presence of purified uPA:PAI-2 complexes (See Figure 3.5).

Relaxed PAI-2 was formed by the incubation of PAI-2 (1 mg/mL) with a 100 fold molar excess of RCL peptide in 10 mM phosphate buffer (pH 8) (Appendix 1) for 48 h at 37°C. Excess RCL peptide was removed using a 30 kDa cut-off spin column. The extent of relaxed PAI-2 formation was determined by incubating PAI-2 with uPA (5:1 molar ratio) for 30 min at 37°C and determining complex formation using SDS-PAGE. This method has previously been shown to result in complete conversion of PAI-2 to the relaxed conformation, forming stable PAI-2/RCL complex with no detectable uPA-inhibitory activity (Saunders et al., 1998; Saunders et al., 2001).

3.2.5.2 BIAcore Analysis

LRP was immobilised to a CM5 BIAcore chip according to manufacturer's instructions. Briefly, the chip was activated using a 1:1 mixture of 0.2M *N*-ethyl-*N'*-(3-dimethylaminopropyl)carbodi-imide and 0.05M *N*-hydroxysuccimide. LRP was coated to the chip at 40 µg/mL in 10 mM sodium acetate buffer (pH 3) for 7 min at 5 µL/min, as previously described (Andersen et al., 2001). The immobilisation resulted in LRP coated to the chip between 15-28 fmol/mm^2. The un-occupied binding sites were

blocked using 1M ethanolamine, pH 8.5 (An example of immobilisation is shown in Appendix 4). Ligands were desalted into running buffer (Appendix 1) before applying to the BIAcore chip at 20 μL/min. Regeneration of the chip was achieved using 1.6 M glycine (pH 3)/EDTA (5 mM). All buffers were filtered and degassed before use. For kinetic analysis, a blank cell was used as the reference cell and data was analysed using BIAevaluation software (Version 4). A one-binding site model with a drifting baseline provided the best fit according to χ^2 values and analysis of residual plots (An example of BIAcore analysis is provided in Appendix 5).

3.3 RESULTS

3.3.1 Candidate Endocytosis Receptors Involved in the Internalisation of PAI-2

It has been shown previously that efficient inhibition of cell surface uPA by PAI-2 on carcinoma cell lines resulted in rapid internalisation of the uPAR/uPA:PAI-2 complex and delivery into endosomes and lysosomes through a RAP-inhibitable mechanism (See Chapter 2) (Al-Ejeh et al., 2004), suggesting internalisation via receptor mediated endocytosis. As already demonstrated (Chapter 2.3.1), LRP was expressed at the surface of PC-3 cells, while VLDLr was barely detectable and megalin (LRP-2) was not detectable. PAI-2 endocytosis was substantially inhibited by both RAP and an anti-catalytic uPA monoclonal antibody (Chapter 2.3.6)

Pre-incubation with a polyclonal antibody against LRP, previously used to inhibit endocytosis of LRP ligands (Stefansson et al., 1995), resulted in ~40% inhibition of PAI-2 endocytosis (Figure 3.1). This may indicate inefficient inhibition by the anti-LRP polyclonal antibody or alternately that the remaining 20-30% of RAP-dependent

endocytosis of PAI-2 may be mediated by VLDLr or other mechanisms. By utilising confocal microscopy to visualise internalised PAI-2, a proportion of the internalised PAI-2 was observed to co-localise with LRP in intracellular vesicles (Figure 3.2). This was confirmed to be RAP-sensitive, as little or no co-localised PAI-2 and LRP could be detected in the presence of RAP. These data also indicate that a small, but significant, component of PAI-2 endocytosis is mediated by a uPA- and LDLR family member-independent mechanism(s), possibly mediated through low affinity binding to cell surface Annexin II heterotetramer, as addressed in Chapter 2. Nevertheless, LRP clearly facilitates a proportion of PAI-2 endocytosis in PC-3 cells.

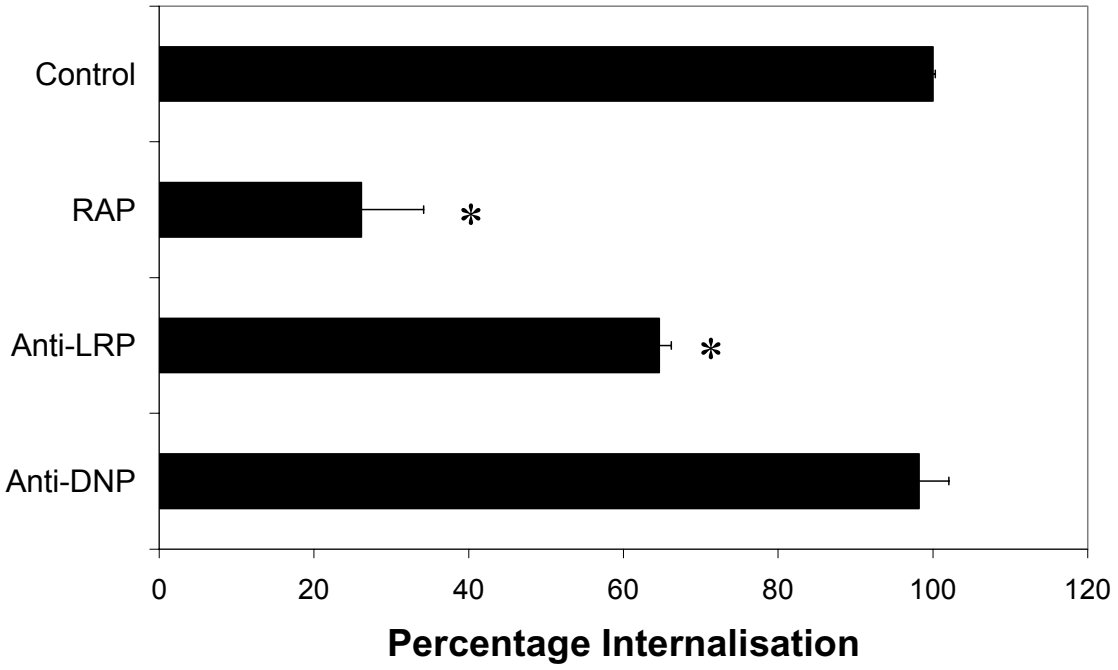

Figure 3.1: PAI-2 endocytosis is inhibited by anti-LRP antibodies. PC-3 cells were treated with either RAP (200 nM), anti-LRP polyclonal antibody (50 µg/mL) or an irrelevant control polyclonal antibody (anti-DNP) (50 µg/mL) prior to analysis of PAI-2:$Alexa_{488}$ internalisation by the fluorescence quenching internalisation assay. Each value for internalised PAI-2 was taken as a percentage of the control, which was calculated as the amount of PAI-2 internalisation in the absence of inhibitors (values are ± SEM, n=3). Values marked with an asterisk are significantly different from the control (*$p<0.05$).

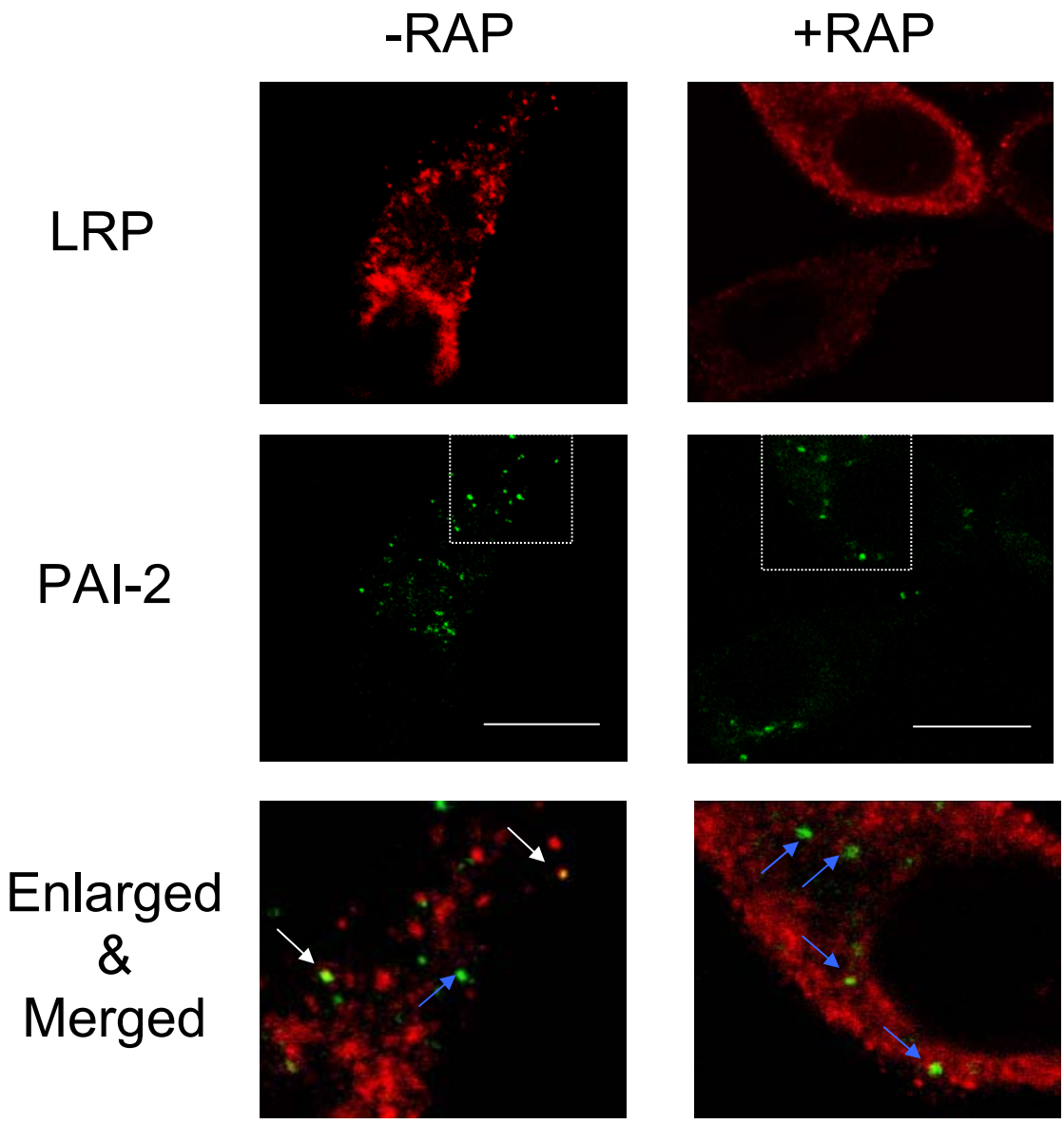

Figure 3.2: The RAP sensitive co-localisation of internalised PAI-2 and LRP. PC-3 cell monolayers were incubated with 10 nM PAI-2:Alexa$_{488}$ for 1 h at 37°C, in the presence or absence of 200 nM RAP. After washing with ice-cold binding buffer the cells were fixed with 3.75% PFA and permeabilised with 0.1% Triton-X. After washing with ice cold PBS, the cells were blocked with PBS containing 0.1% BSA. LRP was detected by probing with an anti-LRP polyclonal antibody (10 µg/mL) and anti-rabbit Cy5 secondary antibody (1:200 dilution). Internalised PAI-2 co-localised with LRP is indicated by white arrows, internalised PAI-2 not co-localised with LRP is indicated with blue arrows. The enlarged and merged images correspond to the white boxed areas in full size PAI-2 images. Scale bars are 10 µm.

3.3.2 The Interaction Between uPA:PAI-2 and LRP

As there is no existing data pertaining to the potential interaction of uPA:PAI-2 with LRP, studies were undertaken to examine the biochemical interactions underlying this mechanism. Initial characterisation of the interaction between uPA:PAI-2 and LRP was undertaken via ligand dot blotting (Figure 3.3). This analysis showed a direct interaction between uPA:PAI-2 and LRP, however no interaction between PAI-2 alone and LRP was detected. The uPA:PAI-2/LRP interaction was inhibited by pre-incubation with either RAP or EDTA, indicating specific, calcium-dependent binding. Deletion of the CD-loop within PAI-2 (Harrop et al., 1999) did not affect binding of uPA:PAI-2 to LRP.

While the use of crude complexes for ligand dot blotting was acceptable, SPR is a much more sensitive assay and the presence of bulk protein would interfere with its measurements. Therefore, prior to SPR analysis, LMW uPA:PAI-2 and HMW uPA:PAI-2 complexes were prepared (section 3.2.7.1). In a method adapted from Saunders et al. (1998), the application of the mixture to a mono-C spin column at pH 6 resulted in the binding of the uPA:PAI-2 complexes to the column while the free PAI-2 was found in the flow-through (Figure 3.4). Following salt elution, the LMW uPA:PAI-2 complexes eluted at 0.1 M NaCl and the HMW uPA:PAI-2 complexes at 0.4 M NaCl (Figure 3.4). Relaxed PAI-2 was formed by the insertion of an RCL peptide. The conversion of PAI-2 from a stressed to relaxed state was confirmed by its lack of ability to form a complex with uPA, instead becoming a substrate for uPA cleavage (Figure 3.5). SPR analysis was undertaken using a BIAcore 2000 to obtain a more detailed characterisation of uPA:PAI-2 binding to LRP (Figure 3.6, 3.7 and Table 3.1).

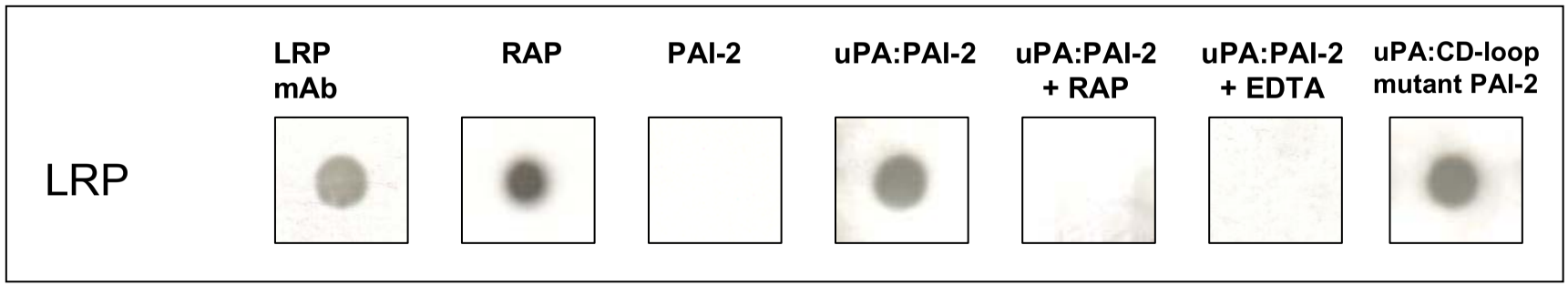

Figure 3.3: Ligand dot blot analysis of the interaction between uPA:PAI-2 and LRP. Immobilised LRP (1 µg) was incubated with various biotinylated ligands or monoclonal antibodies (as shown). For RAP and EDTA inhibition of uPA:PAI-2 binding, membranes were pre-incubated with RAP (100 nM) or EDTA (5 mM). Biotinylated ligands were detected with neutravidin-HRP (1:10,000 dilution) and monoclonal antibodies with rabbit anti-mouse IgG-HRP (1:50 dilution).

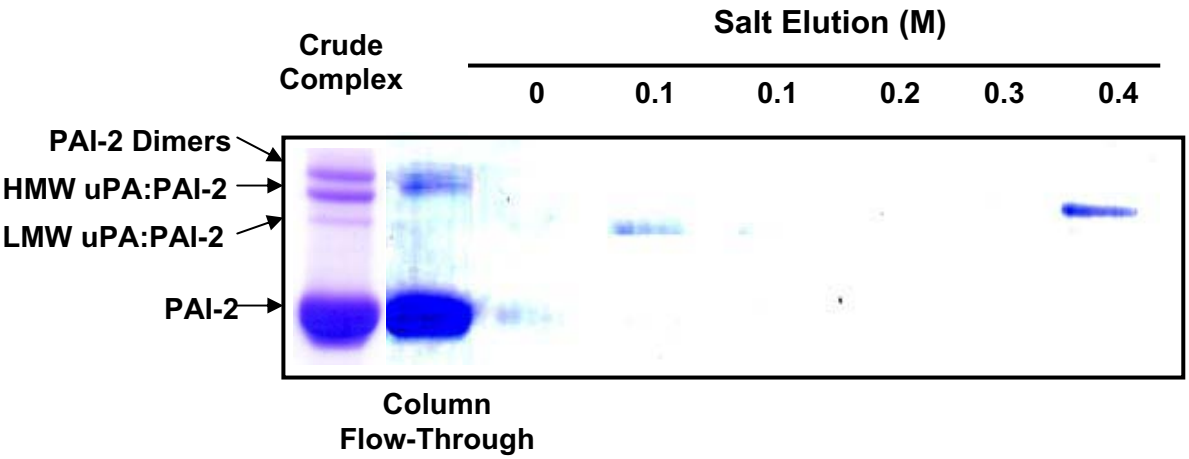

Figure 3.4: The purification of uPA:PAI-2 complexes. A crude mixture of uPA:PAI-2 complexes and free PAI-2 was applied to a mono-C spin column at PBS (pH 6) and centrifuged. Free PAI-2 eluted while uPA:PAI-2 complexes remained bound to the column. The LMW uPA:PAI-2 complexes eluted at 0.1 M NaCl while the HMW uPA:PAI-2 complexes eluted at 0.4 M NaCl, as determined by 12% non-reducing SDS-PAGE and coomassie blue staining.

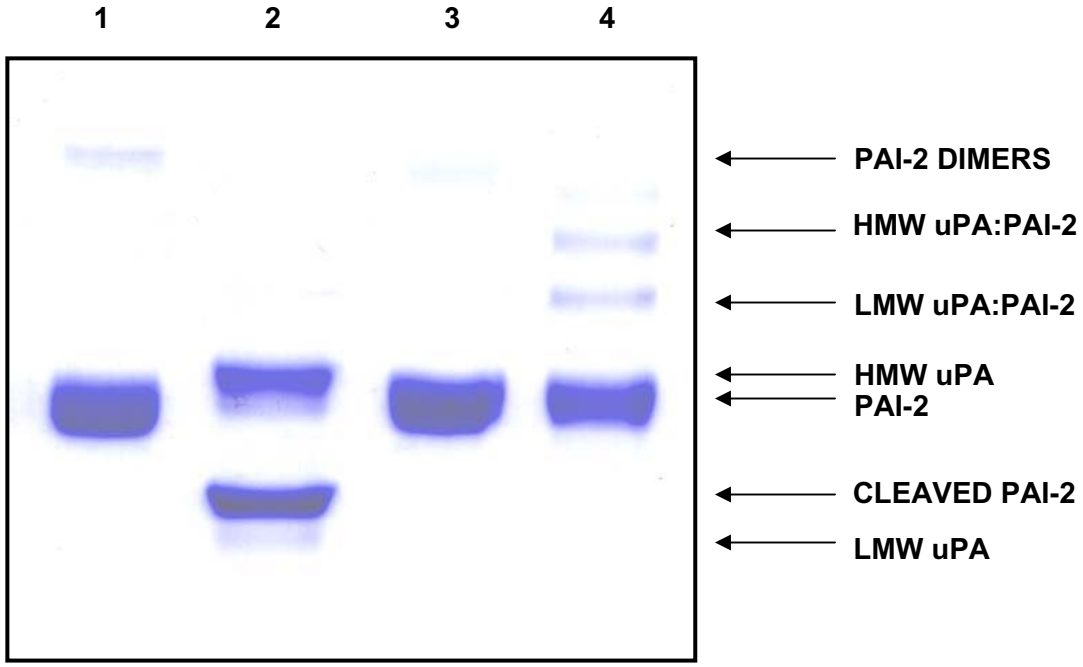

Figure 3.5: The formation of relaxed PAI-2. PAI-2 was incubated with a 100 molar excess of RCL peptide in 10 mM phosphate buffer (pH 8) for 48 h at 37°C. Excess peptide was removed using a 30 kDa cut-off spin column. Relaxed (Lanes 1 and 2) and stressed (Lanes 3 and 4) PAI-2 were incubated in the presence (Lanes 2 and 4) or absence (Lanes 1 and 3) of uPA (5:1 molar ratio) for 1 h at 37°C. Samples were resolved by 12% SDS-PAGE and stained with coomassie blue.

BIAcore data was obtained by measuring the interactions between the uPA:PAI-2 complexes or the free (uncomplexed), components and LRP immobilised onto a CM5 BIAcore chip. In support of the ligand blotting data, no interaction between LRP and PAI-2 (in either the stressed or relaxed conformation) was detected (Figure 3.6). A high affinity interaction, which best fit a one-binding site model, was observed between uPA:PAI-2 and LRP (K_D ~36 nM) (Figure 3.6, 3.7 and Table 3.1). HMW uPA also bound LRP with a one-binding site model, although with ~5.5-fold lower affinity (K_D ~ 200 nM) (Figure 3.6, 3.7 and Table 3.1). No interaction was observed between LRP and a complex of LMW uPA (ie uPA lacking ATF region, 33 kDa) and PAI-2 (Figure 3.6).

Detailed analysis of SPR data for uPA and uPA:PAI-2 binding to LRP revealed that the rate of dissociation of uPA from LRP was not significantly altered upon PAI-2 inhibition (Figure 3.7 and Table 3.1). However, the rate of association of uPA:PAI-2 with LRP was increased ~8-fold compared to the rate of uPA association.

The increase in affinity of uPA:PAI-2 for LRP was also reflected in the enhanced clearance of uPA from the cell surface. For example, uPA was internalised by PC-3 cells with a $t_{1/2}$ of ~100 min, whereas uPA:PAI-2 was internalised with a $t_{1/2}$ of ~20 min (R^2 values of 0.94 and 0.95 respectively) (Figure 3.8). These data also confirm the previous observations, using different techniques, of slow constitutive cell-surface uPA turnover in the absence of exogenous inhibitors (Al-Ejeh et al., 2004).

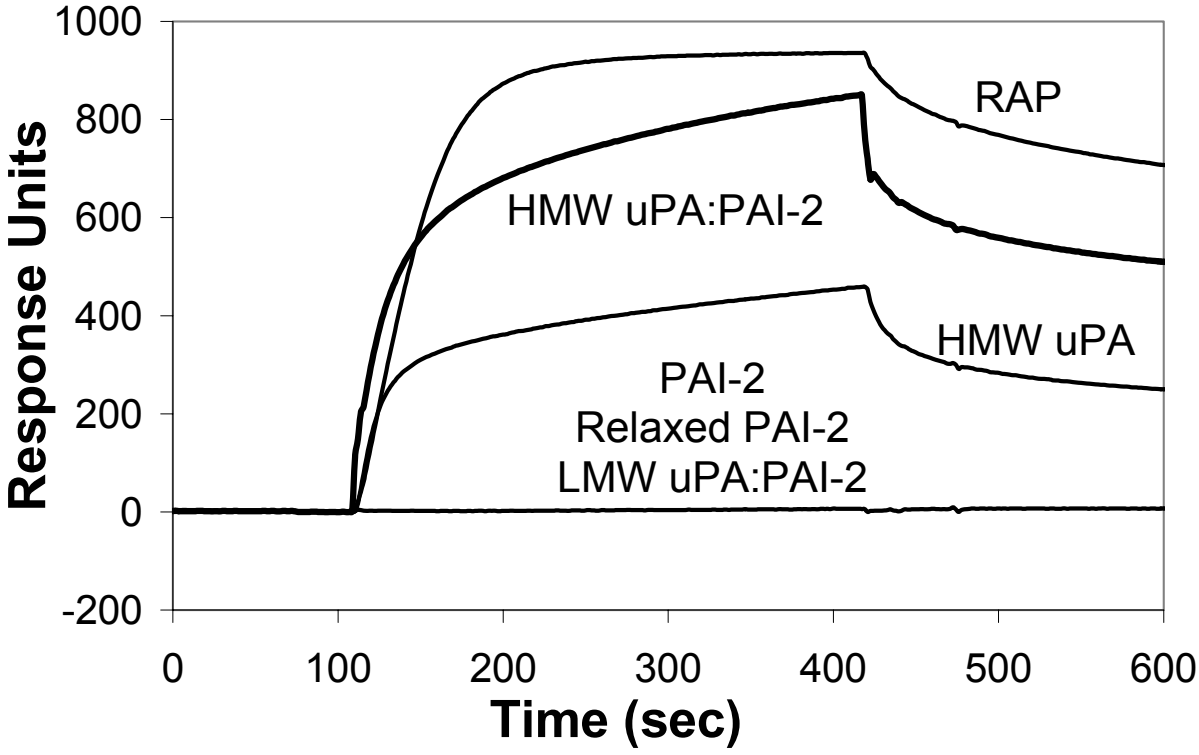

Figure 3.6: Surface plasmon resonance analysis of the interaction between uPA:PAI-2 and LRP. Normalised sensorgrams showing the interaction between 100 nM stressed PAI-2, relaxed PAI-2, HMW uPA, HMW uPA:PAI-2, LMW uPA:PAI-2 and immobilised LRP (~14,000 response units). RAP (100 nM) was used as a positive control. The data shown is representative of at least three independent experiments.

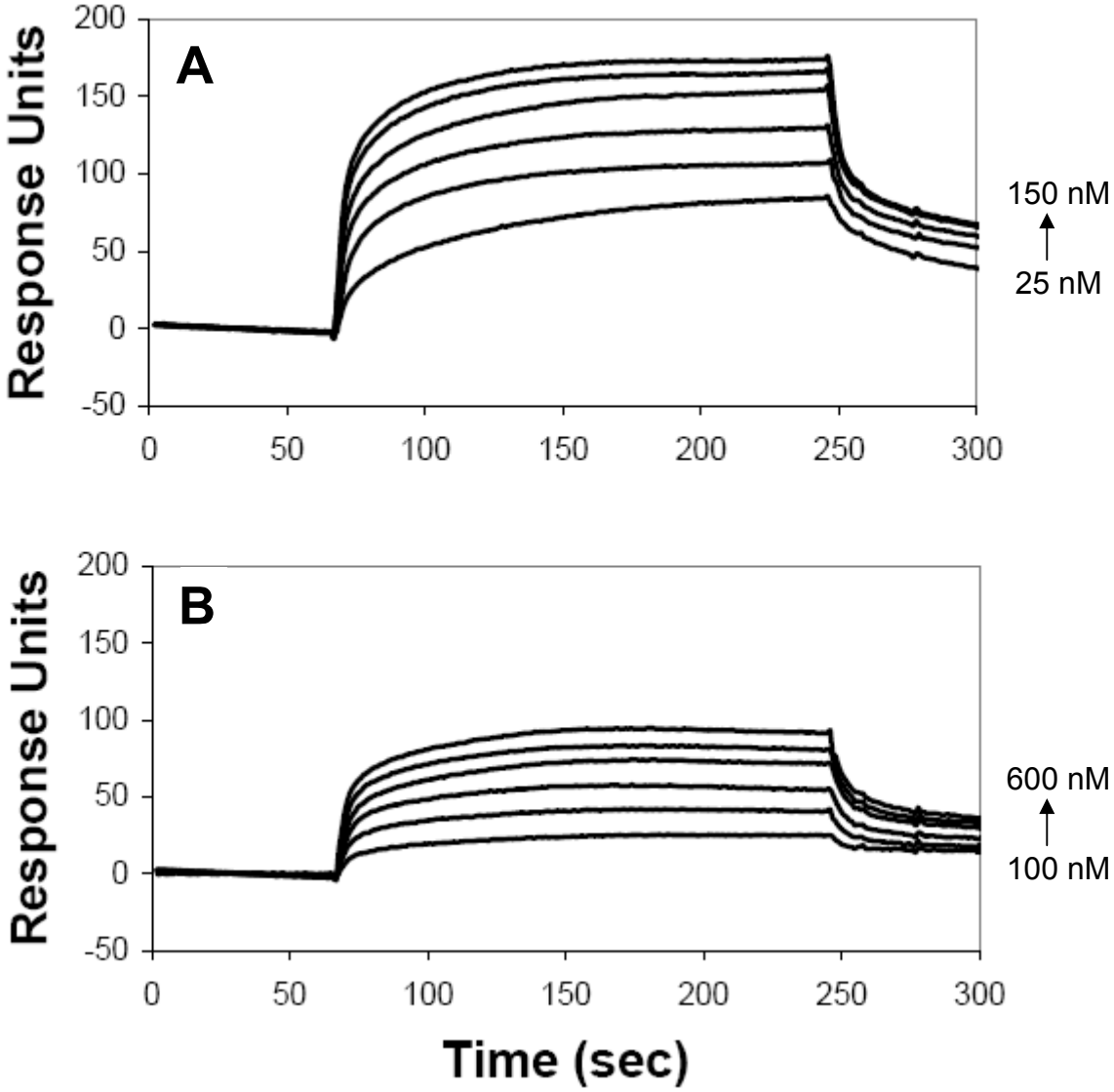

Figure 3.7: The binding of uPA and uPA:PAI-2 to LRP using surface plasmon resonance. **(A)** Normalised sensorgram showing the dose dependent binding of uPA:PAI-2 (25-150 nM) to LRP (~7000 response units). **(B)** Normalised sensorgram showing the dose dependent binding of uPA (100-600 nM) to LRP. Data shown is representative of at least 3 experiments.

Table 3.1: The kinetic parameters of uPA and uPA:PAI-2 binding to LRP. The binding of uPA (100 – 600 nM) and uPA:PAI-2 (25-150 nM) to immobilised LRP was measured by surface plasmon resonance.

Analyte	k_{off}	k_{on}	K_D	χ^2
	S^{-1}	$M^{-1}\ S^{-1}$	M	
uPA	7.78×10^{-3} ($\pm 1.31 \times 10^{-3}$)	3.87×10^{4} ($\pm 0.096 \times 10^{4}$)	2.00×10^{-7} ($\pm 0.29 \times 10^{-7}$)	0.45 (±0.118)
uPA:PAI-2	6.63×10^{-3} ($\pm 0.902 \times 10^{-3}$)	$3.12 \times 10^{5*}$ ($\pm 1.31 \times 10^{5}$)	$3.62 \times 10^{-8*}$ ($\pm 1.94 \times 10^{-8}$)	1.59 (±0.69)

The binding data was fitted using the BIAevaluation software (Version 4). A one site binding model with a drifting baseline yielded the best fit for both analytes (lowest χ^2 value). Values are the average result of three experiments.
(Values are ± SEM, n=3).
* denotes kinetic parameters for uPA:PAI-2 that were significantly different to those obtained for uPA ($p<0.05$).

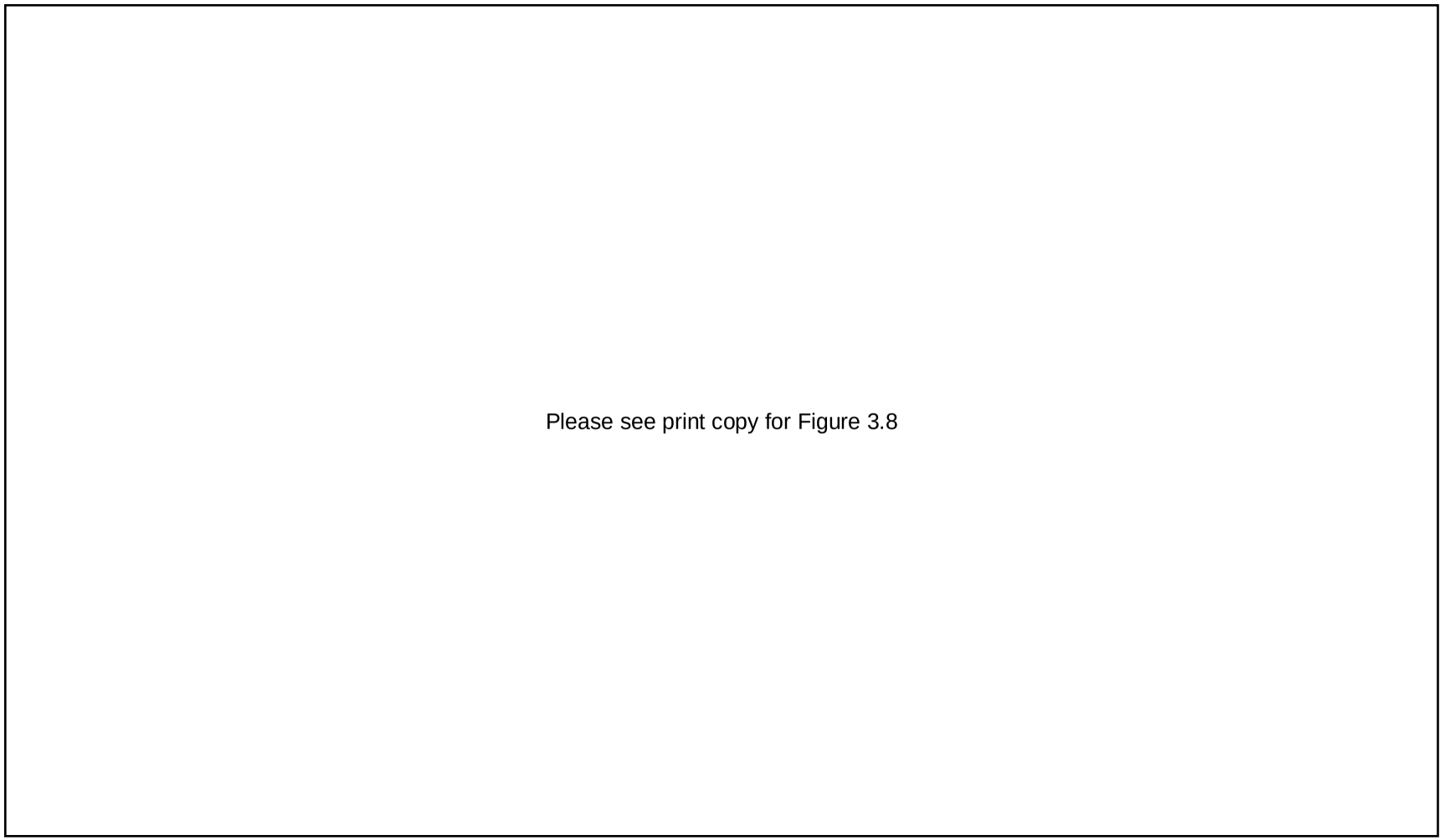

Figure 3.8: Inhibition of uPA by PAI-2 results in enhanced clearance of the uPA:PAI-2 complex. PC-3 cell monolayers, known to have up to 50% unoccupied uPAR (Al Ejeh et al., 2004), were incubated with 10 nM uPA:Alexa488 or uPA:Alexa488 complexed with PAI-2, at 37˚C for the time periods indicated. Cells were then analysed using the fluorescence quenching internalisation assay, data is presented as mean fluorescence units (MFI) (values are ± SEM, n=3). Data was fitted using GraphPad (Version 4, Prism).

3.3.3 Effect of uPAR on uPA:PAI-2 Binding to LRP

uPA is bound to the cell surface via its receptor uPAR, hence *in vivo* interactions between uPA:PAI-2 and LRP are likely to occur in close proximity to, and may be regulated by, uPAR. Using SPR analysis, the binding of uPA:PAI-2 to LRP in the presence of saturating amounts of uPAR resulted in a significant decrease in binding, however the interaction was not completely inhibited (Figure 3.9A). Furthermore, uPAR bound uPA:PAI-2 still bound LRP to a higher level than uPAR bound uPA and also uPA alone (Figure 3.9B). It should be noted that binding of both uPA and uPA:PAI-2 to LRP is reduced in the presence of uPAR, compared to free ligands. However, no interaction between uPAR and LRP was found (Figure 3.9C), confirming the lack of a binding site on uPAR for LRP (Nykjaer et al., 1994).

3.4 DISCUSSION

The efficient inactivation of uPA by PAI-2 at the surface of carcinoma cells is followed by rapid internalisation of the uPA:PAI-2 complex into endosomes and lysosomes (Al-Ejeh et al., 2004). In the previous chapter, definitive data was presented showing that the majority of PAI-2 internalisation is uPA-dependent and RAP-sensitive. The data in this chapter extends this finding to show that the uPA:PAI-2 complex is a novel, high affinity ligand for LRP. This interaction is responsible in part for the receptor-mediated endocytosis of uPA:PAI-2/uPAR and the subsequent clearance of active uPA from the cell surface.

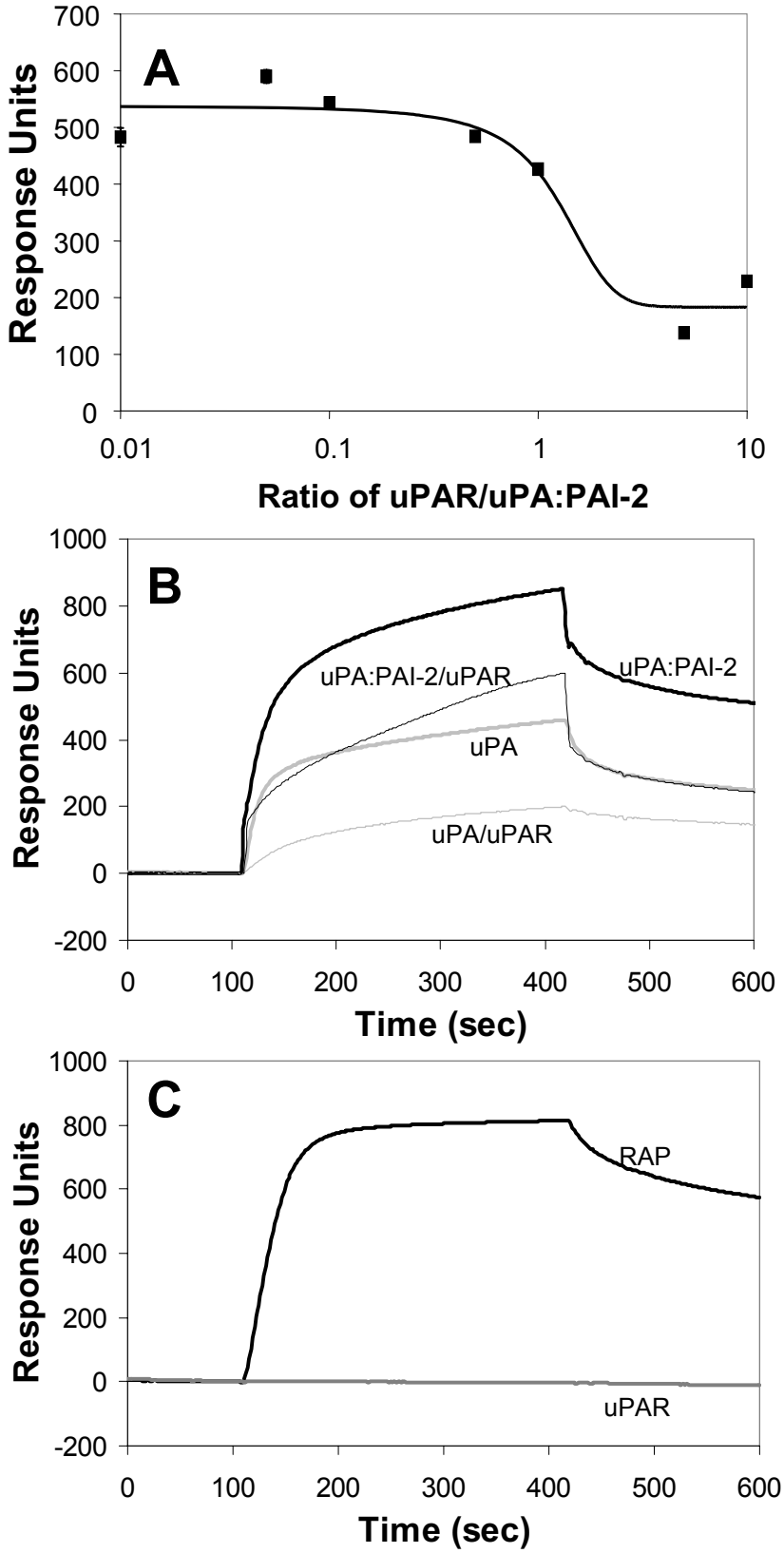

Figure 3.9: Ligation to uPAR reduces but does not prevent the binding of both uPA and uPA:PAI-2 to LRP. (A) Surface plasmon resonance sensorgrams of the binding of uPA:PAI-2 to LRP in the presence of increasing amounts of uPAR. uPA:PAI-2 (100 nM) was incubated with uPAR at the molar ratios indicated for 45 min on ice, prior to binding analysis. Data was fit to a one site competition curve using Graphpad (Version 4, Prism). (Values are ± SD, n=2). **(B)** Sensorgrams of the binding of uPA (grey lines) and uPA:PAI-2 (black lines) to LRP in the presence (thin lines) and absence (thick lines) of a 10 fold molar excess of uPAR. **(C)** Sensorgrams showing the lack of a direct interaction between uPAR (100 nm) (Grey line) and LRP. RAP (100 nM) (Black line) was used as a positive control for LRP binding.

Several lines of evidence implicate LRP as a endocytosis receptor for uPA:PAI-2; internalised PAI-2 co-localised with LRP, pre-incubation with anti-LRP polyclonal antibodies significantly inhibited PAI-2 endocytosis and uPA:PAI-2 bound to LRP with high affinity. Hence, similar to other serpins (Chapter 1.3.3), PAI-2 endocytosis can be mediated via LRP. As inhibition by an anti-LRP polyclonal antibody did not reflect the total amount of RAP inhibition, it is possible that VLDLr, or other unidentified LDLRs, may also be involved in mediating the endocytosis of PAI-2 on the PC-3 cell line. The role of VLDLr in uPA:PAI-2 endocytosis is addressed in the following chapter.

Relatively high concentrations of free PAI-1 (active, latent and cleaved) are able to compete for uPA:PAI-1 binding to LRP (Nykjaer et al., 1994) and free PAI-1 can bind directly to LRP independent of uPA (K_D ~ 93 nM) (Degryse et al., 2004). However, no interaction between stressed or relaxed PAI-2 (discussed further below) and LRP was observed by either SPR or ligand dot blotting. SPR analysis revealed a low affinity interaction between HMW uPA and LRP (K_D ~200 nM), in agreement with previous studies (Kounnas et al., 1993). Critically, inhibition of uPA by PAI-2, and concomitant formation of a uPA:PAI-2 complex, resulted in a ~5.5-fold increase in affinity for LRP (K_D ~36 nM). This may explain in part the enhanced clearance of PAI-2 inhibited uPA observed in both PC-3 (Figure 3.8) and MDA-MB-231 (Al-Ejeh et al., 2004) cells, as shown for uPA:PAI-1 complexes in other cell lines (Andreasen et al., 1994). This in turn facilitates the clearance of cell surface plasminogen activating capability (Zhang et al., 1998) and may possibly mediate cell-signaling events (Herz and Strickland, 2001), as discussed below.

The 12-fold higher affinity of uPA:PAI-1 binding to LRP (K_D ~3 nM) (Kounnas et al., 1993), compared to uPA:PAI-2, may be due to the presence of LRP binding sites within both the uPA and PAI-1 moieties of the uPA:PAI-1 complex. It is thought that

the high affinity binding of uPA:PAI-1 to LRP results from either the combination of low affinity sites in each moiety (Nykjaer et al., 1994), or the unveiling of a cryptic high affinity binding site within PAI-1 (Stefansson et al., 1998). As the high affinity binding of PAI-1 to endocytosis receptors of the LDLR family has been observed whilst in complex with various proteases (Horn et al., 1998; Stefansson et al., 2004), it is most likely that this high affinity binding is mediated through the cryptic high affinity site within PAI-1.

Using synthetic RCL peptides to induce the relaxed conformation of PAI-2 in the absence of uPA (thus mimicking that found in uPA:PAI-2 complex) (Saunders et al., 1998), there was no evidence found for a cryptic high affinity LRP binding site within PAI-2. Furthermore, there was no LRP binding by LMW uPA:PAI-2, which lacks the ATF of uPA, whereas LMW uPA:PAI-1 does bind to LRP (Stefansson et al., 1998). Hence, PAI-2 appears to be unique among protease:serpin complexes (Andreasen et al., 1994; Nykjaer et al., 1994) in lacking an LRP binding determinant. Considering the lack of significant change in dissociation rates between uPA/uPA:PAI-2 and LRP and the marked increase in the association rate of uPA:PAI-2 with LRP compared to free uPA, it is likely that the same site within uPA is responsible for binding to LRP in the free and inhibited molecule. This site within uPA may become more available for LRP binding after the deformation induced by PAI-2 inhibition (possibly reducing steric hindrance to this site), hence increasing the association rate of uPA:PAI-2 for LRP.

Importantly, this data also demonstrates that the increased binding of uPA:PAI-2 to LRP compared with uPA is maintained in the presence of uPAR, even though overall binding is reduced. The reduction in binding of uPA:PAI-2 to LRP upon uPAR binding is consistent with the findings of Nykjaer et al. (1994), who showed that the binding of uPA:PAI-1 to LRP was significantly decreased in the presence of uPAR and that pro-

uPA binding was entirely inhibited. This lowered affinity is most likely due to uPAR hindering the access of LRP to binding sites within the active uPA molecule. Regardless, these data indicate that the enhanced endocytosis of uPA:PAI-2 by LRP is relevant in the cell-surface context, where uPA is bound to uPAR. Incidentally, there was no evidence of a direct interaction between uPAR and LRP. While this is consistent with the findings of Nykjaer et al. (1994), it conflicts with the findings of Czekay et al. (2001), who suggested that uPAR binds to LRP independent of uPA:PAI-1 through a binding site in domain three of uPAR. This discrepancy may be explained by the different techniques used in these studies.

The absence of a high affinity LRP binding site within the PAI-2 moiety has direct implications for cell signaling events mediated upon binding to LDLR family members by other serpins. For example, sustained ERK phosphorylation and subsequent promotion of cell proliferation and migration depends on the high affinity site within the PAI-1 moiety of uPA:PAI-1 binding to VLDLr on MCF-7 cells (Webb et al., 2001) (Further examined in Chapter 4). Furthermore, the ability of PAI-1 to bind LRP independently of uPA, contributes to activation of the Jak/Stat pathway and stimulates cell migration (Degryse et al., 2004). These data suggest the intriguing possibility that PAI-2 may be able to inhibit and clear cell surface uPA, and therefore inhibit plasminogen activation ability, without initiating cell signaling events associated with metastatic potential. If proven, these effects may also partially explain the disparate relationships between PAI-1 and PAI-2 expression and disease outcome in various cancers, as it has been reported that high tumour PAI-2 antigen is related to a favorable overall survival (Foekens et al., 1995; Schmitt et al., 2000) whereas high PAI-1 antigen is related to a negative outcome (Duffy, 2004; Schmitt et al., 2000).

In conclusion, this data presents a mechanism of PAI-2 internalisation by receptor mediated endocytosis involving LRP following inhibition of uPAR-bound uPA. It demonstrated that the interaction between LRP and uPA:PAI-2 is most likely mediated by site/s on the uPA molecule interacting with LRP. This interaction was maintained in the presence of uPAR, confirming the validity of this interaction at the cell surface. Significantly, in contrast to PAI-1, no interaction was observed between either stressed or relaxed PAI-2 and LRP. These findings have important implications for understanding the initiation of downstream cell signaling events mediated upon PAI-1 binding to LDLR family members and their potential role in metastasis. The rapid, LRP mediated endocytosis of PAI-2 upon inhibition of cell surface uPA further validates the use of PAI-2 as an anti-uPA targeting strategy in cancer therapy. It also presents an avenue for intracellular delivery of toxins to cancer cells, increasing specificity and also efficacy of PAI-2 based cancer therapies. The following chapter will aim to address the effects of the differing biochemical interactions between uPA:PAI-2, uPA:PAI-1 and the LDLR family upon cell signaling and thus cancer progression.

Chapter 4

4. Structural basis of the differential signaling by PAI-1 and PAI-2 in Breast Cancer: Implications for metastatic potential

4.1 INTRODUCTION

uPA plays an important role in many physiological processes including metastasis, wound healing, and angiogenesis, through the pericellular activation of plasminogen and degradation of the extracellular matrix (Chapter 1.2) (Dano et al., 1999). The deregulation of uPA expression associated with metastatic cancer increases plasmin activity, catalysing extracellular matrix degradation and promoting migration (Blasi, 1999; Han et al., 2005; Hanahan and Weinberg, 2000). Importantly, uPA can also promote metastasis through protease-independent mechanisms (Chapter 1.3.4) (Han et al., 2005). For example, binding of uPA to its cell surface receptor, uPAR, often initiates motogenic signaling responses (Kjoller, 2002). As uPAR is not a transmembrane receptor, these events are facilitated by interactions with integrins (Resnati et al., 2002) and associated co-receptors, including the epidermal growth factor receptor (EGFR) (Liu et al., 2002).

Whilst both are efficient uPA inhibitors, PAI-1 and PAI-2 are functionally quite distinct and their apparent role(s) in breast cancer invasion and metastasis appear somewhat paradoxical. Clinical studies show that uPA / PAI-1 co-expression has level one evidence as a prognostic marker of progression in early breast cancer (Chapter 1.2.8) (Duffy, 2004; Weigelt et al., 2005) and may have prognostic significance in ovarian, endometrial, bladder and other cancers (Duffy and Duggan, 2004). *In vitro* studies have also shown that uPA and PAI-1 are necessary for lung carcinoma cell invasion through matrigel (Liu et al., 1995) and that PAI-1 deficiency inhibited invasion of transplanted malignant keratinocytes (Bajou et al., 1998). In contrast, high tumour PAI-2 expression has been related to a favourable overall survival (Chapter 1.2.8). Furthermore, a number of observations have shown that PAI-2 reduces tumor growth,

invasion and metastasis using *in vitro* and *in vivo* models via inactivation of cell surface uPA (Foekens et al., 1995; Hang et al., 1998; Kruithof et al., 1995).

Both PAI-1 and PAI-2 are cleared from the cell surface through interactions with endocytosis receptors of the LDLR family such as LRP and VLDLr (Chapter 1.3.3 and 3) (Argraves et al., 1995; Croucher et al., 2006; Herz et al., 1992; Kounnas et al., 1993). Upon PAI-1/2 inhibition of uPA, a covalent complex is formed with increased affinity for these receptors, resulting in an enhanced rate of uPA:serpin complex endocytosis (Croucher et al., 2006; Cubellis et al., 1990; Nykjaer et al., 1994). These interactions can indirectly effect signaling activity by regulating levels of uPA/uPAR on the cell surface (Webb et al., 1999) and also directly transmit signals through receptor cytoplasmic domains (Chapter 1.3.4) (Herz and Strickland, 2001). For example, binding of uPA to uPAR on MCF-7 cells stimulates transient ERK phosphorylation and vitronectin-dependent cell migration (Nguyen et al., 1999; Webb et al., 2001). The inhibition of uPA by PAI-1 sustains this transient ERK phosphorylation and stimulates cell proliferation via the interaction of a cryptic high affinity binding site in PAI-1 for VLDLr (Stefansson et al., 1998; Webb et al., 2001). PAI-1 is also capable of stimulating cell migration independently of uPA, tPA and vitronectin. For example, a direct interaction between PAI-1 and LRP activates the Jak/Stat pathway, resulting in actin filament polarisation, translocation of activated Stat1 into the nucleus, and increased cell migration (Degryse et al., 2004).

Thus, the interactions between uPA:PAI-1 and members of the LDLR family, and the signaling events stimulated by these interactions, have been well characterised. The data presented in Chapter 3 demonstrated that PAI-2 does not contain a cryptic high affinity binding site for LRP and that uPA:PAI-2 endocytosis by PC-3 prostate cancer cells is mediated predominantly by binding sites within the uPA moiety of the complex

(Croucher et al., 2006). The data presented in this chapter indicates that VLDLr binds and mediates the endocytosis of uPA:PAI-2 on breast cancer cells *in vitro*. Furthermore, novel differences in VLDLr binding mechanisms between uPA:PAI-1 and uPA:PAI-2 are highlighted, with important functional implications. Established LRP and VLDLr binding determinants in PAI-1 are absent in PAI-2, leading to distinct downstream signaling events that may explain the disparate relationships between PAI-1 and PAI-2 expression and disease outcome in breast cancer.

4.2 MATERIALS AND METHODS

4.2.1 Proteins and Antibodies

Many proteins, antibodies and reagents used in this chapter are previously described (Chapter 2.2.1 and 3.2.1). Anti-uPAR polyclonal antibody (#399r) and Spectrozyme PL substrate were from American Diagnostica (CT, USA). Transferrin was from Sigma-Aldrich (MO, USA). (Anti-rabbit IgG HRP secondary antibody was from GE Healthcare (Buckinghamshire, UK). Glu-plasminogen was purified from human plasma, as previously described (Ranson et al., 1998). Anti-phospho-tyrosine monoclonal antibody clone PY20 (#P11120) was from BD Biosciences (CA, USA). Anti-phosphorylated ERK (Thr 202/Tyr204) rabbit monoclonal antibody (#91015) and Anti-ERK (#9102) were from Cell Signaling (MA, USA).

Recombinant human VLDLr ligand binding region was a kind gift of Prof. Dieter Blaas (University of Vienna, Vienna, Austria). Recombinant PAI-1 14-1b stable variant and PAI-1^{R76E} mutant on 14-1b backbone were provided by Prof Dan Lawrence (University of Michigan, Michigan, USA) (Stefansson et al., 1998).

4.2.2 Tissue Culture Conditions

The MCF-7 epithelial breast cancer cell line was used for all experiments. Cells were grown, passaged and prepared for experiments as previously described (Ranson et al., 1998). For all experiments, unless otherwise indicated, cells were cultured for 48 h without a change of media and were detached using PBS/EDTA (5mM) either prior to, or during the experiment.

4.2.3 Analysis Of Cell Surface Antigen Expression And Internalisation By Flow Cytometry

MCF-7 cells, grown to 80% confluency over a 48 h period, were detached using PBS/EDTA (5 mM), washed with ice cold binding buffer (Appendix 1) and centrifuged at 300 x *g* at 4˚C. The cells were resuspended at 1 x 10^6 cells/mL in ice-cold binding buffer containing primary polyclonal antibodies or irrelevant isotype control antibody (5 µg/mL) and incubated for 45 min on ice. After three washes with ice-cold binding buffer, the cells were incubated with goat anti-rabbit IgG-FITC (1:50 dilution) for 45 min on ice. In all cases cell surface fluorescence was analysed by dual colour flow cytometry as previously described (Ranson et al., 1998).

Internalisation assays using $Alexa_{488}$ labeled PAI-2 or uPA and $Alexa_{488}$ polyclonal quenching antibody were performed as previously described (Chapter 2.2.2.2) (Croucher et al., 2006).

4.2.4 Surface Plasmon Resonance Analysis

uPA:serpin complexes were prepared as previously described (Webb et al., 2001). Briefly, uPA and serpin (PAI-1 or PAI-2) were incubated at a 1:1 molar ratio for 30 min at 37°C. Complex formation was monitored by SDS-PAGE. These analyses confirmed the complete inactivation of uPA.

VLDLr was immobilised to a CM5 BIAcore chip (BIAcore, Melbourne, Australia) according to manufacturer's instructions. Briefly, the chip was activated using a 1:1 mixture of 0.2M *N*-ethyl-*N'*-(3-dimethylaminopropyl)carbodi-imide and 0.05M *N*-hydroxysuccimide. VLDLr was coated to the chip at 40 µg/mL in 10 mM sodium acetate (pH 3) to a level of ~10,000 response units. Unoccupied binding sites were blocked using 1M ethanolamine, pH 8.5. An example of immobilisation is presented in Appendix 4. Ligands were diluted into running buffer (Appendix 1) before applying to the BIAcore chip at 20 µl/min. Regeneration of the chip was achieved using 100 mM H_3PO_4. For kinetic analysis, a blank cell was used as the reference cell and data was analysed using BIAevaluation software (Version 4). An example of kinetic analysis is presented in Appendix 5.

4.2.5 Plasmin Activity Assay

The plasmin activity assay was performed by Gillian Stillfried (PhD Candidate, University of Wollongong). This data is included with her permission. MCF-7 cells were seeded in 96-well plates at 1 x 10^4 cells/well and cultured for 48h without change of media. Cells were washed and incubated in binding buffer containing purified human uPA (5 nM) for 30 min on ice. Cells were subsequently washed and incubated for 0, 1, 10 or 30 min at 37^{o}C in binding buffer containing PAI-1 or PAI-2 (5 nM). Cells were then washed and incubated with 0.5 µM human glu-plasminogen for 10 min at RT.

Plasmin activity was then measured over 2 h at 37^{o}C using Spectrozyme PL substrate (0.4 mM final concentration). Colour development was recorded at 405 nm.

4.2.6 Confocal Microscopy Analysis of Cellular Phospho-Tyrosine Proteins

MCF-7 cells were grown to ~80% confluency in 8-well chamber slides and serum starved for 4 h. Cells were then incubated in the presence or absence of RAP (100 nM) in binding buffer, at 37°C for 15 min. The cells were then incubated with uPA, uPA:PAI-1, uPA:PAI-1^{R76E} or uPA:PAI-2 (10 nM) in binding buffer, at 37°C for 30 min. Following 2 washes with ice-cold PBS, the cells were fixed with 3.75% para-formaldehyde, permeabilised with 0.1% Triton-X 100, blocked with 1% BSA/PBS and probed with anti-phosphotyrosine (5 μg/mL), for 45 min at 4°C in 1% BSA/PBS. Following a further 2 washes, the cells were incubated with anti-mouse IgG-FITC (1:200) and TO-PRO 3 (1:400) in 1% BSA/PBS for 45 min at 4°C. After washing the cells were analysed by confocal microscopy using a Leica TCS SP system (Leica, Heidlberg, Germany).

4.2.7 Analysis of ERK Activation

ERK activation was analysed essentially as previously described (Webb et al., 2001). Briefly, MCF-7 cells were grown in 24 well plates to ~60% confluency and serum starved for 6 h. The cells were incubated with uPA, uPA:PAI-1, uPA:PAI-1^{R76E} or uPA:PAI-2 (10 nM) for the time periods indicated. The cells were then lysed with ice-cold lysis buffer (Appendix 1) for 5 min, on ice. Cell lysates were centrifuged at 10,000 rpm at 4°C, electrophoresed on 12% gels and transferred to PVDF membranes at

100 V for 1 h. Membranes were blocked with 2% BSA for overnight prior to incubation with either rabbit anti-phosphorylated ERK or rabbit anti-ERK monoclonal antibodies (1:1000) in TBS/0.1% BSA/0.02 % sodium azide for 3 h at room temperature. Following four 15 min washes with TBS/0.05% tween 20, the membranes were incubated with anti-rabbit IgG HRP (1:5000) in TBS/0.05% tween 20/2% skim milk for 1 h at room temperature. Following a further four 15 min washes, the membranes were developed by enhanced chemiluminescence. Blots were stripped by heating in stripping buffer (Appendix 1) for 30 min at 50°C.

4.2.8 Cell Proliferation Assay

MCF-7 cell proliferation assay was performed using the CellTiter 96® AQueous One Solution Cell Proliferation Assay (Promega, USA) essentially as described by Webb et al. (2001). Briefly, MCF-7 cells were seeded at 5000 cells/well in 96 well plates and cultured for 24 h. The media was replaced with 100 μL of serum free RPMI, containing 300 μg/mL glutamine, 5 μg/mL transferrin and 38 nM selenium (Sigma-Aldrich), in the presence of 10 nM uPA, uPA:PAI-1, uPA:PAI-1^{R76E}, uPA:PAI-2 or the media alone. Cells incubated with uPA:PAI-1 were also incubated in the presence or absence of RAP (200 nM). Following culturing for a further 36 h, 20 uL of MTS reagent was added to each well and incubated for 2 h. Absorbance was read at 490 nm. An additional plate was also measured at 0 h to obtain a baseline of cell numbers.

4.2.9 Protein Structure Analysis

The structural analysis of PAI-1 and PAI-2 was performed by Dr Darren Saunders (Cancer Research Program, Garvan Institute of Medical Research). This data is included with his permission. Protein structure analysis and figure preparation was performed using the PyMol software package (DeLano Scientific). Structural co-ordinates were obtained from X-ray crystal structures of the relaxed conformations of both PAI-1 (PDB accession 9pai) (Aertgeerts et al., 1995) and PAI-2 CD-loop deletion mutant (PDB accession 1jrr) (Jankova et al., 2001).

4.3 RESULTS

4.3.1 uPA:PAI-2 Endocytosis is Mediated by uPAR and VLDLr

To confirm the suitability of MCF-7 cells for examining PAI-2 endocytosis and potential associated signaling events, the cell surface expression of uPAR and VLDLr was analysed by flow cytometry. Both VLDLr and uPAR were detected on the surface of MCF-7 cells (Figure 4.1A,B). It was previously shown that LRP can mediate PAI-2 endocytosis in PC-3 cells (Chapter 3) (Croucher et al., 2006). However, LRP was not detected on MCF-7 cells (Figure 4.1C), confirming the findings of previous studies (Webb et al., 1999). Internalisation assays were undertaken to determine whether VLDLr was able to mediate endocytosis of PAI-2. Relatively little PAI-2 internalisation was observed in the absence of exogenous uPA, which was not sensitive to inhibition by RAP (Figure 4.1D). Upon addition of uPA:PAI-2, significant RAP-sensitive internalisation was observed (Figure 4.1D), confirming that both uPAR and VLDLr are necessary for endocytosis of uPA:PAI-2 from the surface of MCF-7 cells.

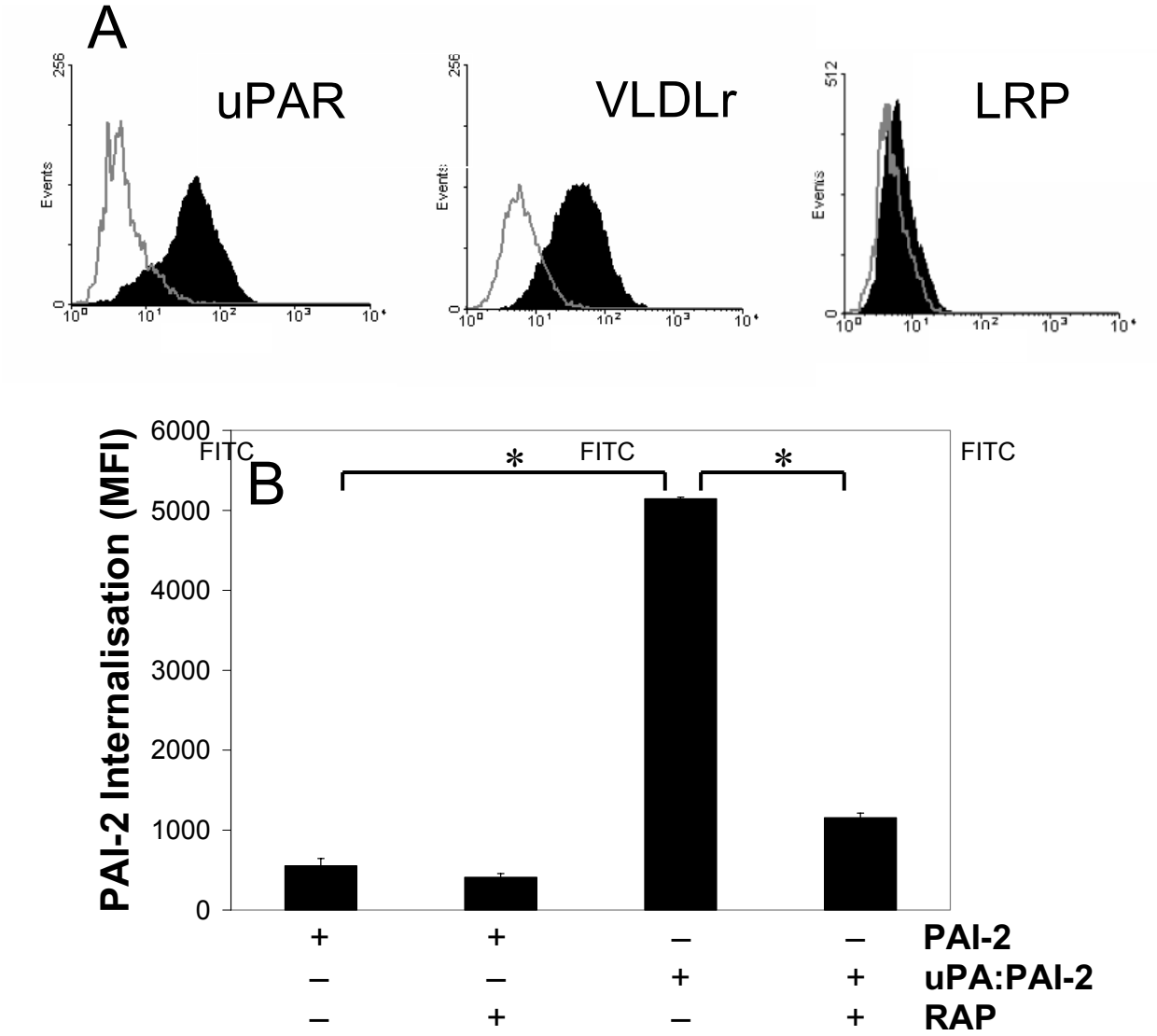

Figure 4.1: uPAR and VLDLr mediate the endocytosis of uPA:PAI-2 by MCF-7 cells. (A) MCF-7 cells were probed with 10 µg/mL primary uPAR, VLDLr or LRP polyclonal antibody. These were detected using anti-rabbit IgG-FITC (1:50 dilution) and the cells analysed by flow cytometry, using propidium iodide to exclude non-viable cells. **(B)** MCF-7 cells were incubated in the presence or absence of RAP (200 nM) for 15 min at 37°C, prior to analysis of PAI-2:$Alexa_{488}$ or uPA:PAI-2:$Alexa_{488}$ internalisation by the fluorescence quenching internalisation assay (mean ± SEM, n = 3; $^{*}p < 0.05$).

4.3.2 PAI-2 Does Not Contain a High Affinity Binding Site for VLDLr

The PAI-1 component of the uPA:PAI-1 complex contains a high affinity VLDLr binding site (Stefansson et al., 1998). However, it was previously shown that PAI-2 does not contain a cryptic high affinity binding site for LRP (Chapter 3) (Croucher et al., 2006). SPR analysis was undertaken to characterise the binding of uPA:PAI-2 to VLDLr, and to compare this with uPA:PAI-1 binding.

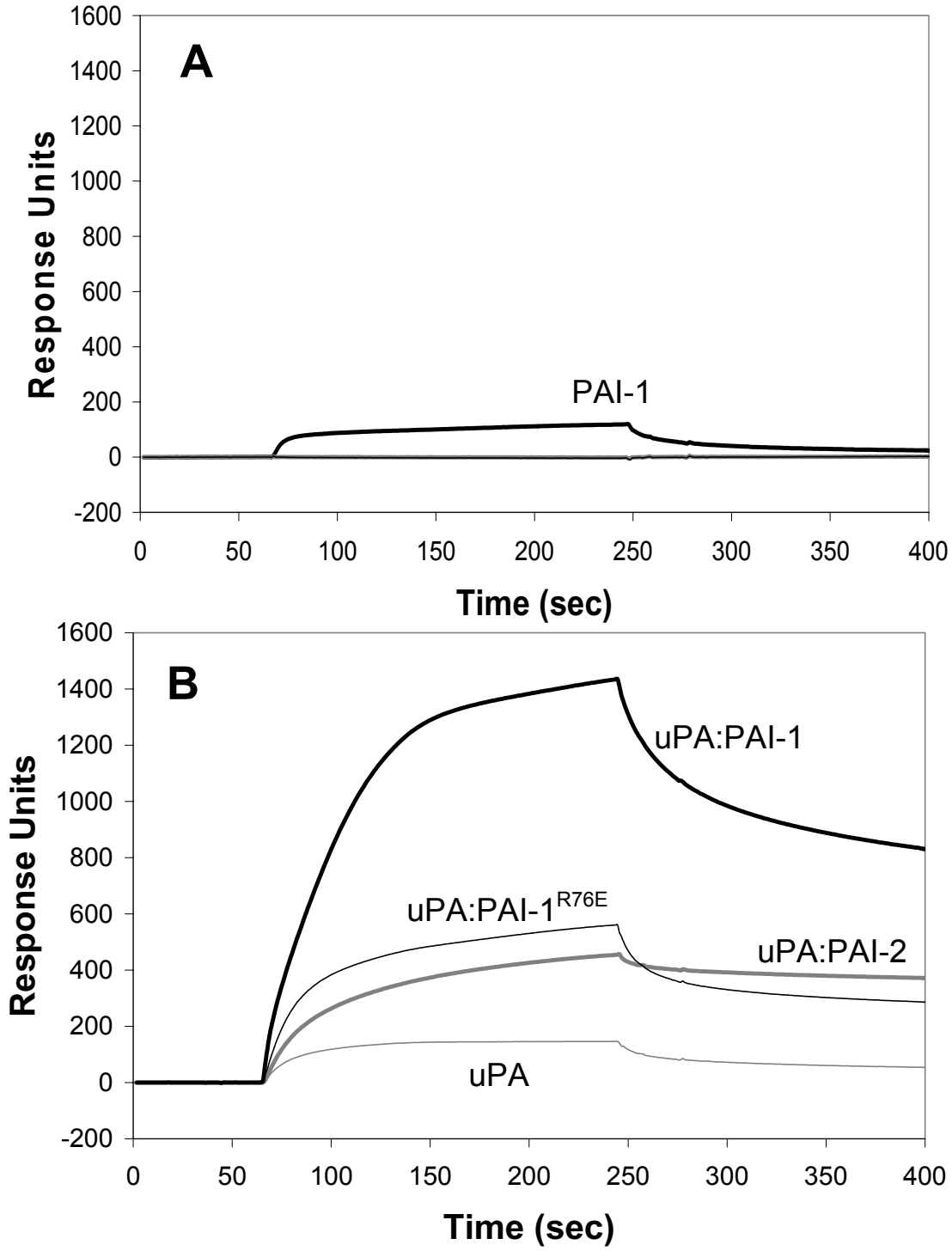

Figure 4.2: Surface plasmon resonance analysis of PAI-1 and PAI-2 binding to VLDLr. (A) sensorgrams showing the interaction between 100 nM PAI-1, PAI-1^{R76E}, PAI-2 and immobilised VLDLr. **(B)** sensorgrams showing the interaction between 100 nM uPA, uPA:PAI-1, uPA:PAI-1^{R76E}, uPA:PAI-2 and immobilised VLDLr. The data shown are representative of at least three independent experiments.

Significantly stronger binding of uPA:PAI-1 to VLDLr compared with uPA:PAI-2 and uPA:PAI-1^{R76E} was observed (Figure 4.2B). Relatively lower binding of PAI-1, and no binding of PAI-2 or PAI-1^{R76E} to VLDLr was detected (Figure 4.2A). uPA proteolytic activity was not necessary for binding of uPA to VLDLr as no difference in binding was observed following PMSF inactivation of uPA (*data not shown)*.

Quantitative analysis showed that PAI-1 binding to VLDLr best fit a 1:1 binding model, with a K_D of ~52 nM (Figure 4.3B and Table 1). uPA and uPA:PAI-1 displayed complicated binding kinetics that best fit a model where both uPA and uPA:PAI-1 contain two separate binding sites of higher and lower affinity capable of binding to VLDLr independently, but in a competitive manner (Figure 4.3A,C and Table 1). The two sites within uPA bound to VLDLr with K_D values of ~209 and ~31 nM. The two sites within uPA:PAI-1 bound to VLDLr with K_D values of ~85 nM and ~1.5 nM (Table 1). Binding of uPA:PAI-1^{R76E} or uPA:PAI-2 to VLDLr best fit a 1:1 binding model with a K_D of ~10 and ~5 nM, respectively (Figure 4.3D,E and Table 1).

4.3.3 Structural Analysis of Serpin/VLDLr Binding

The Arg_{76} residue within helix D of PAI-1 is crucial for binding of PAI-1 and uPA:PAI-1 to LRP and VLDLr (Stefansson et al. 1998; Figure 4.2 above). Although a homologous residue (Arg_{108}) is conserved within helix D of PAI-2 (Huber and Carrell, 1989) PAI-2 does not bind VLDLr (Figure 4.2, Table 4.1) or LRP (Croucher et al., 2006) and uPA:PAI-2 binds with much lower affinity than uPA:PAI-1 (Figure 4.2, Table 4.1).

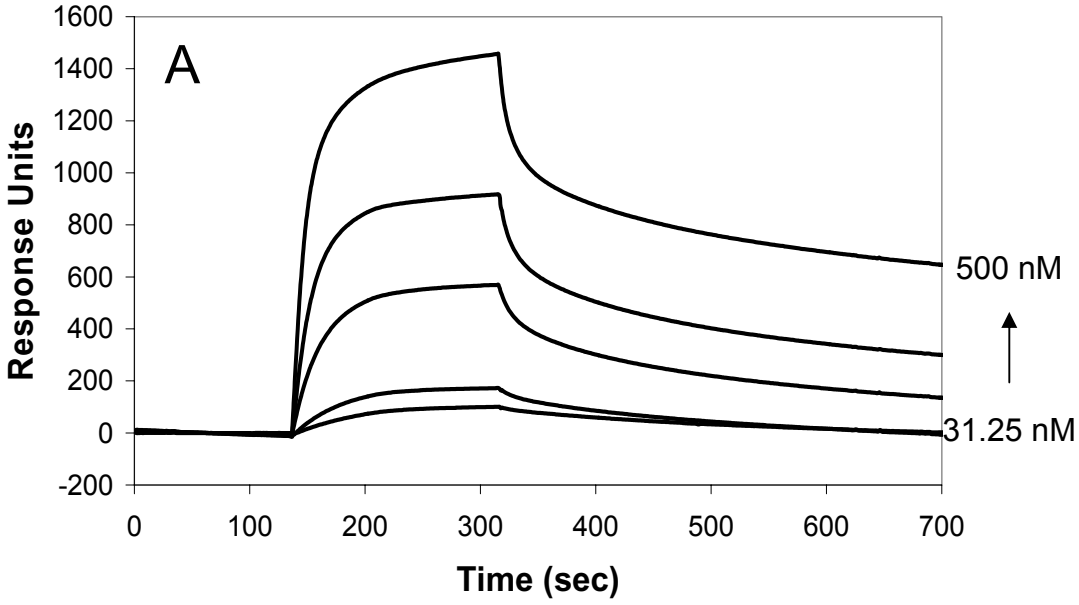
A
Response Units
1600
1400
1200
1000
800
600
400
200
0
-200
0
100
200
300
400
500
600
700
Time (sec)
500 nM
31.25 nM

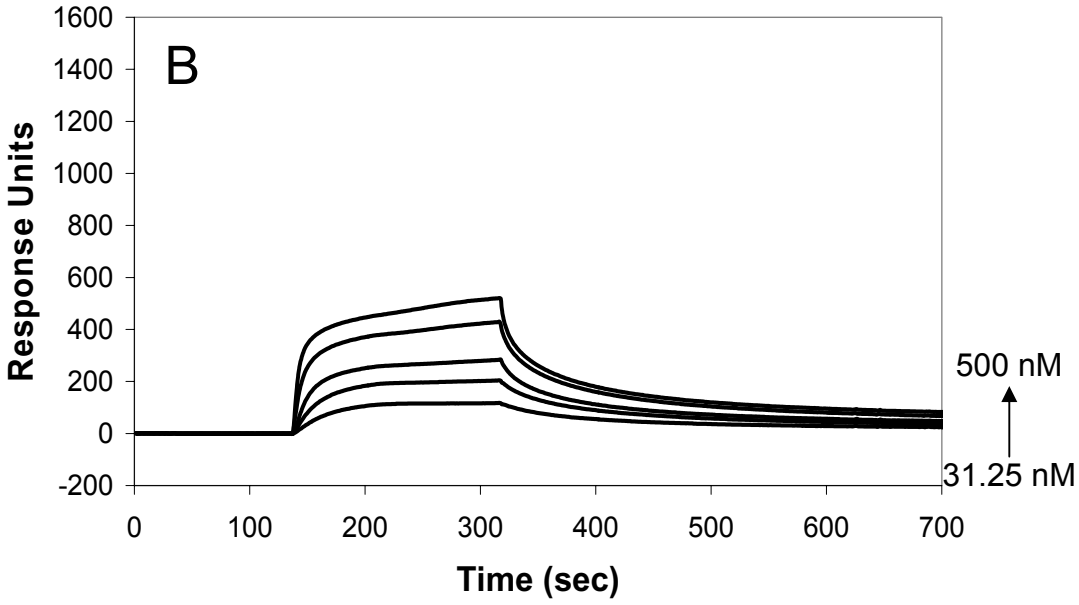
B
Response Units
1600
1400
1200
1000
800
600
400
200
0
-200
0
100
200
300
400
500
600
700
Time (sec)
500 nM
31.25 nM

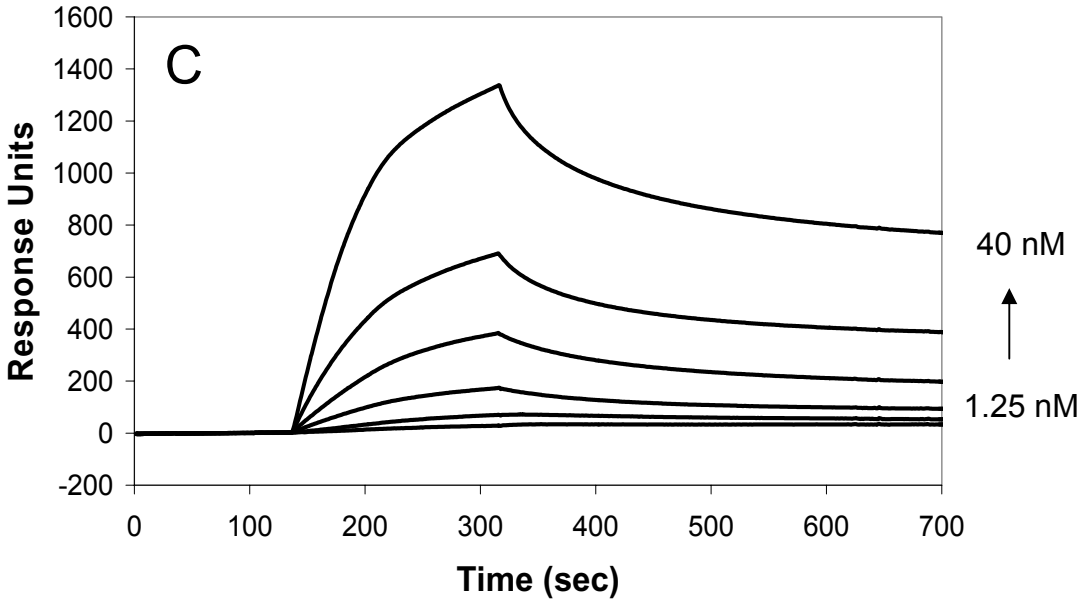
C
Response Units
1600
1400
1200
1000
800
600
400
200
0
-200
0
100
200
300
400
500
600
700
Time (sec)
40 nM
1.25 nM

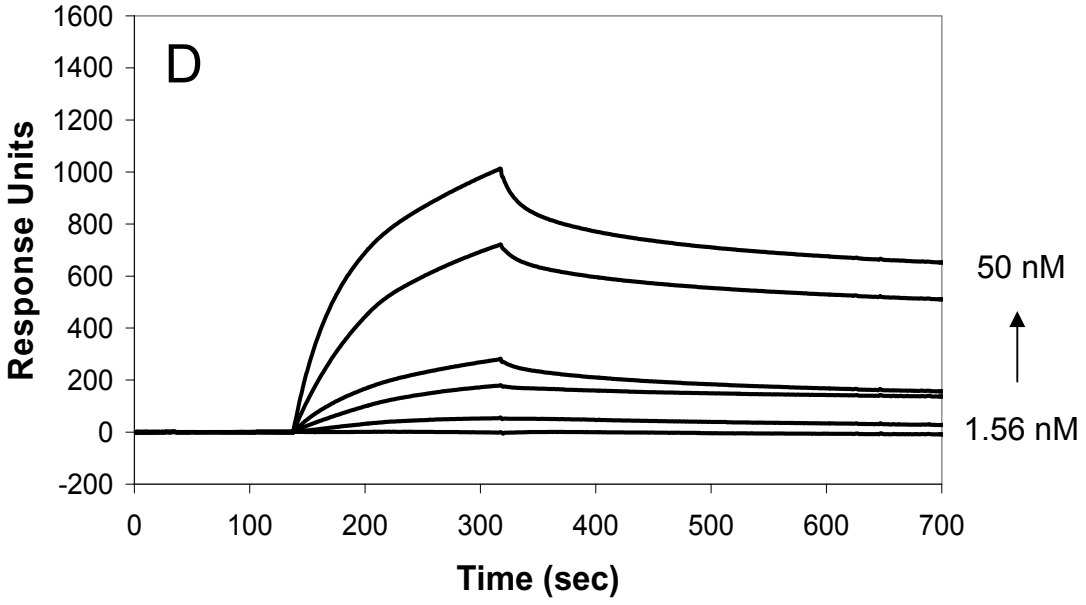
D
Response Units
1600
1400
1200
1000
800
600
400
200
0
-200
0
100
200
300
400
500
600
700
Time (sec)
50 nM
1.56 nM

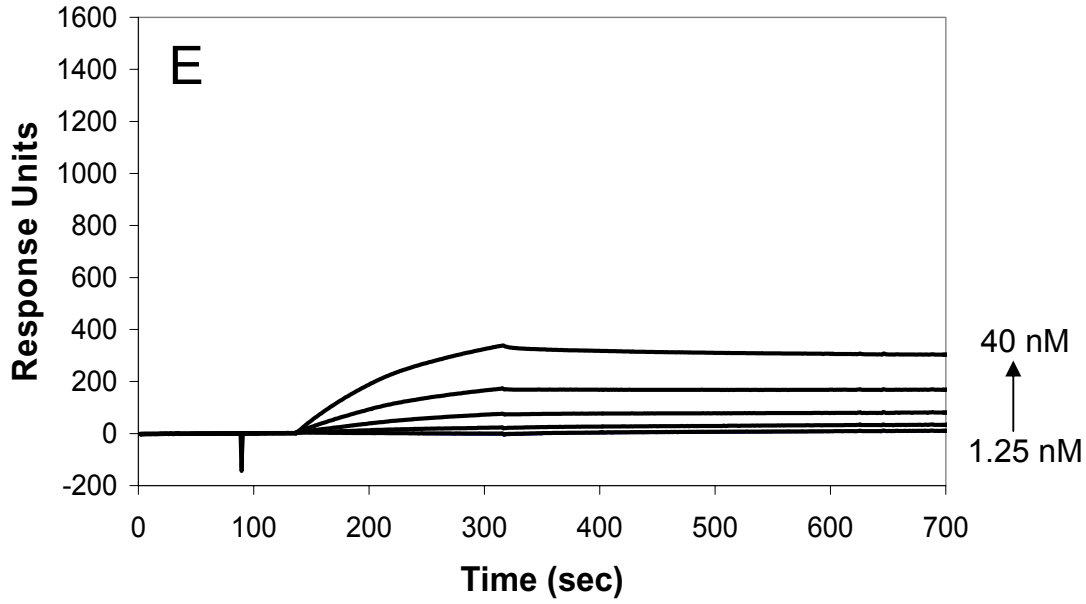

Figure 4.3: Surface plasmon resonance analysis of the interaction between uPA and uPA:serpin complexes with VLDLr. Sensorgrams showing the dose dependent binding of **(A)** uPA, **(B)** PAI-1, **(C)** uPA:PAI-1, **(D)** uPA:PAI-1^{R76E} and **(E)** uPA:PAI-2 to ~10,000 units of immobilised VLDLr, at the concentrations indicated. Data is representative of three experiments.

Many ligands interact with members of the LDLR family via regions of positive electrostatic potential in the ligand and negative electrostatic potential in the receptor (Fisher et al., 2006; Hussain et al., 1999). Therefore, the differential binding of uPA:PAI-1 and uPA:PAI-2 to LDLR members may be heavily influenced by the charge of their respective helix D regions and adjacent residues.

At physiological pH, PAI-2 carries a relatively negative charge (predicted pI = 5.4) compared with PAI-1 (predicted pI = 7), as reflected in the comparative surface electrostatic potentials of the two molecules in the relaxed conformation (Figure 4.4E,F). Helix D of PAI-1 has a mostly basic (+ve) charge, whereas the helix D of PAI-2 is more neutral and surrounded by multiple acidic (-ve) regions. Furthermore, Arg_{76} of PAI-1 is located in the middle of a basic (positively charged) cavity bounded by Lys_{80} and Arg_{136}, whilst the corresponding residue in PAI-2 sits on the edge of a smaller basic region, with Lys_{80} being replaced by Ser_{112} (Figure 4.4E,F).

Table 4.1: The kinetics parameters of PAI-1, PAI-1^{R76E}, PAI-2, uPA and uPA:serpin complexes binding to VLDLr, measured by surface plasmon resonance.

Analyte	Binding Model	k_a (M^{-1} S^{-1})	k_d (S^{-1})	K_D[1] (nM)	χ^2
PAI-1	1:1	9.90×10^4 ($\pm 6.83 \times 10^4$)	4.17×10^{-3} ($\pm 1.19 \times 10^{-3}$)	**51.8** (± 21.9)	8.12
PAI-1^{R76E}	No Binding	-	-	-	-
PAI-2	No Binding	-	-	-	-
uPA	Heterologous Analyte	8.00×10^4 ($\pm 1.08 \times 10^4$)	1.32×10^{-2} ($\pm 0.01 \times 10^{-2}$)	**209** (± 25.1)	13.9
		5.48×10^4 ($\pm 0.74 \times 10^5$)	1.50×10^{-3} ($\pm 0.13 \times 10^{-3}$)	**31.2** (± 5.69)	
uPA:PAI-1	Heterologous Analyte	1.50×10^5 ($\pm 0.20 \times 10^5$)	1.30×10^{-2} ($\pm 0.10 \times 10^{-2}$)	**84.8** (± 1.69)	19.6
		1.00×10^5 ($\pm 0.40 \times 10^4$)	1.30×10^{-4} ($\pm 0.18 \times 10^{-3}$)	**1.51** (± 0.27)	
uPA:PAI-1^{R76E}	1:1	7.79×10^4 ($\pm 0.84 \times 10^4$)	7.08×10^{-4} ($\pm 2.01 \times 10^{-4}$)	**9.95** (± 3.53)	8.2
uPA:PAI-2	1:1	1.73×10^5 ($\pm 0.62 \times 10^5$)	5.61×10^{-4} ($\pm 0.98 \times 10^{-4}$)	**4.68** (± 0.90)	1.9

1. Binding data was fitted using the BIAevaluation 4.0 software. The binding model chosen represents that with the lowest χ^2 value. (Values are the average ± SEM, n=3).

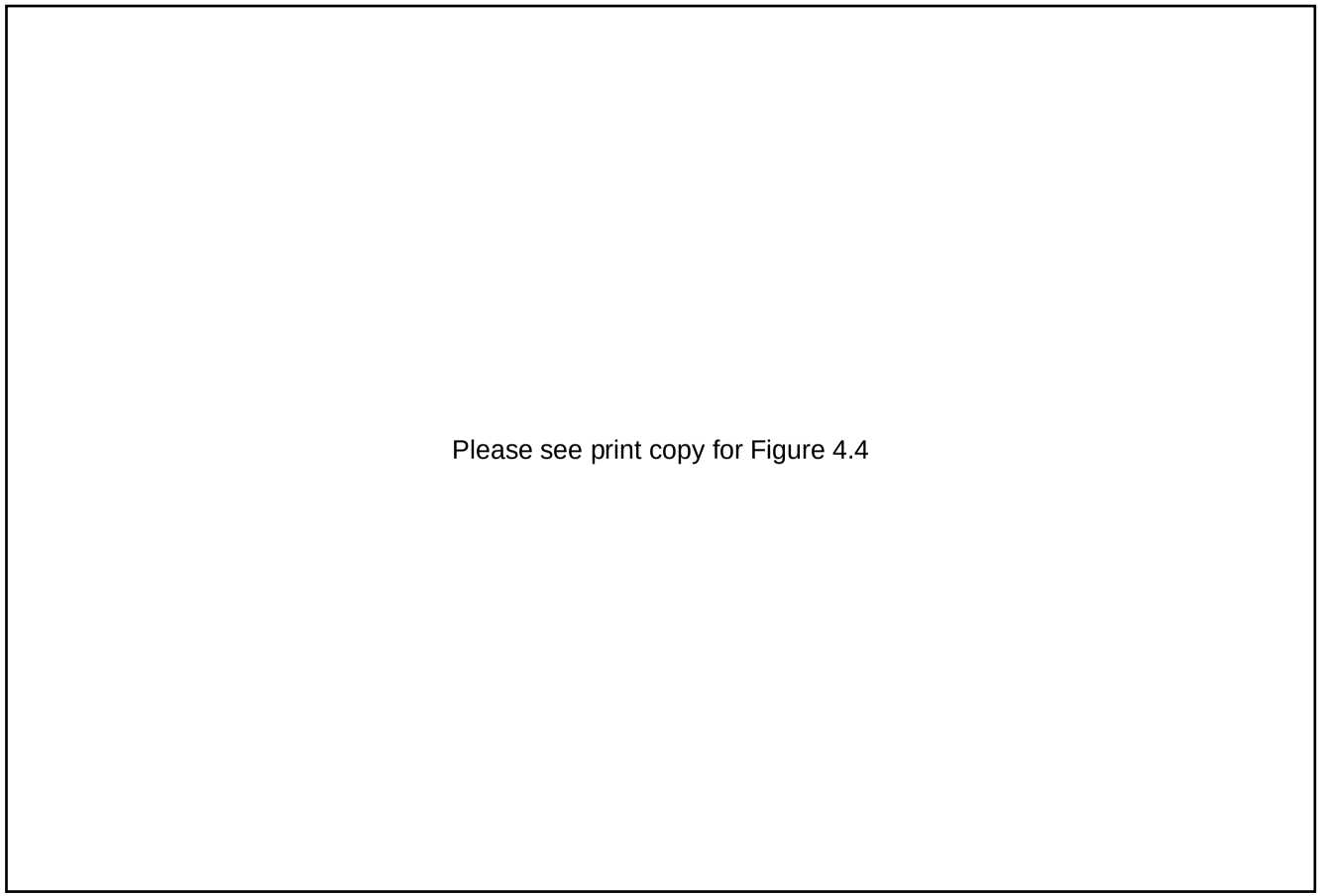

Figure 4.4: Comparison of PAI-1 and PAI-2 VLDLr binding interfaces. (A - D) Ribbon representation showing secondary structure and position of key binding residues within/adjacent to α-helix D of PAI-1 and PAI-2. **(E and F)**. Surface representation showing regions of positive electrostatic potential in blue, regions of negative potential in red and neutral regions in white. Surface position of helix D and key binding residues within or adjacent to this region are outlined in yellow. **(G)** Alignment of helix D sequence from PAI-1 and PAI-2. The putative minimal binding motif (Jensen et al., 2006) in PAI-1 is underlined with necessary basic and hydrophobic residues highlighted in yellow and blue respectively. Analysis performed using PyMol and X-ray crystal structures of the relaxed conformations of both PAI-1 (PDB accession 9pai, Aertgeerts *et al* 1995) and PAI-2 CD-loop deletion mutant (PDB accession 1jrr, Jankova *et al* 2001).

Jensen et al, (2006) proposed a minimal binding motif in LRP ligands, comprising 2 basic residues separated by 2-5 residues and N-terminally flanked by hydrophobic residues. A sequence containing both Arg_{76} and Lys_{80} in helix D of PAI-1 fits this motif, however this sequence is not conserved in PAI-2 (Figure 4.4G). Hence, both the electrostatic environment and surface topography of helix D, particularly surrounding the $Arg_{76/108}$ residue, may explain the observed differences in binding of PAI-1 and PAI-2 to VLDLr and LRP.

4.3.4 Serpin Internalisation is Related to VLDLr Affinity

The effect of serpin inhibition and associated complex formation upon uPA internalisation by MCF-7 cells was analysed using $Alexa_{488}$ labeled uPA. Relatively little internalisation of exogenous uPA was observed after 1 h (Figure 4.5A), as previously reported for PC-3 cells (Chapter 3) (Croucher et al., 2006). However, significantly increased uPA:PAI-1 internalisation (~8.5 fold) was observed in the same timeframe (Figure 4.5A). By comparison, only a ~4-5 fold increase in uPA:PAI-1^{R76E} or uPA:PAI-2 internalisation was observed compared to uPA alone (Figure 4.5A). RAP-mediated inhibition of uPA or uPA:serpin internalisation confirmed the involvement of VLDLr in this process (Figure 4.5A). Hence there was a very strong logarithmic correlation between the affinity of uPA:serpin complexes for VLDLr and uPA internalisation by MCF-7 cells (Figure 4.5B). Therefore, VLDLr affinity may be the rate limiting determinant of uPA/uPAR clearance from the cell surface. Despite this difference in internalisation rate and whilst PAI-2 exhibited a slightly slower rate of uPA inhibition, no significant difference was observed in the ability of PAI-1 or PAI-2 to inhibit cell surface uPA activity on these cells after a 30 min incubation (Figure 4.5C).

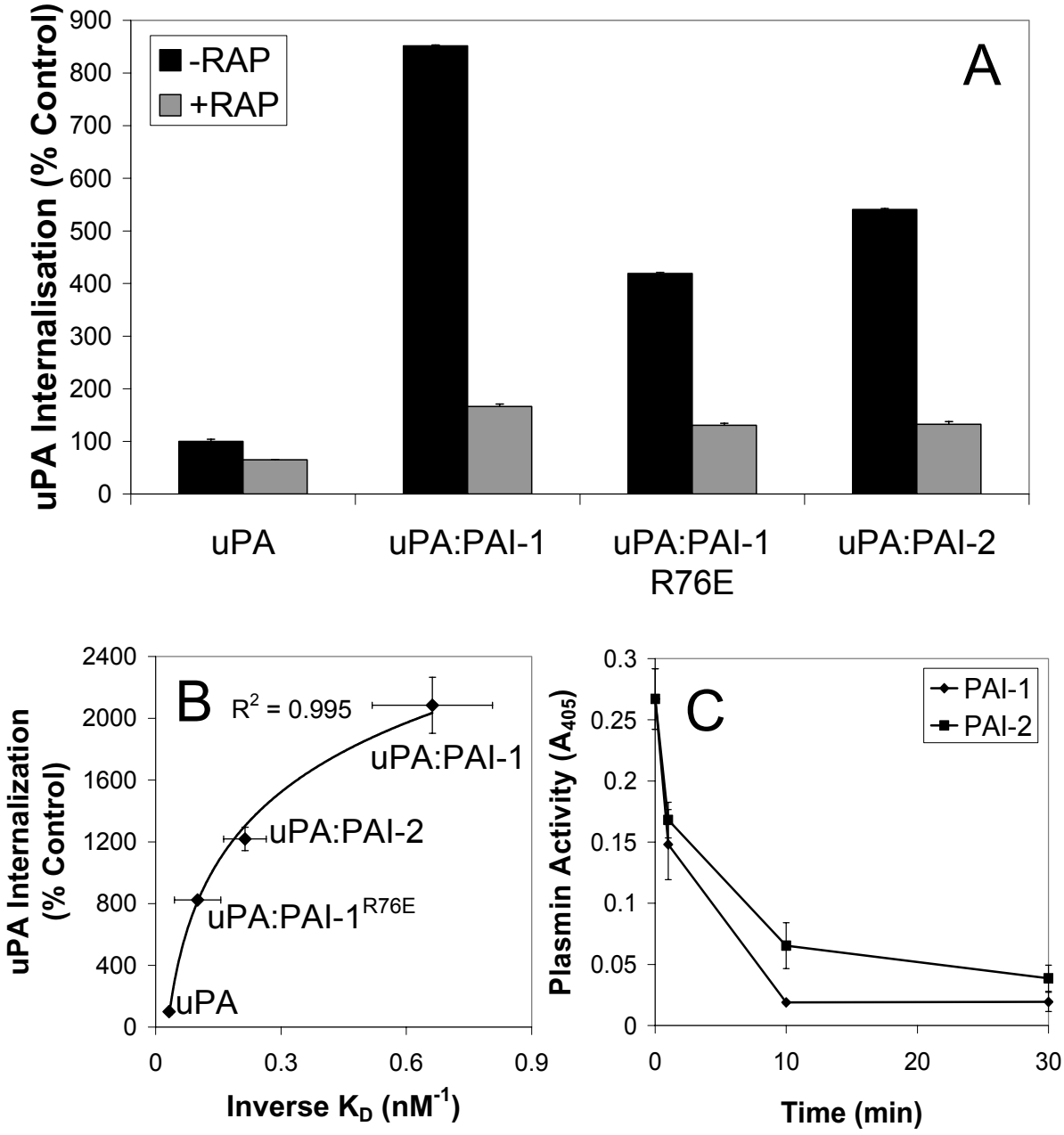

Figure 4.5: VLDLr mediated internalisation of uPA:serpin complexes by MCF-7 cells. (A) MCF-7 cells were incubated in the presence or absence of RAP (200 nM) for 15 min at 37 °C, prior to analysis of uPA:$Alexa_{488}$ internalisation by fluorescence quenching internalisation assay. uPA:serpin complexes were formed by incubation at a 1:1 molar ratio, at 37°C for 30 min. (mean ± SEM, n=3). **(B)** Relationship between the affinity of uPA and uPA:serpin complexes for VLDLr (Table 1, n=3) and RAP sensitive internalisation (Total internalisation minus internalisation in the presence of RAP) (n=2). **(C)** The inhibition of cell surface uPA activity by PAI-1 and PAI-2. MCF-7 cells pre-incubated with uPA (5 nM) at 4°C for 30 min were incubated with PAI-1 or PAI-2 (5 nM) at 37°C for the time periods indicated. uPA activity was measured by the addition of plasminogen (0.5 µM) and Spectrozyme-PL (0.4 mM) for 2 h. Absorbance was read at 405 nm. (mean ± SEM, n=3).

4.3.5 PAI-2 Does Not Induce Mitogenic Signaling in MCF-7 cells

The high affinity VLDLr binding site in PAI-1 has previously been implicated in the initiation of signaling events in breast cancer cells (Webb et al., 2001). The absence of a corresponding high affinity site in PAI-2 suggests potential differences in signaling capacities between these serpins. As a global indicator of intracellular signaling events (Degryse et al., 2004), tyrosine phosphorylation in MCF-7 cells was measured following a 30 min stimulation by uPA, uPA:PAI-1, uPA:PAI-1^{R76E} or uPA:PAI-2. Stimulation by uPA:PAI-1 induced significant cytoplasmic and nuclear tyrosine phosphorylation, which was blocked by the addition of RAP (Figure 4.6). In contrast, tyrosine phosphorylation was not observed following incubation with uPA, uPA:PAI-1^{R76E} or uPA:PAI-2 (Figure 4.6).

Webb et al. (2001) showed that the binding of the PAI-1 high affinity site to VLDLr resulted in the sustained activation of ERK, which otherwise underwent transient activation following the binding of uPA to uPAR. These transient and sustained ERK responses were also observed upon stimulation of MCF-7 cells with uPA or uPA:PAI-1, respectively (Figure 4.7). Stimulation by uPA:PAI-2 or uPA:PAI-1^{R76E} also resulted in a slight increase in ERK phosphorylation however these did not reach the same level or timeframe as that achieved by uPA:PAI-1. Interestingly, a logarithmic correlation (R^2 = 0.9584) was observed between VLDLr affinity (Table 1) and ERK phosphorylation (Figure 4.8A) and a linear correlation (R^2 = 0.9853) between relative uPA internalisation (Figure 4.5) and ERK phosphorylation (Figure 4.8B), suggesting that the level of ERK phosphorylation may directly related to the process of uPA/uPAR/VLDLr endocytosis.

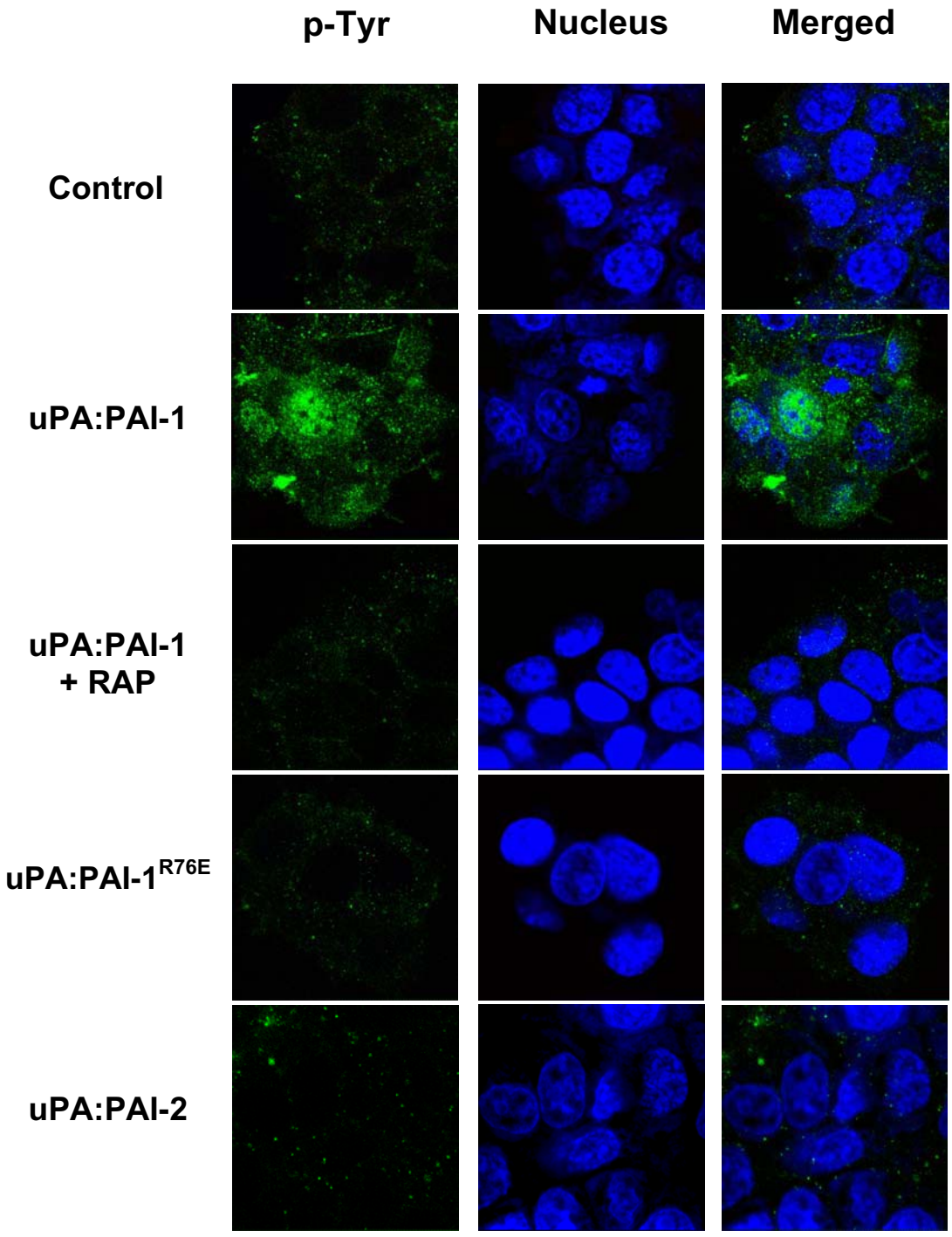

Figure 4.6: uPA:PAI-2 does not induce nuclear/cytoplasmic tyrosine phosphorylation of cellular proteins. MCF-7 cells were serum starved for 4 h and incubated in the presence or absence of RAP (200 nM) for 15 min at 37°C, then incubated with 10 nM uPA, uPA:PAI-1, uPA:PAI-1^{R76E}, uPA:PAI-2 for 30 min at 37°C. The cells were washed with ice cold PBS, fixed with 3.75% PFA and permeabilised with 0.1% Triton-x 100. After incubation with 10 µg/ml anti-phospho tyrosine monoclonal antibody (PY20), the cells were washed and incubated with goat anti-mouse IgG-FITC (1:200 dilution) and TOPRO (1:400). After washing, the cells were analysed by immunofluorescence and confocal microscopy. Scale bars are 10 µm.

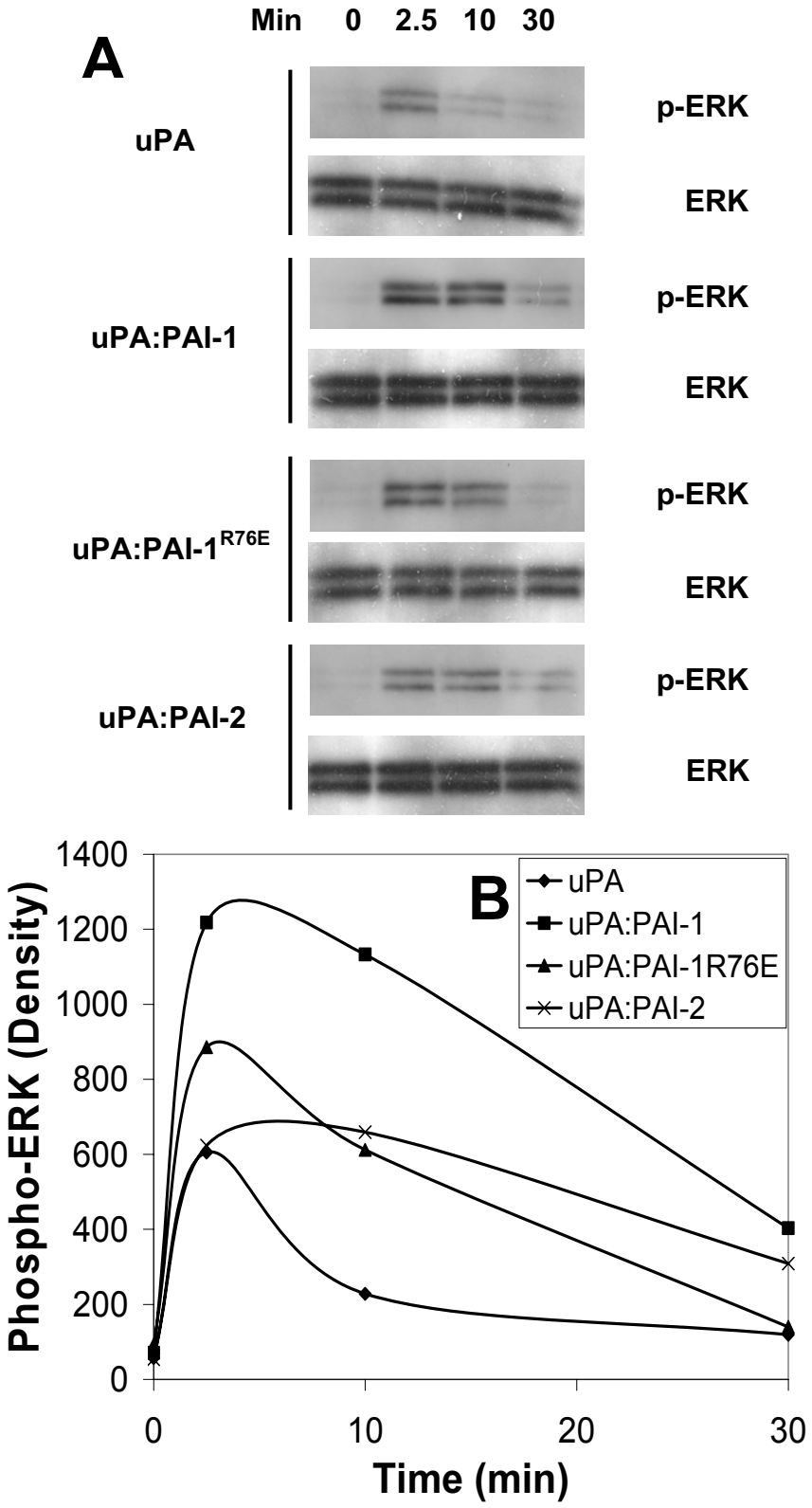

Figure 4.7: Differential ERK phosphorylation in MCF-7 cells upon uPA:PAI-1 and uPA:PAI-2 stimulation. MCF-7 cells were serum starved for 6 h, then stimulated by incubation with 10 nM uPA, uPA:PAI-1, uPA:PAI-1^{R76E} or uPA:PAI-2 for 0, 2.5, 10 or 30 min, in serum free RPMI. **(A)** Cell lysates were analysed for phosphorylated and total ERK by western blotting. **(B)** densitometry analysis of the levels of phosphorylated ERK. Analysis was performed using Quantity One software (BioRad). Data is representative of three separate experiments.

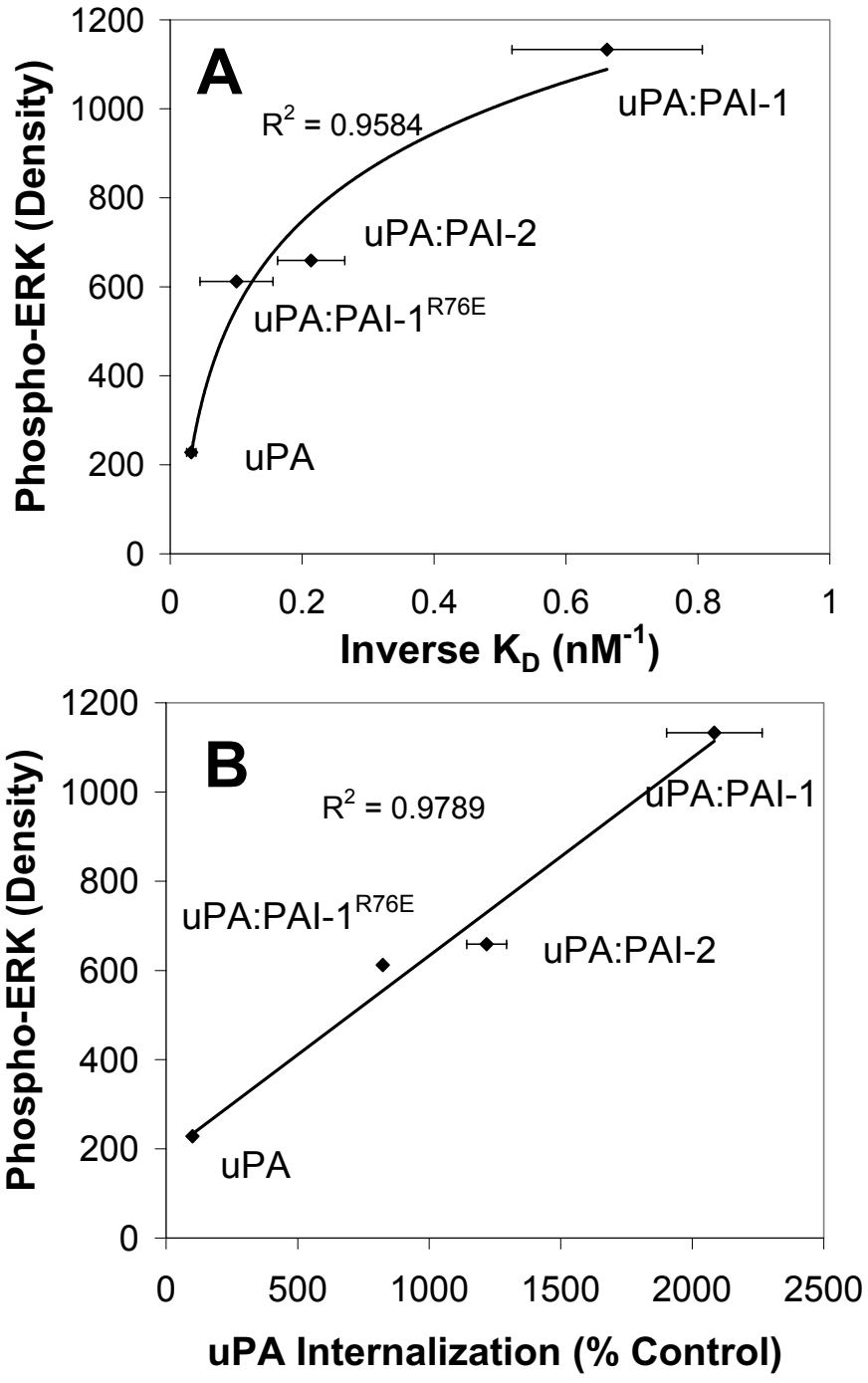

Figure 4.8: The correlation of phosphorylated ERK, VLDLr affinity and RAP sensitive uPA internalisation. Levels of phosphorylated ERK after a 10 min stimulation by 10 nM uPA, uPA:PAI-1, uPA:PAI-1^{R76E} or uPA:PAI-2 (Figure 4.6B) were correlated with **(A)** the affinity of each ligand for VLDLr (Table 1) and **(B)** the relative amount of RAP sensitive internalisation (Total internalisation minus internalisation in the presence of RAP) of each by MCF-7 cells after 1 h (Figure 4.4). Data was fitted to either a linear or logarithmic equation using Microsoft Office Excel 2003 (Microsoft).

As uPA:PAI-1 binding to VLDLr and the resulting sustained ERK phosphorylation is known to induce cell proliferation (Webb et al., 2001), the effect of uPA:PAI-2 on MCF-7 cell proliferation was also examined. A ~60% increase in proliferation of MCF-7 cells (relative to control) was observed after 36 h stimulation with uPA:PAI-1 (Figure 4.9). This effect was inhibited by RAP, again confirming a VLDLr-mediated effect. Consistent with the binding and internalisation data presented above, no effect on cell proliferation was observed following incubation with uPA, uPA:PAI-1^{R76E} or uPA:PAI-2 (Figure 4.9).

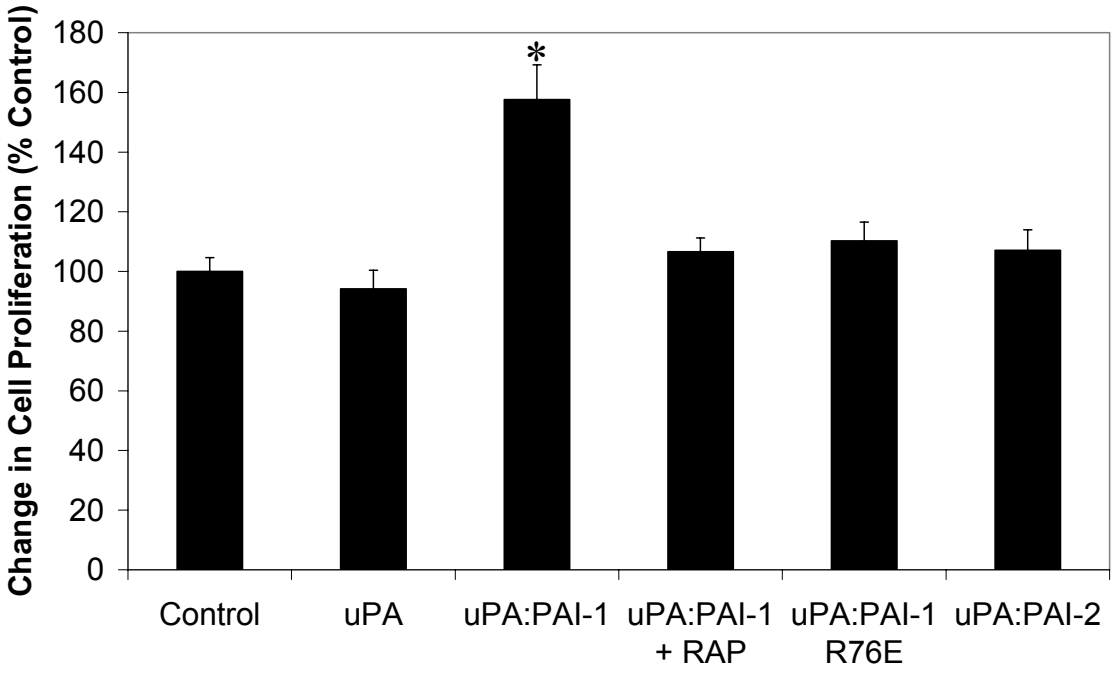

Figure 4.9: uPA:PAI-2 does not stimulate cell proliferation of MCF-7 cells. MCF-7 cells were cultured in RPMI/5% FCS for 48 h then treated with 10 nM uPA, uPA:PAI-1, uPA:PAI-1 plus RAP (200 nM), uPA:PAI-1^{R76E}, uPA:PAI-2 or vehicle in RPMI containing 300 µg/ml glutamine, 5 µg/ml transferrin, and 38 nM selenium. After culturing for 36 h, cell growth was determined by MTS assay. Values of cell growth are relative to the growth of control cells. Values differing significantly from the control are marked with an asterix (*$p<0.05$)

4.4 DISCUSSION

Dysregulation of the uPA system plays a key role in tumour invasion and metastasis, regulating diverse processes such as cell adhesion, migration and proteolysis. This has strong prognostic relevance and provides opportunities for therapeutic targeting (Dano et al., 2005; Duffy, 2004; Ranson et al., 2002; Romer et al., 2004; Schmitt et al., 2000). High uPA and PAI-1 levels are strongly associated with poor prognosis in cancer. (Duffy, 2004; Weigelt et al., 2005). Furthermore, the co-expression of uPA and PAI-1 is the only biomarker to have obtained level 1 significance as an independent marker of poor prognosis in early breast cancer (Weigelt et al., 2005). In contrast, PAI-2 expression in breast carcinomas that also express uPA is correlated with increased relapse-free survival, whilst low levels of PAI-2 are associated with metastasis in non-small cell lung carcinomas, lung cancer, pancreatic cancer and breast cancer (Duffy, 2004; Duffy and Duggan, 2004; Foekens et al., 1995; Foekens et al., 2000; Kruithof et al., 1995).

The results presented here show that VLDLr binds and mediates the endocytosis of uPA:PAI-2 on breast cancer cells *in vitro*. Critically, clear differences were demonstrated in binding mechanisms between uPA:PAI-1 and uPA:PAI-2 for VLDLr which highlight novel and important functional implications of this differential binding. Established LRP and VLDLr binding determinants in PAI-1 are absent in PAI-2, leading to distinct downstream signaling events that may explain the disparate relationships between PAI-1 and PAI-2 expression and disease outcome in breast cancer.

Cellular distribution may be an important factor when considering potential functional roles of PAI-2 in cancer. Others have suggested that intracellular PAI-2 has a role in tumour progression through regulation of apoptosis and

proliferation/differentiation (Medcalf and Stasinopoulos, 2005) (Chapter 1.2.7). Still, others have clearly demonstrated that an extracellular role for PAI-2 is relevant to the inhibition of tumour progression (Chapter 1.2.8). For example, PAI-2 is only significant as a prognostic indicator of positive outcome in association with the expression of uPA (Duffy and Duggan, 2004). Furthermore, inhibition of uPA by over-expression of PAI-2 in tumour xenograft models led to tumour encapsulation, and the reduction or absence of metastases (Laug et al., 1993; Mueller et al., 1995; Praus et al., 1999). Moreover, a detailed clinical study has shown that high PAI-2 expression by tumour-associated fibroblasts was protective in esophageal squamous cell carcinomas (Shiomi et al., 2000).

PAI-1 can promote invasion and metastasis independent of its inhibition of uPA-mediated proteolysis. For example, PAI-1 regulates cell migration through vitronectin binding, blocking cell attachment via uPAR and integrins (Deng et al., 1996; Stefansson and Lawrence, 1996). Alternatively, uPA:PAI-1 stimulates sustained activation of pro-proliferative ERK signaling and subsequent cell proliferation via a high affinity interaction with VLDLr in MCF-7 cells (Webb et al., 2001), which also mediates endocytosis of this complex in various cell lines (Strickland et al., 2002). Given the novel observation that uPA:PAI-2 is endocytosed by VLDLr on MCF-7 cells (Figure 4.1), SPR analysis was undertaken to characterise binding of uPA:PAI-1 and uPA:PAI-2 to VLDLr. These analyses confirmed a high affinity interaction between uPA:PAI-1 and VLDLr. In contrast, the data demonstrated that uPA:PAI-2 binds to VLDLr in a similar manner to uPA:PAI-1^{R76E}, which lacks the high affinity binding site in PAI-1 for VLDLr and LRP (Stefansson et al., 1998). The mutation of Arg_{76} within helix D of PAI-1 results in a 10 fold reduction in the ability of uPA:PAI-1 and trypsin:PAI-1 to

compete for binding to LRP (Stefansson et al., 1998). Interestingly, in this study, this mutation also resulted in a complete abrogation of the binding of free PAI-1 to VLDLr.

It should be noted that whilst previous studies of uPA:PAI-1 binding to VLDLr, using a solid-phase binding assays, reported a 1:1 interaction with K_D values of 14 and 15 nM (Argraves et al., 1995; Mikhailenko et al., 1999), the SPR analyses of uPA:PAI-1 binding to VLDLr presented here indicates a more complex interaction. However, if a simple 1:1 interaction model was force fitted the data, a similar K_D of 24 ± 3 nM was obtained, but with a greatly reduced significance of fit (χ^2 = 38) (Due to the complex nature of this interaction, the analysis of this data is presented in Appendix 5). Heegaard et al. (1995), Kasza et al. (1997) and Skeldal et al. (2006) reported 1:1 binding interactions between uPA:PAI-1 and VLDLr, with K_D values of 0.8, 1.5 and 1.6 nM. These values are almost identical to that obtained for the high affinity VLDLr binding site in PAI-1 in this study (Table 1). Skeldal et al. (2006) also used surface plasmon resonance to investigate the interaction between uPA:PAI-1 and VLDLr and were unable to obtain an acceptable fit using a 1:1 binding site model. They therefore restricted their analysis to only one phase of the clearly two phase association and dissociation data, possibly ignoring the presence of a second lower affinity interaction as observed in this chapter. Although the heterologous analyte model of uPA and uPA:PAI-1 binding to VLDLr does not provide a perfect fit, it is currently the best available model (lowest χ^2 values) and clearly indicates that a 1:1 model is not appropriate or accurate. Indeed the presence of an independent, moderate affinity binding site within the uPA moiety of uPA:PAI-1 (Table 1) has previously been suggested (Stefansson et al., 1998). It could also be expected that a heterologous analyte model would be observed for the binding of uPA:PAI-1^{R76E} as only one residue has

been mutated, although it is likely that the disruption of adjacent residues within this area has significantly altered the biochemistry of the interaction (as discussed below).

It is interesting to note that the interaction between uPA and LRP (Chapter 3) and VLDLr (Chapter 4) present a different number of binding sites on the uPA molecule. uPA bound to LRP with a 1:1 binding site model and a K_D of 200 nM (Table 3.1), whereas uPA bound to VLDLr as a heterologous analyte with two independent binding sites with K_D values of 209 and 31.2 nM (Table 4.1). As a common ~200 nM site exists for both LRP and VLDLR, it is possible that the binding interface presented by VLDLr allows for an interaction with an alternative and higher affinity site on the uPA molecule. Additionally, the increased affinity of uPA:PAI-2 binding to VLDLr (4.68 nM as compared to 36 nM for LRP), which is strongly dependent on sites within uPA, agrees with this hypothesis. This is also supported by the internalisation assay data, in which uPA:PAI-2 is internalised ~2 fold more than uPA on the LRP expressing PC-3 cells (Figure 3.8) and ~5 fold more by the VLDLr expressing MCF-7 cells (Figure 4.5).

Even though the binding models applied to the SPR data may not provide a completely accurate description of the interactions between these uPA:serpin complexes and VLDLR, the strong logarithmic correlation between the affinity of the uPA:serpin complexes for VLDLr and internalisation by MCF-7 cells indicates that the kinetic data does give a solid indication of the *in vitro* interaction. This data also suggests that VLDLr affinity may be the primary determinant of uPA:serpin/uPAR internalisation.. Comparison of structural characteristics of PAI-1 and PAI-2 in their relaxed conformations (Aertgeerts *et al* 1995 and Jankova *et al* 2001), mimicking that present in uPA:serpin complexes, provides a clear explanation for the differential binding of PAI-1 and PAI-2 to VLDLr and LRP (Figure 4.4). Amino acid residues Arg_{76}, Lys_{80} and Lys_{88}

within and adjacent to helix D of PAI-1 contribute to binding of PAI-1 to LRP (Horn et al., 1998). Along with Arg_{118} and/or Lys_{122} (within ß-strand 1A), these residues have also been shown to contribute to the binding of the uPA complexed form of PAI-1 to LRP and VLDLr (Horn et al., 1998; Rodenburg et al., 1998; Skeldal et al., 2006), with Arg_{76} forming part of a cryptic high affinity binding site for LRP exposed by complex formation with uPA (Stefansson et al., 1998). These residues conform with the proposed common binding motif for LRP ligands of 2 basic residues separated by 2-5 residues and N-terminally flanked by hydrophobic residues (Jensen et al., 2006). This motif is not conserved in PAI-2. Whilst the residue corresponding to Arg_{76} in PAI-1 is conserved within helix D of PAI-2 (Arg_{108}), the residue corresponding to Lys_{80} is replaced by a serine (Ser_{112}) in PAI-2 and the adjacent hydrophobic residue is not conserved (Figure 4.4). Furthermore, there are clear differences in the surface topography and overall electrostatic charge between PAI-1 and PAI-2. Previous studies have shown that mutation of basic residues within and adjacent to helix D of PAI-1 can reduce affinity of uPA:PAI-1 for LDLR members (Rodenburg et al., 1998). This mechanism is further supported by a recent detailed description of the interaction between RAP domain 3 and LDLR type-A modules highlighting the importance of electrostatic and hydrophobic interactions between these binding determinants (Fisher et al., 2006). As the modeling is based on the structure of a C-D loop deletion mutant of PAI-2, it is difficult to predict the influence of the C-D loop on LRP/VLDLr binding and a potential to influence the accessibility of Arg_{108} and surrounding residues in helix D cannot be discounted.

uPA:PAI-2 and uPA:PAI-1^{R76E} did not induce the significant global tyrosine phosphorylation observed following incubation of MCF-7 cells with uPA:PAI-1 and an attenuated response was observed following incubation with uPA:PAI-2 or

uPA:PAI-1^{R76E} compared to the elevated and sustained ERK phosphorylation stimulated by uPA:PAI-1 (Figure 4.5). Furthermore, the proliferation of MCF-7 cells stimulated by uPA:PAI-1 was not observed following treatment with either uPA:PAI-2 or uPA:PAI-1^{R76E} (Figure 4.7). Given the striking differences in binding mechanisms described above, these data clearly implicate the high affinity VLDLr binding site on PAI-1 in the initiation of mitogenic signaling events.

Webb et al (2001) have previously shown that the proliferation of MCF-7 cells induced by uPA:PAI-1 is associated with sustained ERK phosphorylation. This sustained ERK phosphorylation was also observed in this study, however not to the same extent as that seen in Webb et al. (2001). This may be due to the divergent nature of cultured cell lines or differences in PAI-1 preparations. Nevertheless, distinct differences were seen in the ability of uPA:PAI-1 and uPA:PAI-2 to initiate ERK phosphorylation in MCF-7 cells. Both the amount of phosphorylated ERK detected and the duration of its activation were increased in the case of uPA:PAI-1. Furthermore, the level of phosphorylated ERK stimulated by uPA:PAI-2 did not exceed that of uPA, however the response was slightly extended. Taken together, these results indicate that upon VLDLr binding, uPA:PAI-1 elicits a mechanism of elevated ERK phosphorylation that uPA:PAI-2 does not. Also, the slight extension of ERK phosphorylation but lack of increased cell proliferation in the case of uPA:PAI-2 suggests that a threshold effect of ERK phosphorylation takes place, where a sufficient level or time of activation must be exceeded to induce proliferative effects. Given the striking differences in binding mechanisms and signaling pathway activation described above, these data clearly implicate the high affinity VLDLr binding site on PAI-1 in these signaling events. The various putative mechanisms of VLDLr-mediated cell signaling induced by uPA:PAI-1 are discussed further in Chapter 5 and also in detail by Strickland et al. (2002).

It is clear that PAI-1 and PAI-2 have differential effects on tumour progression. Whilst both PAI-1 and PAI-2 inhibit cell surface uPA (Figure 4.5C) and consequently decrease pericellular plasminogen activation capacity, PAI-1 has significant additional functional roles stimulating cell proliferation. Therefore, this data proposes a structural basis for this functional difference based on the absence of a high affinity LDLR binding site in PAI-2. Thus, the poor prognosis for breast cancer patients with high uPA/PAI-1 protein levels may be associated with the ability of PAI-1 to initiate mitogenic signaling events through LDLRs. In contrast, the favorable overall survival of patients with high PAI-2 protein expression may be due to uPA inhibition and clearance via LDLRs without the cell signaling events and increased metastatic potential associated with high PAI-1.

Chapter 5

5. Conclusions and Future Directions

The data presented in this thesis provides definitive proof that PAI-2 is internalised by cancer cells following the inhibition of cell surface uPA, contrary to previously published data (Ragno et al., 1995) and the conclusions of various review articles (Andreasen et al., 2000; Andreasen et al., 1997; Schmitt et al., 2000). This internalisation was demonstrated to be mediated through high affinity interactions of the uPA:PAI-2 complex with the endocytosis receptors LRP and VLDLr.

This finding has implications for cancer therapy using PAI-2 as the targeting agent as it provides an opportunity for the intracellular delivery of a cytotoxin (Discussed in Chapter 2). This cytotoxin delivery strategy provides an avenue for future research as a method utilising PAI-2 to transport cytotoxins into the lysosomes of cancer cells would need to be thoroughly optimised. The conditions through which cytotoxins are attached to the PAI-2 molecule and by which they are released once entering the lysosome would need to be established. Also, the choice of a suitable cytotoxin that would be able to escape the lysosome and also be resistant to its acidic conditions is vital to the success of such a therapy.

The established pathways of PAI-2 endocytosis not only provide an avenue for improving PAI-2 cancer therapy, but also provide important information on the prognostic significance of tumour expression of PAI-2 and the related serpin, PAI-1. As both PAI-1 and PAI-2 are potent inhibitors of uPA (Chapter 1.2.5), the disparity between PAI-1 and PAI-2 expression and tumour progression seems illogical (Chapters 1.2.7 and 4). However, the differences observed in this thesis between the biochemical interactions of uPA:PAI-1 and uPA:PAI-2 with receptors of the LDLR family provide a basis for this disparity.

Data obtained through SPR studies consistently showed that PAI-2 does not contain a high affinity site towards LDLR family molecules (Chapters 3 and 4). Whilst

residues within PAI-2 may contribute a small proportion of the binding of uPA:PAI-2 complexes to these receptors, the majority of the interaction is mediated through sites within uPA. This suggests that the interaction of the PAI-1 high affinity site with LDLR family members, the subsequent signaling events and cell proliferation, may contribute to the poor prognosis observed in tumours that over-express PAI-1. Conversely, the lack of this high affinity LDLR site within PAI-2 suggests that PAI-2 is able to inhibit and clear cell surface uPA without inducing these cell signaling events (Summarised in Figure 5.1). Thus, this structural difference between PAI-1 and PAI-2 (Further discussed in Chapter 4) may underlie the disparity in their prognostic impacts.

Despite having only 24% amino acid homology, PAI-1 and PAI-2 still fold into the highly conserved serpin secondary and tertiary structure (discussed in Chapter 1.2.5.1). However, this low sequence similarity may underlie the differences in the interactions of PAI-1 and PAI-2 with co-receptors such as LRP and VLDLr. Mutational analyses are proposed to determine the role of the differing helix D sequences of PAI-1 and PAI-2 and the effect that these have upon binding to LRP and VLDLr. It is hypothesised that replacement of the PAI-2 helix D with that of PAI-1 will increase the affinity of the uPA:PAI-2 complex for VLDLr and LRP, therefore increasing its rate of endocytosis and potential to activate ERK. Further studies will would then be required to refine the residues involved in this high affinity interaction by undertaking site-directed mutagenesis of the PAI-2 helix D to introduce the proposed LDLR binding motif present in the helix D of PAI-1 (Figure 4.4). The possibility of the CD-loop interfering with uPA:PAI-2 binding to LDLRs should be examined by using CD-loop deletion mutants of PAI-2 with both the wild-type and PAI-1 helix Ds in place. The contribution of the uPA moiety to LDLR binding will also be examined using a uPA

mutant with decreased LDLR binding ability ($uPA^{R108A,\ R109A,\ R110A}$) (Skeldal et al., 2006), obtained from Prof. Peter Andreasen (University of Aarhus, Denmark).

While levels of LDLR expression and activity may have varying effects on the cell surface levels of uPAR and thus contribute to the regulation of cell adhesion and migration, the impact of LRP or VLDLr expression varies according to origin of the tissue involved (Discussed in Chapter 1.3.1). As the signaling events mediated by PAI-1 through VLDLr and LRP involve different pathways and have different functional consequences, the response of each individual tumour to PAI-1 stimuli will differ accordingly. However, the activation of ERK upon PAI-1 stimulation has recently been demonstrated in other cell lines (Chen et al., 2006; Soeda et al., 2006), suggesting that high PAI-1 expression will result in ERK activation and cell proliferation in multiple tumour types.

The mechanism of this sustained ERK activation (Chapter 4) has not been elucidated (Strickland et al., 2002), although multiple lines of evidence suggest that EGFR is recruited in response to uPA or uPA:PAI-1 binding and transmits signals through to ERK (Jo et al., 2005; Liu et al., 2002). However, the mechanism of this recruitment has not been addressed. The data obtained in this thesis is highly significant to this process, as it may provide further information to the mechanism behind this process of sustained ERK activation. For example, one hypothesis is that the sustained activation of ERK in MCF-7 cells may be through continuous recycling of uPAR rather than the interaction of VLDLr sites revealed in the uPA:PAI-1 complex (Strickland et al., 2002). That is, uPA:PAI-1/VLDR causes the rapid clearance of uPA/uPAR and recycling of uPAR back to the surface where it is available to bind more uPA. This then allows uPAR to interact with integrins and initiate signaling again. ERK activation in

the presence of PAI-1 is thus sustained because of the "sum of continuous transient responses" (Strickland et al., 2002).

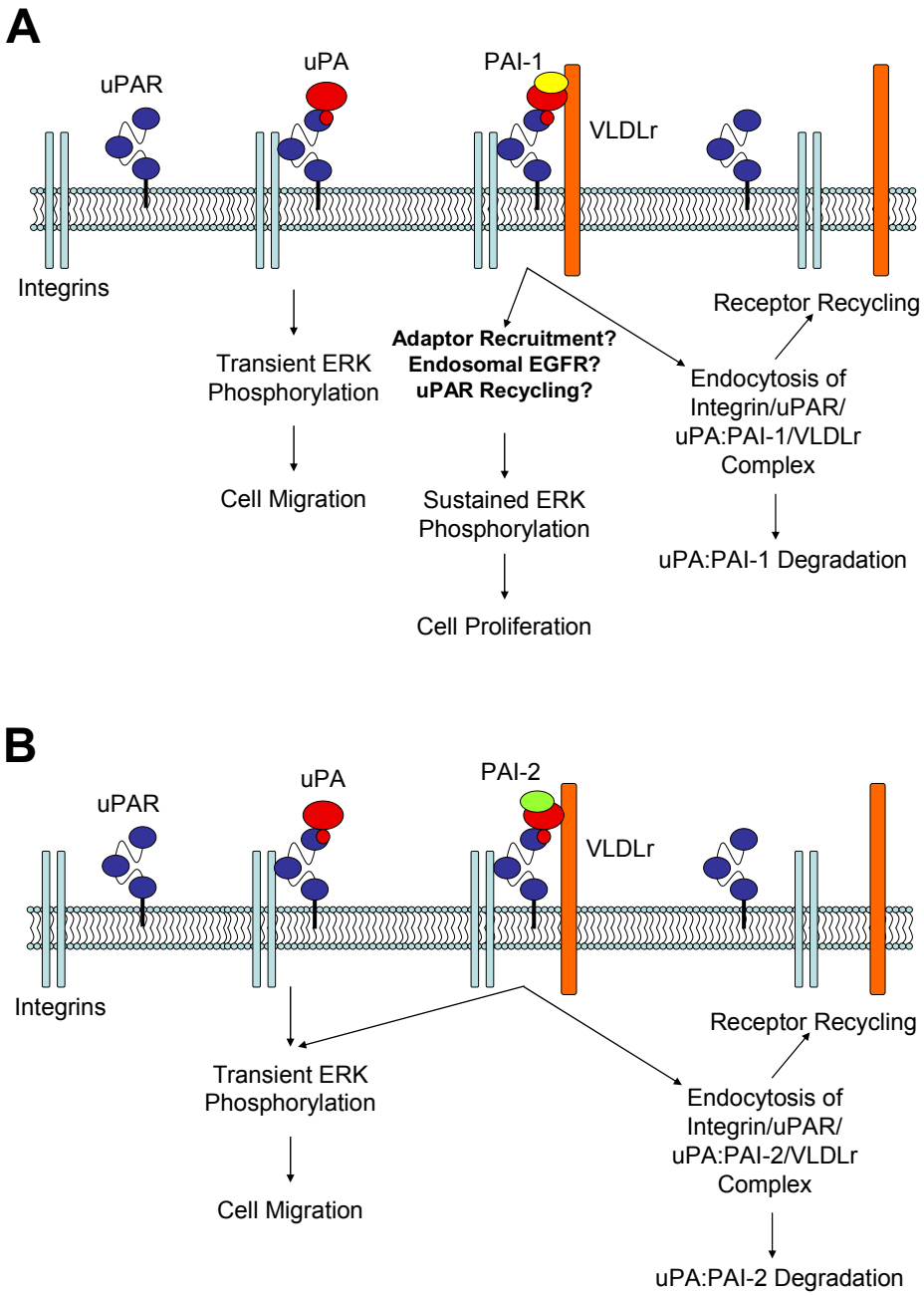

Figure 5.1: Signaling events mediated upon the endocytosis of uPA:PAI-1 and uPA:PAI-2 by VLDLr. The signaling events initiated upon the inhibition of uPAR bound uPA by **(A)** PAI-1 and **(B)** PAI-2, the subsequent interaction of uPA:PAI-1 and uPA:PAI-2 with VLDLr and the endocytosis of these complexes is briefly outlined.

If the uPAR recycling response is involved in PAI-1-mediated cell proliferation then PAI-2 should elicit a similar functional response. Furthermore, the increased level of ERK activation seen after stimulation with uPA:PAI-1 for 2.5 min, compared to that of uPA, uPA:PAI-2 and to a lesser extent uPA:PAI-1^{R76E} (Figure 4.6), does not support this model either, as uPAR would not have had sufficient time to be endocytosed and recycled. Hence, the data presented in this thesis suggests that the "sum of continuous transient reponses" is not the case and therefore it is unlikely that uPA:PAI-1/VLDR signal transduction exerts its effect on cell proliferation via the uPAR recycling model.

The high affinity of uPA:PAI-1 binding to VLDLr may be enough to induce this response, as signaling events mediated through the binding of high affinity ligands to VLDLr have been previously noted. The neural protein reelin binds to VLDLr and also apoER2 with high affinity (KD's of 1.16 nM and 0.2 nM, respectively) (Andersen et al., 2003), this binding induces the phosphorylation of disabled-1 (Dab-1) which is bound to the cytosolic NPxY motif of VLDLr (Benhayon et al., 2003). In a pathway involving Src and P13K activation, these events regulate neuronal migration (Beffert et al., 2004). While the expression of Dab-1 is restricted to neural tissues (Rice et al., 1998), there may be other adaptor proteins capable of transmitting signals through VLDLr upon the binding of high affinity ligands,

Recent studies have also suggested that reelin induces the dimerization of VLDLr, which promotes the phosphorylation of Dab-1 (Strasser et al., 2004). As the uPA:PAI-1 complex presented two independent binding sites by SPR analysis, the possibility also exists that the uPA:PAI-1 complex may be able to mediate the dimerization of VLDLr and influence the activation of adaptor proteins. As both the uPA:PAI-2 and uPA:PAI-1^{R76E} complexes presented only one binding site models, this would explain why sustained ERK phosphorylation was not observed upon the binding

of these ligands to VLDLr. However, the relatively low affinity of the second site in uPA:PAI-1 suggests that this ligand may not be efficient at inducing the dimerization of VLDLr.

Another possibility behind this sustained ERK phosphorylation is the signaling of EGFR from endosomes. uPA binding to uPAR results in the transactivation of EGFR, stimulating ERK phosphorylation and cell migration, whereas transactivation of EGFR by EGF binding resulted in ERK phosphorylation and cell proliferation (Guerrero et al., 2004). However, blocking EGFR activity also inhibits the proliferation associated with uPA:PAI-1 binding to VLDLr (Jo et al., 2005), indicating that EGFR plays a dual role in both the motogenic and mitogenic signaling. As EGF binding to EGFR results in the endocytosis of this complex (Sorkin, 2001), and uPA:PAI-1 results in the endocytosis of the uPAR/uPA:PAI-1/VLDLr/integrin complex, it is possible that EGFR may also be transported to the endosomes with this complex. Therefore, the enhanced signaling of EGFR from the endosomes (Sorkin, 2001) may result in the sustained ERK response associated with the endocytosis of uPA:PAI-1 by VLDLr. However, a mechanism behind the exclusion of EGFR upon uPA:PAI-2 endocytosis is not known.

The results presented in this thesis provide a significant insight into the validation and further applications of PAI-2 as a targeting agent in cancer therapy and also into the biochemical interactions behind the positive prognosis associated with tumour expression of PAI-2. Until now, the cell biology of PAI-2 has remained a largely un-explored part of the plasminogen activation system and this data will hopefully provide a solid basis on which further investigations into the role of PAI-2 as both a cancer therapeutic and a marker of positive prognostic impact can be undertaken.

REFERENCES

Aertgeerts, K., H.L. De Bondt, C.J. De Ranter, and P. Declerck. 1995. Mechanisms contributing to the conformational and functional flexibility of plasminogen activator inhibitor-1. *Nature Structural Biology*. 2:891-897.

Agirbasli, M. 2005. Pivotal role of plasminogen-activator inhibitor 1 in vascular disease. *Int J Clin Pract*. 59:102-6.

Aguirre Ghiso, J.A., D.F. Alonso, E.F. Farias, D.E. Gomez, and E.B. de Kier Joffe. 1999. Deregulation of the signaling pathways controlling urokinase production. Its relationship with the invasive phenotype. *Eur J Biochem*. 263:295-304.

Ahmed, N., K. Oliva, Y. Wang, M. Quinn, and G. Rice. 2003. Downregulation of urokinase plasminogen activator receptor expression inhibits Erk signalling with concomitant suppression of invasiveness due to loss of uPAR-beta1 integrin complex in colon cancer cells. *Br J Cancer*. 89:374-84.

Al-Ejeh, F., D. Croucher, and M. Ranson. 2004. Kinetic analysis of plasminogen activator inhibitor type-2: urokinase complex formation and subsequent internalisation by carcinoma cell lines. *Exp Cell Res*. 297:259-71.

Allen, B.J., S. Rizvi, Y. Li, Z. Tian, and M. Ranson. 2001. In vitro and preclinical targeted alpha therapy for melanoma, breast, prostate and colorectal cancers. *Crit Rev Oncol Hematol*. 39:139-46.

Allen, B.J., Z. Tian, S.M. Rizvi, Y. Li, and M. Ranson. 2003. Preclinical studies of targeted alpha therapy for breast cancer using 213Bi-labelled-plasminogen activator inhibitor type 2. *Br J Cancer*. 88:944-50.

Allen, T.M. 2002. Ligand-targeted therapeutics in anticancer therapy. *Nat Rev Cancer*. 2:750-63.

Andersen, O.M., D. Benhayon, T. Curran, and T.E. Willnow. 2003. Differential binding of ligands to the apolipoprotein E receptor 2. *Biochemistry*. 42:9355-64.

Andersen, O.M., H.H. Petersen, C. Jacobsen, S.K. Moestrup, M. Etzerodt, P.A. Andreasen, and H.C. Thogersen. 2001. Analysis of a two-domain binding site for the urokinase-type plasminogen activator-plasminogen activator inhibitor-1 complex in low-density-lipoprotein-receptor-related protein. *Biochem J*. 357:289-96.

Anderson, H.A., Y. Chen, and L.C. Norkin. 1996. Bound simian virus 40 translocates to caveolin-enriched membrane domains, and its entry is inhibited by drugs that selectively disrupt caveolae. *Mol Biol Cell*. 7:1825-34.

Andreasen, P.A., R. Egelund, and H.H. Petersen. 2000. The plasminogen activation system in tumor growth, invasion, and metastasis. *Cell Mol Life Sci*. 57:25-40.

Andreasen, P.A., L. Kjoller, L. Christensen, and M.J. Duffy. 1997. The urokinase-type plasminogen activator system in cancer metastasis: a review. *Int J Cancer*. 72:1-22.

Andreasen, P.A., L. Sottrup-Jensen, L. Kjoller, A. Nykjaer, S.K. Moestrup, C.M. Petersen, and J. Gliemann. 1994. Receptor-mediated endocytosis of plasminogen activators and activator/inhibitor complexes. *FEBS Lett*. 338:239-45.

Andronicos, N.M., M.S. Baker, M. Lackmann, and M. Ranson. 2000. Deconstructing the interaction of glu-plasminogen with its receptor alpha-enolase. *Fibrinolysis*. 14:327-336.

Andronicos, N.M., and M. Ranson. 2001. The topology of plasminogen binding and activation on the surface of human breast cancer cells. *Br J Cancer*. 85:909-16.

Argraves, K.M., F.D. Battey, C.D. MacCalman, K.R. McCrae, M. Gafvels, K.F. Kozarsky, D.A. Chappell, J.F. Strauss, 3rd, and D.K. Strickland. 1995. The very low density lipoprotein receptor mediates the cellular catabolism of lipoprotein lipase and urokinase-plasminogen activator inhibitor type I complexes. *J Biol Chem*. 270:26550-7.

Asplin, I., U. Misra, G. Gawdi, M. Gonzalez-Gronow, and S. Pizzo. 2000. Selective upregulated expression of the alpha2-macroglobulin signaling receptor in highly metastatic 1-LN prostate carcinoma cells. *Archives of Biochemistry and Biophysics*. 383:135-141.

Astedt, B., C. Lindoff, and I. Lecander. 1998. Significance of the plasminogen activator inhibitor of placental type (PAI-2) in pregnancy. *Semin Thromb Hemost*. 24:431-5.

Bajou, K., C. Maillard, M. Jost, R.H. Lijnen, A. Gils, P. Declerck, P. Carmeliet, J.M. Foidart, and A. Noel. 2004. Host-derived plasminogen activator inhibitor-1 (PAI-1) concentration is critical for in vivo tumoral angiogenesis and growth. *Oncogene*. 23:6986-90.

Bajou, K., A. Noel, R.D. Gerard, V. Masson, N. Brunner, C. Holst-Hansen, M. Skobe, N.E. Fusenig, P. Carmeliet, D. Collen, and J.M. Foidart. 1998. Absence of host plasminogen activator inhibitor 1 prevents cancer invasion and vascularization. *Nat Med*. 4:923-8.

Baker, M.S., S.P. Green, N. Goss, M. Katrantzis, and W.F. Doe. 1990. Plasminogen activator inhibitor 2 (PAI-2) is not inactivated by exposure to oxidants which can be released from activated neutrophils. *Biochem Biophys Res Commun*. 166:993-1000.

Beffert, U., E.J. Weeber, G. Morfini, J. Ko, S.T. Brady, L.H. Tsai, J.D. Sweatt, and J. Herz. 2004. Reelin and cyclin-dependent kinase 5-dependent signals cooperate in regulating neuronal migration and synaptic transmission. *J Neurosci*. 24:1897-906.

Behrendt, N. 2004. The urokinase receptor (uPAR) and the uPAR-associated protein (uPARAP/Endo180): membrane proteins engaged in matrix turnover during tissue remodeling. *Biol Chem*. 385:103-36.

Belin, D., A. Wohlwend, W.D. Schleuning, E.K. Kruithof, and J.D. Vassalli. 1989. Facultative polypeptide translocation allows a single mRNA to encode the secreted and cytosolic forms of plasminogen activators inhibitor 2. *Embo J*. 8:3287-94.

Benhayon, D., S. Magdaleno, and T. Curran. 2003. Binding of purified Reelin to ApoER2 and VLDLR mediates tyrosine phosphorylation of Disabled-1. *Brain Res Mol Brain Res*. 112:33-45.

Berkenpas, M.B., D.A. Lawrence, and D. Ginsburg. 1995. Molecular evolution of plasminogen activator inhibitor-1 functional stability. *Embo J*. 14:2969-77.

Bertram, J.S. 2000. The molecular biology of cancer. *Mol Aspects Med*. 21:167-223.

Bjork, I., K. Nordling, and S.T. Olson. 1993. Immunologic evidence for insertion of the reactive-bond loop of antithrombin into the A beta-sheet of the inhibitor during trapping of target proteinases. *Biochemistry*. 32:6501-5.

Blasi, F. 1993. Urokinase and urokinase receptor: a paracrine/autocrine system regulating cell migration and invasiveness. *Bioessays*. 15:105-11.

Blasi, F. 1999. Proteolysis, cell adhesion, chemotaxis, and invasiveness are regulated by the u-PA-u-PAR-PAI-1 system. *Thromb Haemost*. 82:298-304.

Blasi, F., and P. Carmeliet. 2002. uPAR: a versatile signalling orchestrator. *Nat Rev Mol Cell Biol*. 3:932-43.

Bohuslav, J., V. Horejsi, C. Hansmann, J. Stockl, U.H. Weidle, O. Majdic, I. Bartke, W. Knapp, and H. Stockinger. 1995. Urokinase plasminogen activator receptor, beta 2-integrins, and Src-kinases within a single receptor complex of human monocytes. *J Exp Med*. 181:1381-90.

Boucher, P., P. Liu, M. Gotthardt, T. Hiesberger, R.G. Anderson, and J. Herz. 2002. Platelet-derived growth factor mediates tyrosine phosphorylation of the cytoplasmic domain of the low Density lipoprotein receptor-related protein in caveolae. *J Biol Chem*. 277:15507-13.

Bouchet, C., K. Hacene, P.M. Martin, V. Becette, M. Tubiana-Hulin, S. Lasry, J. Oglobine, and F. Spyratos. 1999. Dissemination risk index based on plasminogen activator system components in primary breast cancer. *J Clin Oncol*. 17:3048-57.

Brownstein, C., A.B. Deora, A.T. Jacovina, R. Weintraub, M. Gertler, K.M. Khan, D.J. Falcone, and K.A. Hajjar. 2004. Annexin II mediates plasminogen-dependent matrix invasion by human monocytes: enhanced expression by macrophages. *Blood*. 103:317-24.

Burgle, M., M. Koppitz, C. Riemer, H. Kessler, B. Konig, U.H. Weidle, J. Kellermann, F. Lottspeich, H. Graeff, M. Schmitt, L. Goretzki, U. Reuning, O. Wilhelm, and V. Magdolen. 1997. Inhibition of the interaction of urokinase-type plasminogen activator (uPA) with its receptor (uPAR) by synthetic peptides. *Biol Chem*. 378:231-7.

Busso, N., S.K. Masur, D. Lazega, S. Waxman, and L. Ossowski. 1994. Induction of cell migration by pro-urokinase binding to its receptor: possible mechanism for signal transduction in human epithelial cells. *J Cell Biol*. 126:259-70.

Cajot, J.F., J. Bamat, G.E. Bergonzelli, E.K. Kruithof, R.L. Medcalf, J. Testuz, and B. Sordat. 1990. Plasminogen-activator inhibitor type 1 is a potent natural inhibitor of extracellular matrix degradation by fibrosarcoma and colon carcinoma cells. *Proc Natl Acad Sci U S A*. 87:6939-43.

Carrell, R.W., and J.A. Huntington. 2003. How serpins change their fold for better and for worse. *Biochem Soc Symp*:163-78.

Castellino, F.J., and V.A. Ploplis. 2005. Structure and function of the plasminogen/plasmin system. *Thromb Haemost*. 93:647-54.

Cavallo-Medved, D., J. Mai, J. Dosescu, M. Sameni, and B.F. Sloane. 2005. Caveolin-1 mediates the expression and localization of cathepsin B, pro-urokinase plasminogen activator and their cell-surface receptors in human colorectal carcinoma cells. *J Cell Sci*. 118:1493-503.

Chakraborti, S., M. Mandal, S. Das, A. Mandal, and T. Chakraborti. 2003. Regulation of matrix metalloproteinases: an overview. *Mol Cell Biochem*. 253:269-85.

Chambers, S.K., C.M. Ivins, and M.L. Carcangiu. 1997. Expression of plasminogen activator inhibitor-2 in epithelial ovarian cancer: a favorable prognostic factor related to the actions of CSF-1. *Int J Cancer*. 74:571-5.

Chapman, H.A., and Y. Wei. 2001. Protease crosstalk with integrins: the urokinase receptor paradigm. *Thromb Haemost*. 86:124-9.

Chaurasia, P., J.A. Aguirre-Ghiso, O.D. Liang, H. Gardsvoll, M. Ploug, and L. Ossowski. 2006. A region in urokinase plasminogen receptor domain III controlling a functional association with alpha5beta1 integrin and tumor growth. *J Biol Chem*. 281:14852-63.

Chazaud, B., R. Ricoux, C. Christov, A. Plonquet, R. Gherardi, and G. Barlovatz-Meimon. 2002. Promigratory effect of plasminogen activator inhibitor-1 on invasive breast cancer cell populations. *American Journal of Pathology*. 160:237-246.

Chen, Y., R.C. Budd, R.J. Kelm, Jr., B.E. Sobel, and D.J. Schneider. 2006. Augmentation of proliferation of vascular smooth muscle cells by plasminogen activator inhibitor type 1. *Arterioscler Thromb Vasc Biol*. 26:1777-83.

Chorostowska-Wynimko, J., E. Skrzypczak-Jankun, and J. Jankun. 2004. Plasminogen activator inhibitor type-1: its structure, biological activity and role in tumorigenesis (Review). *Int J Mol Med*. 13:759-66.

Chorostowska-Wynimko, J., R. Swiercz, E. Skrzypczak-Jankun, A. Wojtowicz, S.H. Selman, and J. Jankun. 2003. A novel form of the plasminogen activator inhibitor created by cysteine mutations extends its half-life: relevance to cancer and angiogenesis. *Mol Cancer Ther*. 2:19-28.

Croucher, D., D.N. Saunders, and M. Ranson. 2006. The urokinase/PAI-2 complex: a new high affinity ligand for the endocytosis receptor low density lipoprotein receptor-related protein. *J Biol Chem*. 281:10206-13.

Cubellis, M.V., P. Andreasen, P. Ragno, M. Mayer, K. Dano, and F. Blasi. 1989. Accessibility of receptor-bound urokinase to type-1 plasminogen activator inhibitor. *Proc Natl Acad Sci U S A*. 86:4828-32.

Cubellis, M.V., T.C. Wun, and F. Blasi. 1990. Receptor-mediated internalization and degradation of urokinase is caused by its specific inhibitor PAI-1. *Embo J*. 9:1079-85.

Cunningham, O., A. Andolfo, M.L. Santovito, L. Iuzzolino, F. Blasi, and N. Sidenius. 2003. Dimerization controls the lipid raft partitioning of uPAR/CD87 and regulates its biological functions. *Embo J*. 22:5994-6003.

Czekay, R.P., K. Aertgeerts, S.A. Curriden, and D.J. Loskutoff. 2003. Plasminogen activator inhibitor-1 detaches cells from extracellular matrices by inactivating integrins. *J Cell Biol*. 160:781-91.

Czekay, R.P., T.A. Kuemmel, R.A. Orlando, and M.G. Farquhar. 2001. Direct binding of occupied urokinase receptor (uPAR) to LDL receptor-related protein is required for endocytosis of uPAR and regulation of cell surface urokinase activity. *Mol Biol Cell*. 12:1467-79.

Czekay, R.P., and D.J. Loskutoff. 2004. Unexpected role of plasminogen activator inhibitor 1 in cell adhesion and detachment. *Exp Biol Med (Maywood)*. 229:1090-6.

Dano, K., P.A. Andreasen, J. Grondahl-Hansen, P. Kristensen, L.S. Nielsen, and L. Skriver. 1985. Plasminogen activators, tissue degradation, and cancer. *Adv Cancer Res*. 44:139-266.

Dano, K., N. Behrendt, G. Hoyer-Hansen, M. Johnsen, L.R. Lund, M. Ploug, and J. Romer. 2005. Plasminogen activation and cancer. *Thromb Haemost*. 93:676-81.

Dano, K., J. Romer, B.S. Nielsen, S. Bjorn, C. Pyke, J. Rygaard, and L.R. Lund. 1999. Cancer invasion and tissue remodeling--cooperation of protease systems and cell types. *Apmis*. 107:120-7.

Darnell, G.A., T.M. Antalis, R.W. Johnstone, B.W. Stringer, S.M. Ogbourne, D. Harrich, and A. Suhrbier. 2003. Inhibition of retinoblastoma protein degradation

by interaction with the serpin plasminogen activator inhibitor 2 via a novel consensus motif. *Mol Cell Biol*. 23:6520-32.

Deckert, M., M. Ticchioni, and A. Bernard. 1996. Endocytosis of GPI-anchored proteins in human lymphocytes: role of glycolipid-based domains, actin cytoskeleton, and protein kinases. *J Cell Biol*. 133:791-9.

Degryse, B., J.G. Neels, R.P. Czekay, K. Aertgeerts, Y. Kamikubo, and D.J. Loskutoff. 2004. The low density lipoprotein receptor-related protein is a motogenic receptor for plasminogen activator inhibitor-1. *J Biol Chem*. 279:22595-604.

Degryse, B., M. Resnati, R.P. Czekay, D.J. Loskutoff, and F. Blasi. 2005. Domain 2 of the urokinase receptor contains an integrin-interacting epitope with intrinsic signaling activity: generation of a new integrin inhibitor. *J Biol Chem*. 280:24792-803.

Deng, G., S.A. Curriden, S. Wang, S. Rosenberg, and D.J. Loskutoff. 1996. Is plasminogen activator inhibitor-1 the molecular switch that governs urokinase receptor-mediated cell adhesion and release? *J Cell Biol*. 134:1563-71.

Deora, A.B., G. Kreitzer, A.T. Jacovina, and K.A. Hajjar. 2004. An annexin 2 phosphorylation switch mediates p11-dependent translocation of annexin 2 to the cell surface. *J Biol Chem*. 279:43411-8.

Dickinson, J.L., E.J. Bates, A. Ferrante, and T.M. Antalis. 1995. Plasminogen activator inhibitor type 2 inhibits tumor necrosis factor alpha-induced apoptosis. Evidence for an alternate biological function. *J Biol Chem*. 270:27894-904.

Dickinson, J.L., B.J. Norris, P.H. Jensen, and T.M. Antalis. 1998. The C-D interhelical domain of the serpin plasminogen activator inhibitor-type 2 is required for protection from TNF-alpha induced apoptosis. *Cell Death Differ*. 5:163-71.

du Toit, P.J., C.H. Van Aswegen, C.M. Steinmann, L. Klue, and D.J. Du Plessis. 1997. Does urokinase play a role in renal stone formation? *Med Hypotheses*. 49:57-9.

Duffy, M.J. 1993. Cellular oncogenes and suppressor genes as prognostic markers in cancer. *Clin Biochem*. 26:439-47.

Duffy, M.J. 2004. The urokinase plasminogen activator system: role in malignancy. *Curr Pharm Des*. 10:39-49.

Duffy, M.J., and C. Duggan. 2004. The urokinase plasminogen activator system: a rich source of tumour markers for the individualised management of patients with cancer. *Clin Biochem*. 37:541-8.

Duggan, C., S. Kennedy, M.D. Kramer, C. Barnes, P. Elvin, E. McDermott, N. O'Higgins, and M.J. Duffy. 1997. Plasminogen activator inhibitor type 2 in breast cancer. *Br J Cancer*. 76:622-7.

Dumler, I., A. Kopmann, A. Weis, O.A. Mayboroda, K. Wagner, D.C. Gulba, and H. Haller. 1999. Urokinase activates the Jak/Stat signal transduction pathway in human vascular endothelial cells. *Arterioscler Thromb Vasc Biol*. 19:290-7.

Ellis, V., S.A. Whawell, F. Werner, and J.J. Deadman. 1999. Assembly of urokinase receptor-mediated plasminogen activation complexes involves direct, non-active-site interactions between urokinase and plasminogen. *Biochemistry*. 38:651-9.

Ellis, V., T.C. Wun, N. Behrendt, E. Ronne, and K. Dano. 1990. Inhibition of receptor-bound urokinase by plasminogen-activator inhibitors. *J Biol Chem*. 265:9904-8.

Estreicher, A., J. Muhlhauser, J.L. Carpentier, L. Orci, and J.D. Vassalli. 1990. The receptor for urokinase type plasminogen activator polarizes expression of the protease to the leading edge of migrating monocytes and promotes degradation of enzyme inhibitor complexes. *J Cell Biol*. 111:783-92.

Falcone, D.J., W. Borth, K.M. Khan, and K.A. Hajjar. 2001. Plasminogen-mediated matrix invasion and degradation by macrophages is dependent on surface expression of annexin II. *Blood*. 97:777-84.

Fan, J., Y.Q. Zhang, P. Li, M. Hou, L. Tan, X. Wang, and Y.S. Zhu. 2004a. Interaction of plasminogen activator inhibitor-2 and proteasome subunit, beta type 1. *Acta Biochim Biophys Sin (Shanghai)*. 36:42-6.

Fan, J., Y.Q. Zhang, P. Li, C. Tong, L. Tan, and Y.S. Zhu. 2004b. Interaction between plasminogen activator inhibitor type-2 and pre-mRNA processing factor 8. *Acta Biochim Biophys Sin (Shanghai)*. 36:623-8.

Felez, J. 1998. Plasminogen binding to cell surfaces. *Fibrinolysis*. 12:183-189.

Fernandez-Soria, V., M.E. Lleonart, M. Diaz-Fuertes, R. Villuendas, R. Sanchez-Prieto, A. Fabra, and Y.C.S. Ramon. 2006. Adenovirus E1A orchestrates the urokinase-plasminogen activator system and upregulates PAI-2 expression, supporting a tumor suppressor effect. *Int J Oncol*. 28:143-8.

Fish, R.J., and E.K. Kruithof. 2006. Evidence for serpinB2-independent protection from TNF-alpha-induced apoptosis. *Exp Cell Res*. 312:350-61.

Fisher, C., N. Beglova, and S.C. Blacklow. 2006. Structure of an LDLR-RAP complex reveals a general mode for ligand recognition by lipoprotein receptors. *Mol Cell*. 22:277-83.

Foekens, J.A., F. Buessecker, H.A. Peters, U. Krainick, W.L. van Putten, M.P. Look, J.G. Klijn, and M.D. Kramer. 1995. Plasminogen activator inhibitor-2: prognostic relevance in 1012 patients with primary breast cancer. *Cancer Res*. 55:1423-7.

Foekens, J.A., H.A. Peters, M.P. Look, H. Portengen, M. Schmitt, M.D. Kramer, N. Brunner, F. Janicke, M.E. Meijer-van Gelder, S.C. Henzen-Logmans, W.L. van Putten, and J.G. Klijn. 2000. The urokinase system of plasminogen activation and prognosis in 2780 breast cancer patients. *Cancer Res*. 60:636-43.

Frandsen, T.L., C. Holst-Hansen, B.S. Nielsen, I.J. Christensen, J.R. Nyengaard, P. Carmeliet, and N. Brunner. 2001. Direct evidence of the importance of stromal urokinase plasminogen activator (uPA) in the growth of an experimental human

breast cancer using a combined uPA gene-disrupted and immunodeficient xenograft model. *Cancer Res*. 61:532-7.

Gao, W., Z. Wang, X. Bai, X. Xi, and C. Ruan. 2001. Detection of soluble urokinase receptor by immunoradiometric assay and its application in tumor patients. *Thromb Res*. 102:25-31.

Gardsvoll, H., K. Dano, and M. Ploug. 1999. Mapping part of the functional epitope for ligand binding on the receptor for urokinase-type plasminogen activator by site-directed mutagenesis. *J Biol Chem*. 274:37995-8003.

Garver, W.S., G.S. Hossain, M.M. Winscott, and R.A. Heidenreich. 1999. The Npc1 mutation causes an altered expression of caveolin-1, annexin II and protein kinases and phosphorylation of caveolin-1 and annexin II in murine livers. *Biochim Biophys Acta*. 1453:193-206.

Genton, C., E.K. Kruithof, and W.D. Schleuning. 1987. Phorbol ester induces the biosynthesis of glycosylated and nonglycosylated plasminogen activator inhibitor 2 in high excess over urokinase-type plasminogen activator in human U-937 lymphoma cells. *J Cell Biol*. 104:705-12.

Gerke, V., and S.E. Moss. 2002. Annexins: from structure to function. *Physiol Rev*. 82:331-71.

Ghosh, S., R. Brown, J.C. Jones, S.M. Ellerbroek, and M.S. Stack. 2000. Urinary-type plasminogen activator (uPA) expression and uPA receptor localization are regulated by alpha 3beta 1 integrin in oral keratinocytes. *J Biol Chem*. 275:23869-76.

Gonias, S.L., L. Wu, and A.M. Salicioni. 2004. Low density lipoprotein receptor-related protein: regulation of the plasma membrane proteome. *Thromb Haemost*. 91:1056-64.

Goretzki, L., M. Schmitt, K. Mann, J. Calvete, N. Chucholowski, M. Kramer, W.A. Gunzler, F. Janicke, and H. Graeff. 1992. Effective activation of the proenzyme form of the urokinase-type plasminogen activator (pro-uPA) by the cysteine protease cathepsin L. *FEBS Lett*. 297:112-8.

Guerrero, J., J.F. Santibanez, A. Gonzalez, and J. Martinez. 2004. EGF receptor transactivation by urokinase receptor stimulus through a mechanism involving Src and matrix metalloproteinases. *Exp Cell Res*. 292:201-8.

Hahn-Dantona, E., J.F. Ruiz, P. Bornstein, and D.K. Strickland. 2001. The low density lipoprotein receptor-related protein modulates levels of matrix metalloproteinase 9 (MMP-9) by mediating its cellular catabolism. *J Biol Chem*. 276:15498-503.

Hajjar, K.A., A.T. Jacovina, and J. Chacko. 1994. An endothelial cell receptor for plasminogen/tissue plasminogen activator. I. Identity with annexin II. *J Biol Chem*. 269:21191-7.

Han, B., M. Nakamura, I. Mori, Y. Nakamura, and K. Kakudo. 2005. Urokinase-type plasminogen activator system and breast cancer (Review). *Oncol Rep*. 14:105-12.

Hanahan, D., and R.A. Weinberg. 2000. The hallmarks of cancer. *Cell*. 100:57-70.

Hang, M.T.N., M. Ranson, D.N. Saunders, X.M. Liang, C.L. Bunn, and M.S. Baker. 1998. Pharmacokinetics of recombinant human plasminogen activator inhibitor type 2 (PAI-2) in control and tumour xenograft bearing mice. *Fibrinolysis*. 12:145-154.

Harbeck, N., R.E. Kates, and M. Schmitt. 2002. Clinical relevance of invasion factors urokinase-type plasminogen activator and plasminogen activator inhibitor type 1 for individualized therapy decisions in primary breast cancer is greatest when used in combination. *J Clin Oncol*. 20:1000-7.

Harbour, J.W., and D.C. Dean. 2000. Rb function in cell-cycle regulation and apoptosis. *Nat Cell Biol*. 2:E65-7.

Harrop, S.J., L. Jankova, M. Coles, D. Jardine, J.S. Whittaker, A.R. Gould, A. Meister, G.C. King, B.C. Mabbutt, and P.M. Curmi. 1999. The crystal structure of plasminogen activator inhibitor 2 at 2.0 A resolution: implications for serpin function. *Structure*. 7:43-54.

Heegaard, C.W., A.C. Simonsen, K. Oka, L. Kjoller, A. Christensen, B. Madsen, L. Ellgaard, L. Chan, and P.A. Andreasen. 1995. Very low density lipoprotein receptor binds and mediates endocytosis of urokinase-type plasminogen activator-type-1 plasminogen activator inhibitor complex. *J Biol Chem*. 270:20855-61.

Herz, J., D.E. Clouthier, and R.E. Hammer. 1992. LDL receptor-related protein internalizes and degrades uPA-PAI-1 complexes and is essential for embryo implantation. *Cell*. 71:411-21.

Herz, J., and D.K. Strickland. 2001. LRP: a multifunctional scavenger and signaling receptor. *J Clin Invest*. 108:779-84.

Hibino, T., Y. Matsuda, T. Takahashi, and P.F. Goetinck. 1999. Suppression of keratinocyte proliferation by plasminogen activator inhibitor-2. *J Invest Dermatol*. 112:85-90.

Higazi, A., R.L. Cohen, J. Henkin, D. Kniss, B.S. Schwartz, and D.B. Cines. 1995. Enhancement of the enzymatic activity of single-chain urokinase plasminogen activator by soluble urokinase receptor. *J Biol Chem*. 270:17375-80.

Horn, I.R., B.M. van den Berg, S.K. Moestrup, H. Pannekoek, and A.J. van Zonneveld. 1998. Plasminogen activator inhibitor 1 contains a cryptic high affinity receptor binding site that is exposed upon complex formation with tissue-type plasminogen activator. *Thromb Haemost*. 80:822-828.

Horn, I.R., B.M. van den Berg, P.Z. van der Meijden, H. Pannekoek, and A.J. van Zonneveld. 1997. Molecular analysis of ligand binding to the second cluster of

complement-type repeats of the low density lipoprotein receptor-related protein. Evidence for an allosteric component in receptor-associated protein-mediated inhibition of ligand binding. *J Biol Chem*. 272:13608-13.

Hoyer-Hansen, G., M. Ploug, N. Behrendt, E. Ronne, and K. Dano. 1997. Cell-surface acceleration of urokinase-catalyzed receptor cleavage. *Eur J Biochem*. 243:21-6.

Hoyer-Hansen, G., E. Ronne, H. Solberg, N. Behrendt, M. Ploug, L.R. Lund, V. Ellis, and K. Dano. 1992. Urokinase plasminogen activator cleaves its cell surface receptor releasing the ligand-binding domain. *J Biol Chem*. 267:18224-9.

Huai, Q., A.P. Mazar, A. Kuo, G.C. Parry, D.E. Shaw, J. Callahan, Y. Li, C. Yuan, C. Bian, L. Chen, B. Furie, B.C. Furie, D.B. Cines, and M. Huang. 2006. Structure of human urokinase plasminogen activator in complex with its receptor. *Science*. 311:656-9.

Huber, K. 2001. Plasminogen activator inhibitor type-1 (part one): basic mechanisms, regulation, and role for thromboembolic disease. *J Thromb Thrombolysis*. 11:183-93.

Huber, R., and R.W. Carrell. 1989. Implications of the three-dimensional structure of alpha 1-antitrypsin for structure and function of serpins. *Biochemistry*. 28:8951-66.

Huntington, J.A., and R.W. Carrell. 2001. The serpins: nature's molecular mousetraps. *Sci Prog*. 84:125-136.

Hussain, M.M., D.K. Strickland, and A. Bakillah. 1999. The mammalian low-density lipoprotein receptor family. *Annu Rev Nutr*. 19:141-72.

Ishikawa, N., Y. Endo, and T. Sasaki. 1996. Inverse correlation between mRNA expression of plasminogen activator inhibitor-2 and lymph node metastasis in human breast cancer. *Jpn J Cancer Res*. 87:480-7.

Jankova, L., S.J. Harrop, D.N. Saunders, J.L. Andrews, K.C. Bertram, A.R. Gould, M.S. Baker, and P.M. Curmi. 2001. Crystal structure of the complex of plasminogen activator inhibitor 2 with a peptide mimicking the reactive center loop. *J Biol Chem*. 276:43374-82.

Jensen, G.A., O.M. Andersen, A.M. Bonvin, I. Bjerrum-Bohr, M. Etzerodt, H.C. Thogersen, C. O'Shea, F.M. Poulsen, and B.B. Kragelund. 2006. Binding Site Structure of One LRP-RAP Complex:Implications for a Common Ligand-Receptor Binding Motif. *J Mol Biol*. 362:700-16.

Jensen, P.H., E.I. Christensen, P. Ebbesen, J. Gliemann, and P. Andreasen. 1990. Lysosomal degradation of receptor-bound urokinase-type plasminogen activator is enhanced by its inhibitors in human trophoblastic choriocarcinoma cells. *Cell. Regul.* 13:1043-1056.

Jensen, P.H., L.I. Cressey, B.T. Gjertsen, P. Madsen, G. Mellgren, P. Hokland, J. Gliemann, S.O. Doskeland, M. Lanotte, and O.K. Vintermyr. 1994. Cleaved

intracellular plasminogen activator inhibitor 2 in human myeloleukaemia cells is a marker of apoptosis. *Br J Cancer*. 70:834-40.

Jensen, P.H., P. Ebbesen, and J. Gliemann. 1989. Low alpha 2-macroglobulin-proteinase complex binding: a common but not exclusive characteristic of malignant cells. *In Vivo*. 3:7-9.

Jensen, P.H., T.G. Jensen, W.E. Laug, H. Hager, J. Gliemann, and B. Pepinsky. 1996. The exon 3 encoded sequence of the intracellular serine proteinase inhibitor plasminogen activator inhibitor 2 is a protein binding domain. *J Biol Chem*. 271:26892-9.

Jensen, P.J., Q. Wu, P. Janowitz, Y. Ando, and N.M. Schechter. 1995. Plasminogen activator inhibitor type 2: an intracellular keratinocyte differentiation product that is incorporated into the cornified envelope. *Exp Cell Res*. 217:65-71.

Jo, M., K.S. Thomas, N. Marozkina, T.J. Amin, C.M. Silva, S.J. Parsons, and S.L. Gonias. 2005. Dynamic assembly of the urokinase-type plasminogen activator signaling receptor complex determines the mitogenic activity of urokinase-type plasminogen activator. *J Biol Chem*. 280:17449-57.

Kamikubo, Y., R. De Guzman, G. Kroon, S. Curriden, J.G. Neels, M.J. Churchill, P. Dawson, S. Oldziej, A. Jagielska, H.A. Scheraga, D.J. Loskutoff, and H.J. Dyson. 2004. Disulfide bonding arrangements in active forms of the somatomedin B domain of human vitronectin. *Biochemistry*. 43:6519-34.

Kanalas, J.J., and S.P. Makker. 1991. Identification of the rat Heymann nephritis autoantigen (GP330) as a receptor site for plasminogen. *J Biol Chem*. 266:10825-9.

Kancha, R., M. Stearns, and M. Hussain. 1994. Decreased expression of the low density lipoprotein receptor-related protein/alpha 2-macroglobulin receptor in invasive cell clones derived from human prostate and breast tumor cells. *Oncology Research*. 6:365-372.

Kanse, S.M., O. Benzakour, C. Kanthou, C. Kost, H.R. Lijnen, and K.T. Preissner. 1997. Induction of vascular SMC proliferation by urokinase indicates a novel mechanism of action in vasoproliferative disorders. *Arterioscler Thromb Vasc Biol*. 17:2848-54.

Kasyapa, C.S., P. Kunapuli, L. Hawthorn, and J.K. Cowell. 2006. Induction of the plasminogen activator inhibitor-2 in cells expressing the ZNF198/FGFR1 fusion kinase, that is involved in atypical myeloproliferative disease. *Blood*.

Kasza, A., H.H. Petersen, C.W. Heegaard, K. Oka, A. Christensen, A. Dubin, L. Chan, and P.A. Andreasen. 1997. Specificity of serine proteinase/serpin complex binding to very-low-density lipoprotein receptor and alpha2-macroglobulin receptor/low-density-lipoprotein-receptor-related protein. *Eur J Biochem*. 248:270-81.

Kawano, T., K. Morimoto, and Y. Uemura. 1968. Urokinase inhibitor in human placenta. *Nature*. 217:253-4.

Kirshner, J., D. Schumann, and J.E. Shively. 2003. CEACAM1, a cell-cell adhesion molecule, directly associates with annexin II in a three-dimensional model of mammary morphogenesis. *J Biol Chem*. 278:50338-45.

Kjoller, L. 2002. The urokinase plasminogen activator receptor in the regulation of the actin cytoskeleton and cell motility. *Biol Chem*. 383:5-19.

Kjoller, L., and A. Hall. 2001. Rac mediates cytoskeletal rearrangements and increased cell motility induced by urokinase-type plasminogen activator receptor binding to vitronectin. *J Cell Biol*. 152:1145-57.

Knauer, M.F., S.B. Hawley, and D.J. Knauer. 1997. Identification of a binding site in protease nexin I (PN1) required for the receptor mediated internalization of PN1-thrombin complexes. *J Biol Chem*. 272:12261-4.

Knauer, M.F., R.A. Orlando, and C.G. Glabe. 1996. Cell surface APP751 forms complexes with protease nexin 2 ligands and is internalized via the low density lipoprotein receptor-related protein (LRP). *Brain Res*. 740:6-14.

Kobayashi, H., M. Schmitt, L. Goretzki, N. Chucholowski, J. Calvete, M. Kramer, W.A. Gunzler, F. Janicke, and H. Graeff. 1991. Cathepsin B efficiently activates the soluble and the tumor cell receptor-bound form of the proenzyme urokinase-type plasminogen activator (Pro-uPA). *J Biol Chem*. 266:5147-52.

Konakova, M., F. Hucho, and W.D. Schleuning. 1998. Downstream targets of urokinase-type plasminogen-activator-mediated signal transduction. *Eur J Biochem*. 253:421-9.

Koshelnick, Y., M. Ehart, P. Hufnagl, P.C. Heinrich, and B.R. Binder. 1997. Urokinase receptor is associated with the components of the JAK1/STAT1 signaling pathway and leads to activation of this pathway upon receptor clustering in the human kidney epithelial tumor cell line TCL-598. *J Biol Chem*. 272:28563-7.

Kounnas, M.Z., J. Henkin, W.S. Argraves, and D.K. Strickland. 1993. Low density lipoprotein receptor-related protein/alpha 2-macroglobulin receptor mediates cellular uptake of pro-urokinase. *J Biol Chem*. 268:21862-7.

Kraynov, V.S., C. Chamberlain, G.M. Bokoch, M.A. Schwartz, S. Slabaugh, and K.M. Hahn. 2000. Localized Rac activation dynamics visualized in living cells. *Science*. 290:333-7.

Kruithof, E.K., M.S. Baker, and C.L. Bunn. 1995. Biological and clinical aspects of plasminogen activator inhibitor type 2. *Blood*. 86:4007-24.

Kruithof, E.K., C. Tran-Thang, A. Gudinchet, J. Hauert, G. Nicoloso, C. Genton, H. Welti, and F. Bachmann. 1987. Fibrinolysis in pregnancy: a study of plasminogen activator inhibitors. *Blood*. 69:460-6.

Kugler, M.C., Y. Wei, and H.A. Chapman. 2003. Urokinase receptor and integrin interactions. *Curr Pharm Des*. 9:1565-74.

Kumar, S., and C. Baglioni. 1991. Protection from tumor necrosis factor-mediated cytolysis by overexpression of plasminogen activator inhibitor type-2. *J Biol Chem*. 266:20960-4.

Kwaan, H.C., J. Wang, K. Svoboda, and P.J. Declerck. 2000. Plasminogen activator inhibitor 1 may promote tumour growth through inhibition of apoptosis. *Br J Cancer*. 82:1702-8.

Kwon, M., T.J. MacLeod, Y. Zhang, and D.M. Waisman. 2005. S100A10, annexin A2, and annexin a2 heterotetramer as candidate plasminogen receptors. *Front Biosci*. 10:300-25.

Laug, W.E., X.R. Cao, Y.B. Yu, H. Shimada, and E.K. Kruithof. 1993. Inhibition of invasion of HT1080 sarcoma cells expressing recombinant plasminogen activator inhibitor 2. *Cancer Res*. 53:6051-7.

Lawrence, D.A., M.B. Berkenpas, S. Palaniappan, and D. Ginsburg. 1994. Localization of vitronectin binding domain in plasminogen activator inhibitor-1. *J Biol Chem*. 269:15223-8.

Lawrence, D.A., S. Palaniappan, S. Stefansson, S.T. Olson, A.M. Francis-Chmura, J.D. Shore, and D. Ginsburg. 1997. Characterization of the binding of different conformational forms of plasminogen activator inhibitor-1 to vitronectin. Implications for the regulation of pericellular proteolysis. *J Biol Chem*. 272:7676-80.

Lee, D.B., N. Jamgotchian, S.G. Allen, F.W. Kan, and I.L. Hale. 2004. Annexin A2 heterotetramer: role in tight junction assembly. *Am J Physiol Renal Physiol*. 287:F481-91.

Lee, S.L., R.B. Dickson, and C.Y. Lin. 2000. Activation of hepatocyte growth factor and urokinase/plasminogen activator by matriptase, an epithelial membrane serine protease. *J Biol Chem*. 275:36720-5.

Leszczyniecka, M., T. Roberts, P. Dent, S. Grant, and P.B. Fisher. 2001. Differentiation therapy of human cancer: basic science and clinical applications. *Pharmacol Ther*. 90:105-56.

Li, Y., D.A. Lawrence, and L. Zhang. 2003. Sequences within domain II of the urokinase receptor critical for differential ligand recognition. *J Biol Chem*. 278:29925-32.

Li, Y., S.M. Rizvi, M. Ranson, and B.J. Allen. 2002. 213Bi-PAI2 conjugate selectively induces apoptosis in PC3 metastatic prostate cancer cell line and shows anti-cancer activity in a xenograft animal model. *Br J Cancer*. 86:1197-203.

Li, Y., N. Wood, P. Grimsley, D. Yellowlees, and P. Donnelly. 1998. In vitro invasiveness of human breast cancer cells is promoted by low density lipoprotein receptor-related protein. *Invasion and Metastasis*. 18:240-251.

Li, Y., N. Wood, P. Parsons, D. Yellowlees, and P. Donnelly. 1997. Expression of alpha2-macroglobulin receptor/low density lipoprotein receptor-related protein

on surfaces of tumour cells: a study using flow cytometry. *Cancer Letters*. 111:199-205.

Liew, M.A., V. McPhun, and M.S. Baker. 2000. Topological localization of plasminogen activator inhibitor type 2. *Cytometry*. 40:32-41.

Lijnen, H.R. 2001. Elements of the fibrinolytic system. *Ann N Y Acad Sci*. 936:226-36.

Lindahl, T.L., O. Sigurdardottir, and B. Wiman. 1989. Stability of plasminogen activator inhibitor 1 (PAI-1). *Thromb Haemost*. 62:748-51.

Lindberg, P., M.S. Baker, and B. Kinnby. 2001. The localization of the relaxed form of plasminogen activator inhibitor type 2 in human gingival tissues. *Histochem Cell Biol*. 116:447-52.

Liu, D., J. Aguirre Ghiso, Y. Estrada, and L. Ossowski. 2002. EGFR is a transducer of the urokinase receptor initiated signal that is required for in vivo growth of a human carcinoma. *Cancer Cell*. 1:445-57.

Liu, G., M.A. Shuman, and R.L. Cohen. 1995. Co-expression of urokinase, urokinase receptor and PAI-1 is necessary for optimum invasiveness of cultured lung cancer cells. *Int J Cancer*. 60:501-6.

Llinas, P., M.H. Le Du, H. Gardsvoll, K. Dano, M. Ploug, B. Gilquin, E.A. Stura, and A. Menez. 2005. Crystal structure of the human urokinase plasminogen activator receptor bound to an antagonist peptide. *Embo J*. 24:1655-63.

Lobov, S., M. Wilczynska, F. Bergstrom, L.B. Johansson, and T. Ny. 2004. Structural bases of the redox-dependent conformational switch in the serpin PAI-2. *J Mol Biol*. 344:1359-68.

Loskutoff, D.J., S.A. Curriden, G. Hu, and G. Deng. 1999. Regulation of cell adhesion by PAI-1. *Apmis*. 107:54-61.

Loukinova, E., S. Ranganathan, S. Kuznetsov, N. Gorlatova, M.M. Migliorini, D. Loukinov, P.G. Ulery, I. Mikhailenko, D.A. Lawrence, and D.K. Strickland. 2002. Platelet-derived growth factor (PDGF)-induced tyrosine phosphorylation of the low density lipoprotein receptor-related protein (LRP). Evidence for integrated co-receptor function betwenn LRP and the PDGF. *J Biol Chem*. 277:15499-506.

Lu, G., H. Maeda, S.V. Reddy, N. Kurihara, R. Leach, J.L. Anderson, and G.D. Roodman. 2006. Cloning and characterization of the Annexin II receptor on human marrow stromal cells. *J Biol Chem*.

Ma, A.S., D.J. Bell, A.A. Mittal, and H.H. Harrison. 1994. Immunocytochemical detection of extracellular annexin II in cultured human skin keratinocytes and isolation of annexin II isoforms enriched in the extracellular pool. *J Cell Sci*. 107 (Pt 7):1973-84.

MacLeod, T.J., M. Kwon, N.R. Filipenko, and D.M. Waisman. 2003. Phospholipid-associated annexin A2-S100A10 heterotetramer and its subunits:

characterization of the interaction with tissue plasminogen activator, plasminogen, and plasmin. *J Biol Chem*. 278:25577-84.

Markus, G. 1996. Conformational changes in plasminogen, their effect on activation, and the agents that modulate activation rates - a review. *Fibrinolysis*. 10:75-85.

Marshall, J.M., A.J. Brown, and C.P. Ponting. 1994. Conformational studies of human plasminogen and plasminogen fragments: evidence for a novel third conformation of plasminogen. *Biochemistry*. 33:3599-606.

Mayor, S., and H. Riezman. 2004. Sorting GPI-anchored proteins. *Nat Rev Mol Cell Biol*. 5:110-20.

Medcalf, R.L., E.K. Kruithof, and W.D. Schleuning. 1988. Plasminogen activator inhibitor 1 and 2 are tumor necrosis factor/cachectin-responsive genes. *J Exp Med*. 168:751-9.

Medcalf, R.L., and S.J. Stasinopoulos. 2005. The undecided serpin. The ins and outs of plasminogen activator inhibitor type 2. *Febs J*. 272:4858-67.

Melchor, J.P., and S. Strickland. 2005. Tissue plasminogen activator in central nervous system physiology and pathology. *Thromb Haemost*. 93:655-60.

Mignatti, P., and D.B. Rifkin. 1993. Biology and biochemistry of proteinases in tumor invasion. *Physiol Rev*. 73:161-95.

Mikhailenko, I., W. Considine, K.M. Argraves, D. Loukinov, B.T. Hyman, and D.K. Strickland. 1999. Functional domains of the very low density lipoprotein receptor: molecular analysis of ligand binding and acid-dependent ligand dissociation mechanisms. *J Cell Sci*. 112 (Pt 19):3269-81.

Mikus, P., and T. Ny. 1996. Intracellular polymerization of the serpin plasminogen activator inhibitor type 2. *J Biol Chem*. 271:10048-53.

Mikus, P., T. Urano, P. Liljestrom, and T. Ny. 1993. Plasminogen-activator inhibitor type 2 (PAI-2) is a spontaneously polymerising SERPIN. Biochemical characterisation of the recombinant intracellular and extracellular forms. *Eur J Biochem*. 218:1071-82.

Misra, U.K., M. Gonzalez-Gronow, G. Gawdi, J.P. Hart, C.E. Johnson, and S.V. Pizzo. 2002. The role of Grp 78 in alpha 2-macroglobulin-induced signal transduction. Evidence from RNA interference that the low density lipoprotein receptor-related protein is associated with, but not necessary for, GRP 78-mediated signal transduction. *J Biol Chem*. 277:42082-7.

Misra, U.K., and S.V. Pizzo. 2001. Receptor-associated protein binding blocks ubiquitinylation of the low density lipoprotein receptor-related protein. *Arch Biochem Biophys*. 396:106-10.

Moestrup, S.K., T.L. Holtet, M. Etzerodt, H.C. Thogersen, A. Nykjaer, P.A. Andreasen, H.H. Rasmussen, L. Sottrup-Jensen, and J. Gliemann. 1993a. Alpha 2-macroglobulin-proteinase complexes, plasminogen activator inhibitor type-1-

plasminogen activator complexes, and receptor-associated protein bind to a region of the alpha 2-macroglobulin receptor containing a cluster of eight complement-type repeats. *J Biol Chem*. 268:13691-6.

Moestrup, S.K., S. Nielsen, P. Andreasen, K.E. Jorgensen, A. Nykjaer, H. Roigaard, J. Gliemann, and E.I. Christensen. 1993b. Epithelial glycoprotein-330 mediates endocytosis of plasminogen activator-plasminogen activator inhibitor type-1 complexes. *J Biol Chem*. 268:16564-70.

Mosesson, M.W. 2005. Fibrinogen and fibrin structure and functions. *J Thromb Haemost*. 3:1894-904.

Mueller, B.M., Y.B. Yu, and W.E. Laug. 1995. Overexpression of plasminogen activator inhibitor 2 in human melanoma cells inhibits spontaneous metastasis in scid/scid mice. *Proc Natl Acad Sci U S A*. 92:205-9.

Mullertz, S., S. Thorsen, and L. Sottrup-Jensen. 1984. Identification of molecular forms of plasminogen and plasmin-inhibitor complexes in urokinase-activated human plasma. *Biochem J*. 223:169-77.

Myers, S.J., and K.K. Stanley. 1999. Src family kinase activation in glycosphingolipid-rich membrane domains of endothelial cells treated with oxidised low density lipoprotein. *Atherosclerosis*. 143:389-97.

Na, Y.R., and H. Im. 2005. The length of the reactive center loop modulates the latency transition of plasminogen activator inhibitor-1. *Protein Sci*. 14:55-63.

Namiranian, S., Y. Naito, V.V. Kakkar, and M.F. Scully. 1995. Bound plasminogen is rate-limiting for cell-surface-mediated activation of plasminogen by urokinase. *Biochem J*. 309 (Pt 3):977-82.

Nguyen, D.H., A.D. Catling, D.J. Webb, M. Sankovic, L.A. Walker, A.V. Somlyo, M.J. Weber, and S.L. Gonias. 1999. Myosin light chain kinase functions downstream of Ras/ERK to promote migration of urokinase-type plasminogen activator-stimulated cells in an integrin-selective manner. *J Cell Biol*. 146:149-64.

Nguyen, D.H., I.M. Hussaini, and S.L. Gonias. 1998. Binding of urokinase-type plasminogen activator to its receptor in MCF-7 cells activates extracellular signal-regulated kinase 1 and 2 which is required for increased cellular motility. *J Biol Chem*. 273:8502-7.

Nguyen, D.H., D.J. Webb, A.D. Catling, Q. Song, A. Dhakephalkar, M.J. Weber, K.S. Ravichandran, and S.L. Gonias. 2000. Urokinase-type plasminogen activator stimulates the Ras/Extracellular signal-regulated kinase (ERK) signaling pathway and MCF-7 cell migration by a mechanism that requires focal adhesion kinase, Src, and Shc. Rapid dissociation of GRB2/Sps-Shc complex is associated with the transient phosphorylation of ERK in urokinase-treated cells. *J Biol Chem*. 275:19382-8.

Nielsen, B.S., M. Sehested, S. Duun, F. Rank, S. Timshel, J. Rygaard, M. Johnsen, and K. Dano. 2001. Urokinase plasminogen activator is localized in stromal cells in ductal breast cancer. *Lab Invest*. 81:1485-501.

Nordengren, J., M. Fredstorp Lidebring, P.O. Bendahl, N. Brunner, M. Ferno, T. Hogberg, R.W. Stephens, R. Willen, and B. Casslen. 2002. High tumor tissue concentration of plasminogen activator inhibitor 2 (PAI-2) is an independent marker for shorter progression-free survival in patients with early stage endometrial cancer. *Int J Cancer*. 97:379-85.

Nykjaer, A., M. Conese, E.I. Christensen, D. Olson, O. Cremona, J. Gliemann, and F. Blasi. 1997. Recycling of the urokinase receptor upon internalization of the uPA:serpin complexes. *Embo J*. 16:2610-20.

Nykjaer, A., L. Kjoller, R.L. Cohen, D.A. Lawrence, B.A. Garni-Wagner, R.F. Todd, 3rd, A.J. van Zonneveld, J. Gliemann, and P.A. Andreasen. 1994. Regions involved in binding of urokinase-type-1 inhibitor complex and pro-urokinase to the endocytic alpha 2-macroglobulin receptor/low density lipoprotein receptor-related protein. Evidence that the urokinase receptor protects pro-urokinase against binding to the endocytic receptor. *J Biol Chem*. 269:25668-76.

Nykjaer, A., and T.E. Willnow. 2002. The low-density lipoprotein receptor gene family: a cellular Swiss army knife? *Trends Cell Biol*. 12:273-80.

Osmak, M., D. Babic, M. Abramic, D. Milicic, I. Vrhovec, and J. Skrk. 2001. Plasminogen activator inhibitor type 2: potential prognostic factor for endometrial carcinomas. *Neoplasma*. 48:462-7.

Pannekoek, H., H. Veerman, H. Lambers, P. Diergaarde, C.L. Verweij, A.J. van Zonneveld, and J.A. van Mourik. 1986. Endothelial plasminogen activator inhibitor (PAI): a new member of the Serpin gene family. *Embo J*. 5:2539-44.

Parton, R.G., and A.A. Richards. 2003. Lipid rafts and caveolae as portals for endocytosis: new insights and common mechanisms. *Traffic*. 4:724-38.

Pelkmans, L., and A. Helenius. 2002. Endocytosis via caveolae. *Traffic*. 3:311-20.

Perlmutter, D.H., G.I. Glover, M. Rivetna, C.S. Schasteen, and R.J. Fallon. 1990. Identification of a serpin-enzyme complex receptor on human hepatoma cells and human monocytes. *Proc Natl Acad Sci U S A*. 87:3753-7.

Pho, M.T., A. Ashok, and W.J. Atwood. 2000. JC virus enters human glial cells by clathrin-dependent receptor-mediated endocytosis. *J Virol*. 74:2288-92.

Pietropaolo, R., and T. Compton. 1999. Interference with annexin II has no effect on entry of human cytomegalovirus into fibroblast cells. *J Gen Virol*. 80 (Pt 7):1807-16.

Plesner, T., N. Behrendt, and M. Ploug. 1997. Structure, function and expression on blood and bone marrow cells of the urokinase-type plasminogen activator receptor, uPAR. *Stem Cells*. 15:398-408.

Ploug, M., and V. Ellis. 1994. Structure-function relationships in the receptor for urokinase-type plasminogen activator. Comparison to other members of the Ly-6 family and snake venom alpha-neurotoxins. *FEBS Lett*. 349:163-8.

Ploug, M., E. Ronne, N. Behrendt, A.L. Jensen, F. Blasi, and K. Dano. 1991. Cellular receptor for urokinase plasminogen activator. Carboxyl-terminal processing and membrane anchoring by glycosyl-phosphatidylinositol. *J Biol Chem*. 266:1926-33.

Ponting, C.P., J.M. Marshall, and S.A. Cederholm-Williams. 1992. Plasminogen: a structural review. *Blood Coagul Fibrinolysis*. 3:605-14.

Praus, M., K. Wauterickx, D. Collen, and R.D. Gerard. 1999. Reduction of tumor cell migration and metastasis by adenoviral gene transfer of plasminogen activator inhibitors. *Gene Ther*. 6:227-36.

Ragno, P. 2006. The urokinase receptor: a ligand or a receptor? Story of a sociable molecule. *Cell Mol Life Sci*. 63:1028-37.

Ragno, P., N. Montuori, and G. Rossi. 1995. Urokinase-type plasminogen activator/type-2 plasminogen-activator inhibitor complexes are not internalized upon binding to the urokinase-type-plasminogen-activator receptor in THP-1 cells. Interaction of urokinase-type plasminogen activator/type-2 plasminogen-activator inhibitor complexes with the cell surface. *Eur J Biochem*. 233:514-9.

Rakic, J.M., C. Maillard, M. Jost, K. Bajou, V. Masson, L. Devy, V. Lambert, J.M. Foidart, and A. Noel. 2003. Role of plasminogen activator-plasmin system in tumor angiogenesis. *Cell Mol Life Sci*. 60:463-73.

Ranson, M., and N.M. Andronicos. 2003. Plasminogen binding and cancer: promises and pitfalls. *Front Biosci*. 8:s294-304.

Ranson, M., N.M. Andronicos, M.J. O'Mullane, and M.S. Baker. 1998. Increased plasminogen binding is associated with metastatic breast cancer cells: differential expression of plasminogen binding proteins. *Br J Cancer*. 77:1586-97.

Ranson, M., Z. Tian, N.M. Andronicos, S. Rizvi, and B.J. Allen. 2002. In vitro cytotoxicity of bismuth-213 (213Bi)-labeled-plasminogen activator inhibitor type 2 (alpha-PAI-2) on human breast cancer cells. *Breast Cancer Res Treat*. 71:149-59.

Resnati, M., I. Pallavicini, J.M. Wang, J. Oppenheim, C.N. Serhan, M. Romano, and F. Blasi. 2002. The fibrinolytic receptor for urokinase activates the G protein-coupled chemotactic receptor FPRL1/LXA4R. *Proc Natl Acad Sci U S A*. 99:1359-64.

Rettenberger, P.M., K. Oka, L. Ellgaard, H.H. Petersen, A. Christensen, P.M. Martensen, D. Monard, M. Etzerodt, L. Chan, and P.A. Andreasen. 1999. Ligand binding properties of the very low density lipoprotein receptor. Absence of the third complement-type repeat encoded by exon 4 is associated with reduced binding of Mr 40,000 receptor-associated protein. *J Biol Chem*. 274:8973-80.

Reuning, U., V. Magdolen, S. Hapke, and M. Schmitt. 2003. Molecular and functional interdependence of the urokinase-type plasminogen activator system with integrins. *Biol Chem*. 384:1119-31.

Rice, D.S., M. Sheldon, G. D'Arcangelo, K. Nakajima, D. Goldowitz, and T. Curran. 1998. Disabled-1 acts downstream of Reelin in a signaling pathway that controls laminar organization in the mammalian brain. *Development*. 125:3719-29.

Ridley, A.J. 2001. Rho GTPases and cell migration. *J Cell Sci*. 114:2713-22.

Rihova, B. 1998. Receptor-mediated targeted drug or toxin delivery. *Adv Drug Deliv Rev*. 29:273-289.

Risse, B.C., N.M. Chung, M.S. Baker, and P.J. Jensen. 2000. Evidence for intracellular cleavage of plasminogen activator inhibitor type 2 (PAI-2) in normal epidermal keratinocytes. *J Cell Physiol*. 182:281-9.

Robert, C., I. Bolon, S. Gazzeri, S. Veyrenc, C. Brambilla, and E. Brambilla. 1999. Expression of plasminogen activator inhibitors 1 and 2 in lung cancer and their role in tumor progression. *Clin Cancer Res*. 5:2094-102.

Rodenburg, K.W., L. Kjoller, H.H. Petersen, and P.A. Andreasen. 1998. Binding of urokinase-type plasminogen activator-plasminogen activator inhibitor-1 complex to the endocytosis receptors alpha2-macroglobulin receptor/low-density lipoprotein receptor-related protein and very-low-density lipoprotein receptor involves basic residues in the inhibitor. *Biochem J*. 329 (Pt 1):55-63.

Romer, J., B.S. Nielsen, and M. Ploug. 2004. The urokinase receptor as a potential target in cancer therapy. *Curr Pharm Des*. 10:2359-76.

Ronne, E., H. Pappot, J. Grondahl-Hansen, G. Hoyer-Hansen, T. Plesner, N.E. Hansen, and K. Dano. 1995. The receptor for urokinase plasminogen activator is present in plasma from healthy donors and elevated in patients with paroxysmal nocturnal haemoglobinuria. *Br J Haematol*. 89:576-81.

Rosenberg, S. 2001. New developments in the urokinase-type plasminogen activator system. *Expert Opin Ther Targets*. 5:711-722.

Sanderson-Smith, M., M. Batzloff, K.S. Sriprakash, M. Dowton, M. Ranson, and M.J. Walker. 2006. Divergence in the plasminogen-binding group a streptococcal M protein family: functional conservation of binding site and potential role for immune selection of variants. *J Biol Chem*. 281:3217-26.

Saunders, D.N., K.M. Buttigieg, A. Gould, V. McPhun, and M.S. Baker. 1998. Immunological detection of conformational neoepitopes associated with the serpin activity of plasminogen activator inhibitor type-2. *J Biol Chem*. 273:10965-71.

Saunders, D.N., L. Jankova, S.J. Harrop, P.M. Curmi, A.R. Gould, M. Ranson, and M.S. Baker. 2001. Interaction between the P14 residue and strand 2 of beta-sheet B is critical for reactive center loop insertion in plasminogen activator inhibitor-2. *J Biol Chem*. 276:43383-9.

Schmitt, M., O.G. Wilhelm, E. Reuning, A. Kruger, N. Harbeck, E. Lengyel, H. Graeff, B. Gansbacher, H. Kessler, M. Burgle, J. Sturzebecher, S. Sperl, and V.

Magdolen. 2000. The urokinase plasminogen activator system as a novel target for tumour therapy. *Fibrinolysis and Proteolysis*. 14:114-132.

Schroeck, F., N. Arroyo de Prada, S. Sperl, M. Schmitt, and M. Viktor. 2002. Interaction of plasminogen activator inhibitor type-1 (PAI-1) with vitronectin (Vn): mapping the binding sites on PAI-1 and Vn. *Biol Chem*. 383:1143-9.

Schwartz, B.S., and J.D. Bradshaw. 1992. Regulation of plasminogen activator inhibitor mRNA levels in lipopolysaccharide-stimulated human monocytes. Correlation with production of the protein. *J Biol Chem*. 267:7089-94.

Sheehan, J.J., and S.E. Tsirka. 2005. Fibrin-modifying serine proteases thrombin, tPA, and plasmin in ischemic stroke: a review. *Glia*. 50:340-50.

Shimizu, T., K. Sato, T. Suzuki, K. Tachibana, and K. Takeda. 2003. Induction of plasminogen activator inhibitor-2 is associated with suppression of invasive activity in TPA-mediated differentiation of human prostate cancer cells. *Biochem Biophys Res Commun*. 309:267-71.

Shiomi, H., Y. Eguchi, T. Tani, M. Kodama, and T. Hattori. 2000. Cellular distribution and clinical value of urokinase-type plasminogen activator, its receptor, and plasminogen activator inhibitor-2 in esophageal squamous cell carcinoma. *Am J Pathol*. 156:567-75.

Shirasuna, K., M. Saka, Y. Hayashido, H. Yoshioka, T. Sugiura, and T. Matsuya. 1993. Extracellular matrix production and degradation by adenoid cystic carcinoma cells: participation of plasminogen activator and its inhibitor in matrix degradation. *Cancer Res*. 53:147-52.

Sidenius, N., and F. Blasi. 2003. The urokinase plasminogen activator system in cancer: recent advances and implication for prognosis and therapy. *Cancer Metastasis Rev*. 22:205-22.

Sier, C.F., N. Sidenius, A. Mariani, G. Aletti, V. Agape, A. Ferrari, G. Casetta, R.W. Stephens, N. Brunner, and F. Blasi. 1999. Presence of urokinase-type plasminogen activator receptor in urine of cancer patients and its possible clinical relevance. *Lab Invest*. 79:717-22.

Silverman, G.A., P.I. Bird, R.W. Carrell, F.C. Church, P.B. Coughlin, P.G. Gettins, J.A. Irving, D.A. Lomas, C.J. Luke, R.W. Moyer, P.A. Pemberton, E. Remold-O'Donnell, G.S. Salvesen, J. Travis, and J.C. Whisstock. 2001. The serpins are an expanding superfamily of structurally similar but functionally diverse proteins. Evolution, mechanism of inhibition, novel functions, and a revised nomenclature. *J Biol Chem*. 276:33293-6.

Simon, D.I., N.K. Rao, H. Xu, Y. Wei, O. Majdic, E. Ronne, L. Kobzik, and H.A. Chapman. 1996. Mac-1 (CD11b/CD18) and the urokinase receptor (CD87) form a functional unit on monocytic cells. *Blood*. 88:3185-94.

Skeldal, S., J.V. Larsen, K.E. Pedersen, H.H. Petersen, R. Egelund, A. Christensen, J.K. Jensen, J. Gliemann, and P.A. Andreasen. 2006. Binding areas of urokinase-type plasminogen activator-plasminogen activator inhibitor-1 complex for

endocytosis receptors of the low-density lipoprotein receptor family, determined by site-directed mutagenesis. *Febs J*.

Soeda, S., K. Shinomiya, T. Ochiai, S. Koyanagi, A. Toda, R. Eyanagi, and H. Shimeno. 2006. Plasminogen activator inhibitor-1 aids nerve growth factor-induced differentiation and survival of pheochromocytoma cells by activating both the extracellular signal-regulated kinase and c-Jun pathways. *Neuroscience*. 141:101-8.

Sorkin, A. 2001. Internalization of the epidermal growth factor receptor: role in signalling. *Biochem Soc Trans*. 29:480-4.

Spyratos, F., C. Bouchet, S. Tozlu, M. Labroquere, S. Vignaud, V. Becette, R. Lidereau, and I. Bieche. 2002. Prognostic value of uPA, PAI-1 and PAI-2 mRNA expression in primary breast cancer. *Anticancer Res*. 22:2997-3003.

Stahl, A., and B.M. Mueller. 1995. The urokinase-type plasminogen activator receptor, a GPI-linked protein, is localized in caveolae. *J Cell Biol*. 129:335-44.

Stefansson, S., M.Z. Kounnas, J. Henkin, R.K. Mallampalli, D.A. Chappell, D.K. Strickland, and W.S. Argraves. 1995. gp330 on type II pneumocytes mediates endocytosis leading to degradation of pro-urokinase, plasminogen activator inhibitor-1 and urokinase-plasminogen activator inhibitor-1 complex. *J Cell Sci*. 108 (Pt 6):2361-8.

Stefansson, S., and D.A. Lawrence. 1996. The serpin PAI-1 inhibits cell migration by blocking integrin alpha V beta 3 binding to vitronectin. *Nature*. 383:441-3.

Stefansson, S., and D.A. Lawrence. 2003. Old dogs and new tricks: proteases, inhibitors, and cell migration. *Sci STKE*. 2003:pe24.

Stefansson, S., G.A. McMahon, E. Petitclerc, and D.A. Lawrence. 2003. Plasminogen activator inhibitor-1 in tumor growth, angiogenesis and vascular remodeling. *Curr Pharm Des*. 9:1545-64.

Stefansson, S., S. Muhammad, X.F. Cheng, F.D. Battey, D.K. Strickland, and D.A. Lawrence. 1998. Plasminogen activator inhibitor-1 contains a cryptic high affinity binding site for the low density lipoprotein receptor-related protein. *J Biol Chem*. 273:6358-66.

Stefansson, S., M. Yepes, N. Gorlatova, D.E. Day, E.G. Moore, A. Zabaleta, G.A. McMahon, and D.A. Lawrence. 2004. Mutants of plasminogen activator inhibitor-1 designed to inhibit neutrophil elastase and cathepsin G are more effective in vivo than their endogenous inhibitors. *J Biol Chem*. 279:29981-7.

Stoppelli, M.P., A. Corti, A. Soffientini, G. Cassani, F. Blasi, and R.K. Assoian. 1985. Differentiation-enhanced binding of the amino-terminal fragment of human urokinase plasminogen activator to a specific receptor on U937 monocytes. *Proc Natl Acad Sci U S A*. 82:4939-43.

Strasser, V., D. Fasching, C. Hauser, H. Mayer, H.H. Bock, T. Hiesberger, J. Herz, E.J. Weeber, J.D. Sweatt, A. Pramatarova, B. Howell, W.J. Schneider, and J. Nimpf.

2004. Receptor clustering is involved in Reelin signaling. *Mol Cell Biol*. 24:1378-86.

Strickland, D.K., S.L. Gonias, and W.S. Argraves. 2002. Diverse roles for the LDL receptor family. *Trends Endocrinol Metab*. 13:66-74.

Strickland, D.K., and S. Ranganathan. 2003. Diverse role of LDL receptor-related protein in the clearance of proteases and in signaling. *J Thromb Haemost*. 1:1663-70.

Stuart, A.D., H.E. Eustace, T.A. McKee, and T.D. Brown. 2002. A novel cell entry pathway for a DAF-using human enterovirus is dependent on lipid rafts. *J Virol*. 76:9307-22.

Syrovets, T., and T. Simmet. 2004. Novel aspects and new roles for the serine protease plasmin. *Cell Mol Life Sci*. 61:873-85.

Tang, H., D.M. Kerins, Q. Hao, T. Inagami, and D.E. Vaughan. 1998. The urokinase-type plasminogen activator receptor mediates tyrosine phosphorylation of focal adhesion proteins and activation of mitogen-activated protein kinase in cultured endothelial cells. *J Biol Chem*. 273:18268-72.

Tarui, T., N. Akakura, M. Majumdar, N. Andronicos, J. Takagi, A.P. Mazar, K. Bdeir, A. Kuo, S.V. Yarovoi, D.B. Cines, and Y. Takada. 2006. Direct interaction of the kringle domain of urokinase-type plasminogen activator (uPA) and integrin alpha v beta 3 induces signal transduction and enhances plasminogen activation. *Thromb Haemost*. 95:524-34.

Tierney, M.J., and R.L. Medcalf. 2001. Plasminogen activator inhibitor type 2 contains mRNA instability elements within exon 4 of the coding region. Sequence homology to coding region instability determinants in other mRNAs. *J Biol Chem*. 276:13675-84.

Tsatas, D., M.S. Baker, and G.E. Rice. 1997. Tissue-specific expression of the relaxed conformation of plasminogen activator inhibitor-2 and low-density lipoprotein receptor-related protein in human term gestational tissues. *J Histochem Cytochem*. 45:1593-602.

Umeda, T., Y. Eguchi, K. Okino, M. Kodama, and T. Hattori. 1997. Cellular localization of urokinase-type plasminogen activator, its inhibitors, and their mRNAs in breast cancer tissues. *J Pathol*. 183:388-97.

van Dam, E.M., T. Ten Broeke, K. Jansen, P. Spijkers, and W. Stoorvogel. 2002. Endocytosed transferrin receptors recycle via distinct dynamin and phosphatidylinositol 3-kinase-dependent pathways. *J Biol Chem*. 277:48876-83.

Van Leuven, F., J. Cassiman, and H. Van Den Berghe. 1979. Demonstration of an alpha2-macroglobulin receptor in human fibroblasts, absent in tumor-derived cell lines. *The Journal of Biological Chemistry*. 254:5155-5160.

Vassalli, J.D., D. Baccino, and D. Belin. 1985. A cellular binding site for the Mr 55,000 form of the human plasminogen activator, urokinase. *J Cell Biol*. 100:86-92.

Vendeville, A., F. Rayne, A. Bonhoure, N. Bettache, P. Montcourrier, and B. Beaumelle. 2004. HIV-1 Tat enters T cells using coated pits before translocating from acidified endosomes and eliciting biological responses. *Mol Biol Cell*. 15:2347-60.

Vilhardt, F., M. Nielsen, K. Sandvig, and B. van Deurs. 1999. Urokinase-type plasminogen activator receptor is internalized by different mechanisms in polarized and nonpolarized Madin-Darby canine kidney epithelial cells. *Mol Biol Cell*. 10:179-95.

von Heijne, G., P. Liljestrom, P. Mikus, H. Andersson, and T. Ny. 1991. The efficiency of the uncleaved secretion signal in the plasminogen activator inhibitor type 2 protein can be enhanced by point mutations that increase its hydrophobicity. *J Biol Chem*. 266:15240-3.

Waisman, D.M. 2005. Annexin A2 may not play a role as a plasminogen receptor. *Br J Haematol*. 131:553-4; author reply 554-6.

Wang, S., M.E. Herndon, S. Ranganathan, S. Godyna, J. Lawler, W.S. Argraves, and G. Liau. 2004. Internalization but not binding of thrombospondin-1 to low density lipoprotein receptor-related protein-1 requires heparan sulfate proteoglycans. *J Cell Biochem*. 91:766-76.

Webb, D.J., D.H. Nguyen, and S.L. Gonias. 2000. Extracellular signal-regulated kinase functions in the urokinase receptor-dependent pathway by which neutralization of low density lipoprotein receptor-related protein promotes fibrosarcoma cell migration and matrigel invasion. *J Cell Sci*. 113 (Pt 1):123-34.

Webb, D.J., D.H. Nguyen, M. Sankovic, and S.L. Gonias. 1999. The very low density lipoprotein receptor regulates urokinase receptor catabolism and breast cancer cell motility in vitro. *J Biol Chem*. 274:7412-20.

Webb, D.J., K.S. Thomas, and S.L. Gonias. 2001. Plasminogen activator inhibitor 1 functions as a urokinase response modifier at the level of cell signaling and thereby promotes MCF-7 cell growth. *J Cell Biol*. 152:741-52.

Wei, Y., D.A. Waltz, N. Rao, R.J. Drummond, S. Rosenberg, and H.A. Chapman. 1994. Identification of the urokinase receptor as an adhesion receptor for vitronectin. *J Biol Chem*. 269:32380-8.

Weigelt, B., J.L. Peterse, and L.J. van 't Veer. 2005. Breast cancer metastasis: markers and models. *Nat Rev Cancer*. 5:591-602.

Wilczynska, M., S. Lobov, P.I. Ohlsson, and T. Ny. 2003. A redox-sensitive loop regulates plasminogen activator inhibitor type 2 (PAI-2) polymerization. *Embo J*. 22:1753-61.

Wilhelm, O.G., S. Wilhelm, G.M. Escott, V. Lutz, V. Magdolen, M. Schmitt, D.B. Rifkin, E.L. Wilson, H. Graeff, and G. Brunner. 1999. Cellular glycosylphosphatidylinositol-specific phospholipase D regulates urokinase receptor shedding and cell surface expression. *J Cell Physiol*. 180:225-35.

Williams, D.L., B. Risse, S. Kim, D. Saunders, S. Orlin, M.S. Baker, P.J. Jensen, and R.M. Lavker. 1999. Plasminogen activator inhibitor type 2 in human corneal epithelium. *Invest Ophthalmol Vis Sci*. 40:1669-75.

Wistedt, A.C., H. Kotarsky, D. Marti, U. Ringdahl, F.J. Castellino, J. Schaller, and U. Sjobring. 1998. Kringle 2 mediates high affinity binding of plasminogen to an internal sequence in streptococcal surface protein PAM. *J Biol Chem*. 273:24420-4.

Wohlwend, A., D. Belin, and J.D. Vassalli. 1987. Plasminogen activator-specific inhibitors produced by human monocytes/macrophages. *J Exp Med*. 165:320-39.

Wright, H.T., and J.N. Scarsdale. 1995. Structural basis for serpin inhibitor activity. *Proteins*. 22:210-25.

Wu, L., S. Arandjelovic, and S.L. Gonias. 2004. Effects of low density lipoprotein receptor-related protein-1 on the expression of platelet-derived growth factor beta-receptor in vitro. *J Cell Biochem*. 93:1169-77.

Xue, W., I. Mizukami, R.F. Todd, 3rd, and H.R. Petty. 1997. Urokinase-type plasminogen activator receptors associate with beta1 and beta3 integrins of fibrosarcoma cells: dependence on extracellular matrix components. *Cancer Res*. 57:1682-9.

Ye, R.D., S.M. Ahern, M.M. Le Beau, R.V. Lebo, and J.E. Sadler. 1989. Structure of the gene for human plasminogen activator inhibitor-2. The nearest mammalian homologue of chicken ovalbumin. *J Biol Chem*. 264:5495-502.

Yebra, M., L. Goretzki, M. Pfeifer, and B.M. Mueller. 1999. Urokinase-type plasminogen activator binding to its receptor stimulates tumor cell migration by enhancing integrin-mediated signal transduction. *Exp Cell Res*. 250:231-40.

Yoshino, H., Y. Endo, Y. Watanabe, and T. Sasaki. 1998. Significance of plasminogen activator inhibitor 2 as a prognostic marker in primary lung cancer: association of decreased plasminogen activator inhibitor 2 with lymph node metastasis. *Br J Cancer*. 78:833-9.

Yu, H., F. Maurer, and R.L. Medcalf. 2002. Plasminogen activator inhibitor type 2: a regulator of monocyte proliferation and differentiation. *Blood*. 99:2810-8.

Zhang, J.C., R. Sakthivel, D. Kniss, C.H. Graham, D.K. Strickland, and K.R. McCrae. 1998. The low density lipoprotein receptor-related protein/alpha2-macroglobulin receptor regulates cell surface plasminogen activator activity on human trophoblast cells. *J Biol Chem*. 273:32273-80.

Zhang, Y.Q., P. Li, M. Hou, X. Wang, J. Fan, L. Tan, and Y.S. Zhu. 2003. Identification of interaction between PAI-2 and IRF-3. *Sheng Wu Hua Xue Yu Sheng Wu Wu Li Xue Bao (Shanghai)*. 35:661-5.

Zhou, A., J.A. Huntington, N.S. Pannu, R.W. Carrell, and R.J. Read. 2003. How vitronectin binds PAI-1 to modulate fibrinolysis and cell migration. *Nat Struct Biol*. 10:541-4.

Zhou, L., Y. Hayashi, T. Itoh, W. Wang, J. Rui, and H. Itoh. 2000. Expression of urokinase-type plasminogen activator, urokinase-type plasminogen activator receptor, and plasminogen activator inhibitor-1 and -2 in hepatocellular carcinoma. *Pathol Int*. 50:392-7.

Zini, J.M., S.C. Murray, C.H. Graham, P.K. Lala, K. Kariko, E.S. Barnathan, A. Mazar, J. Henkin, D.B. Cines, and K.R. McCrae. 1992. Characterization of urokinase receptor expression by human placental trophoblasts. *Blood*. 79:2917-29.

Zoellner, H., J. Wojta, M. Gallicchio, K. McGrath, and J.A. Hamilton. 1993. Cytokine regulation of the synthesis of plasminogen activator inhibitor-2 by human vascular endothelial cells. Comparison with plasminogen activator inhibitor-1 synthesis. *Thromb Haemost*. 69:135-40.

APPENDIX 1: Buffers and Solutions

General Buffers

Phosphate buffered saline (PBS)

NaCl	8 g/L
KCl	0.2 g/L
Na_2HPO_4	1.44 g/L
KH_2PO_4	0.24 g/L
pH 7.4	

50 mM Sodium Phosphate buffer (pH 6)

Na_2HPO_4	6.07 g/L
NaH_2PO_4	1.61 g/L

10 mM phosphate buffer (pH 8)

Na_2HPO_4	0.094 g/L
NaH_2PO_4	2.5 g/L

Tris buffered saline (TBS)

NaCl	8.77 g/L
Tris-base	6.06 g/L
± Tween 20 (TBST)	500 μL/L
pH 7.4	

BIAcore running buffer

HEPES	2.60 g/L
NaCl	8.18 g/L
$CaCl_2$	1 mM
Tween-20	500 μL/L
pH 8 (Chapter 2)	
pH 7.4 (Chapter 3 and 4)	

Cell Culture Assay Buffers

Hanks buffered salt solution (binding buffer)

Phenol red free Hanks buffered salt solution	9.8 g/L
HEPES	4.76 g/L
$CaCl_2$	1 mM
$MgCl_2$	1 mM
Bovine serum albumin	1 g/L
pH 7.4	

Cell lysis buffer

HEPES	13.0 g/L
NaCl	5.84 g/L
1% Nonidet P-40	10 mL/L
EDTA*	2 mM
Sodium Orthovanadate*	0.4 mg/mL
Protease cocktail inhibitor*	1 mL/L
Dithiothreitol*	5 mg/mL

pH 7.4

* Added just before use.

SDS-PAGE and Western Blotting

SDS-PAGE Running buffer

Tris Base	30 g/L
Glycine	144 g/L
SDS	10 g/L

SDS-PAGE Sample Buffer (5X)

Tris Base	12.1 g/L
SDS	0.2% (w/v)
Glycerol	15% (v/v)
Bromophenol Blue	0.1% (w/v)

12% Acrylamide Gels (100 mL stock solution)

1.5 M Tris-base pH 8	25 mL
40% bis-acrylamide stock	30 mL
10% SDS	1 mL
dH_2O	44 mL
10% APS*	50 µL/10 mL
TEMED*	5 µ/10 mL

* Add prior to use to induce polymerisation

4% Acrylamide Gels (100 mL Stock Solution)

0.5 M Tris-base pH 6.8	25 mL
40% bis-acrylamide stock	10 mL
10% SDS	1 mL
dH_2O	64 mL
10% APS*	50 μL/10 mL
TEMED*	5 μ/10 mL

* Add prior to use to induce polymerisation

Coomassie Blue Stain

Methanol	40% (v/v)
Glacial Acetic Acid	10% (v/v)
Coomassie Blue	0.1% (w/v)

Destain

Methanol	40% (v/v)
Glacial Acetic Acid	10% (v/v)

Rapid Destain

Methanol	40% (v/v)
Glacial Acetic Acid	10% (v/v)
Glycerol	4%

Transfer Buffer

Tris-base	3.03 g/L
Glycine	14.4 g/L
Make to 800 mL in distilled water	
Methanol	200 mL

Stripping Buffer

SDS	2% (w/v)
2M Tris pH 6.8	31.2 mL/L
B-mercaptoethanol	0.75% (v/v)

APPENDIX 2: Dual colour flow cytometry

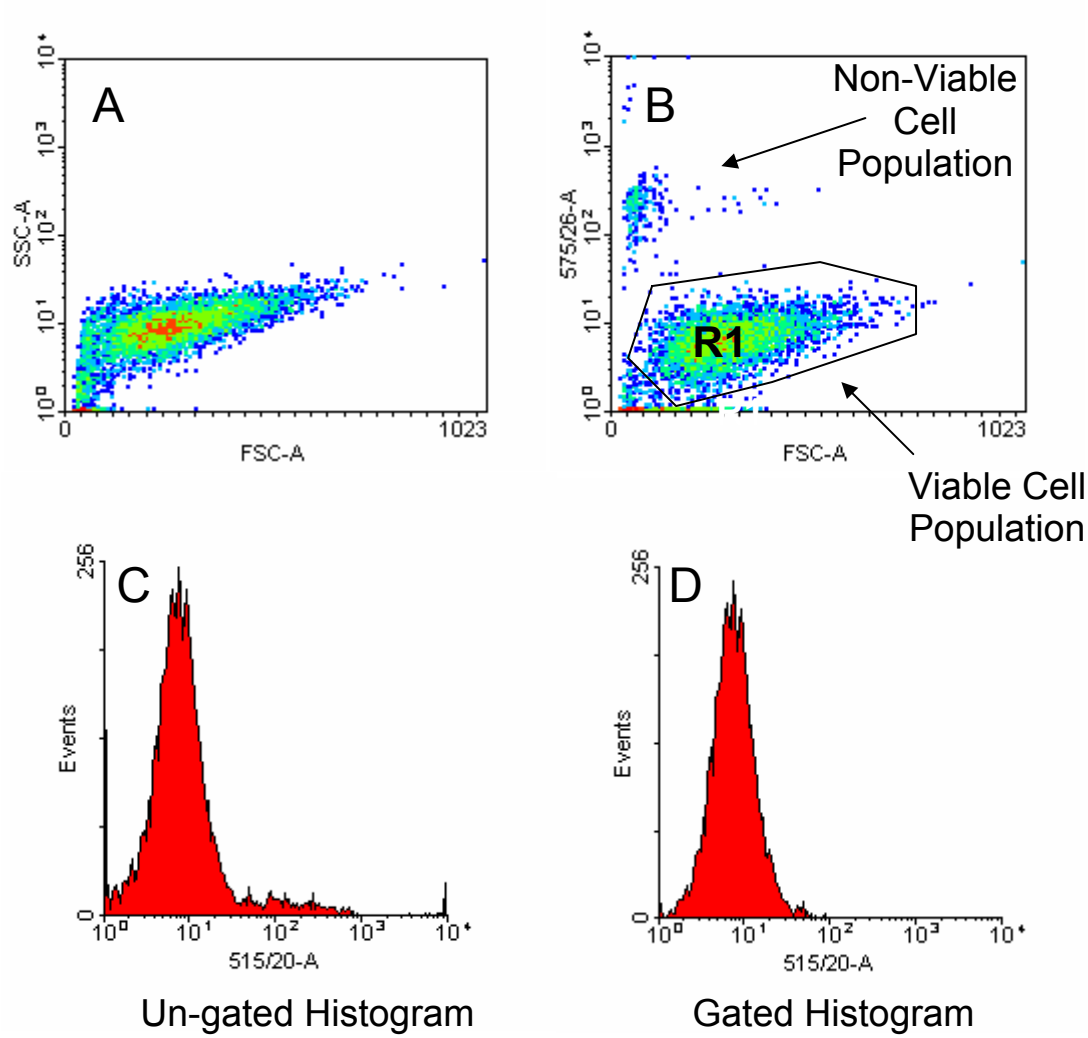

(A) Entire cell population is collected using forward scatter (FSC) and side scatter (SSC) measurements.
(B) Non-viable cells are detected by measuring PI fluorescence (575/26 nm) against FSC. The viable cell population is gated (R1).
(C) Histogram showing FITC fluorescence of entire cell population (515/20 nm).
(D) Histogram showing FITC fluorescence of R1 gated data. Higher fluorescence counts associated with non-viable cells have been removed as a result of gating.

APPENDIX 3: Fluorescence Quenching Internalisation Assay

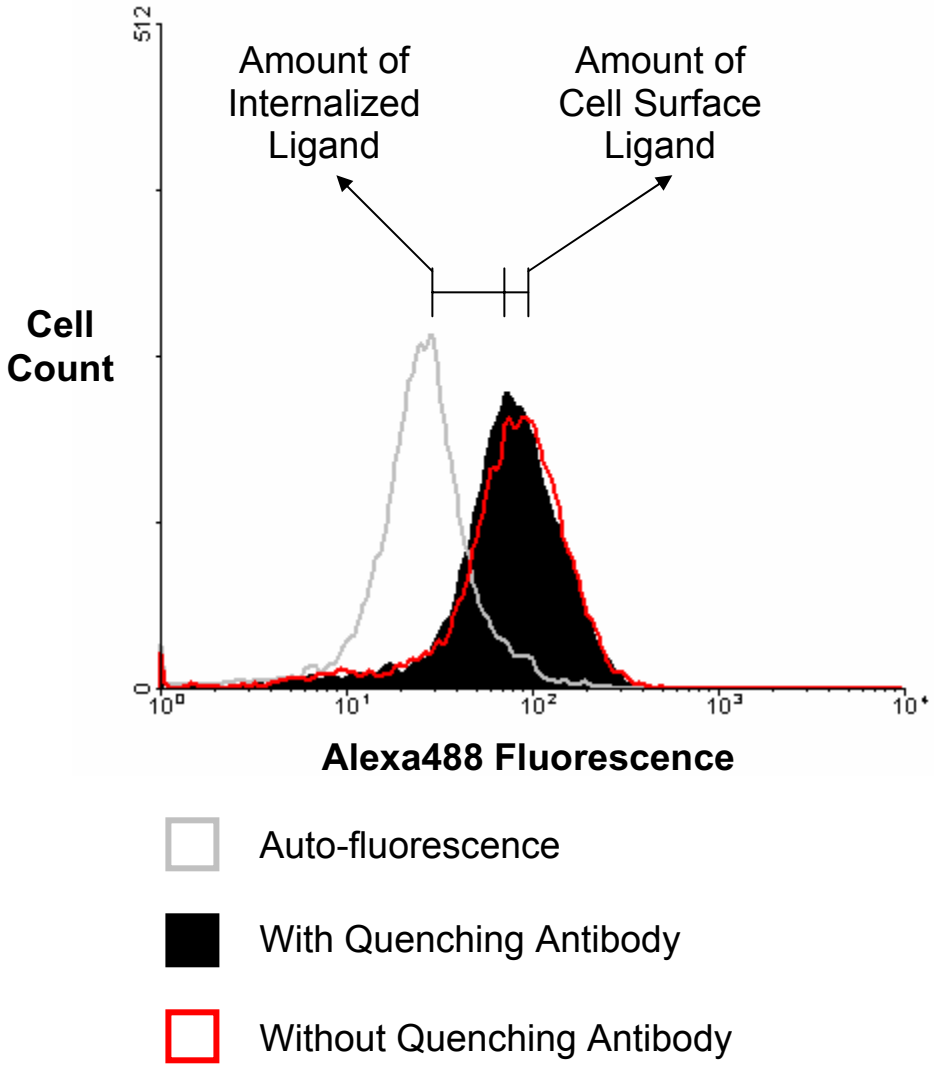

The background level of cell fluorescence is determined by measuring the auto-fluorescence of cells that have undergone all treatments except the addition of $Alexa_{488}$ labeled protein (Grey line). An average is taken of these values and all data blanked to this. Cells incubated with the $Alexa_{488}$ labeled proteins but not the quenching antibody give a measurement of all cell associated protein (Red line). For internalisation rate assays this value is normalised to 100%. Cells incubated with the $Alexa_{488}$ protein and the quenching antibody give a measurement of internalised protein (Black histogram). In this case, there is very little decrease in fluorescence associated with the addition of the quenching antibody, indicating that the majority of cell associated ligand is internalised. For inhibition assays, the value obtained for this measurement in the absence of inhibitors is normalised to 100%.

APPENDIX 4: Immobilisation on CM5 Sensor Chips

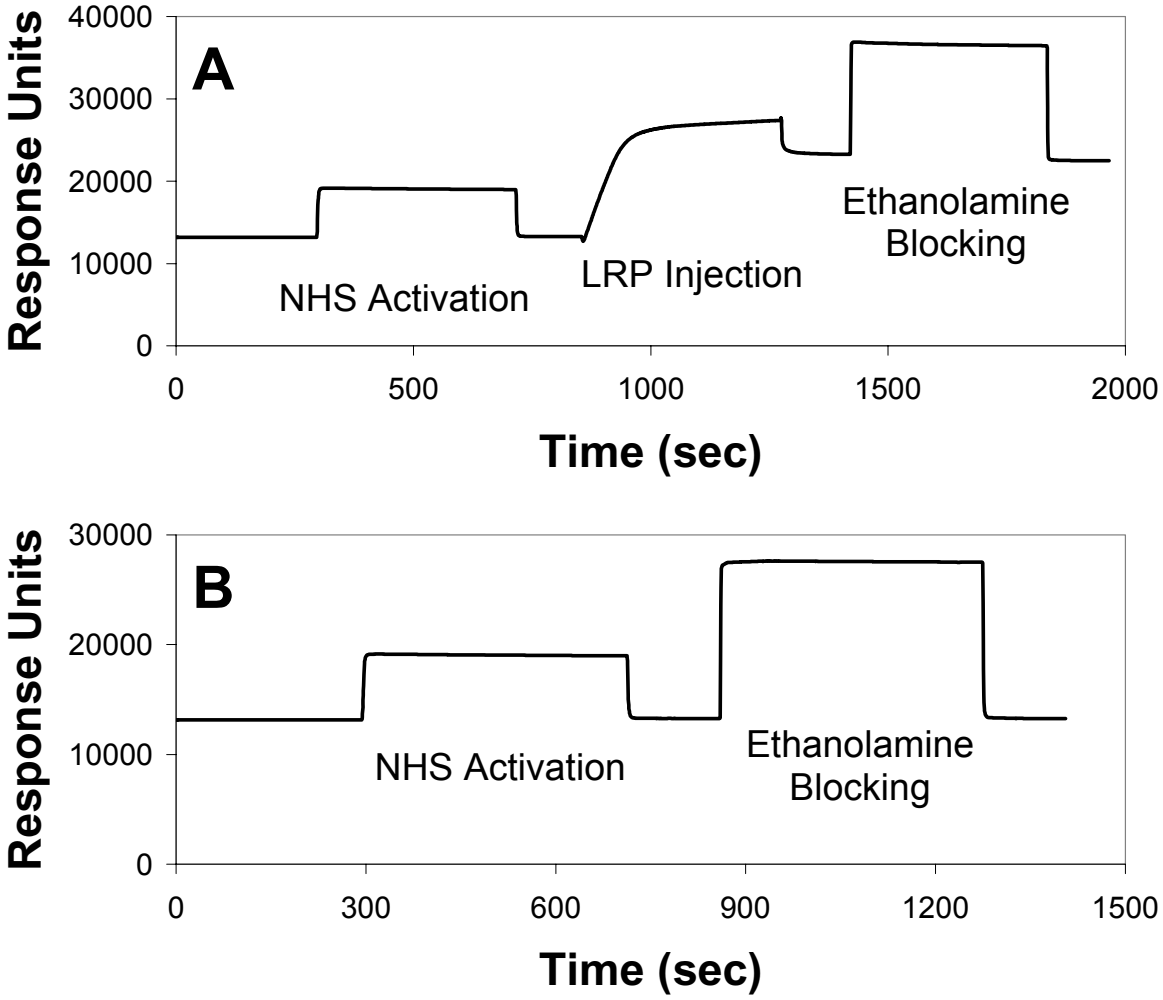

The immobilisation of LRP to a CM5 BIAcore chip (VLDLr and Annexin II heterotetramer were immobilised in a similar manner. The flow cells are activated by a 1:1 mixture of 0.2M *N*-ethyl-*N′*-(3-dimethylaminopropyl)carbodi-imide and 0.05M *N*-hydroxysuccimide (NHS).

(A) the chip was coated by running LRP (40 µg/ml) in 10 mM sodium acetate (pH 3) over it for 7 min at 5 µl/min. The immobilisation of LRP to the chip resulted in an increase in of between 7000-14000 response units (correlating to 15-28 fmol/mm^2, with 1000 response units equaling 1 ng of protein/mm^2). The un-occupied binding sites were blocked using 1M ethanolamine, pH 8.5.

(B) A blank reference cell was prepared by undergoing the activation and blocking steps without the LRP immobilisation step.

APPENDIX 5: BIAcore Kinetic Analysis

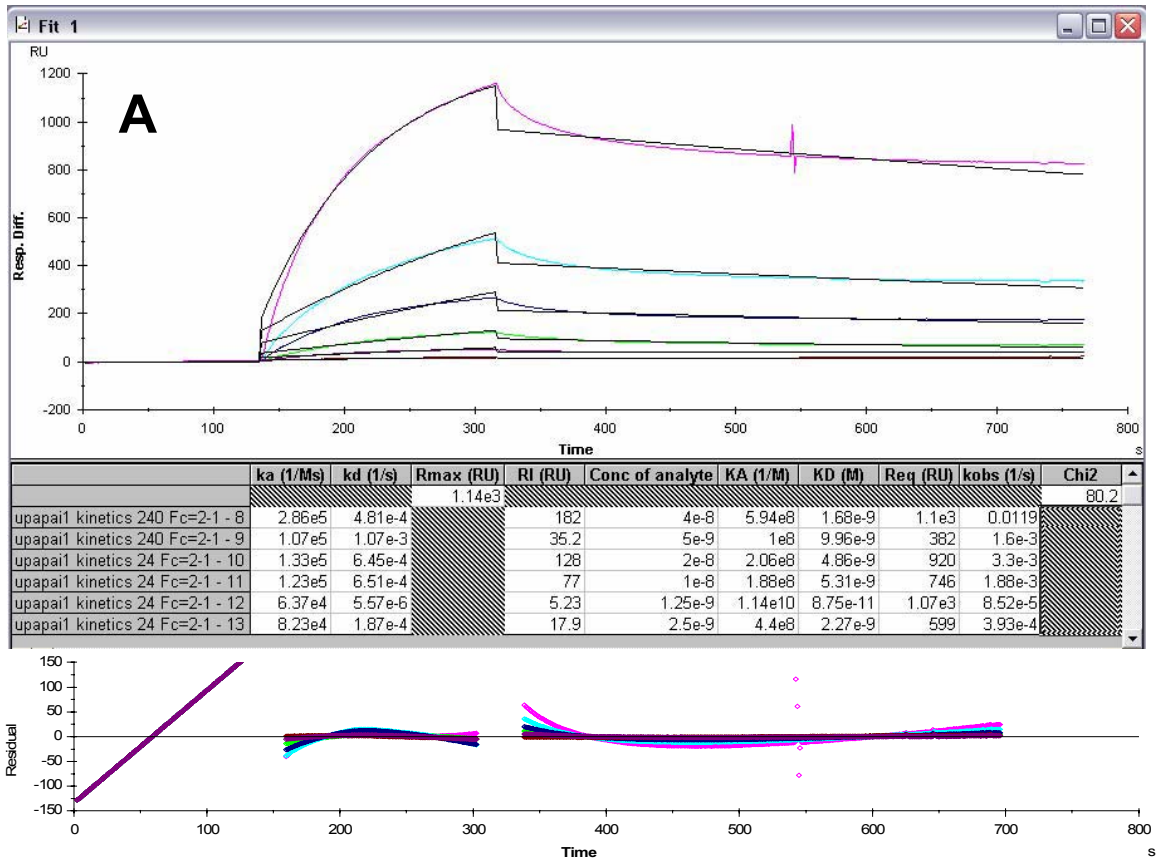

	ka (1/Ms)	kd (1/s)	Rmax (RU)	RI (RU)	Conc of analyte	KA (1/M)	KD (M)	Req (RU)	kobs (1/s)	Chi2
			1.14e3							80.2
upapai1 kinetics 240 Fc=2-1 - 8	2.86e5	4.81e-4		182	4e-8	5.94e8	1.68e-9	1.1e3	0.0119	
upapai1 kinetics 240 Fc=2-1 - 9	1.07e5	1.07e-3		35.2	5e-9	1e8	9.96e-9	382	1.6e-3	
upapai1 kinetics 24 Fc=2-1 - 10	1.33e5	6.45e-4		128	2e-8	2.06e8	4.86e-9	920	3.3e-3	
upapai1 kinetics 24 Fc=2-1 - 11	1.23e5	6.51e-4		77	1e-8	1.88e8	5.31e-9	746	1.88e-3	
upapai1 kinetics 24 Fc=2-1 - 12	6.37e4	5.57e-6		5.23	1.25e-9	1.14e10	8.75e-11	1.07e3	8.52e-5	
upapai1 kinetics 24 Fc=2-1 - 13	8.23e4	1.87e-4		17.9	2.5e-9	4.4e8	2.27e-9	599	3.93e-4	

Screen captures from the BIAevaluation software v4 (BIAcore, Uppsala, Sweden) are shown for the analysis of uPA:PAI-1 binding (1.25 – 40 nM) to immobilised VLDLr by both a **(A)** 1:1 Langmuir binding and **(B)** (following page) a heterogenous analyte – competitive binding model. This data used a local fitting for k_a and k_d measurements, however R_{max} was fitted globally.

Goodness of fit is judged by both the Chi2 (χ^2) value and also the residual plot for the fitting of the data against the theoretical binding model. A χ^2 value of under 10 is assumed to be an acceptable fit, although analysis of the residual plot (the deviation of experimental data from the theoretical fit) can often provide useful information about where the data deviates from the theoretical modeling.

This particular data does not provide a χ^2 of under 10 for the heterogenous analyte – competitive binding model (χ^2 = 15.7), however this was the lowest χ^2 for all of the available models in the newest version of the BIAevaluation software v4.

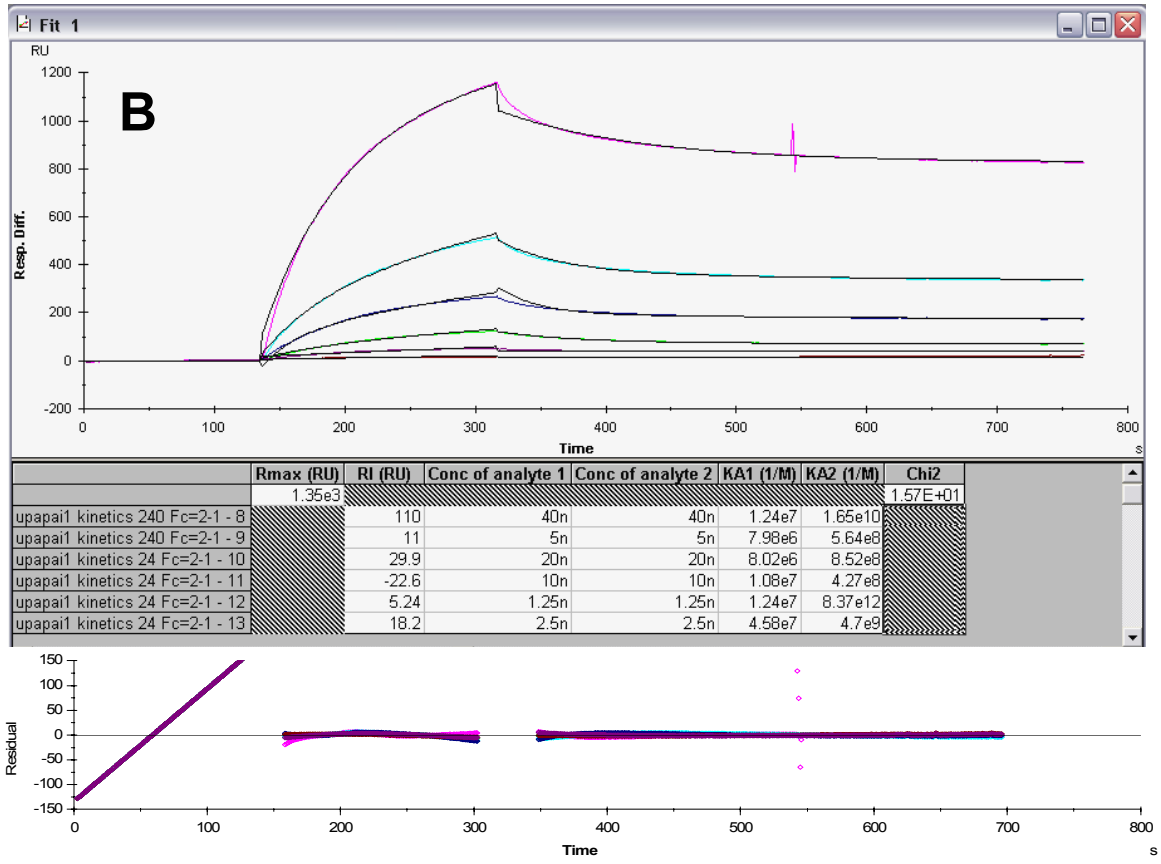

	Rmax (RU)	RI (RU)	Conc of analyte 1	Conc of analyte 2	KA1 (1/M)	KA2 (1/M)	Chi2
	1.35e3						1.57E+01
upapai1 kinetics 240 Fc=2-1 - 8		110	40n	40n	1.24e7	1.65e10	
upapai1 kinetics 240 Fc=2-1 - 9		11	5n	5n	7.98e6	5.64e8	
upapai1 kinetics 24 Fc=2-1 - 10		29.9	20n	20n	8.02e6	8.52e8	
upapai1 kinetics 24 Fc=2-1 - 11		-22.6	10n	10n	1.08e7	4.27e8	
upapai1 kinetics 24 Fc=2-1 - 12		5.24	1.25n	1.25n	1.24e7	8.37e12	
upapai1 kinetics 24 Fc=2-1 - 13		18.2	2.5n	2.5n	4.58e7	4.7e9	

APPENDIX 6: Publications

Please see print copy for Publications